SENSORY NEUROPLASTICITY IN ASTHMA

By

Gregory D. Scott

A THESIS/DISSERTATION

Presented to the Department of Cell & Developmental Biology
and the Oregon Health & Science University
School of Medicine
in partial fulfillment of
the requirements for the degree of

Doctor of Philosophy

June 2012

School of Medicine
Oregon Health & Science University
CERTIFICATE OF APPROVAL

_____

This is to certify that the PhD dissertation of
Gregory D. Scott
has been approved

_____
Mentor/Advisor (Dr. David Jacoby)

_____
Member (Dr. Jeff Gold)

_____
Member (Dr. Allison Fryer)

_____
Member (Dr. Philip Copenhaver)

_____
Member (Dr. Stefanie Kaech Petrie)

_____
Member (Dr. Kelvin MacDonald)

_____
Member (Dr. Stephen Smith)

Table of Contents

LIST OF ABBREVIATIONS

5-HT: 5-hydroxytryptamine or serotonin.

ATP: Adenosine triphosphate.

BDNF: Brain-derived neurotrophic factor

CAM: Cell adhesion molecule.

CC10: Clara cell (airway epithelial) promoter specific to the airway. Used to generate mice with lung-specific eosinophilia.

CCR3: C-C chemokine receptor type 3. Receptor for Eotaxin.

CGRP: Calcitonin gene-related peptide. Pro-inflammatory neuropeptide used to mark a subset of sensory C fibers in the airway.

DNFB: 2,4-dinitrofluorobenzene. Treatment used in acute dermatitis model.

DRG: Dorsal Root Ganglion. Site of spinal sensory neurons of the somatosensory system.

ECP: Eosinophil cationic protein. An eosinophil granule protein.

EDN: Eosinophil-derived neurotoxin. An eosinophil granule protein.

EPO: Eosinophil peroxidase. An eosinophil granule protein.

GDNF: Glial-derived neurotrophic factor. A member of the GFL family of growth factors

GFL: GDNF family ligands. A family of nerve growth factors.

GFR: GDNF family receptor. GFRα receptors are specific to different GFLs.

IB4: Isolectin B4. A lectin that identifies a subpopulation of sensory nerves.

K14: Keratinocyte promoter used to overexpress IL-5 in mouse models of dermatitis causing eosinophil recruitment.

MBP: Major basic protein. An eosinophil granule protein.

NGF: Nerve growth factor. A neurotrophin that binds with high affinity to TrkA.

P75: Low-affinity pan-neurotrophin receptor.

PBS: Phosphate-Buffered Saline.

PGP 9.5: Protein gene product 9.5. Cytoplasmic protein enriched in neuronal and neuroendocrine cells. With little exception PGP 9.5 serves as a pan-neuronal marker.

RAR: Rapidly-adapting receptors. Airway mechanosensors

SAR: Slowly-adapting receptors . Airway mechanosensors

SP: Substance P. A pro-inflammatory neuropeptide expressed in a subset of airway C fibers.

TBS: Tris-Buffered Saline.

TMA: Trimetallic anhydride. Treatment used in chronic dermatitis model.

Trk Receptor: Family of receptor tyrosine kinases. Primary ligands are neurotrophin

Trp Receptor: Transient receptor potential receptor. Family of receptors on sensory nerves involved in sensation of pain, temperature, and other stimuli that produce cough, dyspnea, bronchoconstriction in the airway.

Vagotomy: Cutting parasympathetic and sensory innervation to the airway (which is supplied by the vagus nerve).

VIP: Vasoactive intenstinal peptide. Vasodilatory and anti-inflammatory neuropeptides abundantly expressed most in airway cholinergic nerves but also in sensory neurons.

TRANSGENIC MOUSE STRAINS

IL5/K14: Mouse model of chronic eosinophilic dermatitis where IL-5 is overexpressed in the skin.

K14/PHIL: Transgenic mouse where IL5/K14 mice were crossed with PHIL mice so there is overabundance of IL5 in the skin but no eosinophils.

NJ.1726: Transgenic mouse with overabundant eosinophils specifically in the airway due to overexpression of IL-5 under the clara cell CC10 promoter. Also refererred to as “IL5++/Eos++”.

NJ.1726/PHIL: Transgenic mouse cross between NJ.1726 and PHIL so there is overabundance of IL5 in the airway but not eosinophils.

PHIL: Transgenic mouse lacking eosinophils due to expression of cytotoxic diphtheria toxin under an eosinophil promoter. Also referred to as “No Eos”.

LIST OF TABLES

LIST OF FIGURES

ACKNOWLEDGEMENTS

I am deeply grateful for the support of my mentors, my thesis advisory committee, my collaborators, my friends and family, and my wife, Laura Shula.

My mentors were integral to my professional development as a scientist. Dr. David Jacoby worked tirelessly to help plan experiments and provide constructive feedback on data interpretation, writing, and oral presentations. This included practice sessions and advice on weekends and late at night. I would also like to thank Dr. Allison Fryer for her excellent help both experimentally and with written and verbal communication skills.

In addition, my thesis advisory committee provided helpful ongoing feedback and experimental advice. They focused my efforts and helped me comprehensively consider each avenue of research. All time was offered pro bono with enthusiasm and attentiveness for which I am very grateful.

I also want to acknowledge collaborators who contributed to my dissertation. Dr. James Lee kindly provided transgenic mice for both asthma and dermatitis projects. Dr. Stefanie Kaech Petrie provided advice and help with optics-related experiments. Dr. Kelvin MacDonald provided training and the mouse ventilator equipment necessary for measuring airway mechanics. Dr. Richard Costello provided bronchoscopic biopsies from human subjects. The Pacific Northwest Transplant Bank procured human tracheas. Dr. Jessica Martin taught nodose and jugular ganglion dissections.

I want to extend my sincere thanks to my immediate family, the Scotts (David, Georgie, Andrew, Carrie, Kari, Andy) my in-laws, the Shulas (Bob, Virginia, Lydia, Jerry, Sule), and my extended Scott and Murphy family for providing support through thick and thin. In particular I want to thank my parents David and Georgie Scott for their loving support. I also want to thank

my grandparents, David and Beatrice Murphy, and Douglas and Louis Scott for setting the foundation for any opportunity made available to me.

I also want to thank my friends for their direct and indirect contributions to this dissertation. Both in the lab, at OHSU, and outside of work my friends provided a fresh perspective on my research and work-life balance. This includes: El Gregorio, Matt, Linda, Mark, Helen, Sarah, Deder, Angie, Kalmia, Jesse, Becky, Emily, Noah, Erin, Elad, Kirsten, Jane, Abby, Sarah, Matt, Bart, MD/PhD classmates, Quicksilver, and TSWAC to name a few.

Finally, thank you to my wife, Laura Shula who gave me unparalleled support throughout my dissertation. I simply would not have accomplished this work without her, thank you so much Laura.

ABSTRACT

Asthma is a chronic inflammatory disease of the lung and a significant health burden. Airway sensory neurons in asthma malfunction and contribute to airway hyperreactivity. The upstream changes to neuron structure and the inciting factors behind sensory dysfunction are unknown due to obstacles in characterizing airway innervation. This project aims to offer insight into sensory neuroplasticity, or how sensory neurons change in asthma.

I initially hypothesized that a new method of capturing and quantifying nerves would more accurately and comprehensively measure whole organ innervation. Thus I initially developed a new method permitting the visualization of whole airway innervation and computerized quantification of nerve branching and nerve density (Chapter 3). I then hypothesized that in asthma an inflammatory cell called the eosinophil is important for airway neuroplasticity. Thus I used this new nerve modeling method to show that in a model of chronic allergic inflammatory asthma but not acute allergic inflammatory asthma, increased eosinophils in the airway results in branched outgrowth of airway epithelial nerves (Chapter 4). Furthermore, I showed this branched outgrowth was associated with increased reflex bronchoconstriction, a physiologic characteristic of asthma mediated by airway nerves (Chapter 4). I subsequently used transgenic mice lacking eosinophils to show they were necessary both for sensory nerve branched outgrowth and increased reflex bronchoconstriction (Chapter 4).

Neuronal hypersensitivity and dysfunction in atopic dermatitis, an itchy skin disease, is also associated with changes in nerve density. I hypothesized that eosinophils were important for nerve structural changes. I utilized the same computer modeling approach and found opposite neurotrophic or neuropathic effects caused by eosinophils in a chronic versus acute dermatitis model (Chapter 5). In co-culture experiments, I showed eosinophils produce neurotrophic effects on sensory nerves measured as increased nerve length.

Overall this dissertation shows a new technique for quantification of nerve structure and uses this approach to demonstrate that eosinophils in inflammatory disease are capable of

causing neurotrophic and neuropathic neuroplasticity. Moreover, neuroplasticity caused by eosinophils is associated a major cause of morbidity in asthma, increased reflex bronchoconstriction. Thus the current dissertation describes eosinophil neuroimmune interactions important for pathogenesis and symptom manifestation in allergic airway and skin diseases.

CHAPTER 1: INTRODUCTION

1.1 Asthma

Asthma is a chronic lung disease characterized by airway inflammation and narrowing, which leads to coughing, wheezing, and shortness of breath. It is a widespread problem afflicting 300 million individuals worldwide with incidence rising particularly in children (WHO 2007). Asthma is also responsible for thousands of fatalities each year and is a major contributor to hospitalizations, prescription drug use, and absenteeism costing an estimated $56 billion dollars annually in the United States (WHO 2007; CDC May 2011). Roughly one in four children with asthma and >50% of adults who still have asthma suffer a progressive decline in lung function measured as decreased ability to expire rapidly (Lange, Parner et al. 1998; Sears, Greene et al. 2003; Spahn and Covar 2008). Currently, steroids are the mainstay treatment for asthma despite failure to slow asthma progression or underlying severity (NHLBI 2007). In addition between 5-10% of asthma is resistant to steroids, but steroid resistant asthma accounts for 50% of asthma related health care costs (Barnes and Woolcock 1998; Ito, Chung et al. 2006). Other current treatment options have less favorable side effect profiles and efficacy (NHLBI 2007). Given the importance of asthma and shortcomings of current treatment options, further research is needed to understand novel pathways in asthma pathogenesis. Two predictors of asthma progression and untreatable airway narrowing are an immune cell called the eosinophil and airway hyperresponsiveness (Bumbacea, Campbell et al. 2004). Airway hyperresponsiveness is airway narrowing in response to otherwise innocuous airway stimuli. Eosinophils and airway hyperresponsiveness are discussed later in more detail.

1.2 Asthma Phenotypes

Asthma is probably not a single disease but a collection of diseases with overlapping features. Asthma can be divided into distinct phenotypes based on clinical, trigger-related, and inflammatory disease characteristics (Wenzel 2006). Distinct clinical asthma phenotypes have been identified based on severity, likelihood of exacerbation, airway restriction, response to treatment, and age-of-onset. Distinct trigger-related asthma phenotypes have been identified based on allergy, occupational exposure, aspirin sensitivity, relationship to menses, and exercise as a trigger. Finally, inflammation-specific asthma phenotypes have been identified based on abundance of two inflammatory cells, eosinophils (discussed below) and neutrophils, or lack of either eosinophils or neutrophils. Given the potentially different pathogenesis of each asthma phenotype, it is important to study these different diseases separately in order to reduce confounding variables. The following address allergic asthma since it is the most common asthma subtype (Kim, DeKruyff et al. 2010)

1.3 Allergic Asthma and Atopy

Allergy is defined as a hypersensitivity reaction initiated by immunological mechanisms (Johansson, Bieber et al. 2004). Allergens, or antigens that cause allergy, are typically foreign proteins that include pollen, food, and fungal spores. In allergic asthma, common allergens include pollen, dust mite excrement, cockroach antigen, pet dander, and mold.

The development of allergic disease in different organs often occurs together in the same person. Numerous studies have found positive associations between allergic rhinitis, asthma, atopic dermatitis, allergic conjunctivitis, and food allergies (Sahin-Yilmaz, Nocon et al. ; Spergel ; Worth and Sheikh ; Ellman, Chatchatee et al. 2002; Woods, Thien et al. 2002; Bieber, Leung et al. 2011; Fiocchi, Sampson et al. 2011; Holgate, Canonica et al. 2011; Pawankar, Sanchez-Borges et al. 2011). Atopy is defined as the tendency, usually in childhood or

adolescence, to develop sensitivity to common allergens (Johansson, Bieber et al. 2004). The chronic-exposure allergies of the nose (rhinitis), airway (asthma), eye (conjunctivitis), gastrointestinal tract (food allergy), and skin (atopic dermatitis, eczema) are characterized by acute and chronic symptoms including itch, pain, limited airflow, cough, hypersecretion, intestinal dysmotility, and tissue remodeling. These symptoms are wholly or in part controlled by the peripheral sensory nervous system.

1.4 The Respiratory System

Asthma affects the respiratory system, which is designed to exchange gas between air and blood (Figure 1). The upper respiratory system consists of the nasal cavity, pharynx (throat), and larynx (voice box) but is not affected by asthma and will not be discussed further. The lower respiratory system is made up of extrapulmonary and intrapulmonary compartments (Figure 1). The extrapulmonary compartment consists of large tubular passageways for airflow and includes the trachea below the larynx and the two primary bronchi that come from the trachea splitting at the carina. The intrapulmonary component of the lower respiratory system consists of everything inside the lungs. The primary bronchi divide repeatedly in the lungs to increase overall surface area available for gas exchange. The smallest airway division is called the respiratory bronchiole which connects to thin-walled sacs called alveoli where gas exchange takes place. The airways are made up of distinct cell types localized to specific tissue layers. Air breathed into the lumen first contacts a layer of tightly-bound epithelial cells. Specialized cells called goblet cells that secrete mucus are also located within the epithelium. Below the basement membrane of the epithelial cell layer is the submucosa containing submucosal glands that secrete mucus, airway smooth muscle that contracts to narrow the airway, and blood vessels. The trachea and primary bronchi also contain cartilage below smooth muscle which provides additional structural support. It is in the trachea to bronchioles, also known as the

conducting airways, where asthma narrows lumen diameter, increases airway resistance, and causes symptoms such as wheezing, cough, and shortness of breath.

1.5 Innervation of the Lungs

Airway narrowing is controlled by peripheral nerves that innervate the lungs. The airway contains both autonomic nerves and sensory nerves. The autonomic nervous system is part of the efferent (outgoing signaling) nervous system not under direct conscious control (Langley 1898). The autonomic nervous system is divided into sympathetic and parasympathetic nerve populations. Sympathetic nerves will not be further discussed since in humans they do not directly act on airway smooth muscle to cause airway narrowing or dilation (Proskocil and Fryer 2005). Parasympathetic nerves provide the dominant efferent control of airway narrowing by directly contracting airway smooth muscle (Colebatch and Halmagyi 1963). Parasympathetic nerves store and release the neurotransmitter, acetylcholine, which binds muscarinic receptors on airway smooth muscle causing contraction and airway narrowing (Colebatch and Halmagyi 1963). Release of acetylcholine from parasympathetic nerves is also regulated by muscarinic receptors on the parasympathetic nerves themselves (Fryer and Maclagan 1984). The final nerve population is airway sensory nerves that innervate all lung tissue compartments and transmit information to the central nervous system. The importance of sensory nerves in asthma is in part because they can indirectly cause airway narrowing by activating parasympathetic nerves through a central reflex called reflex bronchoconstriction (discussed later).

1.6 Importance of Airway Nerves in Asthma

The role of sensory nerves in asthma was first demonstrated by studies of lung transplants and studies that blocked the vagus nerve. A study of seven lung transplant

recipients showed that sensory innervation and cough is restored in transplanted tissue after one year (Duarte, Terminella et al. 2008) and a case study found that a human asthmatic recipient of nonasthmatic lungs developed asthma in the new airway after three years (Schwerk, Ballmann et al. 2008). These studies suggest asthma pathogenesis is not restricted to the lungs but that systemic factors such as the peripheral nervous system are important contributing factors. Early surgical studies severed the vagus nerve supply to the airway in patients with severe asthma and showed decreased asthma symptoms (Balogh, Dimitrov-Szokodi et al. 1957) . In animal models, cooling the vagus nerve or vagotomy eliminated allergic airway contractions (Gold, Kessler et al. 1972). Since then a wide variety of changes to sensory nerve function, growth, and signaling components have been identified.

1.7 Airway Sensory Nerves

Asthma disease progression and symptoms involve airway sensory nerves. Sensory nerves are a subpopulation of the peripheral nervous system that sends information about the external and internal environment to the brain. The cell bodies of airway sensory nerves are located in two ganglia, the nodose and jugular ganglia or collectively the vagal ganglia, along the vagus nerve at the base of the skull (Figure 2) (Taylor-Clark and Undem 2006). Axons of airway sensory nerves emerge from vagal ganglia, split, and travel to the brain stem and lung (Taylor-Clark and Undem 2006). Airway sensory nerves can be stimulated by various external stimuli including changes in temperature (eg. cold air), mechanical irritation (eg. by pollen), mechanical stretch, and pollution (eg. sulfur dioxide). Sensory nerves are also activated by endogenous substances such as neurotransmitters and inflammatory mediators as well as by direct sensory agonists such as capsaicin, the active ingredient in hot peppers. Activation of airway sensory nerves causes a variety of effects seen in asthma including airway narrowing, cough, shortness

of breath, increased mucus production, and plasma exudation. As a consequence sensory nerves contribute to both long-term inflammation and acute respiratory symptoms.

1.7.1 Reflex Bronchoconstriction

A principle feature of asthma is reflex bronchoconstriction, or airway narrowing caused by vagal signaling. Sensory nerves cause reflex bronchoconstriction by signaling up to the brain stem via the vagus nerve and back to the lung via parasympathetic nerves, which contracts airway smooth muscle and narrows the airway. Direct electrical (Holtzman, Hahn et al. 1982) or chemical (Nadel, Salem et al. 1965) stimulation of sensory nerves can initiate reflex bronchoconstriction, and this is prevented by cutting the vagus nerve (vagotomy) (Wagner and Jacoby 1999), vagal cooling (Nadel, Salem et al. 1965), chemical depletion of sensory nerves (Forsberg, Karlsson et al. 1988), pharmacologic antagonism of sensory receptors (Nault, Vincent et al. 1999), or genetic sensory depletion in mice (Caceres, Brackmann et al. 2009). One mechanism for airway hyperresponsiveness in asthma, defined as increased bronchoconstriction in response to otherwise innocuous stimuli, is by increased sensitivity of airway sensory nerves to cause reflex bronchoconstriction.

1.7.2 Nerves Populations

The airway contains specialized sensory nerve populations in order to perform its many functions. Sensory populations are identified by both functional and structural characteristics including the stimuli to which they respond, conduction velocity, cell body size, axon diameter, neurotransmitter content, embryologic origin, and tissue location. It is important to note that each criterion used to define different nerve populations has overlapping distributions.

Morphology, Conduction Velocity, and Responsiveness

Sensory nerves are separable into two large subpopulations, A and C fibers, based on morphology, conduction velocity, and stimulus responsiveness (Table 1). These populations were initially identified and mostly characterized in dorsal root ganglion (DRG) of the somatosensory system (Harper and Lawson 1985). A fibers are larger, myelinated, faster conducting, and mechanosensitive nerves. C fibers are smaller, unmyelinated, slower conducting, and more responsive to noxious stimuli (Harper and Lawson 1985; Scott 1992; Julius and Basbaum 2001). The following summarizes how sensory nerves in the vagal ganglion subserving the airways are defined base on similar criteria.

C Fibers

Non-myelinated C fibers make up the majority (> 75%) of the fibers in the vagus nerves (Lee, Shuei Lin et al. 2003) and innervate all airway tissue compartments from the trachea to alveoli (Coleridge and Coleridge 1984). Their body size ranges between 15-30 microns, conduction velocity is between ~0.3- 2m/s, and their general structure and function is similar between mouse, rat, guinea pig, rabbit, cat, and monkey (Scott 1992; Taylor-Clark and Undem 2006; Canning and Chou 2009). Most but not all airway C fibers express the receptor TrpV1, and were historically identified as responsive to capsaicin, a TrpV1 ligand (Undem, Chuaychoo et al. 2004). Stimulation by capsaicin causes defensive airway reflexes including cough and increased bronchoconstriction as well as bradycardia and hypotension (Coleridge and Coleridge 1984). Experimentally, C fiber function is eliminated using capsaicin desensitization through chronic pre-treatment (Jancso, Kiraly et al. 1985; Kuo and Lai 2008) or perineural treatment of the vagus nerve (Zhang, Lin et al. 2008) although the selectivity of capsaicin pre-treament for eliminating C fibers is controversial as discussed below. C fibers respond to additional stimuli including serotonin, hot and cold temperature, smoke, sulfur dioxide, acid, adenosine, bradykinin, and

prostaglandins (Lee, Shuei Lin et al. 2003; Undem, Chuaychoo et al. 2004; Canning and Chou 2009; Kollarik, Ru et al. 2010). To sense exogenous and endogenous stimuli, these nerves express a host of receptors such as TrpA1, TrpV1, adenosine receptors, and purinergic receptors detailed below. These receptors are activated by specific substances associated with asthma which aggravate cough and reflex bronchoconstriction. For example, TrpA1 receptors are activated by unsaturated aldehydes released during inflammation, 5HT receptors are activated by elevated serotonin in asthma, TrpV1 is activated by increased temperatures and acid, and adenosine triphosphate (ATP) stimulates adenosine receptors.

A fibers

A fibers are larger, faster conducting neurons (. In DRGs, their cell body sizes range from C fiber sizes to above 35 microns in diameter (Harper and Lawson 1985; Price 1985). A conduction velocity greater than 2m/s defines an A fiber, and it is further identified as Aα, Aβ, or Aδ if its speed exceeds 30m/s, falls within 14-30m/s, or falls within 2.2-8m/s respectively (Harper and Lawson 1985; Scott 1992). A fibers achieve greater conduction velocity through myelination, and the thickness of myelination corresponds to conduction velocity (Cragg and Thomas 1961). A fiber conduction is more sensitive to temperature than C fibers and so previous studies have experimentally inhibited A fibers by cooling the vagus nerve (Pisarri, Yu et al. 1986). A fibers have unique cytoskeletal requirements for myelinated transduction and thus are enriched for large (200kDa, 160kDa) neurofilament isoforms which are useful for identifying A versus C fibers (Ricco, Kummer et al. 1996; Ruscheweyh, Forsthuber et al. 2007; Zhang, Lin et al. 2008). The 160kDa neurofilament isoform is used in the current dissertation as an A fiber phenotype marker. The limitations of using 160kDa marker (NF160) for A fibers are that previous papers have compared NF160 to substance P which only labels a subpopulation of C

fibers. Thus these studies do not exclude that some C fibers particularly in the jugular ganglion could also could express NF160 (Ricco, Kummer et al. 1996).

A fibers in the airway are divided functionally into slowly-adapting receptors (SARs), rapidly adapting receptors (RARs), and cough receptors (Canning, Mori et al. 2006). SAR and RAR were the first A fibers identified based on their sensitivity to mechanical stretch caused by inflation and deflation of the lungs (Taylor-Clark and Undem 2006). Stretch-responsive nerves (i.e., non-C fibers) were recorded before and during sustained lung inflation and SARs defined as having slower decreases in firing than RARs (Lee, Shuei Lin et al. 2003). Follow-up experiments showed activation of SARs inhibits inspiration and relaxes airway smooth muscle whereas activation of RARs increased inspiratory effort, contracts airway smooth muscle, and causes mucus secretion (Carr and Undem 2001). Thus as you breathe in and out RARs are active whereas SARs are active during inspiration that peaks before start of expiration (Mazzone 2005). The third class of A fibers, cough receptors, are situated in the trachea/bronchi and have slower (Aδ range) conduction velocities of ~5m/s (Canning 2009). They terminate in the airway between the epithelium and smooth muscle with extensive branching. Recent studies suggest that Na^+-K^+-ATPase, $Na^+K^+2Cl^-$, tetrodotoxin-resistant Na^+ channels, Cl^+ channels, and voltage-sensitive K^+ channels on these nerves regulate cough responses (Canning 2009).

Neurotransmitters, Growth Receptors, Tissue Location

A and C fibers also contain unique tissue locations, neurotransmitter content, and growth receptor signaling. The airway epithelium is a tissue compartment uniquely enriched for sensory afferents and more specifically for C fibers. A subpopulation of lung C fibers are also distinguishable from A fibers as containing the inflammatory neuropeptides, substance P,

calcitonin gene-related peptide, and neurokinin A (Widdicombe 2003). Capsaicin-sensitive C fibers release substance P when exposed to capsaicin (Marvizon, Wang et al. 2003). The excitability of airway nociceptors, or pain-sensing neurons, are also increased by reduced extracellular calcium concentration, whereas this treatment had no affect on the exctitability of mechanosensitive (most A fibers) nerves (Undem, Oh et al. 2003). Only 4% of A fibers in the vagal ganglia have been shown to express substance P(Chuaychoo, Hunter et al. 2005). The expression of receptors for neurotrophins also loosely separates C and A fiber populations. A fibers express the TrkC receptor unlike C fibers (Chen, Zhou et al. 1996; Lieu, Kollarik et al. 2011). Also, some C fibers express the receptor for nerve growth factor, TrkA, which A fibers do not appear to express although A fibers were only studied in the nodose ganglian in this study and not in the jugular ganglion (Lieu, Kollarik et al. 2011). A minority of C fibers in the airway do not respond to capsaicin and studies in DRGs suggest they do not contain neuropeptides SP and CGRP but stain positively for the isolectin B4 (IB4) (Kwong, Kollarik et al. 2008). Humans and mice (current dissertation) contain sparser (~1-15%) substance P innervation than rats and guinea pigs (~60%) (Baluk, Nadel et al. 1992; Howarth, Springall et al. 1995; Lilly, Bai et al. 1995). Thus quantifying non-substance P nerves such as IB4-positive C fibers will be important in studies of asthma neuroplasticity. IB4 does not have functional significance other than that it is a legume lectin that binds alpha-D-galactosyl residues on polysacchardies or glycoproteins enriched in some DRGs (Fang, Djouhri et al. 2006). The IB4 C fiber subpopulation also contains unique growth requirements and signaling properties (Stucky and Lewin 1999). IB4+ C fibers are not responsive to NGF but rather to glial-derived neurotrophic factor (GDNF). Whole cell and current clamp experiments on DRGs showed IB4+ nerves contain distinct sodium channels and produce longer action potentials (Stucky and Lewin 1999). Similar to other criteria, however, it is important to note that IB4+ nerves have overlapping distributions with both capsaicin-

insensitive and capsaicin-responsive C fibers. There are intriguing calcium imaging data showing that IB4+ capsaicin-responsive nerves are a population preferentially sensitized by inflammation (Lu and Gold 2008).

Blurring A and C Fiber Characteristics

The properties of airway sensory neurons do not completely segregate using A and C fiber criteria. For example, another population of Aδ fibers derived from the jugular ganglion represent a minority subpopulation of nociceptors which are otherwise usually C fibers. Unlike nodose-derived Aδ fibers (read below), nociceptive jugular-derived Aδ fibers have high thresholds to mechanical stimulation but respond to capsaicin, bradykinin, and hypertonic saline (Undem, Oh et al. 2003). To further complicate categorization, some C fibers are insensitive to capsaicin and more sensitive to A-fiber like mechanical stimuli. These nerves also tend to conduct in the higher C fiber velocity range (0.7 to 1.5m/s) and did not respond to bradykinin, a common C fiber sensory stimulant. It is also important to note that in some studies outside the airways, nerve cooling was imperfect at inhibiting all A-fibers without additional partial suppression of C fibers (Zimmermann 1968). Similarly, there is an under-recognized neuropathic effect of capsaicin pre-treatment on A fibers at higher doses (Lawson and Harper 1984). Thus, using capsaicin pretreatment and nerve cooling to isolate C and A fibers respectively may over- or underestimate the contribution of a certain sensory population. Validation studies from DRG show additional criteria are needed to accurately identify nerve subpopulations since cell number and size counts are not consistent between labs (Tandrup 2004) and even two distinct populations are not always identified based on A/C criteria (Mille-Hamard, Bauchet et al. 1999). More recently, embryologic origin and nerve terminal location have proven useful for improving the categorization of airway sensory nerves.

Embryologic Origin

Studies mostly in guinea pigs have identified unique subpopulations of airway sensory nerves based on their embryologic origin. The airway is innervated by nerves from two different embryologic sources, the epibranchial placode and neural crest cells of the postotic hindbrain (Kwong, Kollarik et al. 2008). The airway's placodal (nodose) and neural crest (jugular) ganglia are situated next to each other on the vagus nerve but they contain different tissue compartment innervation patterns and functional responsiveness (Carr and Undem 2001).

The nodose and not the jugular ganglion supplies faster conducting A fibers (RARs, SARs, neuroepithelial body nerves, and cough receptors) to the large airways (Undem, Carr et al. 2002; Taylor-Clark and Undem 2006) but the jugular ganglion supplies C fibers that innervate these same extrapulmonary (trachea, bronchi) airway locations. Overall the nodose and jugular ganglia each supply ~50% of airway C fibers of both intra- and extrapulmonary locations. Jugular C fibers in guinea pigs are more likely to express neuropeptides (eg. substance P) than nodose C fibers and so may be more involved in neurogenic inflammation (Hunter and Undem 1999). Functionally, nodose but not jugular C fibers are responsive to ATP, adenosine, P2X3, and certain 5HT agonists (Kwong, Kollarik et al. 2008) (95). In terms of purine responsiveness and receptor expression, nodose and jugular airway nerves are less similar to each other than they are to nerves of the same placodal and neural crest origin innervating other organs (Nassenstein, Taylor-Clark et al. 2010). Only nodose and not neural crest nerves in both the airway and esophagus responded to α,β-methylene ATP and expressed P2X3/P2X3 purinergic receptors (Kwong, Kollarik et al. 2008). Esophageal and airway nodose-derived nerves were shown to share serotonin responsiveness (Chuaychoo, Lee et al. 2005; Yu, Ru et al. 2008). For studies of neuroplasticity, embryologic origin is also important for predicting responsiveness to neurotrophin signaling. Using retrograde tracing and single-neuron real-time PCR, Lieu et al.

showed jugular ganglion-derived TrpV1+ C fibers preferentially express TrkA, the receptor for NGF, whereas nodose TrpV1+ C fibers express TrkB, the receptor for BDNF (Lieu, Kollarik et al. 2011). In contrast, all neurons innervating the airway expressed receptors for the GDNF family ligands but there was preferential expression of GFRα3 in jugular neurons (Lieu, Kollarik et al. 2011). This information will be useful for predicting what nerve populations will be affected by neurotrophin signaling.

Nerve Terminal Location

The terminal location of a nerve also helps distinguish sensory subpopulations. Over 90% of sensory nerves in the epithelium are chemo- and temperature sensitive C fibers lacking myelin. Furthermore, epithelial nerves in the upper airways (trachea, primary bronchi) originate from cell bodies in the jugular (neural crest) ganglion and not the nodose (placodal) ganglion (Undem, Chuaychoo et al. 2004). The extracellular matrix between epithelial and smooth muscle compartments is where slow conducting A-fiber cough receptors are located. These nerves are not in the epithelium since stripping the epithelium nor contracting smooth muscle inhibits cough induced by mechanical stimulation or citric acid (Canning 2006). Location is less useful in smooth muscle, mucosal glands, and pulmonary vasculature which are also supplied by efferent autonomic nerves (parasympathetic and sympathetic). The submucosa (including smooth muscle) is where fast conducting stretch receptors, sensory nerves regulating mucus secretion, and pulmonary nerves regulating blood flow are located (Barnes 2001; Widdicombe 2003).

Differences Between Species

Previous studies comparing the sensory innervation of mice versus guinea pigs and humans have found anatomic and functional differences but little is known about their importance or causal mechanism. Most notably, the nodose and jugular ganglia in a mouse are not physically separated from one another unlike in guinea pigs and humans where the jugular ganglion is a distinct swelling caudal from the nodose ganglion (Nassenstein, Taylor-Clark et al. 2010) (Figure 2, Figure 42). A recent study using transgenic mice where neural crest derived neurons (eg. jugular ganglion and not nodose ganglion) were selectively labeled showed that both ganglia exist but are fused in mice (Nassenstein, Taylor-Clark et al. 2010). This study also used retrograde tracing and found that mice contained less jugular-derived C fibers than in guinea pigs. Since jugular C fibers innervate the epithelium of the large airway, this could explain why another study found rat trachea contained fewer cough receptors and the current dissertation found mouse contained fewer epithelial nerves than other species (Mazzone, Reynolds et al. 2009). Since jugular C fibers are involved in cough this may explain why few labs have reported eliciting cough from mice and rats (Canning and Chou 2009). Aside from these macroscopic differences, mouse sensory nerves function similarly to other species and jugular and nodose-derived neurons segregate with the same criteria. For example, in both mice and guinea pigs sensory neuron responsiveness to adenosine tri-phosphate (ATP) and expression of neuropeptides (eg. substance P) (discussed below) is different in jugular versus nodose-derived nerves (Nassenstein, Taylor-Clark et al. 2010).

1.8 Sensory Neuroplasticity in Asthma and Related Diseases

1.8.1 Functional Changes to Sensory Nerves

Asthmatics exhibit hypersensitivity to a wide range of sensory stimulants and individual sensory nerves demonstrate increased firing to various stimuli (Snashall and Baldwin 1982; Ostro, Lipsett et al. 1991; Doherty, Mister et al. 2000). In addition to mechanical stimulation, temperature, and the nine chemical stimuli (capsaicin, serotonin, acid, ATP, nicotine, bradykinin, adenosine, distilled water, hypertonic saline) known to directly cause action potential discharge from airway sensory nerves there are many additional mediators (e.g., histamine, prostaglandins) associated with sensory nerve activation (Taylor-Clark and Undem 2006).

Physiologic Changes

Airway sensory nerves are generally more responsive to stimulants in humans with asthma and in animal models of asthma. For example, stimulation with sulfur dioxide or capsaicin caused more airway narrowing and cough in asthmatic patients compared to healthy control subjects (Snashall and Baldwin 1982; Doherty, Mister et al. 2000). This phenomenon is also called airway hyperresponsiveness due to sensory nerve hypersensitivity. In another meta-analysis, asthmatics self-reported hyperresponsive, and exposure history to acid, particulate sulfate, and particulates smaller than 2.5 microns in diameter was correlated with severity of asthma sensory symptoms (cough, shortness of breath) (Ostro, Lipsett et al. 1991). In models of asthma where animals were sensitized to allergen and given aerosol doses of allergen, sensory nerves were also hyperresponsive. The original study in rabbits showed that allergen sensitization and challenge caused decreased lung conductance which was reduced by vagal cooling and abolished by vagotomy (Karczewski and Widdicombe 1969). More recently, two labs simultaneously reported that sensitized rats exhibited increased physiologic responses to intravenous capsaicin (Kuo and Lai 2008; Zhang, Lin et al. 2008). In terms of A fibers, which are typically capsaicin-insensitive, RARs in allergen sensitized with and without challenge (but not untreated rats), were sensitive to capsaicin and caused enhanced breathing responses (Zhang,

Lin et al. 2008). Lieu et al. showed that A fibers which are normally capsaicin-insensitive exhibit calcium responses to capsaicin after allergen exposure (Lieu, Myers et al. 2012).

Increased Nerve Excitability/Sensitivity

At a cellular scale, asthma and other models of tissue inflammation are associated with increased sensitivity/excitability and greater ion flux. After aerosol allergen, C fibers in sensitized rats exhibited increased action potentials per second (Kuo and Lai 2008) and C fiber baseline activity was greater in sensitized animals even before allergen challenge (Zhang, Lin et al. 2008). Zhang et al. also used single unit electrophysiology to show that A fibers responded to capsaicin only in allergen sensitized animals (Zhang, Lin et al. 2008). When these same two studies measured C fiber mechanical sensitivity to lung inflation, one found it increased after allergen sensitization and challenge (Zhang, Lin et al. 2008) while the other found no change (Kuo and Lai 2008). These different results were not discussed by the authors but may result from different technical experience with the protocol given that both studies used the same experimental setup and analysis but obtained 10-fold differences in control values. Increased mechanical sensitivity and A fiber hyperexcitability was shown by a study using an ex vivo preparation of the lung and vagus. Vagal nerves from allergen sensitized guinea pigs showed increased mechanical sensitivity 10 minutes after exposure to antigen (Riccio, Myers et al. 1996). Sensory nerves from non-sensitized guinea pigs did not show increased mechanical sensitivity indicating that the inflammatory process of asthma can also acutely enhance excitability of A fibers.

Previous studies also suggest increased calcium signaling is part of inflammation-induced nerve hyperexcitability. In the lower limbs, injection of Freund's adjuvant is known to cause inflammation resulting in increased sensory nerve excitability and increased neurotransmitter release. In a follow-up study, Freund's adjuvant was injected into the hindpaw

and DRG sensory nerve calcium flux was measured using fluorescence-based microscopy (Lu and Gold 2008). Inflammation was associated with increased resting intracellular calcium, and increased magnitude of evoked calcium flux. Additional testing using retrograde tracing and immunohistochemistry showed that the sensory nerves most affected by inflammation caused by adjuvant were capsaicin-insensitive IB4+ C fibers (Lu and Gold 2008). IB4 is a marker that roughly selects for C fibers insensitive to capsaicin that also tend not to synthesize neuropeptides (eg. substance P). These changes in sensory excitability persisted over at least 3 days following inflammation. Conversely, high intracellular calcium in airway nerves inhibits nerve activity but this has not been studied in models of asthma (Undem, Oh et al. 2003).

1.8.2 Structural Changes to Sensory Nerves

The growth and retraction of sensory nerves have been studied in asthma only at a larger scale with measures of nerve population density. At a cellular scale, neuroplastic changes have been studied in other inflammatory diseases, infectious diseases, and nerve damage models. The data are mixed with studies finding neuronal outgrowth, neuronal retraction, or no structural change. Similarly, studies conflict and show both increased and decreased neurotransmitter and receptor content. In general, the degree of insult or inflammation may play a role in determining which structural changes the resident peripheral nerves exhibit. The variable results reported for nerve structural changes may also be a consequence of undersampling individual nerve structure and undersampling organ-wide innervation heterogeneity. This is addressed in Chapter 3. In addition, variable changes to nerves may occur in different subtypes of each inflammatory disease that contain unique cellular infiltrates. For example, eosinophils (discussed below) are one of the most common inflammatory cells seen in asthma but still only account for roughly 50% of overall disease. If eosinophils cause

structural changes to nerves but other common inflammatory cells do not, then nerve structural changes would be variable in studies that did not adequately control for asthma subtypes.

Changes in Nerve Density

There is little agreement on whether nerve density changes in airway disease for both human and animal models. The current dissertation uses a new method and shows regional heterogeneity throughout the lung which may explain disparate results from previous studies using conventional methods that undersample nerve structure and airway-wide nerve distribution (see below). The earliest study to show increased nerves was performed in 1992 on sectioned bronchial autopsy tissue of severe asthmatics and non-asthmatics. Ollerenshaw and Woolcock reported an increase in substance P-positive nerves in the lamina propria and smooth muscle of asthmatic tissue and concluded that either substance P production increased or nerves were growing (Ollerenshaw and Woolcock 1992). In patients with persistent cough there was also a significant increase in epithelial CGRP but not the pan-neuronal marker, PGP 9.5, or SP indicating that increased CGRP probably resulted from CGRP synthesis rather than nerve outgrowth (O'Connell, Springall et al. 1995). PGP 9.5 is a pan-neuronal marker for airway nerves discussed in more detail below. In another study of humans with chronic bronchitis, sensory nerves expressing VIP and located next to mucosal glands were shown to increase (O'Connell, Springall et al. 1995). In infant rhesus monkeys chronically exposed to ozone and allergen, there was an increased density of epithelial nerves 6 months after treatment (Kajekar, Pieczarka et al. 2007). Similarly, in infant rhesus monkeys chronically exposed to cigarette smoke the density of substance P-expressing nerves increased in the epithelium (Yu, Zheng et al. 2008).

However, other human studies using forceps biopsies of airway tissue from severe asthmatics did not find any change in the quantity of substance P, CGRP, VIP, or the pan-neuronal marker, PGP 9.5 (Howarth, Springall et al. 1995; Lilly, Bai et al. 1995; Chanez, Springall

et al. 1998). In patients with chronic bronchitis caused by cigarettes or chronic cough, there was also no change in the density of PGP 9.5, substance P, or CGRP-expressing nerves (Lucchini, Facchini et al. 1997; Groneberg, Niimi et al. 2004). In contrast, Goldie et al. reported a non-significant decrease in overall PGP 9.5 nerve density in biopsies from mild asthmatics (Goldie, Fernandes et al. 1998). Two human studies also report decreased VIP (Ollerenshaw, Jarvis et al. 1989) and NPY nerves (Chanez, Springall et al. 1998) in biopsies from asthmatics but both results were not replicated by other labs (Howarth, Springall et al. 1995; Chanez, Springall et al. 1998; Groneberg, Folkerts et al. 2004) and animal studies report similar across-the-board variability for these two nerve markers (Dinh, Groneberg et al. 2004; Wu, Benders et al. 2012). CGRP and SP density have also been shown to decrease in a guinea pig asthma model (Mapp, Lucchini et al. 1998).

The conventional methods used by previous studies undersample individual nerves and organ-wide heterogeneity which may explain the wide range of baseline nerve densities and variable results in airway disease. To begin with, each study typically uses autopsy or biopsy material from one or two airway locations. The airway is known to have heterogeneous innervation (Widdicombe 1995), an observation I have corroborated, and biopsies are unable to capture large-scale regional changes in nerve structure or density (Howarth, Springall et al. 1995). Perhaps more importantly, each study uses tissue sectioning which samples a cross-section (usually 5-15 microns) worth of morphologic information about nerves that are long three-dimensional branching cells (Larson, Schelegle et al. 2003). Low sampling with tissue sectioning in a few cases led to studies missing entire nerve subpopulations known to exist such as epithelial substance P positive nerves (Howarth, Springall et al. 1995), which I easily identified using my imaging method in humans and for the first time in mice. Importantly, after reporting a lack of substance P nerves with repeated biopsies of multiple subjects, Howarth et al.

discovered one instance of epithelial innervation in post-mortem derived sources of tissue (Howarth, Springall et al. 1995). Estimates of nerve density marked with antibodies against neurotransmitters such as substance P, CGRP, VIP are also prone to disease-related changes in neurotransmitter expression. Typically this is addressed with a more stable unreleased neuronal marker, PGP 9.5. PGP 9.5 is a brain-enriched ctyoplasmic protein discovered in 1981 by 2D-PAGE (Jackson and Thompson 1981), and has since become a pan-neuronal marker used in many studies of the peripheral nervous system (Day and Thompson 2010). PGP 9.5 is a ubiquitin hydrolase and although levels of PGP 9.5 change with nerve development or injury it remains highly enriched in neurons and neuroendocrine cells relative to other sources (Wilkinson, Lee et al. 1989; Schofield, Day et al. 1995; Olerud, Chiu et al. 1998; Day and Thompson 2010). It is unknown if any nerves in the airway do not express PGP 9.5 So far alternative transgenic approaches to label airway nerves can only label parasympathetic nerves efficiently (Tallini, Shui et al. 2006) and a new adeno-associated virus transfection approach remains unavailable to the broader community (Kollarik, Carr et al. 2010).

Neurotransmitter and Receptor Plasticity

In addition to branched outgrowth, hypersensitivity has been linked to changes in neurotransmitter and sensory receptor content (Carr and Undem 2001). In addition to immunohistochemistry, transcript and protein levels of signaling molecules were measured in airway vagal ganglia following retrograde tracing from the lungs and total content was measured in tissue and airway compartments. Ex vivo preparations of sensory nerves allow one to examine specific pathways using chemical, electrical, and mechanical stimuli with pharmacologic manipulation. Overall these studies have found that in asthma sensory nerves increase synthesis of signaling molecules linked to airway narrowing, cough, and inflammation. New signaling machinery decreases activation thresholds and causes phenotypic changes that

also lead to sensory hypersensitivity and new stimuli generating action potentials. Molecules implicated in nerve growth, such as neurotrophins, not only cause branched outgrowth but are associated with changes in sensory neurotransmitter and receptor content. It is important to note that most of these molecules are enriched in sensory neurons but are also made by non-neuronal cells (Sternini, Su et al. 1995; Fernandes, Fernandes et al. 2012). Many studies did not or could not distinguish neuronal from non-neuronal sources.

Serotonin Receptors

Serotonin (5-HT) is a biogenic amine with seven receptors (all GPCRs except 5-HT_3 which is ionotropic) and numerous effects on the airway (Hoyer, Hannon et al. 2002). Serotonin directly stimulates airway sensory neurons, contracts airway smooth muscle, potentiates parasympathetic cholinergic firing, and causes epithelial release of acetylcholine (Karczewski and Widdicombe 1969; Dupont, Pype et al. 1999; Cazzola and Matera 2000; Moffatt, Cocks et al. 2004; Chuaychoo, Lee et al. 2005). In terms of sensory nerves, serotonin activates nodose-derived intrapulmonary C fibers through the ionotropic 5-HT_3 receptor (Chuaychoo, Lee et al. 2005). In some but not all studies, serotonin was also shown to activate A fibers (Karczewski and Widdicombe 1969; Dixon, Jackson et al. 1979; Fox, Barnes et al. 1993). Recent data from ex vivo electrophysiology of the trachea suggested serotonin failed to activate Aδ fibers (Fox, Barnes et al. 1993) but earlier studies of dogs showed RAR (A-fibers) produced airway narrowing and vigorous vagal action potential discharge in response to serotonin (Dixon, Jackson et al. 1979). In rabbits, serotonin caused reflex bronchoconstriction that was also linked to increased RAR firing since serotonin-induced airway narrowing decreased with vagal cooling and was abolished by vagotomy (Karczewski and Widdicombe 1969). C fibers may play a role in serotonin reflex bronchoconstriction since vagal cooling may inhibit C fiber firing (mentioned above).

Serotonin and its receptors have been shown to play an important role in causing asthma symptoms. Specific to sensory nerves serotonin inhibits cough and causes reflex bronchoconstriction. Serotonin levels in the plasma are elevated with asthma and associated with clinical severity (Lechin, van der Dijs et al. 2002). Treatment of asthmatics with tianeptine, a serotonin uptake enhancing drug, rapidly improved asthma symptoms whereas buspirone treatment increased plasma serotonin and worsened asthma symptoms (Lechin, van der Dijs et al. 2002). Tianeptine has also shown promise in the treatment of asthma in larger blinded, placebo controlled studies involving 25,000 patients (Lechin, van der Dijs et al. 2004). In terms of sensory nerves, serotonin given intravenously suppresses cough in cats and humans (Kamei, Hosokawa et al. 1986; Stone, Worsdell et al. 1993), and a serotonin antagonist given to cats enhanced cough responses (Kamei, Hosokawa et al. 1986). Unlike cough, however, serotonin signaling causes increased airway narrowing in animal models of asthma. In an early study on allergic rats, increased airway resistance to inhaled allergen was blocked by methysergide, a non-specific serotonin antagonist (Nagase, Dallaire et al. 1996). In humans, the effect of inhaled serotonin in asthmatics is controversial with some studies reporting responsiveness (Hajos 1962) and others not (Cushley, Wee et al. 1986). However, this and numerous human studies blocking serotonin signaling do not isolate neuronal from non-neuronal signaling. A more recent study in mice implicated vagal signaling caused by serotonin signaling on neuronal 5-HT_{2a} receptors (Cyphert, Kovarova et al. 2009). In this study, intravenous serotonin caused greater airway resistance in allergic mice, than in non-sensitized mice. Administration of 4-chloro-DL-phenylalanine, an inhibitor of serotonin synthesis, or vagotomy prevented allergen-induced increases in serotonin airway narrowing. Similarly, the nonspecific serotonin receptor antagonist, methiothepin, and the 5-HT_{2a} antagonist, ketanserin, prevented increased serotonin airway responses but the 5-HT_{3a} antagonist, ondansetron, had no effect. The authors also

showed that capsaicin pre-treatment (which inhibits capsaicin-sensitive nerves) did not prevent this affect, but they could not inhibit capsaicin-insensitive nerves lacking TrpV1 which in mice make up ~60% of airway C fiber. (Kollarik, Dinh et al. 2003). A study of ferret tracheal nerves using immunohistochemistry also showed capsaicin treatment doesn't completely eliminate airway sensory nerves (Dey, Satterfield et al. 1999).

Tachykinins

Tachykinins are a group of neurotransmitters that are synthesized by sensory neurons and stored throughout nerve processes (Lembeck 1953; Joos 2001; Chuaychoo, Hunter et al. 2005). There are numerous tachykinins but the two most commonly implicated in asthma are substance P (SP) and neurokinin A (NKA) which act on their receptors NK1 and NK2 (DeVane 2001). Substance P and NKA induces airway bronchoconstriction, plasma excudation, mucus secretion, eosinophil degranulation, and increased acetylcholine release, and increased inflammation (Evans, Belmonte et al. 2000; Barnes 2001; O'Connor, O'Connell et al. 2004). In a recent meta-analysis of human trials using tachykinin NK1 and/or NK2 antagonists, these blockers significantly decreased airway hyperresponsiveness in asthmatics (Ramalho, Soares et al. 2011).

In terms of airway nerves, substance P and NKA unlike another tachykinin, neurokinin B, are localized to a subpopulation of unmyelinated sensory C fibers (Uddman, Hakanson et al. 1997). It is important to note that humans and mice (current dissertation) contain sparser (~1-15%) substance P innervation than rats and guinea pigs (~60%) (Baluk, Nadel et al. 1992; Howarth, Springall et al. 1995; Lilly, Bai et al. 1995). In asthmatics, substance P levels are increased in the lumen (sputum and bronchoalveolar lavage but decreased in the tracheal tissue (Joos, Germonpre et al. 2000). Decreased tissue substance P and increased substance P in the lumen may suggest that substance P is released from neurons or denuded tissue into the airway

lumen. Epithelial denudation can also indirectly increase substance P/NKA levels because it synthesizes a potent degrading enzyme of tachykinins called neutral endopeptidase (NEP) (Dusser, Jacoby et al. 1989; Frossard, Rhoden et al. 1989). There are also controversial results (mentioned above) showing increased substance P nerves in human asthma and animal models (Ollerenshaw, Jarvis et al. 1991).

Airway sensory nerves release substance P in response to numerous asthma stimulants including cigarette smoke, capsaicin, histamine, bradykinin, and mechanical perturbation (Lundberg and Saria 1983; Andre, Campi et al. 2008). Sensory nerves also contain neurokinin receptors and potentially respond to substance P via local reflexes in asthma (Verleden 1996). This local reflex is also called an axon reflex, and is defined as neuronal signaling in peripheral tissues that does not involve the cell body or synapses. An electrophysiology study looked at nodose-derived nerves from guinea pigs sensitized to ovalbumin (allergy model) (Weinreich, Moore et al. 1997). They showed nerves from non-sensitized guinea pigs did not respond to substance P but nearly all nerves from allergen sensitized guinea pigs responded electrically and with calcium influx to substance P. They hypothesized based on pharmacologic testing that vagal afferent nerves contained NK-2 receptors that were not functional until after allergen sensitization although the mechanism is unknown.

Substance P is also linked to a broader phenomenon of A fiber phenotypic transitioning in models of asthma where A fibers begin expressing C fiber-specific markers and responding to C fiber stimulants. In guinea pigs sensitized and challenged with ovalbumin, A fiber mechanical sensitivity was shown to increase approximately 4-fold and at the same time there was an increase in substance P and NKA activity in the lungs (Fischer, McGregor et al. 1996; Riccio, Myers et al. 1996). Whereas in untreated guinea pigs, A fibers projecting to the large airways do not express substance P (Riccio, Myers et al. 1996), after allergen challenge greater than 10% of

these nerves began expressing substance P (Fischer, McGregor et al. 1996). In a follow-up study, substance P synthesis in A fibers caused by allergen was prevented by vagotomy (Chuaychoo, Hunter et al. 2005). Inflammation of the hindpaw caused *de novo* expression of the tachykinin gene, preprotachykinin, and substance P production in large-diameter low mechanical threshold A fibers (Neumann, Doubell et al. 1996). The authors went on to speculate that allodynia, a disease where light touch is perceived as pain, can result from inflammation causing mechanosensitive A fibers to synthesize and release C fiber nociceptive neuropeptides like substance P. The same phenomenon in asthma research has been coined allodyspnea or allotussive responses, to surmise why asthmatics experience severe shortness of breath or urge to cough where there is only mild compromise of lung function or little mechanical stimulation(Undem and Carr 2002).

TrpV1 and TrpA1 Receptors

The transient receptor potential (TRP) family consists of 28 cation channels grouped in mammals into six superfamilies: TrpC, TrpV, TrpM, TrpA, TrpML, TrpP. All channels are Ca^{2+} permeable and some (such as TrpA1) are equally permeable for monovalent cations. Two channels, TrpV1 and TrpA1, are implicated in asthma primarily through their roles as sensory neuron receptors(Colsoul, Nilius et al. 2009). Both TrpV1 and TrpA1 cause acute affects of asthma such as cough as well as aggravate long-term inflammation possibly through neurogenic tachykinin release.

TrpV1

TrpV1 is a non-selective cation channel expressed primarily but not exclusively on nociceptive sensory neurons that can be activated by numerous aggravants for asthmatics including capsaicin, heat, ethanol, citric acid, anandamide (a neuronal lipid mediator), and others (Jia, McLeod et al. 2002; Gatti, Andre et al. 2006; Cantero-Recasens, Gonzalez et al.

2010). In humans there is a genetic and expression-level association of TrpV1 with asthma and cough respectively. In children with asthma, a single-nucleotide polymorphism in TrpV1 function is associated with decreased wheezing and cough in childhood asthma (Cantero-Recasens, Gonzalez et al. 2010). In a biopsy study of patients with chronic cough, the number of TrpV1+ nerves in the epithelium increased and was correlated with cough (Groneberg, Niimi et al. 2004).

Studies of animal models show a role for TrpV1 in different aspects of airway disease through increased expression, sensitization by inflammatory mediators, and A fiber phenotypic switching. TrpV1 activation has been linked to increased airway narrowing (Lin, Hayes et al. 2009; Delescluse, Mace et al. 2012), cough (Gatti, Andre et al. 2006; McLeod, Jia et al. 2007), potentiation of cholinergic signaling (Stretton, Belvisi et al. 1992), and longer term airway neurogenic inflammation (Trevisani, Gazzieri et al. 2004). TrpV1 is also sensitized by inflammatory mediators such as prostaglandins (Moriyama, Higashi et al. 2005) and bradykinin (Premkumar and Ahern 2000). In allergic guinea pigs, two different TrpV1 antagonists also prevented airway hyperreactivity to histamine (Delescluse, Mace et al. 2012). Similar to phenotypic switching of A fibers to synthesize substance P, nodose-derived A fibers (neurofilament 160/200 positive) also increased synthesis of TrpV1 (normally enriched in C fibers) after chronic airway inflammation (Zhang, Lin et al. 2008). Newer data show phenotypic switching of A fibers to a C fiber phenotype is also apparent at TrpV1's transcriptional and functional levels. In allergen-sensitized guinea pigs, TrpV1 mRNA increased in Aδ nodose-derived cough receptors in the trachea and exhibited *de novo* responsiveness to capsaicin with ovalbumin challenge or exogenous neurotrophin administration (Lieu, Myers et al. 2012).

TrpA1

TrpA1 is another member of the Trp receptor family that was recently implicated in asthma. TrpA1 is expressed on airway C fibers and responds to numerous sensory and inflammatory stimulants including oxidants (Bessac, Sivula et al. 2008), noxious cold (Colsoul, Nilius et al. 2009), ozone in air pollution (Taylor-Clark and Undem 2010), isothiocyanates in mustard oil (Jordt, Bautista et al. 2004), and unsaturated aldehydes from cigarette smoke (Andre, Campi et al. 2008). Surprisingly, pungent general anesthetics (isoflurane, halothane) were also recently shown to cause bronchoconstriction through activation of TrpA1 in guinea pigs (Eilers, Cattaruzza et al. 2010). In mouse vagal ganglia, TrpA1 was expressed on TrpV1-expressing sensory neurons sensitive to capsaicin (Nassenstein, Kwong et al. 2008).

In a mouse model of asthma, TrpA1 knockout and pharmacologic blockade prevented airway hyperreactivity (Caceres, Brackmann et al. 2009). In guinea pigs and mice, sensory activation caused by ozone was also prevented by genetic and pharmacologic blockade (Taylor-Clark and Undem 2010). TrpA1 receptors are also strongly linked to cough in pharmacologic studies of guinea pigs and humans (Birrell, Belvisi et al. 2009; Taylor-Clark, Nassenstein et al. 2009).

TrpA1 is also helps establish airway inflammation. In guinea pigs and mice cigarette smoke-induced inflammation was shown to be prevented blocking TrpA1 or genetic ablation (Andre, Campi et al. 2008). Similarly in a mouse asthma study, TrpA1 knockout or antagonism prevented increased cytokine expression and eosinophilic inflammation (Caceres, Brackmann et al. 2009). This may in part result from TrpA1 indirectly causing neurogenic inflammation. TrpA1 deficiency through knockout or pharmacologic antagonism prevented release of tachykinins (presumably from neurons) in to the airway lumen (Caceres, Brackmann et al. 2009).

Purinergic Receptors

Purinergic receptors are a group of receptors that respond to extracellular purines and pyrimidines such as adenosine or adenosine-5-triphosphate (ATP). There are two main families of purinergic receptors, P1 receptors respond to adenosine and adenosine 5 monophosphate (AMP) and P2 receptors respond to ATP, UTP and derivatives (Ralevic and Burnstock 1998). Airway sensory nerves contain both P1 and P2 purinergic receptors and asthmatics exhibit sensory hyperresponsiveness to purinergic agonists. The mechanism behind asthmatic hypersensitivity to purinergic stimuli is unknown but may involve changes to purinergic receptor expression and interaction with tachykinin signaling (eg. substance P, neurokinin A). In addition, P1 versus P2 receptors may be acting on different capsaicin-sensitive and capsaicin-insensitive C fiber populations in the airway (Vaughan, Szewczyk et al. 2006).

P1 Purinergic Receptors (Adenosine Receptors)

The A1 and A2A subtypes of P1 receptors appear to be important mediators of C fiber activity in the large airways. In an ex vivo lung preparation, adenosine-induced depolarization of nodose C fibers was mimicked by A1 and A2A agonists and blocked by A1 and A2A antagonists (Chuaychoo, Lee et al. 2006). In humans, adenosine or AMP causes airway contraction (Cushley, Tattersfield et al. 1983), increased respiration (Watt and Routledge 1985), dyspnea (Burki, Alam et al. 2006), and cough (Basoglu, Pelleg et al. 2005).

In studies of asthma, elevated levels of adenosine monophosphate (AMP), the ligand for P1 receptors, have been reported in the airways of asthmatics (Driver, Kukoly et al. 1993). Inhalation of AMP causes bronchoconstriction in atopic asthmatics but not in non-atopic normal subjects (Cushley, Tattersfield et al. 1983). Activation of P1 purinergic receptors on sensory nerves may not only directly cause bronchoconstriction but contribute to inflammation by causing increased release of neuropeptides. A2 activation in anesthetized guinea pigs was also

shown to mediate airway contraction that was dependent on serotonin signaling and was inhibited by capsaicin nerve depletion (Manzini and Ballati 1990). In twenty asthmatics, inhaled AMP caused cough and significantly increased NKA and substance P release into the airways (Crummy, Livingston et al. 2005). In animal models of asthma, the A1 subtype of P1 receptors was shown to be mediate adenosine activation of sensory nerves leading to increased airway resistance. A1 genetic knockdown, pharmacologic antagonism, or vagotomy in ventilated mice all prevented increased airway resistance caused by adenosine (Hua, Erikson et al. 2007). None of these affects was observed with genetic knockout of A2A, A2B, or A3 receptors. In another study, the bronchoconstriction effect of adenosine was not inhibited by capsaicin-sensitive nerve depletion suggesting the relevant nerves are capsaicin insensitive C fibers (Vaughan, Szewczyk et al. 2006).

P2 Purinergic Receptors (ATP Receptors)

ATP can stimulate airway sensory nerves through two subtypes of P2 receptors, P2X and P2Y (Vaughan, Szewczyk et al. 2006). Electrophysiologic data demonstrated that ATP stimulates all C fibers regardless of subtype (Kollarik, Dinh et al. 2003) but it appears to induce bronchoconstriction and cough through capsaicin-sensitive and capsaicin-insensitive nerves respectively. ATP potentiated cough potentially through P2X4 activation of capsaicin-insensitive neurons in guinea pigs (Kamei, Takahashi et al. 2005). ATP increased critic acid-induced cough but not capsaicin-induced cough and it was blocked by an antagonist of P2X1-4 and not by an antagonist of P2X1,2,3,5,7. However, ATP-induced bronchoconstriction in mice was inhibited by capsaicin depletion indicating the P2X4 receptors are likely on capsaicin-sensitive C fibers (Vaughan, Szewczyk et al. 2006).

1.9 Mechanisms of Neuroplasticity in the Lungs and in Other Organs

Studies of neuroplasticity in asthma are limited to two groups of signaling molecules, neurotrophins and GDNF family ligands. The extensive data available from other research fields outside the lungs in development, nerve injury, and disease provide useful additional information about these mechanisms.

1.9.1 Airway Mechanisms of Neuroplasticity: Neurotrophins and GDNF Family Ligands

Studies of the mechanism of neuroplasticity in asthma have predominantly focused on neurotrophins, a class of secreted signaling proteins with well-described roles in growth, survival, and differentiation. Newer research is also implicating a different family of secreted signaling proteins called glial-derived neurotrophic factor family ligands (GFLs).

Neurotrophins

Neurotrophins are a family of signaling molecules involved in many forms of neuroplasticity including neuron survival, neurite outgrowth, myelination, and differentiation (Sofroniew, Howe et al. 2001; Lu, Pang et al. 2005). The four known mammalian neurotrophins are: nerve growth factor (NGF), brain-derived neurotrophic factor (BDNF), neurotrophin 3 (NT-3), and neurotrophin 4 (NT-4). Each neurotrophin binds preferentially to one of three tyrosine kinase receptors (TrkA, TrkB, TrkC) with NGF binding TrkA, BDNF and NT-4 binding TrkB, and NT-3 binding TrkC (Lindsay 1996). Each neurotrophin also binds non-selectively to the $p75^{NTR}$ transmembrane glycoprotein receptor (Sofroniew, Howe et al. 2001; Lu, Pang et al. 2005). In asthma, eosinophils, the hallmark inflammatory cell of asthma, may be a significant source of

neurotrophin production. Cultured eosinophils have been shown to make more NGF (127 pg/10^6 cells) and NT-3 (112 pg/10^6 cells) than peripheral blood mononuclear cells and neutrophils (Kobayashi, Gleich et al. 2002). Other common sources of neurotrophins include schwann cells, fibroblasts, or neurons themselves.

In airway sensory ganglia, expression of neurotrophin receptors depends on nerve phenotype. TrpV1+ C fibers were shown by single cell PCR to express TrkA and TrkB depending on localization to the jugular or nodose ganglion respectively (Lieu, Kollarik et al. 2011). In the same study, A fibers from the nodose ganglion were shown to express TrkB and TrkC (Lieu, Kollarik et al. 2011). Using immunolabeling, nerves in the lung have been shown to stain positively for TrkA, B, C, and $p75^{NTR}$ although further phenotyping was not performed (Nassenstein, Dawbarn et al. 2006; Nassenstein, Kammertoens et al. 2007).

Neurotrophin levels are elevated in the lungs of asthmatics, released upon allergen challenge, and levels appear to depend on allergy and eosinophilia. In an early study, patients with severe allergic asthma had elevated NGF levels in their serum (Bonini, Lambiase et al. 1996). However, only allergic and not non-allergic asthma patients had elevated NGF (132 pg/ml vs. 4.9 pg/ml) and NGF correlated with two markers of the allergic asthma subtype (serum IgE and eosinophil cationic protein). In two follow-up studies, NGF and BDNF, were also elevated in the BAL of allergic asthmatics (Virchow, Julius et al. 1998; Braun, Lommatzsch et al. 1999). In one study, patients underwent repeated BAL sampling after allergen challenge and there was an increase in BDNF and NGF 18 hours but not 20 minutes after challenge, suggesting neurotrophins are involved in non-acute asthmatic responses. In a sputum screen of 242 patients with asthma, BDNF levels were significantly increased in patients with severe asthma (Hastie, Moore et al. 2010). In animal models of asthma or antigen exposure, NGF and BDNF are also elevated and exogenous administration or genetic overexpression of neurotrophins causes

airway hyperreactivity (Braun, Lommatzsch et al. 1999; Braun, Quarcoo et al. 2001; de Vries, van Rijnsoever et al. 2001; Yu, Zheng et al. 2008). Moreover, pharmacologic or genetic inhibition of BDNF, NGF, or TrkA/B/p75 prevents airway hyperreactivity and in some studies prevented airway inflammation (Tokuoka, Takahashi et al. 2001; Braun, Lommatzsch et al. 2004; Nassenstein, Dawbarn et al. 2006; Nassenstein, Kammertoens et al. 2007).

A few studies have directly addressed the role of neurotrophin signaling on airway neuroplasticity. Data from three separate labs suggest that inappropriate sensory responses in asthma are caused by NGF- or BDNF-induced A fiber phenotype changes to a C-fiber like phenotype. In two studies, the authors injected NGF into the airways and showed it caused de novo expression of a nociceptive C fiber-specific neuropeptide, substance P, in otherwise mechanically sensitive A fibers (Hunter, Myers et al. 2000; Dinh, Groneberg et al. 2004). A fiber production of substance P was also increased in a guinea pig asthma model, and both substance P production and airway hyperreactivity were blocked by tyrosine kinase inhibitors, which interfere with trk signaling (de Vries, Engels et al. 2006). A fibers may also become more sensitive to additional NGF exposure since expression of trkA, typically a C fiber neurotrophin receptor, also increased (Dinh, Groneberg et al. 2004). Recently, another study showed Aδ mechanosensors responsible for cough began synthesizing TrpV1 after allergen challenge or exogenous BDNF treatment (Lieu, Myers et al. 2012). Lieu et al. showed allergen exposure or BDNF treatment also caused capsaicin-induced calcium responses in Aδ fibers isolated from the nodose nerves that were unresponsive to capsaicin without treatment.

A different lab studying asthma in mice suggested $p75^{NTR}$ signaling is important for sensory hyperreactivity. The authors used bone marrow transplants between wildtype and $p75^{NTR}$ knockouts and found airway hyperreactivity was eliminated in mice lacking non-hematopoietic $p75^{NTR}$. Furthermore, the authors suggest sensory nerves are the important non-

hematopoietic $p75^{NTR}$-containing cells because they alone stained for $p75^{NTR}$ (Nassenstein, Kammertoens et al. 2007). However, the authors base this on immunolabeling without demonstrating controls and do not address other studies studies showing $p75^{NTR}$ mRNA and protein on other non-hematopoietic lung cells such as smooth muscle (Freund-Michel and Frossard 2008), schwann cells (Chen, Zeng et al. 2009), and epithelium (Othumpangat, Gibson et al. 2009). Thus it is unclear in which non-hematopoietic cell(s)' $p75^{NTR}$ signaling is responsible for airway hyperreactivity

Neurotrophin cleavage by extracellular proteases is a potentially important regulatory mechanism that has not been explored in asthma. Neurotrophins are secreted outside the cell in a precursor form and enzymatically cleaved by the serine protease, plasmin, or matrix metalloproteinases (Airaksinen and Saarma 2002). Regulation of this step may be critical to their effects since pro-neurotrophins bind p75 with equal or higher affinity than neurotrophins and potentially cause opposing effects. Both proBDNF and proNGF binding to $p75^{NTR}$ causes apoptosis unlike the pro-survival and trophic effects of Trk receptor binding by mature neurotrophins (Lu, Pang et al. 2005).

GDNF Family Ligands

Glial-derived neurotrophic factor (GDNF) family ligand (GFLs), similar to neurotrophins, are secreted proteins made by numerous cells that influence cell differentiation, and survival. Members of this group include GDNF, neurturin, artemin, and persephin. Also similar to neurotrophins, GFLs are secreted as precursors and enzymatically cleaved outside the cell. All GFLs signal through RET, a receptor tyrosine kinase, but each binds uniquely to one of four GDNF-family receptor-α (GFRα) receptors.

Despite being a new field in asthma neuroplasticity research, GDNF and neurturin have been implicated in exacerbating and mitigating asthma respectively. GDNF levels in sputum are

elevated in patients with severe eosinophilic and neutrophilic asthma (Hastie, Moore et al. 2010). By single-cell PCR and retrogradely labeling, airway neurons were shown to express GFRα1, GFRα2, GFRα3, and RET. Unlike neurotrophin receptors, GDNF family receptors were not preferentially expressed by either airway A or C fibers, but are equally expressed in all populations (Lieu, Kollarik et al. 2011). In the airway of allergen sensitized and challenged guinea pigs, epithelial cells were shown by immunofluorescence to produce GDNF (Lieu, Myers et al. 2012). Topical application of GDNF also caused a C-fiber phenotypic switch in nodose Aδ fibers as measured by increased TrpV1 transcript.

One study has implicated neuturin as a protective GFL using knockout mice and exogenous treatment (Michel, Theresine et al. 2011). Neurturin knockout mice after allergen sensitization and challenged showed increased allergen-specific IgE, increased IL-5, increased eosinophils (lung and BAL), and augmented airway hyperreactivity. Intranasal pre-treatment with neurturin decreased the same cytokines and inflammation in both allergic wildtype and neurturin knockout mice. However airway hyperreactivity was not measured after neurturin treatment.

1.9.2 Neurotrophin and GDNF Family Ligand Neuroplasticity Outside the Lung

Branched outgrowth.

Research outside the lung has linked inflammation and neuropathy to nerve outgrowth and neurotrophins. In bowel inflammation, NGF and TrkA were shown to increase and appendicitis was associated with increased nerves (di Mola, Friess et al. 2000; Nemeth, Rolle et al. 2003). In a heart inflammation model, neurotrophin content increases along with sympathetic nerve hyperinnervation (Hasan, Jama et al. 2006; Xin, Pan et al. 2010). In the skin,

neurotrophin levels increase with pain and itch and are associated with increased epidermal nerve density (Stucky, Koltzenburg et al. 1999; Hefti, Rosenthal et al. 2006; Ikoma, Steinhoff et al. 2006; Paterson, Schmelz et al. 2009; Peleshok and Ribeiro-da-Silva 2012). In these disease models, indirectly reducing neurotrophins or administering blocking antibodies of NGF or BDNF prevented inflammation, arrhythmia, hyperalgesia and allodynia (Hasan, Jama et al. 2006; Hefti, Rosenthal et al. 2006; Li, Xu et al. 2008; Xin, Pan et al. 2010).

More in-depth studies show neurotrophin signaling promotes specific nerve populations outgrowth and axonal and dendritic branching. NGF was initially described by Hamburger and Levi-Montalcini as essential for nociceptive sensory and sympathetic nerve survival (Levi-Montalcini 1987). This involved retrograde transport of survival signals from nerve endings to the cell bodies. Since then exogenous neurotrophin administration and genetic knockdown of neurotrophins and Trk receptors have mapped how different nerve populations' survival depends on each neurotrophin signaling pathway (Huang and Reichardt 2001). Neurotrophin signaling also produces or maintains outgrowth in adult nerves similar to disease models mentioned above. This was originally shown in vitro by Campenot who demonstrated local NGF promoted advance of sympathetic nerves (Campenot 1977). Subsequently NGF, BDNF, and NT-3 acting through TrkA, TrkB, and TrkC were shown to promote axon growth while gradients of neurotrophins steered directionality (Huang and Reichardt 2001). More recently, skin overexpression of NGF, BDNF, NT-3, and NT-4 increased nerve densities of specific populations, neuropeptide-containing C fibers and sympathetic nerves, myelinated sympathetic nerves around the hair follicle, touch mechanosensors, and myelinated hair follicle nerves, respectively (Albers, Wright et al. 1994; Albers, Perrone et al. 1996; Botchkarev, Botchkareva et al. 1998; Tolwani, Cosgaya et al. 2004; Krimm, Davis et al. 2006). Some overexpression studies also suggest neurotrophins cross-talk or compete with one another in different tissue

compartments. In a large skin study involving knockouts of all four neurotrophins (NGF, BDNF, NT-3, NT-4) and receptors (p75, trkA-C) different neurotrophins and receptors were shown to cross-promote or inhibit survival of nerve subpopulations. TrkA-sensitive peptidergic C and Aδ nerves were promoted by NGF and NT-3 but suppressed by BDNF, NT-4, and p75. Peptidergic C fibers, however, were promoted by p75 as well as NGF and NT-3. (Rice, Albers et al. 1998).

Neurotrophins have a number of growth and branching-promoting pathways in a neuron. Signaling through Trk receptors is followed by phospholipase C (PLC, IP3, DAG), RAS-ERK (Ras, Raf, Mek, Erk), and PI-3 kinase (PI-3K, Akt) signaling pathways, which have been independently linked to neuronal growth (Huang and Reichardt 2001). Downstream pro-survival and pro-proliferation signaling involves activation of protein kinase C, activation of CREB, and inhibition of apoptosis. In addition, neurotrophins cause cytoskeletal rearrangements in part through acting on Rho family G proteins (Rac, Rho, CDC42 etc) that regulate F-actin polymerization and turnover (Tada and Sheng 2006).

Exogenous NT-3 and BDNF have also been shown to cause dendritic outgrowth in cortical and sympathetic neurons (Jan and Jan 2010). BDNF activates the PI3K-mTOR and MAPK pathways to control cell size and promote dendrite growth (Dijkhuizen and Ghosh 2005) and NGF causes dendritic arborization in tandem with bone morphogenic proteins (Lein, Johnson et al. 1995; McAllister, Lo et al. 1995).

Neurotrophins also cause branching of axons. In the elegant retinal patterning system of *Xenopus laevis,* BDNF plays a critical role by non-specifically promoting axonal branching which is selectively suppressed by ephrin/Eph signals (Marler, Becker-Barroso et al. 2008). This was confirmed by BDNF microinjection studies into *Xenopus laevis* (Marshak, Nikolakopoulou et al. 2007) . The way position-dependent axonal branching is achieved is by patterned positioning of Ephrin/Eph and suppression of BDNF-induced branching. To add complexity, trkB was shown

to directly cooperate with EphA to promote branching via PI3K/Akt signaling. Loss of p75 receptor causes disorganization of the same retinotectal system but the downstream mechanism is unknown (Lim, McLaughlin et al. 2008). In a live cell imaging study this process of retinal branching was observed in vivo using fluorescence microscopy and manipulated by exogenous BDNF administration (Alsina, Vu et al. 2001). A second mechanism involving NT-3 is partially understood. Arborization of sensory nerves onto motorneurons may act through Wnt and NT-3 since trkC and NT-3 are required for terminal arborization (Rice, Albers et al. 1998) and motorneurons selectively make Wnt (Krylova, Herreros et al. 2002). Wnt is a family of secreted proteins that act on cell surface receptors and are involved in numerous development and homeostasis pathways (Logan and Nusse 2004).

A smaller amount of evidence links GDNF family ligands (GFLs) to branching and growth of peripheral nerves. GDNF, artemesin, and neurturin (but not persephin) cause increased survival of peripheral nerves in culture (Baloh, Tansey et al. 1998; Mikaels, Livet et al. 2000), but they are not required for sensory neuron survival during development (Baudet, Mikaels et al. 2000). There were also no deficits in C fiber innervation in knockouts of GFRα1, GFRα2, or GFRα3 suggesting they do not require GFLs during development. Rather, GFLs appear to be required for postnatal survival and growth of specific subpopulations of DRG sensory nerves. Approximately half of DRG neurons expressed RET or one or more of the GFRα receptors. Overall there are three distinct subgroups of RET-containing DRG neurons, two of which are identified based on labeling with isolectin B4 (IB4); small TrkA+ and IB4+ neurons, small IB4+ TrkA-, and myelinated medium and large neurons. In sensory neurons from adult mice, each GFL promoted survival, GDNF and neurturin combined increased survival, but artermin combined with other GFLs did not. This matches GFR receptor expression data where GFRα3 was expressed on most GFL-containing neurons and GFRα1 and GFRα2 were present in distinct

nerve populations. GDNF may also be required for postnatal targeting of peripheral innervation to respective tissue compartments since GDNF heterozygous knockouts exhibited reduced A fiber mechanoreceptors in the skin (Airaksinen and Saarma 2002). The data on GFL-promotion of branching are unclear and do not focus on adult sensory neurons. In embryonic dopaminergic neurons, neurturin, artemesin, and persephin (10-fold lower potency) promoted branching morphogenesis (Zihlmann, Ducray et al. 2005) but GDNF did not in two other studies (Schafer and Mestres 1999). In another study of dopaminergic neurons, GFL-mediated branching and GFL-mediated elongation were consistently mutually exclusive growth events (Costantini and Isacson 2000) but this has not been tested in peripheral nerves. In transected motor neurons, GDNF promoted arborizing and sustained regrowth of motorneurons (Boyd and Gordon 2003)

Phenotypic Switching

Additional studies of neurotrophin signaling and phenotypic switching come from hypersensitivity and allodynia research in the somatosensory system. After inflammation peripheral nerves not only become more sensitive (e.g., hyperalgesic) but they also respond to new stimuli and produce new sensations. Originally, this was thought to result from C fiber hypersensitivity in the skin, but some data also implicate A fiber transitioning to a more nociceptive C fiber phenotype. For example, mechanosensitive A fibers in health do not transmit pain but after injury/inflammation they begin expressing C fiber signaling proteins (eg. substance P, TrpV1) and facilitate nociception (Neumann, Doubell et al. 1996). This is thought to result in allodynia, where light touch is perceived as painful.

Pharmacologic and genetic studies have implicated NGF and BDNF in causing hypersensitivity. Local or systemic NGF causes thermal and mechanical hyperalgesia, and inflammation-induced hyperalgesia can be blocked by NGF antagonism (Lewin, Ritter et al.

1993; Ma and Woolf 1997). In another study where rats were given adjuvant to cause plantar inflammation and hypersensitvity, intrathecal administration of a TrkB-Fc fusion protein that sequesters BDNF/NT-4 prevented light touch hypersensitivity (Mannion, Costigan et al. 1999).

Manipulating neutrophins also produces phenotypic switching in sensory ganglia. Intraplantar injection of NGF causes hyperalgesia and increases C fiber-enriched pre-protrachykinin A (gene precursor for tachykinins) and CGRP mRNA both of which are reversed by anti-NGF treatment (Woolf 1996). In another study, NGF caused Aβ fiber hypersensitivity which was reversed by an antagonist of the substance P receptor, NK1 (Thompson, Dray et al. 1995). BDNF signaling was shown recently to mediate inflammatory bladder hypersensitivity through augmented TrpV1 expression on BDNF-sensitive nerves (presumably A fibers). When the colon is inflamed (by tri-nitrobenzene sulfonic acid) it causes hyperreactivity in the non-inflamed bladder and serves as a model of central inflammatory neuroplasticity. Inflammation caused increased peripheral nerve expression of TrpV1 and coincided with increased BDNF in the corresponding lumbar DRG (Xia, Gulick et al. 2012). Moreover, treatment with a neurotoxin or intrathecal BDNF neutralizing antibody prevented hyperreactivity. Furthermore, multiple studies suggest central sources of BDNF may be important for developing hyperalgesia. After nerve injury, BDNF expression increased in DRG and more specifically in larger diameter neurons (Zhou, Chie et al. 1999; Li, Xian et al. 2006).

GFLs have also been linked to sensory phenotypic switch after nerve injury or inflammation. Overall the data support a critical role for GFLs but the data are mixed as to what sensory subpopulation is the principle target for GDNF, artemesin, and neurturin. After chronic nerve compression, GDNF expression levels changed in tandem with markers of A fiber phenotypic transitioning to a C fiber phenotype (loss of neurofilament, increased CGRP and IB4) (Chao, Pham et al. 2008). However, a different study also using chronic nerve compression did

not replicate the change in CGRP expression (Keast, Forrest et al. 2010). After sciatic nerve transection in this study followed by lentiviral overexpression of GDNF, DRG cell size increased and expressed greater CGRP and IB4 (Tannemaat, Eggers et al. 2008). In DRGs, GDNF, artemin, and neurturin also increased TrpV1 calcium signaling and created capsaicin sensitivity in otherwise insensitive neurons (Malin, Molliver et al. 2006). The functional TrpV1 phenotypic transitioning was replicated in vivo where artemin, neurturin, or GDNF injection caused thermal hyperalgesia. Two notable findings were that inflammation only increased GFRα3 in DRGs and every GFL was more potent than NGF at causing phenotypic transitioning. As noted below, transgenic overexpression of GDNF did not replicate the finding that GDNF causes thermal hyperalgesia (Albers, Woodbury et al. 2006). In another study, overexpression of artemin in the skin also led to increased TrpV1 in DRG and heat hyperalgesia as well as increased TrkA, TrpA1, and cold hypersensitivity (Elitt, McIlwrath et al. 2006). In this study it was difficult to separate trophic effects from phenotypic transitioning since artemin overexpression increased the number of DRG neurons overall. Overexpression of GDNF caused mechanical hypersensitivity rather than heat hyperalgesia caused by artemin, and appeared to act by increasing IB4-positive conduction velocity and expression of TrpA1 and acid-sensitive channels (Albers, Woodbury et al. 2006). However, in a different study, the same GDNF-overexpressing mice did not exhibit increased TrpV1 or thermal hyperalgesia suggesting further studies are needed to confirm how GDNF overexpression changes phenotypic transitioning (Molliver, Lindsay et al. 2005).

It is important to note that the role of neurotrophin and GFL signaling in phenotypic transitioning is still controversial. For example, a recent study does not support the role of substance P in hyperalgesia or the role of neurotrophins in phenotypic transitioning (Malcangio, Ramer et al. 2000). The authors injected intrathecal NGF and found that it causes hyperalgesia but not increased A-fiber SP release. In addition, NT-3 injection increased SP expression but did

not cause thermal hyperalgesia. Similarly, GFLs do not always produce phenotypic transitioning and in some cases are linked to preventing hyperalgesia. Furthermore this may depend on whether GFLs are signaling centrally or peripherally. In one study of nerve injury-induced hyperalgesia, intrathecal but not peripheral administration of GDNF prevented both mechanical and thermal hypersensitivity (Boucher, Okuse et al. 2000).

1.9.3 Time-dependence of neuroplasticity

Some studies show a time-course of neuroplasticity or a critical period during development when an insult causes neuroplasticity. The critical period has been suggested for the skin, colon, and airway in terms of establishing neuroplasticity. Colonic inflammation of postnatal rats only caused persistent sensory hyperresponsiveness if inflammation occurred earlier in life (8-21 days) and not in older rats (>21 days) (Al-Chaer, Kawasaki et al. 2000). In some (but not all) skin studies, hyperinnervation and hyperalgesia only occurs after inflammation if it is performed in infants (Torsney and Fitzgerald 2003).

Previous data have also described the time course of changes to a nerve's structure or phenotype in response to inflammation. In one study, after inflammation lumbar DRGs transiently increased expression of TrpA1 and TrpV1 peaking at 1 and 7 days respectively (Malin, Molliver et al. 2011).

1.10 Eosinophils in Asthma and Neuroplasticity

Eosinophils are inflammatory cells commonly seen in asthma. My understanding of the role of these cells has expanded from solely a defense against infection to include activators of neuroplasticity, agents of tissue remodeling, and immunoregulatory cells. In terms of neuroplasticity, eosinophils are capable of causing trophic changes, phenotypic transitioning, and pathologic changes to nerves.

1.10.1 Introduction

Eosinophils are a subpopulation (~2-4%) of white blood cells originally identified by Paul Ehrlich by their characteristic acidophilic cytoplasmic granules (Ehrlich and Lazarus 1900; Young, Lowe et al. 2006). They are typically between 10-14 microns in diameter and often contain a bi-lobed nucleus. Eosinophil cytoplasmic granules are made of four basic protein components, major basic protein (MBP), eosinophil peroxidase (EPO), eosinophil-derived neurotoxin (EDN), and eosinophil cationic protein (ECP) (Hamann, Barker et al. 1991). These granule proteins were initially thought of as cytotoxic molecules that defended the host against parasitic infection (Meeusen and Balic 2000). More recently they have also been shown to act in non-cytotoxic ways including: antagonizing muscarinic receptors on parasympathetic nerves (Jacoby, Costello et al. 2001), suppressing T cell proliferation (Throsby, Herbelin et al. 2000), and stimulating mucus secretion (Lundgren, Davey et al. 1991). Eosinophils are also present in healthy tissues and appear to be involved in tissue remodeling (Blanchard and Rothenberg 2009). Eosinophils in these contexts appear to contribute to uterus maturation during estrus, mammary gland development, involution of the thymus, antigen presentation, and negative selection of CD8 T cells (Rothenberg and Hogan 2006).

Development and Trafficking

Eosinophils are produced in the bone marrow from hematopoietic stem cells through tightly regulated differentiation, expansion, and survival. In vitro and genetic ablation studies identified transcription factors (GATA-1, PU.1, and C/EBP) and cytokines (IL-5, IL-3, and GM-CSF) as necessary for eosinophil differentiation followed by egress from bone marrow (Rothenberg and Hogan 2006). The Th2 cytokine, IL-5, is uniquely critical for further expansion and recruitment of eosinophils.

IL-5

IL-5 is a cytokine synthesized predominantly by Th2 lymphocytes that acts on the IL-5 receptor (IL-5R) which is expressed mostly but not exclusively on eosinophils. IL-5R is a heterodimeric receptor made of an alpha and beta subunit (Rosenberg, Phipps et al. 2007). The alpha subunit is unique to IL-5R and the beta subunit is common to the receptors for IL-5, IL-3, and GM-CSF. IL-5R downstream signaling involves the Janus kinase/signal transducer and activator of transcription (JAK/STAT) pathway and PI3-kinase.

IL-5's role in eosinophil trafficking has been demonstrated in vivo by multiple studies. When IL-5 or IL-5R is pharmacologically or genetically inhibited in models of asthma there is a profound decrease in eosinophilia (Corry, Folkesson et al. 1996; Pauwels, Brusselle et al. 1997; Lach-Trifilieff, McKay et al. 2001). Conversely, exogenous IL-5 administration or genetic overexpression of IL-5 causes eosinophil influx targeted to the source of IL-5 production (Lagente, Pruniaux et al. 1995; Lee, McGarry et al. 1997; Ochkur, Jacobsen et al. 2007). IL-5 does not appear to be necessary for eosinophil survival since genetic knockout of IL-5 did not eliminate the presence of eosinophils in blood or bone marrow. Rather these mice showed loss of eosinophil expansion and recruitment to tissue infected with a parasite (Kopf, Brombacher et al. 1996).

Eotaxin

Eotaxin is another potent eosinophil chemoattractant shown to recruit and activate eosinophils and in some studies to act synergistically with IL-5. Eotaxin is a member of the C-C subfamily, a large family of chemokines (chemoattractant cytokines) that contain two adjacent cysteines near their N-terminus. Unlike other C-C chemokines, eotaxin binds only to one receptor, CCR-3, although CCR-3 can bind other chemokines, RANTES and MCP-3 (Daugherty, Siciliano et al. 1996; Gerber, Zanni et al. 1997). Eotaxin can independently attract and activate

eosinophils, polymerizing their intracellular actin, producing reactive oxygen species, and promoting degranulation (Griffiths-Johnson, Collins et al. 1993; Elsner, Hochstetter et al. 1996; Ochkur, Jacobsen et al. 2007). The potentiating effects of eotaxin and IL-5 have also been shown in vivo for asthma studies. In one study, IL-5 and eotaxin overexpression in a double transgenic mouse model caused eosinophil activation and degranulation as well as profound airway remodeling and airway hyperreactivity (Ochkur, Jacobsen et al. 2007). This mouse model is used in the current dissertation. Another study showed antigen in combination with IL-5 and eotaxin (overexpresed by vaccinia virus gene transfer) was required to cause airway hyperreactivity. Eotaxin-induced recruitment of eosinophils into the airways (measured in BAL) was potentiated 4-fold by the presence of IL-5 (Mould, Ramsay et al. 2000).

1.10.2 Importance in asthma

Eosinophilic inflammation is one of the few useful non-clinical markers for asthma, a heterogeneous group of diseases. Eosinophilic asthma is the most common asthma phenotype (> 50%) and encompasses a disproportionate amount of allergic- (high IgE) and corticosteroid-resistant asthma (Wenzel, Schwartz et al. 1999; Wenzel 2006). Eosinophils are associated with resistance to treatment and clinical approaches that target eosinophils outperform standard guidelines. In one study of children, the presence of eosinophilic inflammation predicted the child's ability to reduce corticosteroid doses (Zacharasiewicz, Wilson et al. 2005).

In animal models of asthma, pharmacologic or genetic ablation of eosinophils reduces lung pathology and airway hyperreactivity whereas increasing eosinophils alone can reproduce these symptoms (Lee, McGarry et al. 1997; Lee, Dimina et al. 2004; Fulkerson, Fischetti et al. 2006). This has been shown in mice lacking airway eosinophilia through genetic strategies including eosinophil-selective cytotoxicity (PHIL mice used in the current dissertation), halting

development, or knocking out eosinophil trophic and chemoatractant molecules, IL-5 and eotaxin. Although the link between eosinophils and airway remodeling is well established there is some controversy as to whether eosinophils directly cause airway hyperreactivity. Another mouse model (Δdbl GATA) where eosinophils were ablated through mutation of a high affininty site on GATA-1, a myeloid differentiation transcription factor, did not show any decrease in airway hyperreactivity (Humbles, Lloyd et al. 2004). It is still unclear why PHIL and Δdbl GATA approaches to eliminate eosinophils resulted in such different effects on airway hyperreactivity but one possible explanation is the use of different mouse strains (Balb/C versus C57/B6). Different mouse strains are known to be more or less susceptible to airway hyperreactivity (Reinhard, Eder et al. 2002) and produce opposite responses to asthma-related cytokines (Foster, Hogan et al. 1996; Hogan, Matthaei et al. 1998).

Selective recruitment of eosinophils has been achieved by injection or genetic overexpression of IL-5 and eoxtaxin (Mould, Ramsay et al. 2000). The current dissertation uses a mouse model with lung-specific overexpression of IL-5 under an airway epithelial cell promoter, CC10, which results in chronic eosinophilia and hallmarks of asthma (Lee, McGarry et al. 1997).

In humans, eosinophils have been shown to be a useful clinical biomarker and treatment target. In two human studies, treatment targeting to lower sputum eosinophilia below 3% or 2% significantly reduced the number of severe exacerbations compared to standard treatment guidelines (Green, Brightling et al. 2002; Jayaram, Pizzichini et al. 2006). Recently, two small (20 and 61 patients) human trials tested an anti-IL-5 monoclonal antibody (Mepolizumab) in patients with corticosteroid-resistant eosinophilic asthma. Anti-IL5 treatment in both studies led to drops in blood (300 to 40, 664 to 64 per mm^3) and sputum (8 to 1%, 16.6 to 1.3%) eosinophils. The decrease in eosinophils in this subtype of asthma was associated with reduced number of exacerbations and less need for steroid treatment. These human studies in select

asthma subpopulations and the strain-specific effects in animal asthma models suggest treating asthma in the future will depend on identifying the subtype of asthma.

1.10.3 Eosinophils and Neuroplasticity in Asthma and Other Diseases

Eosinophils have been shown to cause a wide range of trophic and pathologic affects on nerves. There is emerging evidence in different diseases that eosinophils can preferentially localize next to nerves. Remarkably, the manifestations of some diseases can be prevented not only by ablating eosinophils or their recruitment, but also by separating eosinophils from nerves.

Eosinophil Recruitment to Nerves

Studies that showed eosinophils migrating to neurons were performed in nerve injury and inflammatory disease models. In an early study, transecting the sciatic nerve caused an influx of eosinophils within the nerve itself (Beuche 1991). Three to ten days after transection, the sciatic nerves were removed and disaggregated and all cells counted. Eosinophils within the injured nerve comprised roughly half of the total inflammatory cells, far greater than the percentage of eosinophils in blood (< 8%). Eosinophils are also associated with the optic nerve in a mouse model of multiple sclerosis (Milici, Carroll et al. 1998). Similarly, in antigen challenged guinea pigs and in humans with fatal asthma, eosinophils are located inside the nerve bundles, around the parasympathetic ganglia, and along nerve fibers (Costello, Schofield et al. 1997). The density of eosinophils associated with nerves is greater than eosinophils associated with blood vessels or airway tissues. In the inflamed bowel or skin, eosinophils and their granules were also shown to preferentially localize next to nerves (Dvorak, Onderdonk et al. 1993; Hogan, Mishra et al. 2001; Foster, Simpson et al. 2011). These studies and others demonstrate that eosinophils can selectively migrate towards nerves.

Role of Neuropeptides

Neuropeptides include the tachykinins, substance P and neurokinin A, as well as calcitonin gene-related peptide (CGRP), vasoactive intestinal peptide (VIP), secretin, and secretoneurin. Neuropeptides are made by many cell types including neurons; predominantly, sensory neurons (Barnes 2001; Undem and Carr 2002; Veres, Rochlitzer et al. 2009). Neuropeptides regulate inflammatory responses and are associated with diseases involving eosinophil-nerve interactions such as asthma, rhinitis, inflammatory bowel disease, atopic dermatitis, conjunctivitis, and myelitis (Barnes 2001; Carr and Undem 2001; Heppt, Dinh et al. 2004; Fischer, Wussow et al. 2005). The role of neuropeptides in eosinophil recruitment has been demonstrated in vivo and in vitro. In vitro studies have shown that isolated human eosinophils move up substance P, CGRP, secretoneurin, VIP, and secretin concentration gradients with EC50s in the picomolar range (Dunzendorfer, Meierhofer et al. 1998). In vivo, intradermal injections of substance P cause eosinophil recruitment to human skin (Smith, Barker et al. 1993). Lesional pruritis nodularis, a skin disease characterized by itchy bumps on the arms and legs, is associated with increased CGRP expression in neurons and with increased nerve-associated eosinophils (Liang, Jacobi et al. 2000). Substance P, neurokinin A, and CGRP also prime human eosinophils isolated from allergic patients to migrate toward other chemotactic factors, such as platelet activating factor (PAF) and leukotriene B4 (Numao and Agrawal 1992). Thus, neuropeptides can prime and directly recruit eosinophils to nerves.

Other diseases also suggest there may be a relationship between neuropeptides and eosinophil recruitment. For example, in ulcerative colitis, vernal keratoconjunctivitis, seasonal allergic conjunctivitis, and cervical ripening in preparation for labor there is an increase in neuronal substance P that coincides with increased eosinophils (Knudsen 1996; Collins, Usip et al. 2002; Jonsson, Norrgard et al. 2005; Mantelli, Micera et al. 2010). It is tempting to speculate

that increased eosinophil presence in these inflammatory states is mediated by neuropeptide signaling. It will be important for future studies in each disease, or biologic process, to confirm whether neurons or another cell type are the source of neuropeptides.

Role of Cytokines and Chemokines

Recruitment of eosinophils to nerves is an active process and requires chemotactic signals. These signaling proteins are cytokines capable of generating an immune response, and also are chemokines that cause leukocyte migration. In antigen challenged guinea pigs and in humans dying of fatal asthma, there are more eosinophils associated with airways nerves than anywhere else in the lungs (Costello, Schofield et al. 1997). Associated eosinophils are those within 8µm of a nerve, since 8µm is the diameter of an eosinophil. Blocking the pleiotropic cytokine, tumor necrosis factor (TNF), in antigen challenged guinea pigs prevents eosinophils localizing along airway parasympathetic nerves (Nie, Jacoby et al. 2009). The eotaxin family members are potent chemokines responsible for eosinophil recruitment from blood vessels and bone marrow. Blocking the receptor for eotaxin, CCR3, prevents eosinophil localization to airway nerves in vitro and in vivo (Fryer, Stein et al. 2006). CCR3 is a receptor for many cytokines in addition to eotaxin including RANTES (Regulated upon Activation, Normal T-cell Expressed, and Secreted) and MCP-3 (Monocyte-Specific Chemokine 3) (Erin, Williams et al. 2002). Thus, while eotaxin has been shown in nerves, other chemokines, although they have not yet been demonstrated in nerves, may also be important for eosinophil recruitment to nerves. This is important because it appears that the presence of eotaxin alone is not sufficient to recruit eosinophils to nerves. Although eotaxin is constitutively expressed in human and guinea pig airway parasympathetic nerves in vitro (Fryer, Stein et al. 2006) and eotaxin-3 is expressed in airway nerves of allergen sensitized rhesus monkeys, there is no association of eosinophils and nerves in the absence of antigen challenge (Chou, Daugherty et al. 2005).

Role of Acetylcholine, Substance P, Leukotriene B4, and Platelet Activating Factor

Nerves may also indirectly recruit eosinophils. The neurotransmitters, acetylcholine and substance P stimulate macrophages and epithelial cells in vitro to secrete chemotactic factors for eosinophils (Koyama, Sato et al. 1998; Sato, Koyama et al. 1998). In these studies, chromatography and antagonist experiments suggested that macrophage and epithelial cell – derived chemotactic factors were the lipid mediators leukotriene B4 and PAF (Koyama, Sato et al. 1998; Sato, Koyama et al. 1998). Another study demonstrated that neuropeptides substance P, neurokinin A, and CGRP directly prime eosinophils to migrate towards PAF and leukotriene B4 (Numao and Agrawal 1992). This priming effect was blocked by inhibiting substance P signaling or CGRP receptors. I can speculate that neurotransmitters acetylcholine and/or substance P induce resident macrophages or epithelial cells to secrete chemotactic factors for eosinophils. A role for acetylcholine mediated eosinophil recruitment is supported by the in vivo observation that, in a guinea pig model of allergic asthma, treating animals with tiotropium, an antagonist of acetylcholine M3 muscarinic receptors, prevented eosinophil influx into lungs (Bos, Gosens et al. 2007). Alternatively, like other inflammatory cells (neutrophils and macrophages) eosinophils express muscarinic receptors and it is possible that acetylcholine may directly recruit eosinophils to the nerves (Gosens, Zaagsma et al. 2006).

Role of Cell Adhesion Molecules (CAMs)

Following recruitment, eosinophils adhere to neurons using cell adhesion molecules (CAMs). Two cell adhesion molecule families participate in eosinophil-nerve binding, immunoglobulin superfamily CAMs (VCAM, ICAM, NCAM) and integrin CAMs (VLA-4, LFA-1). These two groups of adhesion molecules serve as ligands and counter-ligands for one another. In nerve cells, VCAM and ICAM expression augments leukocyte binding to nerves. Conversely, blockade of VCAM, ICAM, LFA-1, and/or VLA-4 inhibits leukocyte binding to nerves (Birdsall,

Lane et al. 1992; Sawatzky, Kingham et al. 2002) showing that all these CAM's are important in eosinophil adhesion to nerves.

CAM expression on nerves is both constitutive and inducible. Although VCAM is constitutively expressed on parasympathetic nerves, adhesion of eosinophils to nerves also requires ICAM expression (Sawatzky, Kingham et al. 2002). Tumor necrosis factor (TNF) up-regulates adhesion molecules, VCAM and ICAM, on neuroblastoma and cortical neurons and increases leukocyte adhesion to nerves (Birdsall, Lane et al. 1992). In parasympathetic nerves isolated from trachea and maintained in cell culture, ICAM can be induced by TNF-alpha and interferon gamma (IFNγ) in a dose-related manner (Sawatzky, Kingham et al. 2002). Dexamethasone, an anti-inflammatory corticosteroid, blocks tumor necrosis factor- and interferon gamma- induced ICAM expression in parasympathetic neurons from humans and guinea pigs resulting in decreased eosinophil adhesion to parasympathetic nerves (Nie, Nelson et al. 2007). Interferon gamma and tumor necrosis factor induced ICAM expression was also blocked by an inhibitor of NFκB, a pro-inflammatory transcription factor. Thus, not only interferon gamma and tumor necrosis factor but also NFκB can increase CAM expression in nerves that results in increased eosinophil adhesion to these nerves.

Chemokines and inflammatory cytokines increase eosinophil adhesion through CAMs and switch eosinophil CAM binding preference from VCAM to ICAM (Sawatzky, Kingham et al. 2002). Eotaxin, though considered primarily to be key to eosinophil migration also switches eosinophil dominant CAM binding from VCAM to ICAM (Schleimer, Sterbinsky et al. 1992). Conversely, blocking the CCR3 eotaxin receptor prevented increased eosinophil binding to primary parasympathetic nerves after treatment with pro-inflammatory cytokines that increased ICAM expression (Fryer, Stein et al. 2006). However, not all nerves respond to

inflammatory cytokines. For example, neuroblastoma cells do not recapitulate the dexamethasone-induced decrease in eosinophil adhesion seen in primary parasympathetic neurons (Nie, Nelson et al. 2007).

Eosinophils are also abundant in the gut and localize to enteric nerves during inflammation. The role of ICAM and VCAM in enteric nerves is not known, but expression of another cell adhesion molecule, NCAM, was increased in enteric nerves of rats infected by parasites (O'Brien, Fitzpatrick et al. 2008). Eosinophils were also increased along the nerves in these infected animals. Therefore, NCAM may also be important in eosinophil adhesion to nerves.

There is some evidence that, in vivo, adhesion of eosinophils to nerves is also mediated by inflammation and CAMs. Antigen challenge of an allergen-sensitized guinea pig increases tumor necrosis factor in the airways (Kelly, Denis et al. 1992) and increases ICAM and eotaxin expression by airway nerves (Nie, Nelson et al. 2007). Dexamethasone, Etanercept, or a CCR3 eotaxin receptor antagonist blocked eosinophil association with nerves (Fryer, Stein et al. 2006; Nie, Nelson et al. 2007; Nie, Jacoby et al. 2009) by inhibiting respectively, ICAM, TNF, or eotaxin receptors on airway nerves. These studies demonstrate eosinophil-nerve interactions are reversible at many different levels.

Neuroplasticity caused by eosinophils

Chronic inflammatory diseases with underlying eosinophil involvement are associated with symptoms such as excessive pain, cough, itch, enteric dysmotility, and bronchoconstriction all of which could be due to excessive neural activity (Carr and Undem 2001). Conversely, eosinophils are also associated with ataxia and neuropathies that are associated with loss of neural activity. The impact of eosinophils on nerves has been studied 1) by measuring

physiologic effects of eosinophil depletion or inhibition in vivo, 2) by injecting eosinophil products into neuronal tissue compartments in vivo, 3) by cataloging changes to nerves in eosinophilic diseases, and 4) by co-culturing eosinophil and nerves. The consequences of eosinophil-nerve interactions range from increased neuronal growth and increased activation to growth inhibition and nerve damage all of which lead to aberrant neurotransmission.

Eosinophils Increase Neuronal Growth

In some inflammatory diseases the presence of eosinophils is associated with excessive neuronal growth. Increased eosinophil association with nerves following enteric parasitic infection coincides with an increased density of nerves expressing the growth and plasticity marker, growth associated protein-43 (GAP-43) (O'Brien, Fitzpatrick et al. 2008). Lesional skin from humans with prurigo nodularis contains both increased numbers of eosinophils and increased nerves compared to normal skin in the same patients (Johansson, Liang et al. 2000). Histologic studies of human acute appendicitis biopsies also found increased eosinophils along with a doubling of nerves and a doubling of ganglion cells. In the appendicitis study, the increase in nerves was significant but may have been underestimated since nerve-specific immunolabeling was not performed and small unmyelinated and difficult-to-visualize fibers may have been missed (Singh, Malhotra et al. 2008). Sensory nerves in airway tissues from patients with asthma were reported to be longer than nerves from non-asthmatic patients. This study, though intriguing, may be limited by the dependence on two dimensional tissue sections to quantify the length of neurons that are complex three dimensional objects branching and undulating through tissue. The distribution of potential neuron lengths obtainable in one tissue section is dependent on the angle between the tissue section plane and the nerve as well as upon the degree of nerve straightness or uniform directionality/anisotropy (Ollerenshaw, Jarvis

et al. 1991). Despite these limitations this study suggests airway nerves grow excessively in asthma. Since asthma is associated with eosinophils, and in co-culture, eosinophils can cause excessive nerve growth (Kobayashi, Gleich et al. 2002), eosinophils may be a mechanism for increased nerve length. These three different diseases in three distinct organs: skin, gastrointestinal tract, and airway demonstrate there is an association between eosinophils and increased nerves that remains to be confirmed. Whether increased nerves are actually due to increased nerve cell numbers, branching, length, or undulation needs to be determined.

The physiologic consequences of increased nerves have been studied in neuropathic pain. Hyperinnervation of peripheral tissues by sensory neurons increases their receptive field size and increases the likelihood of multiple receptive fields (Sandkuhler 2009). These changes result in sensitivity to otherwise sub-threshold stimuli (Chu, Faltynek et al. 2004). Similar changes occur with eosinophil-related diseases. This may explain how patients with eosinophilic disorders are sensitive to sub-threshold mechanical and chemical stimuli that do not initiate a response in normal subjects. For example, patients with prurigo nodularis are hypersensitive to light touch (Johansson, Liang et al. 2000) and irritants that do not provoke an effect in normal lungs, cause bronchoconstriction and cough in patients with asthma (Carr and Undem 2001). Dexamethasone and steroids are used to treat all of these diseases. Although dexamethasone is an anti-inflammatory drug, it also decreases ICAM in nerves (Nie, Nelson et al. 2007) which would decrease eosinophils around nerves. Inhibition of eosinophil and nerve interactions may be an additional mechanism for dexamethasone and other steroids' effectiveness in vivo. However, steroids given after eosinophil influx might not be able to reverse pre-exisiting eosinophil-nerve association since airway eosinophilia predicts steroid resistance in patients with asthma (Wenzel, Schwartz et al. 1999; Wenzel 2006).

One mechanism by which eosinophils have been shown to increase nerve outgrowth is through release of neurotrophins. Eosinophils have been shown to synthesize and release NGF, BDNF, and NT-3 (Kobayashi, Gleich et al. 2002; Noga, Englmann et al. 2003). In co-culture, eosinophils prevent apoptosis of nerves cells and promote neurite outgrowth (Kobayashi, Gleich et al. 2002; Morgan, Kingham et al. 2004).

Eosinophils Regulate Neuropeptide Synthesis and Release

Neuropeptides regulate inflammatory responses and are associated with diseases involving eosinophil-nerve interactions (Liang, Jacobi et al. 2000; Barnes 2001; Carr and Undem 2001; Heppt, Dinh et al. 2004; Fischer, Wussow et al. 2005). As discussed above, increased neuropeptides is also linked to altered neuronal phenotype which may underlie the changed responses to stimuli that are characteristic of eosinophilic diseases, for example dermatitis-related itchiness in response to touch.

Eosinophils are associated with increased synthesis of neuropeptides in nerves. Nasal biopsies from patients with seasonal allergic rhinitis, perennial allergic rhinitis, and aspirin-sensitive rhinitis contain increased eosinophils and increased expression of VIP in mucosal nerves (Groneberg, Heppt et al. 2003; Heppt, Dinh et al. 2004; Fischer, Wussow et al. 2005). Nasal nerves from patients with seasonal allergic rhinitis also exhibited increased expression of substance P and NPY (Heppt, Dinh et al. 2004). Lesional pruritis nodularis, a skin disease characterized by itchy bumps on the arms and legs, is also associated with increased CGRP expression in neurons and with increased nerve-associated eosinophils (Liang, Jacobi et al. 2000). Similarly, airway neurons in sensitized guinea pigs synthesize substance P de novo following antigen challenge (with presumed eosinophil influx) (Carr and Undem 2001).

Other diseases also suggest there may be a relationship between eosinophils and neuropeptides synthesis. In ulcerative colitis increased substance P and increased eosinophils

are observed but have not been correlated (Jonsson, Norrgard et al. 2005). Increased tear and plasma substance P production in vernal keratoconjunctivitis and seasonal allergic conjunctivitis also coincide with increased eosinophil accumulation in the finely innervated ocular surface mucosa (Mantelli, Micera et al. 2010). Finally, cervical ripening in preparation for labor and delivery are characterized by increased neuronal expression of substance P, CGRP, and VIP along with increased eosinophils (Knudsen 1996; Collins, Usip et al. 2002).

In vitro, eosinophils or their products can directly release neuropeptides from nerves. In addition, eosinophils isolated from patients with allergic rhinitis and/or asthma increase neuronal release of substance P when co-cultured with sensory neurons from rats (Garland, Necheles et al. 1997). Administration of eosinophil major basic protein increased substance P release from cultured sensory neurons (Garland, Necheles et al. 1997). Increased substance P release was specific to eosinophil major basic protein as other eosinophil granule proteins, eosinophil cationic protein and eosinophil-derived neurotoxin, as well as eosinophil products, leukotriene D4, platelet activating factor, and hydrogen peroxide, did not cause substance P release (Garland, Necheles et al. 1997).

Eosinophil Adherence to Neurons and Subsequent Disinhibition or Activation of Neurons By Eosinophil Granule Proteins

Eosinophils selectively migrate to airway parasympathetic nerves in asthma and in antigen challenged guinea pigs (Costello, Schofield et al. 1997). These eosinophils are activated since major basic protein is deposited along the nerves in lungs of asthmatic humans and antigen challenged guinea pigs (Costello, Schofield et al. 1997; Evans, Fryer et al. 1997). Eosinophils are a mechanism of airway hyperreactivity since treatments that prevent eosinophil influx into lungs (Elbon, Jacoby et al. 1995; Fryer, Costello et al. 1997) or shift them away from nerves (Evans, Jacoby et al. 2001; Fryer, Stein et al. 2006; Nie, Jacoby et al. 2009) prevents

airway hyperreactivity in antigen challenged guinea pigs. As discussed above, recent studies of severe asthmatics shows eosinophil depletion also prevents asthma exacerbations and reduces the need for steroids (Haldar, Brightling et al. 2009; Nair, Pizzichini et al. 2009).

Eosinophils cause airway hyperreactivity in antigen sensitized and challenged guinea pigs by disrupting a cholinoreceptor responsible for limiting acetylcholine release from parasympathetic neurons. Parasympathetic neurons induce airway smooth muscle contraction by releasing acetylcholine which stimulates muscarinic receptors on airway smooth muscle. Acetylcholine also stimulates M2 muscarinic receptors located prejunctionally on airway parasympathetic neurons which limits further release of acetylcholine and prevents excessive bronchoconstriction (Fryer and Maclagan 1984). Eosinophil major basic protein is an endogenous allosteric antagonist of M2 muscarinic receptors (Jacoby, Gleich et al. 1993). Release of MBP from eosinophils blocks M2 muscarinic receptors resulting in disinhibition of acetylcholine release from parasympathetic neurons leading to increased acetylcholine release and increased bronchoconstriction. Sensory nerves also express M2 muscarinic receptors which pain studies suggest may be associated with airway sensory hyperresponsiveness through M2 inhibition by MBP. Sensory nerve M2 expression is increased in nerve-injury models of hyeralgesia (Hayashida, Bynum et al. 2006) and knockdown of M2 using inhibitory RNA prevented inhibition of hyperalgesia by muscarine (Cai, Chen et al. 2009). Thus eosinophil-mediated release of MBP might inhibit M2 receptors on sensory nerves and increase sensory responsiveness to otherwise innocuous stimuli.

More recently, eosinophil granule proteins were shown to activate sensory neurons. Instillation of eosinophil cationic protein or eosinophil MBP, into rat trachea in vivo increased baseline activity of unmyelinated airway sensory nerve fibers (Lee, Gu et al. 2001). In vitro, administration of major basic protein onto cultured sensory neurons also increased capsaicin-,

acid-, and ATP- evoked action potentials (Gu, Wiggers et al. 2008; Gu, Lim et al. 2009). In follow-up experiments, eosinophil major basic protein was shown to increase the decay and recovery time of action potentials via potassium channels (Gu, Lim et al. 2009). This increased excitability of sensory neurons via eosinophil MBP or eosinophil cationic protein is a potential mechanism for the sensory hypersensitivity associated with eosinophilic diseases.

Adhesion of eosinophils to nerves through ICAM and VCAM also activates nerves. Following whole eosinophil or eosinophil membrane adhesion to isolated nerves in culture, the neurons activate a pro-inflammatory transcription factor, NFκB (Curran, Morgan et al. 2005). This stimulatory effect is dependent upon ICAM activation and involves intracellular kinase signaling and reactive oxygen species. Eosinophil adhesion via the other major nerve CAM, VCAM, activates a different transcription factor, AP-1, which is also associated with neuroplasticity and inflammatory responses (Walsh, Curran et al. 2004). These data show that eosinophil adhesion to the nerves via ICAM and VCAM is sufficient to change nerve function even in the absence of eosinophil degranulation.

Eosinophils Can Also Inhibit Nerve Growth and Cause Nerve Cell Damage

In some diseases and experimental systems, eosinophils inhibit neuronal growth and cause neuropathic damage. Case-control studies of demyelinating diseases (e.g. eosinophilic myelitis, neuromyelitis optica) demonstrate increased eosinophils, as well as eosinophil cationic protein, eosinophil-derived neurotoxin, eotaxin, and IL-5 in cerebrospinal fluid. In eosinophilic myelitis, demyelination is associated with eosinophil cationic protein in the spinal cord indicating the presence of activated eosinophils in the central nervous system (Osoegawa, Ochi et al. 2003). Patients with another demyelinating disease, neuromyelitis optica, also have increased eosinophil cationic protein and additionally have increased IL-5 and eotaxin in cerebrospinal fluid and also in active spinal cord lesions demonstrated histologically (Lucchinetti,

Mandler et al. 2002; Correale and Fiol 2004). Eosinophil cationic protein levels in cerebrospinal fluid are also significantly elevated with cerebrovascular disease, acute central nervous system infections, and brain tumor malignancies (Hallgren, Terent et al. 1983). The presence of eosinophils products in the cerebrospinal fluid is important because neurotoxic effects were observed upon administration of eosinophils, or their granule proteins, to peripheral or to central neurons. Injection of eosinophils, eosinophil cationic protein, or eosinophil-derived neurotoxin into the cerebral cortex or cerebrospinal fluid of guinea pigs or rabbits was shown to cause axonal damage, vacuolization, and destruction of central and peripheral neurons (Newton, Walbridge et al. 1994). In a mouse model of multiple sclerosis, eosinophil influx into the optic nerve was one of the earliest events following induction of the autoimmune disease and preceded nerve demyelination and the development of motor paralysis (Milici, Carroll et al. 1998). Conversely, egress of eosinophils from the optic nerve preceded remyelination and disease remission. Eosinophils may also be more active in disease since eosinophils derived from a patient with hypereosinophilia and peripheral neuropathy killed more peripheral nerves in co-culture than eosinophils from healthy subjects (Sunohara, Furukawa et al. 1989). Thus, eosinophils have the capacity to damage and kill nerves in the central nervous system and are associated with demyelinating diseases.

Eosinophils may also mediate pathologic and cytotoxic changes in the peripheral nervous system. Co-culturing eosinophils with a cholinergic nerve cell line inhibited neurite outgrowth without increasing apoptosis (Kingham, McLean et al. 2003). In vivo, in a murine model of enteric eosinophilic inflammation, eosinophils were seen next to damaged axons suggesting a neuropathic interaction with myenteric nerves (Hogan, Mishra et al. 2001). Eosinophils are found next to nerves in the gut, thus if eosinophils inhibit peripheral neurons,

the resulting disruption of myenteric control might cause gastric dysmotility characteristic of inflammatory bowel disease.

Dependence on Inflammatory Environment, Timing, and Tissue Distribution

Eosinophils are capable of causing trophic or pathologic changes to nerves, increasing nerve outgrowth and nerve activity, changing neuropeptide content, and killing neurons. Thus, it is odd that injured (Beuche 1991) and inflamed (Milici, Carroll et al. 1998) nerves selectively recruit eosinophils unless there are unrecognized beneficial interactions between eosinophils and nerves. The surrounding environment appears to influence an eosinophil's impact on nerves. For example, eosinophils mediate virus-induced airway hyperreactivity only in allergen sensitized guinea pigs and not in non-sensitized guinea pigs (Adamko, Yost et al. 1999). Depletion of eosinophils is not protective in virus infected guinea pigs unless the guinea pigs are also sensitized to a protein. Thus, the role of eosinophils is dependent upon atopic status. Timing also determines the impact of eosinophils on nerves. In guinea pigs, airway hyperreactivity one day after ozone exposure is mediated by eosinophil recruitment to parasympathetic nerves (and subsequent blockade of nerve M2 muscarinic receptors) (Yost, Gleich et al. 2005). In contrast, three days following ozone exposure the role of eosinophils is changed so they are now protective against ozone-induced airway hyperreactivity. These eosinophils are synthesized from the marrow after ozone exposure and their protective role on airway hyperreactivity may be due to different effects on nerves than harmful eosinophils. The concentration and tissue distribution of eosinophil products also mediate their effect on nerves. For example, a low concentration of eosinophil derived neurotoxin as may be seen in vivo, is not cytoxic and is rather anti-viral and chemoattractant (Yang, Rosenberg et al. 2003) unlike the neurotoxicity caused by directly injecting eosinophil-derived neurotoxin into cerebrospinal fluid (Durack, Ackerman et al. 1981). Thus, the effect of eosinophils on nerves is dependent on atopic

status, on the time after a specific challenge, on dosing and tissue distribution of eosinophils and their products.

Eosinophil-Nerve Interactions as a Therapeutic Target

Recent data from animal models of allergic airway disease and also from human asthma show that inhibiting eosinophil-nerve interactions represent a potentially useful therapeutic target. Treatment of guinea pig asthma models with Etanercept®, a TNF blocker, or with dexamethasone, a corticosteroid, inhibited eosinophil localization next to nerves and prevented airway hyperreactivity without changing the overall quantity of eosinophils in the lungs (Evans, Jacoby et al. 2001; Nie, Jacoby et al. 2009). Importantly, these medications are approved for human use and may be efficacious in some patients with asthma. In human asthma, dexamethasone reduces symptoms and reduces the relapse rate. Similarly, Etanercept reduces hyperresponsiveness and exacerbations in severe steroid-dependent asthma (Berry, Hargadon et al. 2006; Nie, Jacoby et al. 2009).

Newer muscarinic and neurokinin receptor antagonists show promise in recent animal and human trials (Veres, Rochlitzer et al. 2009; Peters, Kunselman et al. 2010). Older studies of nonselective anticholinergic drugs and selective neurokinin receptor antagonists concluded that these compounds were ineffective (Westby, Benson et al. 2004). Newer studies, demonstrate triotropium, an anticholinergic agent selective for M3, or CS-003, a combined antagonist of NK-1, NK-2, and NK-3 receptors reduce bronchoconstriction and airway hyperreactivity in humans with asthma (Veres, Rochlitzer et al. 2009; Peters, Kunselman et al. 2010). It is tempting to speculate that these medications act in part by disrupting eosinophil-nerve interactions (Costello, Jacoby et al. 2000). A better understanding of eosinophil-nerve interactions within the gut, skin, eye, upper airway, lung, and other organs will hopefully elucidate therapeutically useful signaling pathways.

1.11 Atopic Dermatitis, Eosinophils in the Skin, and Peripheral Neuroplasticity

Using a similar three-dimensional imaging and computer modeling approach, the current dissertation also investigated eosinophil-induced neuroplasticity in models of atopic dermatitis, an itchy skin disease. This was a continuation of previous research showing eosinophils are associated with increased nerves in atopic dermatitis and cause sensory nerve growth in vitro (Foster, Simpson et al. 2011).

1.11.1 Atopic Dermatitis and Eosinophils

Atopic dermatitis is a prevalent skin disease characterized by debilitating itch and chronic inflammation. Atopic dermatitis affects 10% of children in the U.S. and sufferers often have a family history of asthma and allergic rhinitis (Correale, Walker et al. 1999). The itch sensation typically precedes lesions of excoriations or scratches made by the patient. Within acute lesions of allergic (extrinsic) atopic dermatitis, eosinophils and their granule proteins are elevated and electron micrographs show that eosinophils degranulate upon entering the skin (Cheng, Ott et al. 1997; Rho, Kim et al. 2004). Eosinophil levels are also increased in circulation of patients with atopic dermatitis (Akdis, Akdis et al. 1999). Similar to asthma, the recruitment of eosinophils to the skin in atopic dermatitis coincides with elevated levels of skin IL-5 and eotaxin (Yawalkar, Uguccioni et al. 1999; Taha, Minshall et al. 2000; Leung, Boguniewicz et al. 2004). Atopic dermatitis, like asthma, is also a heterogeneous disease with intermittent eosinophilia caused by variable recruitment and degranulation (Cheng, Ott et al. 1997).

1.11.2 Sensory Neuroplasticity and Eosinophils in Atopic Dermatitis

The skin is innervated by a network of peripheral sensory nerves that cause itch in atopic dermatitis. Unlike in asthma where changes in nerve density are controversial, there is general agreement that nerve density increases in the skin of patients with atopic dermatitis (Tobin, Nabarro et al. 1992; Ostlere, Cowen et al. 1995; Sugiura, Omoto et al. 1997; Urashima and Mihara 1998; Foster, Simpson et al. 2011). In addition most studies showed increased nerve density in lesional skin versus non-lesional skin in the same patient. A recent study showed that in lesional skin from patients with atopic dermatitis, eosinophil granule proteins are located next to regions of increased nerve density. The same study demonstrated that transgenic mice with skin-specific IL-5 overexpression and subsequent eosinophilia had increased epidermal nerve density. This suggests eosinophils are associated with the nerve outgrowth seen in atopic dermatitis. This study went on to show eosinophils also cause sensory nerve outgrowth in vitro. The mechanism of eosinophil-induced nerve growth required that eosinophils were viable and was not contact-dependent suggesting release of a soluble neurotrophic factor. Adding an inhibitor to nerve growth factor did not prevent eosinophil-induced nerve branching suggesting that a different soluble factor is causing branched outgrowth.

1.12 Summary and Hypothesis

Airway sensory hyperresponsiveness is an important part of asthma and previous studies demonstrated nerve hyperresponsiveness is associated with nerve structural and phenotype plasticity. However, the current methods for characterizing airway nerve structure are limited by undersampling both individual nerve structure and their organ-wide distribution. After testing conventional methods (discussed at the beginning of Chapter 3), I hypothesized that a three-dimensional organ-wide quantification of airway nerve structure would more comprehensively capture neuroplasticity (Chapter 3). I then used my new three-dimensional

computer mapping approach in tandem with airway function experiments to test the hypothesis that airway sensory hyperresponsiveness is caused by eosinophil-induced changes to the three-dimensional structure of sensory nerves (Chapter 4). This was tested in both chronic and acute mouse models of asthma. Finally, I used three-dimensional computer mapping of skin sensory nerves to test the hypothesis that eosinophils cause sensory neuroplasticity in chronic and acute mouse models atopic dermatitis, an allergic skin disease characterized by itch (Chapter 5).

CHAPTER 2: GENERAL METHODS

2.1 Animal Care

The majority of animal experiments were performed using mice and tissue from larger animals was used for testing nerve modeling techniques. Mice were used because of their widespread use, availability of transgenic lines specific to asthma studies, and availability of experimental reagents. The limitations of mice include their small size, less differentiated airway tissue compartments, lack of abundant submucosal glands, and diminished cough response. Subsequent studies in larger animals (eg. guinea pigs) were performed given their increased anatomic and functional similarity to humans. All animals were treated humanely with regard for alleviation of suffering in accordance with the standards established by the U.S. Animal Welfare Act as set forth in the National Institutes of Health guidelines (NIH 2002). All protocols involving animals were approved by the Institutional Animal Care and Use Committee at Oregon Health & Science University.

Wildtype C57BL/6 mice and transgenic mice (PHIL and NJ.1726 discussed below) on a C57BL/6 background were housed in a pathogen-free facility run by the Department of Comparative Medicine. For allergen sensitization experiments, cohorts of similarly-aged and sexed C57BL/6 wildtype mice were ordered from Jackson Laboratory (Bar Harbor, ME). Tissue from an IL-5 and eotaxin-2 double transgenic line were provided by the Lee laboratory (Mayo Clinic, Scottsdale, AZ). In non-survival experiments, mice were euthanized with an intraperitoneal injection of 120 mg/kg pentobarbital in PBS. Death was verified by lack of a blink reflex and pain withdrawl reflex caused by pinching lower limb.

Tissue from Dunkin-Hartley guinea pigs (Elm Hill Labs, Chelmsford, MA) was provided by the Fryer laboratory at Oregon Health and Sciences University. Canine airway tissue samples

were provided by the Victor Monterosso in the Department of Comparative Medicine at Oregon Health and Sciences University.

2.2 Transgenic Mice Lacking Eosinophils (PHIL)

PHIL mice ("NoEos") were used in order to test if eosinophils were necessary for structural and functional neuroplasticity in various studies. I maintained a colony of a transgenic mouse line called "PHIL" that systemically and selectively lacks eosinophils. The mouse line contains a transgene made of an eosinophil-specific (EPO) promoter linked to a diphtheria toxin A chain open reading frame (Lee, Dimina et al. 2004). Diphtheria toxin A chain is the cytocidal portion of ditpheria toxin (whereas the B chain is involved in cell entry). In the bone marrow, newly differentiated eosinophils uniquely activate the EPO promoter so in PHIL mice this causes DTA production and eosinophil self-destruction upon differentiation. Since EPO is specific to the eosinophil lineage, PHIL mice lack eosinophils but contain all other hematopoietic cells. In studies of acute allergic inflammatory asthma, PHIL mice were shown to contain less airway pathology and reduced hyperreactivity compared to Wildtype controls (Lee, Dimina et al. 2004).

2.3 Transgenic Model of Chronic Allergic Inflammatory Asthma with Airway Eosinophilia (NJ.1726)

A mouse model of chronic allergic inflammatory asthma called "NJ.1726" or "IL5++" was used to measure the long-term impact of airway eosinophils on structural and functional neuroplasticity. The chronic allergic inflammatory asthma transgenic mouse model called "NJ.1726" contains overabundant eosinophils specifically in the airways (Crosby, Shen et al. 2002). This was accomplished by overexpression of IL-5 under an airway-specific promoter, CC10. CC10 is a promoter specific to Clara cells, a specialized airway epithelial cell. IL-5 over-expression causes increased survival and recruitment of eosinophils. Thus CC10 driven

expression leads to marked increases in airway eosinophils and not other tissue compartments. These mice were shown to have chronic lung pathology and abnormal lung mechanics characteristic of asthma.

2.4 Transgenic Mouse Model of Severe Chronic Allergic Inflammatory Asthma (IL5/Eot2)

A mouse model of chronic severe asthma called "IL5/Eot2" was used to measure the long-term impact of activated degranulating eosinophils on structural and functional neuroplasticity. I obtained tissue from a model of severe chronic allergic inflammatory asthma caused by transgenic activation and activation of eosinophils to the lung (Ochkur, Jacobsen et al. 2007). In this mouse model, two eosinophil cytokines are overexpressed, IL-5 and eotaxin-2. IL-5 overexpression is driven by a systemic T-cell promoter, CD3, and eotaxin-2 airway-specific overexpression is driven by CC10, the same promoter used to drive IL-5 in NJ.1726 mice. Compared to other transgenic asthma models, these mice exhibit increased lung remodeling, increased eosinophil activation/degranulation, and worsened lung mechanics characteristic of severe asthma. Tissue from this mouse line was provided by the Lee laboratory.

2.5 Genotyping

In order to identify distinct mouse offspring, mice were genotyped by PCR and agarose gel electrophoresis. Briefly, ear tissue was collected from mice under urethane anesthesia. The Red-Extract-N-Amp kit (Sigma, XNAT) was used according to manufacturer's instructions. Briefly, after DNA extraction a proprietary PCR master mix (containing polymerase, magnesium chloride, deoxynucleotide triphosphates) was added with 250nM of each primer (see below) and run through a PCR reaction using a 96 well Veriti Thermal Cycler (Applied Biosystems). The temperature and duration for PCR denaturation steps was 95°C and 30 seconds, and for

extension steps it was 72°C for 1 minute. The annealing steps for PHIL were run at 53°C for 1 minute and for NJ.1726 it was 56.5°C for 1 minute. Both PCR reactions were cycled 35 times.

PHIL Primers:

"EPO F221"	5'-AAG-TAT-GAT-GGG-GGT-GTT-TC-3'
"DTA R224"	5'-GAG-CGG-GTT-TTC-ATT-ATC-TAC-3'

NJ.1726 Primers:

"CC1 F"	5'-CAG-TGC-TTG-ACT-TTA-AAG-AGG-3'
"115.2 R"	5'-TGG-CAG-TGG-CCC-AGA-CAC-AGC-3'

2.6 Measuring Mouse Airway Mechanics In Vivo

In order to measure airway mechanics, in particular reflex bronchoconstriction, mice were artificially ventilated as described by Mitzner in 1999 (Brown, Walters et al. 1999). Mice were anesthetized, paralyzed, and mechanically ventilated and subsequently given aerosol stimulants while measuring airway narrowing (Figure 7). The intubation protocol was developed by K. MacDonald and published previously (MacDonald, Chang et al. 2009). Mice were anesthetized by intraperitoneal injection of Ketamine (Hospira, 100 mg/kg) and Xylazine (Vedco, 5 mg/kg). The mouse was secured vertically, the tongue gently lifted out and to the side of the mouse's mouth, and the vocal cords were visualized with a pediatric otoscope (2mm specula). A guide wire was then inserted into the trachea. An endotracheal tube (custom silicon-covered 20G IV catheter) is then inserted along the guide wire into the trachea and the mouse is placed into the ventilator circuit. Mouse temperature is maintained throughout the experiment between 34-36 degrees Celsius using a heating pad and rectal thermometer.

Lung mechanics were measured with a low dead-space lung ventilator system and end-inflation occlusion (Ewart, Levitt et al. 1995). The ventilator system consists of a differential pneumotachograph (ML141, AD Instruments), an in-line pressure transducer, solenoid gas

valves, custom electronic hardware, two expiratory limb water columns for positive end-expiratory pressure (2 cm H2O) and sighing (25 cm H2O) to prevent atelectasis, and an Analog-to-Digital converter for interfacing with computer acquisition software (LabChart Pro). The ventilator was powered by a 100% oxygen source gas. A gas-pressurized (30 PSIG) metering valve is connected directly to an electronically controlled solenoid valve. The outlet of this valve is then connected to the endotracheal tube via a manifold made from small-bore tubing. The manifold also contains ports for measurement of pressure at the trachea and inspiratory airflow (via pressure differential pneumotachograph). The manifold then connects to the second expiratory solenoid. The timing of the solenoids is controlled electronically. During normal ventilation the inspiratory and expiratory times were 175 and 300 ms respectively. Mice were ventilated at 125 breaths/min with a 0.3 ml tidal volume and paralyzed with succinylcholine (5 mg/kg) to eliminate respiratory effort. 3-lead electrocardiogram tracings were also digitally recorded throughout the experiment.

In-line with the respiratory circuit was an Aeroneb nebulizer for delivering aerosolized pharmacologic agonists to stimulate airway sensory nerves. This setup offers specific advantages including: uniform particle size (4-6uM volume mean diameter), direct nebulization into the ventilation circuit without additional gas flow, complete nebulization of all medication, and the ability to nebulize small (10µl) volumes and avoid airway trapping. Complete nebulization of the drug occured within 1-2 seconds and visually aerosol enters the mouse airway within 2 seconds.

2.7 Measuring Reflex Bronchoconstriction in Ventilated Mice

In order to measure neuronal airway narrowing, reflex bronchoconstriction was measured in ventilated mice. In ventilated mice, airway responsiveness was measured as changes in airway resistance caused by aerosol administration of serotonin (5-HT) (Sigma) as shown in

Figure 8. I obtained half-log dose-response curves to nebulized serotonin at concentrations of 1, 3, 10, 33, and 100mM in 10 µl volumes (0.1762, 0.5286, 1.762, 5.8146, and 17.62 mg/mL). Before each dose mice were given a deep inflation (sigh) at 25 cm H2O. Increasing concentrations of serotonin were then administered via nebulizer in 10 µL volumes with increasing concentrations of serotonin. After each dose, I performed end-inflation maneuvers every 10 seconds for 2 min (Figure 8). Resistance was calculated from pressure and flow data collected during these maneuvers as the difference of peak inflation pressure and end-inflation pressure and dividing by inspiratory flow rate. The peak values of resistance obtained at 20 and 30 seconds following each dose were then averaged. Airway resistance at baseline was subtracted and data were expressed as cmH2O/ml/s.

Following the serotonin dose-response, mice were vagotomized to eliminate reflex (neuronal) bronchoconstriction, and the same serotonin dose-response was performed. While the mouse was ventilated and kept warm, the anterior cervical region was exposed and the carotid sheath was isolated using blunt dissection. The working field was kept hydrated by room temperature PBS. The vagus nerve was then gently separated from the carotid artery by blunt dissection with Dumont #5 forceps (Fine Science Tools, Foster City, CA) and cut. After vagotomy, mice were administered the same serotonin doses and airway resistance was measured. Upon completion of serotonin administration, mice were euthanized by an overdose of anesthesia followed by cervical dislocation.

2.8 In vitro constriction of isolated mouse trachea:

In order to measure contractility of airway smooth muscle, isolated tracheas were used in an organ bath experimental setup. Constrictions of the isolated trachea were measured *in vitro* as shown in Figure 6 and previously reported by my laboratory (Murray and Jacoby 1992). Mice were killed with sodium pentobarbital (Sigma, 150 mg/kg i.p). The tracheas were removed

and placed in a 5 ml organ bath (Radnoti Glass Technology Inc., Monrovia, CA) containing Kreb's solution bubbled with a 95%O_2-5%CO_2 gas mixture. The segments were supported by loops of thread (3.0; silk) through the lumen of the trachea, with the lower thread tied to a supportive hook and the upper thread tied to a Grass FT03 isometric force transducer (Grass Instrument Co, Quincy, MA). The segments were equilibrated in the bath at 0.3 g tension for 30 min, and washed with Krebs solution every 10 min. Tracheas were further equilibrated with three 1.5 minute contractions caused by 10 μM acetylcholine chloride (Acros Organics, Geel). Tracheas were then washed and contractions of tracheal segments were induced with electrical field stimulation (EFS; 20 V, 0.2 msec pulse duration, 30 sec on, 30 sec off) at increasing frequencies of 1,3,10, and 30Hz. At each frequency, stimulation was repeated until three equivalent sequential contractions were obtained. Afterward, tracheas were washed for 5 minutes and then contracted with increasing doses of acetylcholine (0.33, 1, 3.3, 10, 33, 100, 330 μM). Tracheas were washed four times over 15 minutes and then contracted with increased doses of methacholine chloride (Sigma) (0.33, 1, 3.3, 10, 33 μM). Finally, tracheas were washed and then contracted with 100mM potassium chloride. Tension recordings were made on a Powerlab/8SP (ADinstruments, Castle Hill, Australia).

2.9 Measurement of plasma extravasation by Evan's Blue:

In an attempt to measure neurogenic inflammation, the leakage of Evan's Blue dye into the airways was measured. Mice were anesthetized by intraperitoneal injection of ketamine (100 mg/kg) and xylazine (5 mg/kg) and subsequently ventilated as described above. Evan's Blue Dye (Sigma) 20 mg/kg in 0.9% saline was injected into the jugular vein. Twenty-five minutes after injection, the mice were given an overdose of anesthesia, the chest cavity was rapidly exposed, and the lungs excised and perfused with PBS. Lung tissue was frozen in liquid

nitrogen and stored at -80˚C. Lungs were homogenized, incubated in formamide at 60˚C for 18 hours, and the supernatant collected following centrifugation at 5000xg for 30 minutes. Optical density at 620nm (A_{620}) was measured with a spectrophotometer for samples and standards of known Evan's Blue concentration. I used a formula derived specifically for murine inflamed lungs using a turbidity correction factor: $A_{corrected} = 1.1649*A_{620} + 0.004$ (Moitra, Sammani et al. 2007).

2.10 Tissue Harvesting for Immunohistochemistry

In order to image peripheral nerves, airways, skin, esophagus, and intestinal tissue were rapidly harvested and fixed for use in nerve imaging studies. For airway epithelial nerves, rapid en-bloc removal of airways, heart, and esophagus and immersion in Zamboni's fixative (American MasterTech Scientific) resulted in better preservation of nerve morphology (presumably by preventing autolysis) than vascular perfusion or airway lavage of fixative. Airways were also manually compressed in fixative to facilitate diffusion of fixative into alveoli. Tissues were left in fixative overnight at 4°C and then washed 5 x 1 hour and overnight in TBS (pH 7.4).

2.11 Whole Mount Airway Dissection

In order to expose the whole airway for imaging, I developed a microdissection protocol. Under a light-dissecting microscope with transmitted and reflected light sources, a ventral midline incision was made from the trachea to distal-most-bronchioles. Adventitial tissue consisting of fat, lymph nodes, fascia were removed by gentle pulling and sharp dissection. After securing airways to a Sylgard (Dow-Corning Corporation, Midland, Michigan) plate with dissecting pins (10130-05, Fine Science Tools, Foster City, CA), airway parenchyma and pulmonary vessels were carefully removed by blunt and sharp dissection using Dumont forceps and spring microscissors (91501-09, Fine Science Tools, Foster City, CA). Tissue opacity was

visualized as tissue transparency when using transmitted light and epithelium was visible at the highest dissecting microscope magnification.

2.12 Whole Mount Immunostaining

For more completely imaging innervation throughout the organ I developed a whole mount immunostaining protocol. Immunostaining tissue whole mounts was performed using extensive tissue permeabilization and long antibody incubation and washing steps. Tissues were blocked overnight at (4% Normal Goat Serum, 1% Triton X-100, 5% powered milk in TBS pH 7.4) then treated with antiserum/antibodies for 3 days. Tissues were washed in TBS five times for one hour per wash and then washed in TBS overnight at 4°C followed by overnight immersion secondary antibody. When available, smaller secondary antibodies made of the $F(ab)_2$ antibody fragment were used because of improved tissue penetration. Tissues were then washed in TBS 5 x 1 hour and mounted on a charged microscope slide with aqueous mountant (Vectorlabs, H-1200). Tissues that deformed undesirably before mounting were temporarily secured using 1mm glass pieces. For example, airways were secured in a lumen-up configuration with this method before mounting and sealing. Coverslips (22x22x1.5mm) were weighed down by 100g weights and sealed with Cytoseal 60 (Richard-Allan Scientific, 8310-16).

2.13 Cryosectioning

In order to improve signal-to-noise (improved antibody penetration, reduced light scatter/absorption, reduced spherical aberration with confocal microscopy) and reduce variability caused by tissue thickness changes and folding, airway, DRGs, and esophagus immunohistochemistry was performed on cryosections. Tissues were fixed overnight in Zamboni's fixative at 4°C and washed 5 x 1 hour in TBS then overnight in 18% sucrose (w/v in PBS). The next day tissues were moved into 1:1 18% sucrose and OCT (Optimal Cutting Temperature compound, Tissue Tek #4583) for 5 hours then immersed in OCT in a plastic block

mold for freezing at -80°C. When consistent orientation was needed tissues were held by forceps and the bottom layer of OCT hardened on a dry ice-cooled metal block. A second freezing technique was used to selectively cut parallel to tissue layers. Tissues in a drop of OCT were placed on a cooled cryostat tissue block holder epithelium facing up and quickly freeze-flattened with a dry ice-cool metal cylindrical rod.

2.14 Mouse Model of Acute Allergic Inflammatory Asthma

In order to measure structural and functional neuroplasticity in asthma, I used a common mouse model of allergic inflammatory airway hyperreactivity. Over the period of a month mice were sensitized to a foreign protein, ovalbumin (Sigma, 5253), and challenged with repeated airway exposures to model acute allergic airway hyperreactivity. Ovalbumin was dissolved overnight in PBS at 4°C. On day 1, 6-8 week old mice were given a 100 µl intraperitoneal injection of ovalbumin (40 μg) in a 30% v/v adjuvant solution (Imject Alum, Thermo Scientific, #77161) in PBS. On day 14, mice were given 400ug of ovalbumin in the same 30% v/v adjuvant solution. On day 24, 26, and 28 mice were administered an allergen "challenge" by administration of ovalbumin alone without adjuvant into the airways. Mice were initially anesthetized with Ketamine (100 mg/kg) and Xylazine (5 mg/kg) and restrained in a vertical position. Ovalbumin (in 25 µl of PBS) was given intra-tracheally and the mouse was kept vertical until liquid visibly drops from the oral cavity into the airways. Mice were kept warm and watched until they recovered from anesthesia. To minimize mortality, 2% ovalbumin was only given at day 24, and 1% was administered at days 26 and 28. Tissue harvesting was performed three days later on Day 31.

2.15 Human Tissue

To quantify neuroplasticity in humans, human tracheal tissue was obtained from anonymous organ donors via the Pacific Northwest Transplant Bank. All families provided

informed consent for use of these tissues. De-identified and fixed human bronchoscopic airway biopsy tissue were provided by the Costello and McGarvey laboratories under patient consent and institutional approval by the Royal College of Surgeons in Ireland (Dublin, Ireland) and the Center for Infection and Immunity at Queens University Belfast (Belfast, Ireland). Human DRGs were obtained from recently deceased humans by National Disease Research Interchange (NDRI, Philadelphia, PA). Eosinophils were isolated from blood drawn from normal volunteers.

2.16 Human Airway Biopsy Dissection for Imaging Epithelium

In order to test the usefulness of computer modeling in clinically-obtained tissue, human airway biopsies were stained for nerves and quantified. Human airway biopsies were dissected with a light microscope to isolate epithelium for immunostaining and imaging. Forceps biopsies pinched off airway tissue into a rounded configuration with epithelium on the outside. Initially tissue was opened and secured in a flattened epithelium-down position on a sylgard surface with dissecting pins. Submucosa was subsequently removed by applying weak traction and sharp dissecting. Tissue opacity was visualized as tissue transparency when using transmitted light and epithelium was visible at the highest dissecting microscope magnification (Figure 9).

2.17 Human Eosinophil Isolation

Human eosinophils were isolated and purified in order to perform sensory nerve/eosinophil co-culture experiments. Eosinophils were isolated from human blood by density centrifugation and antibody-based magnetic purification. After informed consent, a human participant provided 180ml of blood. Blood was collected into three 60ml syringes pre-filled with 1.5ml of 0.5M ethylenediaminetetraacetic acid (EDTA), an anti-coagulant. Blood was diluted 1:1 in 0.5% Bovine Serum Albumin in PBS and gently layered over Ficoll-Paque PLUS (GE Healthcare, #17-1440-03) in 50ml conical tubes. Blood was spun in a centrifuge at 600 x gravity

(g) for 30 minutes at room temperature with minimal centrifuge braking. After the spin, blood was separated into distinct layers. The top yellow layer is serum, the interface is monocytes, a white hazy layer near the bottom contains granulocytes (eosinophils and neutrophils), and red blood cells are located at the bottom. Layers above the granulocytes and red blood cells were aspirated and the red blood cells were subsequently lysed. To lyse the red blood cells, the remaining solution containing granulocytes and red blood cells were repeatedly exposed to a cycle of 10 seconds distilled sterile water followed by return to isotonicity with 10x PBS. Between each cycle, non-lysed cells were purified by centrifugation at 300xg for 10 minutes at 4°C. After four red blood cell lysis cycles, the cell pellet turns from red to white, and remaining cells are predominantly (>95%) granulocytes. Cells were counted and Trypan Blue (Gibco, #15250) exclusion is performed to ensure >97% viability. Eosinophils were subsequently purified by an antibody-based magnetic isolation system (Miltnyi Biotec, #130-092-010). Granulocytes were labeled with a cocktail of biotinylated antibodies (CD2, CD14, CD16, CD19, CD56, CD123, CD235a) and then with an anti-biotin secondary antibody conjugated to magnetic beads. This permits a negative selection of eosinophils as the only cell type to traverse a strong magnetic field due to lack of labeling. Eosinophils were subsequently counted and purity determined by Hemacolor staining (Harleco, 65044A-85) and differential counting. Eosinophil purity was greater than 95%.

2.18 Isolation of Airway Sensory (Nodose/Jugular) Ganglia

Murine nodose and jugular ganglia were isolated in order to perform sensory nerve/eosinophil co-culture experiments and nerve immunohistochemistry experiments. Airway sensory ganglia (nodose and jugular ganglia) were harvested after removal and fixation of the airways. The peri-tracheal neck region was exposed and kept immersed in sterile PBS or Zamboni's fixative depending if nerve culturing or immunostaining was planned. Initially the

superficial neck layer (dermis, platysma muscle and veins) was removed and the deeper neck muscles (sternocleidomastoid, thyrohyoid, cricothyroid) were blunt dissected to view the carotid sheath containing the carotid artery, carotid vein and jugular nerve. The jugular nerve was carefully dissected up to the jugular foramen at the base of the skull. The nodose and jugular ganglion were visualized as a swelling at the base of the jugular foramen.

2.19 Isolation of Mouse Dorsal Root Sensory Ganglia

Murine DRG sensory neurons were isolated in order to perform sensory nerve/eosinophil. Isolation of lumbar DRGs (L3-L5), an abundant source of sensory nerves, was performed after harvesting airway tissue and airway sensory (nodose/jugular) ganglia. Mice were rotated to a prone position, sprayed with 70% v/v ethanol, and the posterior skin and fascia removed to expose the dorsal spinal column. The caudal half of the spinal column was cut along vertebral transverse processes, removed from the mouse, bisected by a midline sagittal cut, and placed in ice-cold Hanks-buffered salt solution (HBSS). The spinal column halves were broken along their longitudinal axes at the vertebral pedicles to allow access to the inner portion of the vertebral foramen. Dorsal root ganglia were visualized as large translucent white swellings next to the foramen wall abutting the pedicle break line and connected to a spinal nerve. Ganglia were gently pulled and cut from their spinal dorsal root and spinal nerve attachments and placed in 10% Fetal Bovine Serum (FBS) (v/v in Dulbecco's Modified Eagle Medium). Three different sets of sterile forceps and scissors were used for skin and spinal column removal, column longitudinal breaking, and DRG isolation.

2.20 Culturing Dorsal Root Ganglia

Sensory nerves from dorsal root ganglia were cultured in order to measure the isolated effects of eosinophils on sensory nerves. Human and mouse DRGs were cultured using enzymatic disassociation, enrichment through differential cell adherence, and plating on coated

slides. Human DRGs were cut from attached spinal nerves and spinal roots shown in Figure 10. DRGs in 10% FBS (v/v in Dulbecco's Modified Eagle Medium) are pelleted by spinning 300 x g for 10 minutes and disassociated in 10ml 0.05% collagenase (Sigma-Aldrich) with penicillin-streptomycin (Cellgro) 4 hours at 37°C with gentle shaking. Cells were then spun at 300 x g for 10 minutes to remove collagenase and further digested in 1ml 1.25% Trypsin-EDTA (Gibco) for 15 minutes at 37°C with gentle shaking. Disassociated cells were spun again at 300 x g for 10 minutes, resuspended in 10% FBS (v/v in Dulbecco's Modified Eagle Medium) with penicillin-streptomycin, and plated overnight on a 100mm polystyrene culture plate (Corning Inc.) in a humidified incubator at 35.5°C and 5% CO_2.

The next day the culture supernatant was enriched for non-adherent cells including sensory neurons whereas adherent monocytes and fibroblasts remained attached to the plate. The supernatant was removed from the culture plate, spun at 300 x g for 10 minutes, and resuspended in C2 medium plus penicillin-streptomycin. For neurotrophin treatment experiments, purified Nerve Growth Factor (Harlan Laboratories, Indianapolis) or Brain-Derived Neurotrophic Factor (Chemicon) was added to C2 medium at 50ng/ml.

Cells were counted and plated on matrigel (BD Biosciences) coated 4-well chamber slides (Lab Tek) and 60mm (Corning Inc.) tissue culture-grade plates at various concentrations depending on the experiment. In some experiments, cytosine arabinoside (Sigma), a drug that purifies cultures by inhibiting DNA synthesis, was added a day later (2µM). DRG cultures were incubated at 35.5°C.

2.21 Retrograde Tracing of Airway Sensory Ganglia

Airway-specific nerves in vagal ganglia were labeled using retrograde tracer with a lipophilic fluorescent dye. On day 29 of the sensitization protocol animals were anesthetized by intraperitoneal injections of Ketamine (100 mg/kg) and Xylazine (5 mg/kg) dissolved in PBS. The

mid cervical trachea was exposed and a Hamilton syringe inserted into the airway lumen between tracheal cartilage rings allowing for a 50 µl injection of the retrograde tracer, DiI (2% dissolved in DMSO then 1:10 dilution in saline). Animals were given two weeks for DiI labeling to extend into neuron cell bodies innervating the airway. Any animals displaying behaviors of persistent pain or infection were immediately euthanized. Post mortem analysis confirmed that DiI labeling remained confined to respiratory tissues.

2.22 Skin Dissection to Image Epithelial Nerves

In order to quantify neuroplasticity in skin epithelium, skin was manually dissected and epidermal nerves stained and imaged using confocal microscopy. Epidermal imaging was performed on microdissected skin obtained from the base of the ear. The concave half of the ear was initially separated from the convex half and intervening cartilage using sharp dissection. The base of the concave half of ear skin was manually plucked free of large hairs using forceps and manually securing the tissue. Afterwards, a rectangular strip of skin was isolated that extended from the base of the ear up 1 cm and extended the full width of the tissue section. The tissue was then flipped epidermis-side down and secured with dissecting pins for removal of deeper dermis layers. Similar to airway tissue, forceps were used to pull dermis for clean sharp dissection. Epidermis was also visible using the higher magnification zoom on the light dissecting microscope.

2.23 Quantifying Neuronal Substance P and NF160kDa

Early analysis of whole mount airways stained with neurofilament 160KDa used blinded manual counting of nerves in images with de-identified (random number) names. The number of distinct NF160kDa nerves were counted per high-powered 20x field (425 µm x 425 µm) in each image and averaged. For later substance P analysis, 3D 20x images of the primary bronchi

were acquired with the laser scanning confocal microscope. 3D images were flattened using maximum intensity projection, gaussian filtered, and thresholded by intensity to identify nerves labeled with the pan-neuronal marker PGP 9.5 (in the green 488 nM channel). Substance P signal was captured in the red channel (555nM) and the average intensity of substance P signal was calculated for each pixels co-localized to neuronal (PGP 9.5) pixels.

2.24 Statistical Analysis

For nerve mapping data (Chapters 3, 4, and 5) one-way ANOVA repeated measures with Tukey's post-hoc test was used. For comparing manual quantification of branchpoints and nerve length to nerve mapping in Chapter 3, one sample two-tailed t-tests were used. For comparing reflex bronchoconstriction and trachea contractions in organ bath experiments a mixed-effects two-way ANOVA was performed with Bonferroni's post-test. For comparing nerve length in sensory nerve and eosinophil co-cultures in Chapter 5, paired two-tailed t-tests were used. For comparing neuronal substance P in maximum intensity projections of the airway, non-parametric two-tailed Mann-Whitney test was used. Data were analyzed using GraphPad Prism 5 (GraphPad Software, La Jolla California).

2.25 Nerve Imaging and Analysis

The protocol developed for imaging and quantifying nerve structure is discussed in Chapter 3.

CHAPTER 3: QUANTIFYING NERVE ARCHITECTURE USING THREE-DIMENSIONAL COMPUTATIONAL MAPPING; APPLICATION TO LUNG, ESOPHAGUS, SKIN AND INTESTINE.

3.1 Abstract:

Here I demonstrate a method using a computational approach to measure nerve architecture that will allow for more complete nerve quantification and measurement of structural peripheral neuroplasticity in development and disease. I have used the lungs as a primary test organ to show the utility of my approach and demonstrate my computer analysis substantially outperforms manual scoring in quantifying three-dimensional nerve structures. In mouse lungs, I detected airway epithelial nerves that have not been previously identified due to their patchy distribution, and quantified their three-dimensional morphology using my computer mapping approach. Additionally I show this approach can be used in humans and in other organs (esophagus, intestines, skin) where neuroplasticity is known to contribute to disease pathogenesis.

3.2 Introduction:

Nerve architecture is highly complex, three dimensional, and unique to each tissue. It is important to accurately measure nerve architecture since it can change (structural neuroplasticity) during development or disease resulting in altered nerve signaling. Neuroplasticity changes may include swelling, central and peripheral sprouting, reduced axon diameter, and nerve retraction. Three-dimensional nerve architecture has been inferred from either tissue sections or from whole mounts where data are acquired in three dimensions, but is routinely flattened to two dimensions for analysis. However, morphologically complex nerve

architecture including branching axonal processes and dendritic spines are under-sampled in two-dimensional images. Even though stereotactic tissue sectioning increases sample size and reduces sampling bias (Hyde, Harkema et al. 2006), it still requires an impractical amount of sampling for accurate quantification of heterogeneous nerve distribution, complex nerve structure, and rare subpopulations of nerves. Thus, all these two-dimensional approaches may be inaccurate due to under-sampling.

In the clinic measurement of peripheral neuropathy in skin currently requires trained pathologists to manually count the number of nerves crossing the basement membrane in 3-4 thick (50 µm) tissue sections in a labor intensive process (Lauria, Cornblath et al. 2005). However, this method of quantifying neuroplasticity from skin tissue sections has 25% variability between laboratories, wide inter-subject variability, with sensitivity that is unable to diagnosis milder disease (Lauria, Cornblath et al. 2005).

Confocal microscopy of whole mounts can image the branching structure of entire nerves as well as capture organ-wide heterogeneity of nerve density and see rare subpopulations. However, using confocal microscopy to model nerve architecture has multiple problems due to tissue thickness. These include difficulty fixing and labeling tissues homogeneously as well as imaging problems because thick tissues can absorb or diffract laser light. Even when these are solved, there is currently no method to quantify complex three-dimensional morphology of peripheral nerves. Three-dimensional analysis is currently available for larger scale imaging methods, such as magnetic resonance imaging (Manniesing, Viergever et al. 2006) and x-ray computed tomography (Bauer, Pock et al. 2010), and smaller scale methods like cryo-electron microscopy (Jiang, Ji et al. 2006), and fluorescent microscopy of cortical neurons [3DMA (http://www.ams.sunysb.edu/~lindquis/3dma/3dma.html)].

My goal was to develop an efficient method to map nerve architecture in three dimensions throughout an organ, with sufficient resolution to quantify nerve density, length, branching, and neurotransmitter content. The method I describe here images nerves throughout whole organs and tissue biopsies and, by designing new and adapting existent computer programs, produces three-dimensional maps of nerve architecture that can be quantified.

3.3 Results:

Airways were imaged from the larynx to the terminal bronchioles, including the whole circumference (ventral and dorsal sides) and carina and secondary bifurcations (see Figure 17). I acquired all images using laser scanning confocal microscopy of whole mounts. Although I also used the newer super-resolution structured illumination microscopy to acquire images, this method did not provide a practical balance of scan speed, multi-color imaging, depth resolution, and post-processing time.

3.3.1 IMAGING AIRWAY EPITHELIAL INNERVATION IN MICE

3.3.2 Tissue preparation and Image Acquisition

Lungs were removed from C57Bl/6 mice and immediately fixed to minimize neuronal apoptosis. Airways, from the larynx to the terminal bronchioles, were dissected free of connective tissue and alveoli (the parenchyma) and permeablized. Airway nerves were labeled with a pan-neuronal antibody (PGP 9.5) (Thompson, Doran et al. 1983). Non-specific binding was significantly reduced by extensive washing after PGP 9.5 incubation. Furthermore, PGP antibodies were identified using a $F(ab')_2$-conjugated secondary antibody because that also reduced non-specific binding and because they penetrate whole tissues better than whole secondary antibodies (Brandon 1985). Images of nerves (labeled with PGP 9.5 $F(ab')_2$-conjugated

secondary antibody) in airways of a whole mouse lung that is also labeled with 4',6-diamidino-2-phenylindole (DAPI) for cell nuclei, α-smooth muscle actin (α-SMA) for smooth muscle, and substance P (for a nerve population implicated in inflammatory disease and cough) (Barnes, Chung et al. 1998) are shown in Figure 15 and in Supplementary Video 1a. Whole airway morphology can be imaged, capturing the depth from the lumen to adventitial layers and length from the larynx to the terminal bronchioles (Figure 15 and in Supplementary Video 1a and 1b). In Figure 15 and Supplementary Video 1a and 1b note the large and small scale nerve heterogeneity (Figure 15a-d) including decreased density of nerves proximal-to-distal (Figure 15a), transverse submucosal inter-cartilage nerves (Figure 15b, Figure 15c), adventitial nerve bundles and ganglia (Figure 15b), undulating large-diameter nerves in smooth muscle (Figure 15c), branching small-diameter epithelial C fibers (Figure 15d), and rare epithelial substance P nerves (Figure 15d).

3.3.3 3D layer boundaries in large field of view images could be identified using a novel program that calculates boundary layer dimensions.

Airways are lined with epithelial cells (epithelium) that are separated from airway smooth muscle (in the submucosa) by a basement membrane and connective tissue (lamina propria). Since these each harbor distinct nerve populations, it is important in images that capture multiple tissue layers to distinguish the different layers which is not trivial due to variable thickness and folding. To do this, confocal images were resampled in an orthogonal orientation (Figure 16a) and layer boundaries in 10-15 representative tissue image slices were manually identified using ImageJ software (Abramoff, Magalhaes et al. 2004) (Figure 16b). I wrote macros that converted these to data readable by Matlab (Mathworks, Natick

Massachusetts). I created Matlab software that uses tri-cubic interpolation to calculate the three-dimensional shape of each tissue layer (Figure 16c).

The layers identified by Matlab, matched those identified by staining smooth muscle with antibodies to alpha smooth muscle actin, and by autofluorescence of elastin fibers and DAPI staining of nuclei to identify the epithelium (Thiberville, Moreno-Swirc et al. 2007). This method for identifying epithelium was validated using E-Cadherin immunostaining (data not shown).

3.3.4 Nerve structure can be mapped in three dimensions

Identification of PGP 9.5 labeled nerves in whole lung is complicated by signal drop off in deep tissue layers, non-neuronal PGP labeling especially in epithelial cells, auto fluorescence, and by variable brightness at the nerve cell membrane making it difficult to determine the edge of the nerve. I mitigated these problems by applying two filtering methods; coherence-enhancing diffusion (CED; demonstration shown in Figure 18) and Hessian-based filtering (HBF). I used the commercial program, Imaris (Bitplane, Zurich), to generate tessellated, three dimensional maps of nerves (Figure 15e and Figure 15f, Supplementary Video 1c). Nerve images were loaded into Imaris and user-defined control points were selected in the image using the Filament Tracer function. Imaris then used active contour mapping to fit nerve model data between control points.

3.3.5 Identification of nerve branching by computational analysis of nerve maps is superior to manual human analysis.

Computer analysis of the nerve maps identified more out of plane nerve branchpoints than human analysis of the original images could (Figure 19a-c). Nerve branchpoints are defined by the computer as the contact point between three or more neurites on the map created by Imaris. I trained volunteers in the use of Space Software (Dow M., and Scott G., http://lcni.uoregon.edu/~dow/#Space_software) to rotate three-dimensional nerve images to any arbitrary angle and to identify branchpoints using examples. Branchpoints were further designated as "in-plane" if they contained three branches visible within the non-rotated image (ie parallel to the objective, x/y field of view, colored red in Figure 19a and b) or "out-of-plane" if at least one branch was not visible in the non-rotated image (colored blue in Figure 19a and b).

Human analysis did not find additional branchpoints beyond those identified by computer. Conversely, nerve mapping analysis by computer identified significantly more (50 vs. 39.33±3.0 per observer) branchpoints than human analysis of the images (Figure 19c). Computer analysis of nerve maps identified significantly more out-of-plane branchpoints than humans (Figure 19c, see Supplementary Video 2). The missed out-of-plane branchpoints, were subsequently confirmed by human analysis of the images, once volunteers knew where to look.

3.3.6 Measurement of nerve length using by computational analysis of three-dimensional nerve maps is superior to manual two-dimensional analysis

Nerve length was measured in nerve maps by the computer. Nerves were also manually traced by connecting line segments in three-dimensional images or in flattened two-dimensional projections of three-dimensional images using maximum intensity projection, analogous to camera lucida tracing (Figure 19d-e). Nerve length was significantly (25.3 ± 8.8%) less when

measured using 2D tracing of flattened images versus 3D computer calculations. Nerve lengths using 3D manual tracing were not significantly different from the computer mapping measurement (Figure 19e), but were considerably more labor intense and time consuming.

3.3.7 Computer mapping demonstrates marked epithelial nerve heterogeneity as a function of their anatomic location in the airways

I demonstrate that nerves are present throughout the epithelial layer of airways from the trachea to the secondary bronchi in Wildtype C57Bl/6 mice (Figure 20). Epithelial nerves had a patchy distribution, complex three-dimensional morphology with repeated branching (Figure 20a), and tortuous fiber projections between epithelial cells (Figure 15d, Video 1a and 1b).

Quantification of nerve maps demonstrated regional heterogeneity of epithelial nerve branches and length with density markedly decreasing from the trachea to secondary bronchi (Figure 20). Past the secondary bronchi, epithelial nerves were only infrequently observed (data not shown). Within the trachea, both nerve branching and nerve length were greatest at the top of the trachea and at the dorsal midline (lumenal to the trachealis muscle) and decreased going down the trachea and moving around toward the front of the trachea (Figure 20b, Supplementary Videos 3a).

Decreased nerve branching was not caused by decreased nerve length for dorsal to lateral or to ventral locations since the number of branches/unit length also decreased (Figure 21). Both nerve length and nerve branching continued to decrease into the primary and secondary bronchi. A notable exception to this trend is a dramatic increase in nerve length and nerve branching at airway bifurcations (carina, secondary bifurcation, Figure 20b).

3.3.8 Clinical Potential: Mapping Human Airway Nerves

I was able to preserve the delicate epithelial nerve morphology in both human tracheas obtained at autopsy and in guinea pig tracheas. I performed similar tissue preparation and analysis as in mice with the additional step of dissecting epithelium free of deeper tissues to reduce light absorbance/scatter during image acquisition. Nerves were stained, imaged and mapped with the computer, and morphology quantified. For two guinea pig tracheas, mean epithelial nerve branching was 81±5.0 branchpoints per 135 µm x 135 µm field and nerve length was 3233.6±254.1 per 135 µm x 135 µm field (Figure 22a). In three human autopsy tracheas, mean epithelial nerve branching was 23.2±22.7 branchpoints per 135 µm x 135 µm field and nerve length was 1915.2±1127.4 µm per 135 µm x 135 µm field (Figure 23a and Figure 23b, Supplementary Videos 4a, 4b). Although these data appear to demonstrate that nerves are less dense, both in branching and length, in human than in guinea pig trachea, there is more variability in the human tracheas so additional data would be required before a species comparison could be made.

Because airway tissues from living humans are predominantly obtained by endobronchial forceps biopsy and are typically only about 1 mm across, it was important to determine whether I could image nerves in samples this small that were obtained this way. Samples obtained through bronchial forceps biopsies could also be crushed or the epithelium abraded, both of which could damage nerve architecture. I initially demonstrated that nerve architecture was preserved and quantifiable in forceps biopsies from an otherwise discarded dog airway (Figure 22b). Bronchoscopic forceps tissue obtained from human volunteers, also showed quantifiable nerve architecture in biopsies taken from the carina and from the secondary bifurcation of the airways (Supplementary Video 4c, 4d). Innervation of columnar and

squamous epithelium in biopsy tissue specimens are demonstrated in Figure 23c and Figure 23d respectively.

3.3.9 Application in skin, esophagus and intestine

Nerve supply is unique in each organ system. To test whether I could quantify nerve architecture in organs outside of the lungs, I mapped epithelial nerves in murine skin, esophagus, and intestine. Similar to the airway, nerve morphology was preserved and quantifiable. In skin (Figure 24a), epithelial nerve branching was 167±43.8 branchpoints per 135 µm x 135 µm field and nerve length was 3356.6±699.4 µm per 135 µm x 135 µm field (n=8; 5 replicates/mouse). In esophagus (Figure 24b) and colon (Figure 24c), there were 72 and 166 branchpoints and nerve length was 1659.7 µm and 3564.4 µm per 135 µm x 135 µm field respectively (n=1).

3.3.10 Mapping a Subpopulation of Airway Nerves

I mapped and quantified the uncommon subpopulation of epithelial nerves in mouse lung that contain substance P (Figure 25). Substance P positive nerves accounted for 8.1% of total nerve branchpoints and 18.4% of total neurite length. Similar to total nerves, as identified by PGP 9.5, substance P containing nerves decreased progressively going down the airway from trachea to secondary bronchi (Figure 26, Supplementary Videos 3b). However, in contrast to total epithelial nerves where branching and length are highest on the dorsal surface, substance P-containing nerve branching and length were lowest on the dorsal surface of the trachea, and increased moving ventrally (Figure 26, Supplementary Videos 3b). This proximal/distal and ventral/dorsal distribution of substance P containing nerves was seen regardless of whether branchpoints or nerve length were quantified, or whether data were expressed as a percent of

total nerves (identified by PGP9.5 staining; Figure 26). Increased substance P nerve branching, measured dorsal to ventral, was independent of nerve length (Figure 27). In contrast, decreased substance P nerve branching, measured proximal to distal, was dependent of nerve length (Figure 27). Also in contrast to epithelial nerves as a whole, there was no increase in substance P containing nerves at airway bifurcations (compare Figure 20 to Figure 26).

Using this method I was able to map substance P containing nerves in human autopsy tracheas (not shown), human airway biopsies (Figure 28b and Supplementary Video 4c and 4d), guinea pig airway Figure 28a), and mouse skin (Figure 28c).

3.4 Discussion

Nerves are capable of exhibiting an astonishing array of rapid and long-term structural changes including nerve swelling, fragmentation, retraction, growth, and branching (Kerschensteiner, Schwab et al. 2005; Chakrabarty, McCarson et al. 2011). Previous work has shown that in disease, structural neuroplasticity coincides with functional neuroplasticity (Di Giulio, Tenconi et al. 1989; Lauria, Cornblath et al. 2005; Oh, Jong et al. 2006). However, my ability to measure these change in vivo has been hindered by my inability to sample and quantify three-dimensional nerve morphology in tissues. For example, human studies have linked increased nerve density to cough (O'Connell, Springall et al. 1995), heart arrhythmia (Cao, Fishbein et al. 2000), and inflammatory pain (Fitzgerald and Beggs 2001). However, these studies used tissue sections that provided only a limited view of nerve morphology, restricting their measurement of neuroplasticity to changes in nerve density; that would have missed most changes in nerve architecture.

Here I present a new computational method that accurately maps the three dimensional architecture of nerves and allows quantification of nerve length, branching, and

neurotransmitter content. This method allows for a large sampling of complex peripheral nerves to be analyzed at a high level of detail in a reasonable amount of time in human, dog, guinea pig and mouse airways and in mouse skin, esophagus and colon. The strength of this method is demonstrated by my ability to identify and quantify novel, regional, heterogeneity in epithelial nerves and reveal an uncommon nerve population in mouse airways.

I used whole mount confocal microscopy because it captured full nerve structure compared to traditional methods that include tissue sectioning and flattened confocal images. Additionally confocal microscopy had superior efficiency compared to super-resolution microscopy while retaining sufficient resolution to capture nerve morphology. I avoided dehydration, embedding, tissue sectioning, and two-dimensional image analysis in order to minimize distortion artifacts. For example, both paraffin embedding and dehydration have been shown to alter nerve length, nerve surface area, and nerve volume (Hanani, Ermilov et al. 1998; Muhlfeld, Papadakis et al. 2010). In addition, serial tissue sectioning introduces distortions that cannot be sufficiently corrected to accurately quantify the architecture of a nerve fiber when restacking images to create a three dimensional map. The microtome knife alone will introduce non-isotropic distortions that prevent accurate image alignment by computer of nerve segments even after nonlinear co-registration. Two-dimensional image analysis of nerve density also varies with tissue stretch (Karaosmanoglu, Aygun et al. 1996; Freytag, Seeger et al. 2008).

I used computational modeling to map nerves; this used all three-dimensional image data, reduced analysis error, and reduced the time it takes to analyze data. Typically after three-dimensional nerves are imaged or reconstructed from serial sections, data are flattened or manually segmented. This is not optimal because flattening discards all depth data acquired in the original images. My results show image flattening underestimates nerve length and

branching, particularly when nerves are oriented out-of-plane in the z direction. Nerves are also variably planar so flattening causes unpredictable reductions in nerve length and branching. Thus, it is impossible to infer three-dimensional nerve architecture from a flattened image. Manual reconstruction (eg camera lucida) on the other hand is effective at reproducing three-dimensional nerve morphology but is time consuming and subject to human variability.

I developed a novel computational approach to mapping and quantifying nerve architecture. I found computational mapping identified branchpoint features in three dimensional data that were consistently missed by human graders. This was true even though human graders were shown in-plane and out-of-plane branchpoints beforehand and taught to obliquely rotate images. Out-of-plane branchpoints identified by computer nerve mapping, that were originally missed by the human graders, were subsequently confirmed by the human graders. I suspect that with extensive image rotation and re-slicing human grader performance would improve but at a significant cost of time. Overall, I found my computer approach reduced the time to analyze the images and improved accuracy of analyzing three-dimensional nerve structure compared to human performance (Figure 19). By using a data format that has been standardized by engineers and that is compatible with most modeling software, this approach will allow images obtained by different people across multiple laboratories to be analyzed similarly, eliminating variability.

Using my imaging approach I found epithelial nerves throughout the large airways that had a heterogeneous distribution. However, in mice, epithelial nerves were thought to either not exist, or to only supply neuroepithelial cells (Karlsson, Sant'Ambrogio et al. 1988; Adriaensen, Brouns et al. 2003). My data show that epithelial nerves although present throughout the airways, were patchy, and were prohibitively infrequent to capture accurately

with tissue sectioning. I show that epithelial nerves also have a complex morphology, with extended undulating root-like branching patterns that would have been under sampled by cross-section.

I mapped epithelial nerves throughout the airways to demonstrate that I could quantify nerve architecture in the context of significant organ-wide heterogeneity. Using computer mapping I quantified epithelial nerve distribution and found that it fluctuates, with dense patches near airway bifurcations, and that average nerve length and branching decreases distally. A map that includes both fine nerve architecture and organ wide distribution has not been previously created. Heterogeneity of epithelial nerve density may be anatomically important for sensing inhaled particles since inhalants accumulate along the dorsal trachea and airway bifurcations (Lambert, O'Shaughnessy et al. 2011).

I used this method of sampling to image a sparse subpopulation of epithelial nerves in order to test its sensitivity. In the lungs, a subset of afferent C-fibers produce substance P and are associated with the symptoms of asthma and with neurogenic inflammation (Groneberg, Quarcoo et al. 2004; Canning and Chou 2009). Thus I imaged substance P epithelial nerves in mouse airways, analyzed their three-dimensional structure, and quantified their regional heterogeneity. Surprisingly, my data showed a dorsal-to-ventral distribution of substance P expressing epithelial nerves that was opposite to the distribution of all epithelial nerves. This demonstrates the sensitivity of organ-wide nerve sampling, but also shows nerve distribution as a whole is not necessarily predictive of the distribution of individual subpopulations. Given that substance P nerves were present at low density (only 8% of branchpoints were substance P positive) and heterogeneously distributed, I predict that an impractically large number of tissue sections would have been necessary to capture substance P-positive epithelial nerve

distribution. The lack of special distribution of substance P nerves at airway bifurcations suggests that substance P-induced epithelial release of nitric oxide (Figini, Emanueli et al. 1997) or eosinophil chemoattractants (Koyama, Sato et al. 1998) are not preferentially concentrated where the airway splits. Substance P-expressing nerves in the epithelium may also be less involved in sensing large diameter inhalants since these particles tend to deposit on the dorsal trachea and airway bifurcations (Lambert, O'Shaughnessy et al. 2011).

Clinical studies in living patients require use of biopsies, including from the airways, skin and intestine. Airway tissues can be obtained by fiberoptic bronchoscopy with endobronchial forceps biopsy that offers the methodological advantage of allowing quantification of nerves before and after any treatment and additionally of correlating nerve quantification with disease (as assessed by clinical findings or laboratory tests). I have shown this method will keep the three-dimensional nerve morphology intact and can quantify nerve architecture in biopsy specimens. A major advantage of this method is that by not sectioning the tissue or flattening nerve images, I am able to see all nerves in the biopsy limiting errors from under sampling. Similar to mouse, the density of substance P fibers in humans is rare. Using tissue sections cut from human airway biopsies some studies found no substance P containing nerves, while others estimated that epithelial nerves that express substance P covered one-tenth the area compared to all nerves identified by PGP 9.5 (Howarth, Springall et al. 1995; O'Connell, Springall et al. 1995). Even using human biopsy specimens, my method was sufficiently sensitive to identify these rare substance P positive nerves.

I demonstrate the feasibility of using my approach in multiple organs to robustly quantify nerves by showing that I am able to map and quantify neural architecture in mouse skin, esophagus and colon. It is known that nerves in the gastrointestinal system and skin are

highly heterogeneous in mouse and rat and humans. For example, colon contains a patchwork of hypoganglionic regions surrounded by dense nerve clusters (Sibaev, Franck et al. 2003). In human skin, nerve density can vary by up to 50% depending upon patient age and skin region (McArthur, Stocks et al. 1998). My method will allow detailed quantification of nerves in all these organs.

Changes in nerve structure are likely connected to nerve function. Nerve restructuring has been associated with increased excitability in pain, itch, arrhythmia, dysmotility, and airway hyperreactivity (Janse, Peretz et al. 1999; Lauria, Cornblath et al. 2005; Grossmann, Gorodetskaya et al. 2009; Janig, Grossmann et al. 2009). Disease-associated neuroplasticity has been implicated in a variety of organ systems. For example, increased epithelial nerve density in the lungs is associated with cough (O'Connell, Springall et al. 1995), increased epidermal nerves are present in atopic dermatitis and may contribute to itch (Foster, Simpson et al. 2011) and both increased nerve density and neuropathic changes in inflammatory bowel disease may contribute to intestinal dysmotility (Hogan, Mishra et al. 2001). Neuroplasticity studies have also highlighted therapeutic targets including studies of nerve lesions, heart arrhythmia, and inflammatory pain. In these studies, treatment of neuronal swelling with protease antagonists, reduced axon diameter with calpain antagonists, sympathetic outgrowth with clodronate, and epithelial hyperinnervation with antibodies to nerve growth factor each had therapeutic benefit (Woolf 1996; Terada, Yasuda et al. 1998; Wernli, Hasan et al. 2009; Beirowski, Nogradi et al. 2010).

Data from my current study demonstrate that nerve mapping matches or outperforms manual scoring and adequately samples organ-wide innervations to measure rare subpopulations. I quantified epithelial three-dimensional nerve length and branching and

demonstrated their organ-wide distribution. With this approach I describe previously unrecognized murine airway epithelial innervation. I also demonstrated its potential use in pre-clinical and clinical studies of large animals and human biopsy specimens as well as applicability in other organs, including skin, esophagus, and colon. Finally, the ability of this approach to capture organ-wide heterogeneity of rare nerve populations was highlighted by quantifying the substance P containing subpopulation of airway epithelial nerves.

Individual and organ-wide heterogeneity of peripheral nerves makes it difficult to adequately sample disease neuroplasticity using traditional methods. Undersampling likely contributes to opposite findings of hyper- and hypoinnervation in diabetes (Sharma and Thomas 1974; Di Giulio, Tenconi et al. 1989; Sorensen, Molyneaux et al. 2006), asthma (Ollerenshaw, Jarvis et al. 1991; Howarth, Springall et al. 1995; Goldie, Fernandes et al. 1998), and inflammatory pain (Fitzgerald and Beggs 2001; Sorensen, Molyneaux et al. 2006). A follow-up quantification of nerve structure using my computational mapping approach could solve these conflicting data and identify specific changes in nerve architecture that would implicate a causal mechanism and functional consequences of neural plasticity in airway disease. For example, mapping would allow identification of directional growth of all nerves or of a subpopulation of nerves that may point to a cellular source for neurotrophins since nerves follow a concentration gradient (Markus, Patel et al. 2002). Nerve subpopulations also have unique sensitivities to neurotrophins and other growth factors (Baudet, Mikaels et al. 2000), thus identifying whether plasticity is pan-neuronal or not would be important to identifying which neurotrophins are relevant to disease. In addition to measuring nerve length and branching, the data accumulated could be used to measure nerve swelling, nerve surface area, nerve branch angles or more complicated structural characteristics including tortuosity (Kallinikos, Berhanu et al. 2004). These may be important since my method will make it possible to quantify subtle changes in

nerve architecture at earlier time points and in milder disease. For example, nerve swelling is thought to precede changes in density in neuropathic disease (Lauria, Cornblath et al. 2005). My technique is applicable to pre-clinical and clinical human research and other organs with suspected disease neuroplasticity. I expect this method will significantly advance our understanding of neuroplasticity in disease.

3.5 Methods:

Tissues from the airway, skin, and gastrointestinal system were harvested from wildtype 6-8 week old C57Bl/6 mice. Airway tissue included the whole airway from trachea to alveoli, gastrointestinal tissue included cervical esophagus and descending colon, and skin was harvested from the base of the ear.

In addition epithelial nerves were mapped in guinea pig and human tracheal epithelium, as well as canine and human airway forceps biopsies. Human tracheal tissue was obtained from anonymous cadaveric organ donors via the Pacific Northwest Transplant Bank. All families provided informed consent for use of these tissues. De-identified and fixed human airway biopsy tissues were provided by Dr. Richard Costello, and were obtained from consenting patients and with institutional approval by the Royal College of Surgeons in Ireland (Dublin). Pathogen-free female Dunkin-Hartley guinea pigs were obtained from Elm Hill Labs (Chelmsford, MA) in filtered crates. Canine airways were provided by the Department of Comparative Medicine at Oregon Health and Sciences University. All animals were treated in accordance with the standards established by the U.S. Animal Welfare Act as set forth in the National Institutes of Health guidelines. All protocols involving animals were approved by the Institutional Animal Care and Use Committee at Oregon Health & Science University.

3.5.1 Tissue dissection

Harvested tissues were immediately fixed in Zamboni's fixative (MasterTech Scientific, FXZAMPT) overnight at 4°C. In order to expose epithelial nerves for imaging, airway and gastrointestinal lumina were opened by ventral midline incisions. In skin samples, hair was manually removed. I avoided enzymatic hair removal (eg. Nair®) in order to minimize epithelial damage. For skin, intestine, and guinea pig, canine, and human airway tissue the submucosa was removed in order to reduce the duration of immunostaining and tissue light scatter, absorbance, and spherical aberration.

After fixing, immunostaining was performed at 4°C. Tissues were blocked overnight with 4% Normal Goat Serum, 1% Triton X 100, 5% powered milk in Tris-Buffered Saline pH 7.4, then treated with rabbit polyclonal antiserum against human PGP 9.5 (a nerve-specific protein, Abd Serotec, 7863-0504) for 3 days. Tissues were washed in Tris-Buffered Saline (TBS) 5 x 1h then overnight at 4°C followed by overnight immersion in goat anti-rabbit 488 secondary antibody (Invitrogen, A-11070). Tissues were then washed in TBS 5 x 1h and mounted on a charged microscope slide with aqueous mountant (Vectorlabs, H-1200). 1mm coverslip pieces temporarily secured tissues in a lumen-up configuration before mounting. Coverslips (22x22x1.5mm) were weighed down by 100g weights and sealed with Cytoseal 60 (Richard-Allan Scientific, 8310-16). Labeling substance P nerves and smooth muscle was performed with rat-anti substance P (BD Pharmigen, clone NC1) and mouse anti-alpha smooth muscle actin (Sigma, clone 1A4) primary antibodies followed by goat anti-rat 555 (Invitrogen, A21434) and anti-mouse 647 (Invitrogen, A21235) secondary antibodies.

3.5.2 Generation of deformable surfaces for identifying three-dimensional layer boundaries

Using ImageJ, images were resampled to an x-z orthogonal orientation and 10-15 representative tissue layers were traced and saved as region files (Figure 16). My ability to identify layers by tissue morphology was validated in some sections by stains of lamina propria (laminin and collagen IV), smooth muscle (alpha smooth muscle actin), luminal epithelium (e-cadherin and DAPI), and basement membrane elastin autofluorescence,. Custom software written for Matlab loads layer region files and generates three-dimensional matrices of layer surfaces using tricubic interpolation. The software outputs layer information as both serial binary masks and masked image data for use in analysis.

3.5.3 Diffusion Filtering to Identify Nerve Structure

Nerve signal is enhanced by filtering methods designed to reduce image noise and enhance edges, linear shapes, and tubular structures. Coherence-enhancing diffusion (CED) is an anisotropic diffusion filtering method for filtering linear structures such as nerves (Weickert 1999). A three-dimensional diffusion tensor is adapted to linear structures allowing for elongated smoothing kernels along edges. CED has been used in software designed for diffusion tensor magnetic resonance imaging, microtubule identification in electron microscopy tomographs, analysis of fabrics, and fingerprint analysis. My second approach was originally developed by Frangi to identify blood vessels in angiograms and uses the Hessian matrix of second derivative image data to calculate curvature (Frangi, Niessen et al. 2001). I used open-source Matlab implementations of CED and Frangi filter made available by D.J. Kroon (http://www.mathworks.com/matlabcentral/fileexchange/24409-hessian-based-frangi-vesselness-filter). Diffusion time and gaussian sigma parameters were adjusted for signal intensity variation due to tissue thickness.

3.5.4 Quantification of Nerve Structural Characteristics

For computing nerve branching and three-dimensional length from nerve maps I used commercially-available image processing software, Imaris (Bitplane, Zurich). The program's image filtering, 64-bit capability, and user interface allow for adaptive contour fiber tracking and generation of tessellated nerve maps. The user defines controls points and the computer generates three dimensional best fitted nerve maps to intervening image data. Control points were created using the Filament tracer module of Imaris. Subregion analysis was used for images with homogenous density. Imaris also supports VMRL standard vector graphics for generating bit-mapped masks from tessellated data. With nerve structure mapped, structural characteristic can be quantified by the computer, including nerve length, branching, density, surface area, measures of tortuoisity, and branch angle. Nerve length and branching were calculated for the current study and expressed in microns or number of branchpoints per 135 µm x 135 µm field.

Although not used in the current study, I adapted software for 3D printing (http://www.freesteel.co.uk) to create masks from nerve map data (data not shown). These (bitmapped) masks are useful in colocalization studies.

3.5.5 Comparison of Computer Nerve Mapping Analysis to Manual Human Quantification

Manual quantification of branchpoints in three-dimensional images of airway nerves was compared to my computer nerve mapping approach. Three blinded human observers were given six 63x image stacks and branchpoints were counted as the convergence of three or more neurites or "branches". Branchpoints were designated as "out-of-plane" if a branch was

oriented in a different direction to the original image (ie not parallel to the objective (x,y) field of view). Conversely, branchpoints designated as “in-plane” contained three branches viewable within the non-rotated image. Human counters were given a priori instructions on viewing non-rotated (orthogonal) images and rotated (oblique) images, and shown examples of in-plane and out-of-plane branches.

Nerve length was compared to two forms of manual quantification. In six 63x image stacks, nerves were manually traced in ImageJ as connected line segments in 3D image data (“3D Manual”) or flattened 2D maximum intensity projections of the 3D data (“2D Manual”). In both the 2D and 3D manual approaches, nerve length was calculated as the sum of Cartesian lengths for each tracing segment.

CHAPTER 4: HYPERINNERVATION AND INCREASED REFLEX BRONCHOCONSTRICTION ASSOCIATED WITH EOSINOPHILS IN A MODEL OF CHRONIC ALLERGIC INFLAMMATORY ASTHMA

4.1 Introduction

As discussed in Chapter 1, asthma is an inflammatory disease characterized by hyperresponsiveness of airway peripheral nerves. Previous data are inconclusive as to whether nerve hyperresponsiveness and chronic inflammation are linked by inflammation-induced changes to nerve growth and morphology. Based on other diseases (Chakrabarty, McCarson et al. 2011; Foster, Simpson et al. 2011), I hypothesized that epithelial nerves undergo branched outgrowth in association with increased nerve responsiveness. However, the heterogeneous distribution of epithelial nerves throughout the airway and their individual three-dimensional branching structure make it difficult to study using tissue sectioning and two-dimensional analysis. I used a three-dimensional computational approach (as described in Chapter 3) to increase organ-wide sampling and quantify individual nerve structure.

The current chapter also addresses the role of eosinophils as an inflammatory mechanism of neuroplasticity in asthma. Eosinophils are a biomarker and therapeutic target in asthma and have been implicated in sensory neuroplasticity outside the airway. However, the various subtypes and heterogeneous inflammation in asthma make it difficult in humans to isolate the role of one inflammatory cell type. Thus I used transgenic mice where eosinophils were selectively eliminated or upregulated in the airway. In a chronic eosinophilic asthma model, I quantified nerve structure and reflex (neural) bronchoconstriction and found eosinophils were associated with branched outgrowth of epithelial nerves and increased reflex

bronchoconstriction. In two control groups lacking eosinophils there was no increase in branched outgrowth of epithelial sensory nerves and no increased reflex bronchoconstriction. Ex vivo organ bath experiments demonstrated smooth muscle was not hyper-contractile in eosinophilic mice. I conclude that eosinophils are important for long-term remodeling of epithelial nerves and airway hyperresponsiveness in asthma.

4.2 Methods

4.2.1 Animal Care and Euthanasia

Wildtype C57BL/6 mice and transgenic mice (PHIL and NJ.1726 discussed in Chapter 2) all on a C57BL/6 background were housed in a pathogen-free facility run by the Department of Comparative Medicine. For allergen sensitization experiments, cohorts of similarly-aged (6-8 weeks) female C57BL/6 wildtype mice were ordered from Jackson Laboratory (Bar Harbor, ME). In non-survival experiments, mice were euthanized with an intraperitoneal injection of 120 mg/kg pentobarbital in PBS. All animals were treated humanely with regard for alleviation of suffering in accordance with the standards established by the U.S. Animal Welfare Act as set forth in the National Institutes of Health guidelines (NIH 2002). All protocols involving animals were approved by the Institutional Animal Care and Use Committee at Oregon Health & Science University.

4.2.2 Mouse Models of Chronic and Acute Allergic Inflammatory Asthma

I utilized a transgenic mouse line called “PHIL” (“NoEos”) that has selective ablation of eosinophils as discussed in Chapter 2 “Transgenic Mice Lacking Eosinophils (PHIL)”. I also used a transgenic mouse model of chronic allergic inflammatory asthma called “NJ.1726” (“IL5++/Eos++”) that contains overabundant eosinophils specifically in the airways caused by IL-

5 overexpression as discussed in Chapter 2 “Transgenic Model of Chronic Allergic Inflammatory Asthma with Airway Eosinophilia (NJ.1726)” (Crosby, Shen et al. 2002). I also used an ovalbumin mouse model of acute allergic inflammatory asthma. Over the period of a month mice were sensitized to a foreign protein, ovalbumin (Sigma, 5253), and challenged with repeated airway exposures to model acute allergic airway hyperreactivity as discussed in Chapter 2 “Mouse Model of Acute Allergic Inflammatory Asthma”.

4.2.3 Measuring Mouse Airway Mechanics In Vivo

In order to measure mouse airway mechanics in vivo, mice were anesthetized, paralyzed, and mechanically ventilated and subsequently given aerosol stimulants while measuring airway narrowing (Figure 7) as discussed in Chapter 2 “Measuring Mouse Airway Mechanics In Vivo”. In ventilated mice airway responsiveness was measured as changes in airway resistance caused by aerosol administration of serotonin (Figure 8) as discussed in Chapter 2 “Measuring Reflex Bronchoconstriction in Ventilated Mice”.

4.2.4 Imaging Airway Nerves

In order to harvest tissues for immunohistochemistry, airways were rapidly harvested and fixed for use in nerve imaging studies as discussed in Chapter 2 “Tissue Harvesting for Immunohistochemistry”. Microdissection was used to expose the whole airway for imaging as discussed in Chapter 2 “Whole Mount Airway Dissection”. Immunostaining tissue whole mounts was performed as discussed in Chapter 2 “Whole Mount Immunostaining”.

4.2.5 Measuring Trachea Constrictions Ex Vivo

Finally, constrictions of the isolated trachea were measured *in vitro* as described in Chapter 2 “In vitro constriction of isolated mouse trachea”.

4.3 Results

4.3.1 Chronic Eosinophilic Asthma Mice Have Increased Nerve Branching and Total Neurite Length

Using computer modeling analysis of three-dimensional epithelial nerve structure, NJ.1726 mice (++IL5/++Eos) had roughly double both the number of branchpoints (83.8 ± 7.0 vs 39.6 ± 10.4) and total neurite length (2126.4µM ± 415.4 vs. 1084.3µM ± 166.2) versus wildtype littermates (Figure 31). NJ/PHIL (++IL5/NoEos) and PHIL (No Eos) mice contained wildtype amount of nerve length and branching.

4.3.2 Increased Reflex Bronchoconstriction in Chronic Allergic Inflammatory Asthma Mice

Mice with chronic lung eosinophilic asthma and wildtype littermates exhibited bronchoconstriction to serotonin that was prevented by vagotomy (Figure 30). The chronic allergic inflammatory asthma mice (n=9) exhibited increased reflex bronchoconstriction before vagotomy compared to wildtype mice (n=7) (compare red to black lines in Figure 30) as well as mice lacking eosinophils with increased IL-5 (++IL5/NoEos, n=3) or without increased IL-5 (NoEos, n=3). After vagotomy, bronchoconstriction in the mouse model of chronic allergic inflammatory asthma was not significantly different from other mouse groups (lower panel of Figure 30) although there was a variable non-significant response at the highest serotonin dose.

4.3.3 No Change in Smooth Muscle Responsiveness in Chronic Eosinophilic Asthma Model

Ex vivo constrictions were measured using trachea isolated from mice with chronic eosinophilic asthma and wildtype littermates. There was no significant difference between mice with chronic eosinophilic asthma (n= 12) and wildtype littermates (n=17) at any dose of acetylcholine or methacholine (Figure 32). There was also no difference in cholinergic neuronal contraction between mice with chronic eosinophilic asthma (n= 14) and wildtype littermates (n=19) measured using electrical field stimulation (Figure 32).

4.3.4 Nerve Branching and Neurite Length is Unchanged in a Mouse Model of Acute Allergic Inflammatory Asthma

Using computer modeling analysis of three-dimensional epithelial nerve structure, ovalbumin sensitized and challenged mice did not have significantly different numbers of branchpoints (67.94 ± 14.2 vs 73.7 ± 21.7) or total neurite length (2063 µM ± 228.8 vs. 1981µM ± 499.2) versus untreated wildtype controls (Figure 33).

4.4 Discussion

The current study used three-dimensional nerve quantification with computer modeling to investigate asthma structural neuroplasticity and the potential role of eosinophils. I found chronic airway eosinophilic asthma was associated with increased branched outgrowth of epithelial nerves. This increase in nerve branching and length was also associated with potentiated reflex bronchoconstriction in vivo. Eosinophils were necessary for both nerve outgrowth and airway hyperresponsiveness.

I used a new approach for studying neuroplasticity that increases organ-wide sampling and quantifies three-dimensional structure of individual nerves. Studies using electron microscopy and more recent immunofluorescence studies have demonstrated that innervation density depends on positional variables including: proximal-to-distal location (Shimosegawa and Said 1991; Baluk, Nadel et al. 1992; Larson, Schelegle et al. 2003), distance from airway bifurcations (Chapter 3), costal versus mediastinal location (Larson, Schelegle et al. 2003), and tissue layer (Dey, Satterfield et al. 1999). Furthermore, epithelial nerves discussed in the current study exhibit marked local heterogeneity in a patchwork configuration (Chapter 3). At higher magnification than used to measure nerve density, individual nerves are also complex elongated branching structures. This small and large-scale structural heterogeneity is likely under-sampled by previous methods using tissue sections or flattened projections. Under-sampling may contribute to variable results in the literature finding increased, no change, and decreased innervation in asthma (Ollerenshaw, Jarvis et al. 1991; Howarth, Springall et al. 1995; Lilly, Bai et al. 1995; Chanez, Springall et al. 1998; Goldie, Fernandes et al. 1998). This variability is also seen in animal studies of nerve density and airway disease (Mapp, Lucchini et al. 1998; Kajekar, Pieczarka et al. 2007). I have recently shown that three-dimensional imaging and structural analysis using computer modeling can quantify both organ-wide heterogeneity and individual nerve structure. This technique also outperformed humans at detecting three-dimensional branchpoints and nerve length missed by tissue sectioning or image flattening.

Although epithelial nerves in mouse airways were only recently described outside of neuroepithelial bodies (Chapter 3), previous studies have looked at this nerve population outside of the lung in vagal ganglia in order to study their phenotype and phenotypic transitioning with inflammation. These studies have identified signaling mechanisms that inform the interpretation of the current study on eosinophils and epithelial neuroplasticity. A

recent phenotypic characterization of mouse airway sensory nerves demonstrated that most jugular ganglion-derived C fibers (presumed source of epithelial nerves in mouse large airways) express neurotrophin receptors which are commonly implicated in inflammatory neuroplasticity. One population of jugular C fibers expressed TRKA, the receptor for nerve growth factor (NGF), whereas the other jugular C fibers tended to express TRKB, the receptor for brain-derived neurotrophic factor (BDNF). Importantly, both of NGF and BDNF are synthesized and stored by eosinophils and release of NGF from eosinophils is increased in allergic diseases including asthma (Noga, Englmann et al. 2003; Raap and Braunstahl 2010). Thus in asthma, lung eosinophils may release NGF or BDNF to induce epithelial nerve outgrowth and exacerbate airway hyperresponsiveness. Jugular C fiber nerves were also shown to express receptors for glial cell-derived neurotrophic factor (GDNF) family ligands (GFLs), another family of signaling molecules implicated in neuroplasticity. In fetal lung explants, GDNF caused increased nerve outgrowth overall and GDNF gradients served as a directional cue for individual growing neurites (Tollet, Everett et al. 2002).

My data also suggest that epithelial nerve outgrowth is only a long-term consequence of eosinophilia. In future studies it will be important to further characterize the critical period and duration of eosinophilia necessary for causing eosinophil remodeling of nerves and other tissues (Humbles, Lloyd et al. 2004; Lee, Dimina et al. 2004). A study of early postnatal airway exposure in monkeys demonstrated decreased innervation density (with increased eosinophils) after 6 months of exposure and increased innervation density after recovering for 6 months (Larson, Schelegle et al. 2004; Kajekar, Pieczarka et al. 2007). Similarly, neuroepithelial cells increased with antigen sensitization in guinea pigs but decreased acutely after antigen challenge (Bousbaa and Fleury-Feith 1991). Data from cutaneous studies of injury and inflammation also narrow the potential critical period/duration. In studies of skin inflammation and injury in adult animals,

nerve hyperinnervation and increased receptive field size generally occurred within 25 to 56 days (Diamond, Holmes et al. 1992; Yen, Bennett et al. 2006) . Studies in the skin (Yen, Bennett et al. 2006; Almarestani, Longo et al. 2008) also suggest that only severe nerve injury or inflammation causes nerve density to initially decrease (as in the airway), and that neonates are more capable of nerve remodeling (Ruda, Ling et al. 2000). Future transgenic studies using inducible ablation and upregulation of eosinophils will be useful in determining the severity- and time-dependence of eosinophil-induced neuroplasticity. Inducible transgenic models can also distinguish any confounding effects of transgene insertion on lung development. Also, it will be important to resolve the difference in nerve branching and length between the control mice in the models of chronic versus acute allergic inflammatory asthma. This could reflect differences in environmental exposure that changed baseline nerve growth.

Previous nerve injury and plasticity studies are unclear whether branched outgrowth is pathologic or beneficial to the host and is associated with hypo- or hypersensitivity (Fitzgerald and Beggs 2001; Torsney and Fitzgerald 2003; Sorensen, Molyneaux et al. 2006; Tomita, Kubo et al. 2007) . Thus I combined nerve structural analysis with measuring vagus nerve-mediated airway responsiveness. My data show airway hyperreactivity is associated with epithelial nerve outgrowth. This agrees with data from others organs where branched outgrowth was linked to increased receptive field size and hypersensitivity (Torsney and Fitzgerald 2003). However, other studies found branched outgrowth is associated with failed reinnervation and hyposensitivity (Tomita, Kubo et al. 2007). Similar to the time-dependent decreased and increased innervation density described above, I suspect future studies will find both increased and decreased epithelial nerve sensitivity depending on the time after insult. It is important to note that hypersensitivity in airway A fibers has been shown to occur rapidly and in association with neurotrophin-dependent phenotypic changes. Data from three separate labs have shown

altered A fiber responses caused by allergen, NGF-, and BDNF-induced changes to a C-fiber like phenotype (TrpV1+, SP+, capsaicin responsive) (Hunter, Myers et al. 2000; Dinh, Groneberg et al. 2004; de Vries, Engels et al. 2006; Lieu, Myers et al. 2012). Remarkably, a recent study showed that allergen exposure or BDNF treatment caused TrpV1 expression in Aδ placodal fibers and *de novo* capsaicin calcium responses in isolated nerves (Lieu, Myers et al. 2012).

The nerve length and reflex bronchoconstriction data also suggest that IL-5 overexpression may cause an intermediate phenotype. IL-5 has previously been independently linked to increased airway smooth muscle contraction (Rizzo, Yang et al. 2002) but to the authors knowledge has not been linked to sensory neuroplasticity.

The untreated and wildtype control mice in the acute versus chronic asthma experiments contained different nerve branching and growth which may be caused by different surrounding environment. This has been shown previously to influence an eosinophil's impact on nerves. For example, eosinophils mediate virus-induced airway hyperreactivity only in allergen sensitized guinea pigs and not in non-sensitized guinea pigs (Adamko, Yost et al. 1999). Depletion of eosinophils is not protective in virus infected guinea pigs unless the guinea pigs are also sensitized to a protein. Perhaps environmental exposures caused different amounts of baseline nerve branching and growth.

The heterogeneous long and short-term manifestations of asthma make it difficult to study long-term cause-effect relationships. I used three-dimensional nerve modeling in a chronic transgenic asthma model in order to more fully quantify airway neuroplasticity and specifically manipulate eosinophil numbers. With this approach I detected significant outgrowth of epithelial nerves and increased reflex bronchoconstriction caused by eosinophils. This study

highlights the understudied long-term effects of eosinophils on the airway and the potential clinical benefit of preventing long-term eosinophilia in asthma.

CHAPTER 5: NEUROTROPHIC AND NEUROPATHIC EFFECTS OF EOSINOPHILS ON SENSORY NERVES IN THE SKIN

5.1 Introduction

Similar to previous asthma studies and the current dissertation (Chapter 4), nerve density in the skin was previously demonstrated to be increased in patients with atopic dermatitis and in an eosinophilic transgenic mouse model of dermatitis. Foster et al. showed with sensory nerve and eosinophil co-culture experiments that eosinophils induced nerve branching through a contact-independent mechanism (Foster, Simpson et al. 2011). Previous studies have shown eosinophils can synthesize, store, and release soluble mediators such as neurotrophins that influence nerve growth. This is important because nerve outgrowth is associated with skin diseases characterized by itch such as atopic dermatitis and prurigo nodularis. Thus eosinophil-induced neuroplasticity may be an important mechanism underlying chronic itch.

My goal was to advance a previous study of atopic dermatitis (Foster, Simpson et al. 2011) by using a three-dimensional computer mapping technique in conjunction with models of dermatitis in wildtype mice and mice lacking eosinophils. In the past, quantification of nerves was performed using conventional tissue sectioning, which is susceptible to undersampling error and missing nerve structure. In order to overcome this, I used my computer mapping to increase data sampling and quantify three-dimensional nerve structure. I tested if nerve structure changes in mouse models of dermatitis, if eosinophils are necessary for neuroplasticity, and if dermatitis severity and time course impact neuroplasticity. I quantified nerve structure in both a transgenic eosinophilic model of chronic dermatitis and two chemical treatment models of dermatitis, one with an acute (5 day) time course and one with a subacute (15 day) time course. Treatment with the compound, 2,4-Dinitrofluorobenzene (DNFB) was

used for the acute dermatitis model and treatment with Trimetallic Anhydride (TMA) was used for the subacute (15 day) dermatitis model. I also performed co-culture experiments using human DRGs and eosinophils in order to test if eosinophils were sufficient for nerve growth.

5.2 Methods

5.2.1 Animal Care and Euthanasia

Mouse colony maintenance and dermatitis treatment protocols were performed by the Lee Laboratory at the Mayo Clinic in Scottsdale, Arizona. PHIL (discussed in Chapter 2) and K14/PHIL mice all on a C57B/6 background were housed in a pathogen-free facility at the Mayo Clinic. For chemical treatment dermatitis experiments, cohorts of wildtype BALB/cJ mice were purchased commercially and PHIL mice were maintained in-house. In non-survival experiments, mice were euthanized with an intraperitoneal injection of 30 mg/kg pentobarbital in PBS followed by carbon dioxide inhalation. All animals were treated humanely with regard for alleviation of suffering in accordance with the standards established by the U.S. Animal Welfare Act as set forth in the National Institutes of Health guidelines (NIH 2002). All protocols involving animals were approved by the Institutional Animal Care and Use Committee at the Mayo Clinic.

5.2.2 Imaging Epidermal Nerves

Skin was harvested and processed for imaging epidermal nerves as discussed in Chapter 2 “Skin Dissection to Image Epithelial Nerves”, “Tissue Harvesting for Immunohistochemistry”, and “Whole Mount Immunostaining.”

5.2.3 Transgenic Model of Chronic Dermatitis with Skin Eosinophilia (IL5/K14)

I used a transgenic mouse model of chronic dermatitis called IL5/K14 that contains overabundant eosinophils specifically in the skin (Foster, Simpson et al. 2011). This is accomplished by overexpression of IL-5 under a skin-specific promoter found in keratinoctytes, K14, on a C57BL/6 background. IL-5 causes increased survival and recruitment of eosinophils, thus K14 driven expression leads to marked increases (greater than 30-fold) in skin eosinophils. Some IL5/K14 mice develop spontaneous skin lesions which were shown to contain increased major basic protein. An additional double-transgenic control mouse was generated (K14/PHIL) where IL-5 is overexpressed in the skin but eosinophils are ablated. This double-transgenic isolates the impact of IL-5 independent of eosinophils.

5.2.4 Chemical Treatment Model of Acute Dermatitis using 2,4-Dinitrofluorobenzene

For the chemical treatment model of acute dermatitis, age-matched wildtype and PHIL mice were sensitized and challenged with 2,4-Dinitrofluorobenzene (DNFB) over a five day period. Before treatment mice were placed under isoflurane anesthesia via nose cone. On day 0 and day 1 mice were sensitized to DNFB by topical application to the dorsal skin. Fur was removed from a 3 cm square of dorsal skin and 25 µl of 0.5% DNFB in vehicle (acetone/olive oil = 3:1) was applied topically. On day 5 mice were simultaneously challenged with DNFB by topical application to the left ear and challenged with vehicle control to the right ear. 25 µl of 2% DNFB in vehicle (acetone/olive oil = 3:1) was spread over the dorsal side of the left ear and vehicle was spread over the dorsal side of the right ear. On day 6 mice were anesthetized by pentobarbital (30 mg/kg) injection and euthanized by carbon dioxide inhalation.

5.2.5 Chemical Treatment Model of Subacute Dermatitis using Trimetallic Anhydride

For the chemical treatment model of subacute dermatitis, age-matched wildtype and PHIL mice were sensitized and challenged with trimetallic anhydride (TMA) over a 14 day period. Before treatment mice were placed under isoflurane anesthesia via nose cone. On day 0 and day 5 mice were sensitized to TMA by topical application to the dorsal skin. Fur was removed from a 3 cm square of dorsal skin and 50 µl of 5% TMA in vehicle (acetone/olive oil = 3:1) was applied topically. On days 6 through 14 mice were simultaneously challenged with TMA by topical application to the left ear and challenged with vehicle control to the right ear. 15 µl of 2% TMA in vehicle (acetone/olive oil = 3:1) was spread over the dorsal side of the left ear and vehicle was spread over the dorsal side of the right ear. On day 15 mice were anesthetized by pentobarbital injection (30 mg/kg) and euthanized by carbon dioxide inhalation.

5.2.6 Nerve Density Quantification of Mouse Skin

From (Foster, Simpson et al. 2011). 60x images were taken of an entire 5 µm section through each mouse skin biopsy. Photographs were blinded to the human grader and nerve number was counted manually in the epidermis and dermis. Quantification of nerves per area or nerves per unit length of basement membrane did produce different results.

5.3 Results

5.3.1 Epidermal Nerve Density is Increased in a Chronic Dermatitis Model with Skin Overexpression of IL-5 and Eosinophilia

Foster et al. showed nerve density was more than doubled in the epidermis of IL5/K14 mice with chronic dermatitis due to IL-5 overexpression and eosinophilia in the skin (Foster, Simpson et al. 2011) (Figure 34). In the dermis, the density of nerves was not significantly different between IL5/K14 and wildtype mice (data not shown). Quantification of nerves per area or nerves per unit length of basement membrane did not produce different results.

5.3.2 Epidermal Nerve Branching and Length are Not Changed in Mice with Skin Overexpression of IL-5 and Absence of Eosinophils.

I found that nerve length and branching in the epidermis were not significantly different between wildtype and K14/PHIL mice (Figure 35). Three-dimensional epidermal nerve structure was quantified in four wildtype mice and four mice overexpressing IL-5 in the skin but lacking eosinophils (K14/PHIL). Nerves were modeled with the computer and three-dimensional nerve length and branching were quantified.

5.3.3 Chemical Treatment Model of Subacute Dermatitis is Not Associated With Structural Neuroplasticity.

Wildtype and PHIL mice lacking eosinophils were treated over 14 days with TMA which resulted in eosinophilic inflammation, swelling of the treated ear, and itch (personal communication with the Lee laboratory). I imaged epidermal innervation in TMA treated and untreated ears and used computer modeling to quantify three-dimensional nerve branching and length. Nerve branching and length were not significantly different between TMA and untreated ears in Wildtype and PHIL mice (Figure 36). PHIL mice exhibited decreased itch of the TMA treated ear compared to wildtype mice (personal communication with the Lee laboratory).

5.3.4 Decreased Nerve Branching and Length in a Chemical Treatment Model of Acute Dermatitis is Prevented by Loss of Eosinophils.

Wildtype and PHIL mice lacking eosinophils were treated over 5 days with DNFB which resulted in eosinophilic inflammation, swelling of the treated ear, and itch (personal communication with the Lee laboratory). I imaged epidermal innervation in DNFB treated and untreated ears and used computer modeling to quantify three-dimensional nerve branching and length. In wildtype mice epidermal nerve branching and length was significantly decreased in the DNFB treated ear versus the vehicle treated ear. However, in PHIL mice lacking eosinophils, there was not a significant decrease in nerve length or branching in the DNFB treated versus untreated ear (Figure 37). PHIL mice exhibited decreased itch of the DNFB treated ear compared to wildtype mice (personal communication with the Lee laboratory).

5.3.5 Co-culture of Human Sensory Neurons with Human Eosinophils Increases Nerve Length

Human sensory nerves from dorsal root ganglia were cultured with and without human eosinophils from peripheral blood and nerve length and branching were quantified. Confirming previous studies in mouse DRG, co-culture with human eosinophils was associated with increased length of human DRG sensory nerves (Figure 38). There was no change in branching. Previous studies showed this effect was not caused by co-cultured mast cells and eosinophil-induced outgrowth depended on eosinophil-viability (Foster, Simpson et al. 2011).

5.4 Discussion

Here I show that a chronic mouse model of dermatitis contains increased epidermal nerves and that an acute model of dermatitis contains decreased nerve branching and length.

Surprisingly I found that eosinophils were needed for both the neurotrophic effects of increased nerves in my chronic dermatitis model and the neuropathic effects of decreased nerves in my acute DNFB dermatitis model. I also show that isolated human eosinophils co-cultured with human sensory nerves cause neurotrophic nerve outgrowth replicating earlier findings using mouse DRGs. These opposite forms of sensory neuroplasticity caused by eosinophils were both associated with itch which may coincide with known distinct mechanisms of acute versus chronic itch in dermatitis.

5.4.1 Neuroplasticity Timecourse and Dependence on Inflammatory Insult

Different neuroplasticity was observed in wildtype mice in my dermatitis models which may be caused by both capturing nerves at acute versus chronic time points after insult and caused by using different severities of inflammatory insult. These data from IL5/K14, TMA, and DNFB dermatitis models may reflect the normal timecourse of peripheral neuroplasticity after nerve insult (Rajan, Polydefkis et al. 2003). Unlike nerve increases which were seen in a chronic IL5/K14 transgenic model of dermatitis and in humans with longstanding atopic dermatitis, nerve branching and length decreased acutely in a short DNFB treatment model of dermatitis. Early nerve retraction after insult is commonly reported in other models of nerve injury and inflammation (Kerschensteiner, Schwab et al. 2005). Thus the short timecourse of DNFB treatment may have only allowed time for the initially retraction of epidermal nerves but not subsequent regrowth and hyperinnervation. Unlike the loss of nerves with 5 day DNFB treatment, fifteen day treatment with TMA did not change nerve branching or length. One possibility based on the time course of neuroplasticity is that TMA initially decreased nerve length/branching and was subsequently repaired. Alternatively TMA treatment may not have been as severe as DNFB at causing inflammation to change nerve structure at all. Previous

studies have shown nerve retraction and regrowth after injury/inflammation depends on the severity of the initial insult. A milder insult tends to cause less nerve retraction and permits subsequent nerve regrowth and hyperinnervation whereas severe nerve injury (eg. excision, transection, nerve sheath removal) causes permanent nerve loss without regrowth (Rajan, Polydefkis et al. 2003; Yen, Bennett et al. 2006; Almarestani, Longo et al. 2008). By producing a more severe insult than TMA, DNFB may have consequently caused a detectable amount of nerve retraction and prevented nerve repair.

In terms of neurotrophic effects, unlike in the K14 transgenic chronic model of dermatitis, subacute 14 day TMA treatment was not associated with increased innervation. Most studies suggest a longer timecourse is needed for peripheral regeneration. With skin inflammation and injury in adult animals, nerve hyperinnervation and increased receptive field size generally occurred within 25 to 56 days (Diamond, Holmes et al. 1992; Yen, Bennett et al. 2006). If nerves were re-growing after TMA treatment, they may have ultimately hyperinnervated the dermis given additional time as was seen in the chronic transgenic model of dermatitis. However other studies have shown hyperinnervation can occur in much shorter (3 day) time spans (Chakrabarty, McCarson et al. 2011). Only one day elapsed after the last TMA treatment before harvesting the skin. Perhaps a longer recovery period would reveal TMA-induced hyperinnervation.

5.4.2 Neurotrophic Effects of Eosinophils

My data in the eosinophilic transgenic model of chronic dermatitis show eosinophils are necessary for nerve outgrowth and that Il-5 alone does not cause epidermal neuroplasticity. Mice with overabundant skin eosinophils due to IL-5 overexpression (IL5/K14) have previously been shown to contain increased epidermal nerves (Foster, Simpson et al. 2011). To test if

eosinophils in the IL5/K14 mouse model are necessary for epidermal nerve outgrowth I utilized double transgenic K14/PHIL mice where IL-5 was overexpressed by the same K14 promoter but eosinophils were absent. In contrast to IL5/K14 mice, K14/PHIL mice did not show increased epidermal nerve branching or length compared to wildtype littermates. Thus eosinophils are necessary for chronic sensory nerve outgrowth which may contribute to long term itch and neurogenic inflammation in atopic dermatitis. Aside from atopic dermatitis, eosinophil inflammation is also associated with increased nerves in another itchy skin disease, prurigo nodularis, as well as enteric parasitic infection, asthma, and appendicitis (Ollerenshaw, Jarvis et al. 1991; Liang, Jacobi et al. 2000; O'Brien, Fitzpatrick et al. 2008; Singh, Malhotra et al. 2008). Eosinophils are known to produce neurotrophic compounds including members of the neurotrophin signaling family, NGF, BDNF, and NT-3 which serve as nerve survival and growth guidance cues (Kobayashi, Gleich et al. 2002; Noga, Englmann et al. 2003). In co-culture, peripheral blood eosinophils from healthy patients prevent nerve apoptosis and promote neurite outgrowth (Kobayashi, Gleich et al. 2002; Morgan, Kingham et al. 2004). Here I show human eosinophils from peripheral blood also promote growth of human sensory nerves in co-culture experiments. Eosinophils also produce cationic granule proteins that at lower concentrations are non-toxic and have been shown to be both chemoattractant and cause neuroplasticity in cholinergic nerves. For example EDN is chemoattractant for dendritic cells (Yang, Rosenberg et al. 2003) and MBP/EPO increases acetylcholine signaling molecules (M2 muscarinic receptor, choline acetyltransferase, vesicular acetylcholine transferase) in co-cultured cholinergic nerves (Durcan, Costello et al. 2006)

5.4.3 Neuropathic Effects of Eosinophils

Opposite of eosinophil neurotrophic effects in IL5/K14 mice, eosinophils were responsible for the neuropathic effects of decreased nerves and branching in my DNFB model of acute dermatitis. Eosinophils in other diseases are also associated with decreased nerves or neurotoxicity in multiple sclerosis, neuromyelitis optica, and eosinophilic myelitis (Milici, Carroll et al. 1998; Lucchinetti, Mandler et al. 2002; Osoegawa, Ochi et al. 2003; Correale and Fiol 2004). Eosinophils are also known to produce neurotoxic compounds. As mentioned above eosinophil granule proteins at low doses are neurotrophic and chemoattractant, but at higher doses granule proteins have been shown to be profoundly neurotoxic. Injection of eosinophil cationic protein, eosinophil derived neurotoxin, or eosinophils themselves into cerebrospinal fluid or cerebral cortex causes widespread neuropathy (axon fragmentation, swelling, complete destruction) (Newton, Walbridge et al. 1994). In a murine model of enteric eosinophilic inflammation, eosinophils were seen next to damaged axons suggesting a neuropathic interaction with myenteric nerves (Hogan, Mishra et al. 2001). Unlike my current results and others studies that showed eosinophils in co-culture produce neurotrophic effects, eosinophils can also cause neurotoxicity in culture. Peripheral eosinophils from a patient with peripheral neuropathy were shown to kill more co-cultured nerves than eosinophils isolated from healthy patients (Sunohara, Furukawa et al. 1989). Co-culturing eosinophils with a cholinergic nerve cell line did not kill nerves but inhibited neurite outgrowth (Kingham, McLean et al. 2003).

5.4.4 Factors Determining Neurotrophic Versus Neuropathic Effects of Eosinophils

Surprisingly, eosinophils were necessary for both increased nerves in my chronic transgenic model of dermatitis and eosinophils were necessary for decreased nerves in my acute DNFB dermatitis model. These differential effects of eosinophils on nerve architecture

can be regulated by a variety of factors including the concentration of eosinophil-derived mediators, the activation state of eosinophils, and regulation at individual granule proteins themselves.

As discussed above, the concentration of eosinophil-derived neuromediators influences their neurotrophic versus neuropathic effect. Low concentrations of eosinophil granule proteins caused adhesion-dependent neurotrophic effects on co-cultured nerves whereas supra-physiologic administration of granule proteins causes profound neurotoxicity. Neurotrophic factors that are made by eosinophils, such as NGF and BDNF, are also known to act on nerves in a concentration-dependent manner (Markus, Patel et al. 2002). Thus the amount of eosinophil accumulation and proximity to nerves will influence the "dose" of eosinophil-derived mediators influencing a nerve.

The opposite neurotrophic and neurotoxic effects of eosinophils on nerves may reflect different activation states and extracellular release mechanisms of eosinophils. Eosinophils have distinct "hypodense" and "normodense" activation states with different sensitivities to perform inflammatory effector functions (Czech, Dichmann et al. 2001; Kaatz, Berod et al. 2004), and 2) eosinophils have differential release mechanisms including regulated secretion, piecemeal degranulation, or cytolysis and release of all intact granule proteins (Moqbel and Coughlin 2006). Eosinophils have been shown to activate and release neurotrophins and low levels of granule proteins which induce neurotrophic effects and neuroplasticity. Eosinophils can be activated by platelet activation factor, a pro-inflammatory lipid mediator, or by IL-5/IgA to release a dose-dependent amount of NGF and BDNF (Kobayashi, Gleich et al. 2002; Noga, Englmann et al. 2003). Eosinophils can induce plasticity of cholinergic nerves which depends on eosinophil activation by adherence, eosinophil release of NGF, but also on eosinophil granule proteins, MBP and EPO (Durcan, Costello et al. 2006). In contrast, eosinophils can be activated

to fully lyse and release formed granule proteins extracellularly which have been shown to be cytotoxic (Erjefalt, Sundler et al. 1996; Erjefalt, Korsgren et al. 1997; Erjefalt, Greiff et al. 1999). This neurotoxicity may be caused by proteins in eosinophil granules, which when injected into the cerebral cortex or cerebrospinal fluid at high concentrations causes profound neuropathy (Newton, Walbridge et al. 1994) . Interestingly, another level of activation at the scale of an individual granule protein may play a role in regulating neuroplasticity caused by eosinophil release of intact granules. Individual eosinophil granules express receptors for inflammatory signals (eg. interferon gamma) and can independently secrete granule proteins (eg. ECP) depending on the extra-granule environment (Neves, Perez et al. 2008).

In addition, differential effects of eosinophils on nerves may be caused by different populations defined by the age of eosinophils. Eosinophils are resident at homeostatic levels in some tissues and there is a pool of pre-existing circulating eosinophils readily recruited upon stimulation but new eosinophils are also synthesized and recruited to diseased tissue. These resident, old, and new eosinophil populations have been shown to exhibit opposite effects in animal models of asthma. In guinea pig models of asthma, my lab has shown pre-formed resident or early arriving “old” eosinophils exacerbate airway hyperreactivity whereas newly synthesized “new” eosinophils reduce airway hyperreactivity upon entering the lungs three days after antigen challenge . Thus overall eosinophil age, activation, and mechanisms of extracellular release may provide further regulation of neuroplasticity. For example, new eosinophils might cause neurotrophic effects by localizing close to nerves or adhering to nerves and releasing neurotrophins or low levels of granule proteins. Alternatively activated or old eosinophils such as those derived from the patient with peripheral neuropathty might release neurotoxic quantifies of granule proteins.

5.4.5 Opposite Forms of Neuroplasticity Both Associated with Itch

Unexpectedly, I found opposite forms of neuroplasticity in my acute versus chronic dermatitis model that were both associated with itch. Previous data have shown itch is caused by multiple independent signaling mechanisms. In general these can be divided into three forms with distinct sensory nerve populations (Wilson, Gerhold et al. 2011): 1.) histamine- and serotonin-induced itch caused by activating $5HT_3$ and H1 histamine receptor-expressing C fibers, 2.) antihistamine-insensitive itch induced by the anti-malarial, chloroquine, which activates a different C fiber population that express an orphan receptor, MrgprA3, and 3.) another antihistamine-insensitive itch caused by an endogenous poorly characterized compound, BAM8-22 (Liu, Tang et al. 2009). Only a subset of patients with dermatitis benefit from antihistamine treatment suggesting that non-histamine forms of itch are also important (Rukwied, Lischetzki et al. 2000; Steinhoff, Neisius et al. 2003). In addition there are populations of sensory nerves that may reduce itch sensations indirectly through the release of anti-inflammatory peptides such as VIP (Roosterman, Goerge et al. 2006). These unique forms of itch may be caused by different lesions and different underlying inflammatory signaling seen in acute versus chronic dermatitis. Acute dermatitis lesions are spongiotic (edematous) papulo-vesicular (raised vesicles) erythematous (red) lesions that contain increased eosinophils as well as increased mast cells and IL-4 producing Th2 cells (Maintz and Novak 2007; Bieber 2008). In general acute lesions are characterized by Th2-type inflammation with increased IL-4, IL-5, and IL-13 (Maintz and Novak 2007). On the other hand, chronic dermatitis lesions are thickened with hypertrophy of the epidermis, fibrotic, and contain nodular plaques (Correale, Walker et al. 1999; Maintz and Novak 2007; Bieber 2008). Both the presence of eosinophils and IL-5 levels stay elevated in chronic lesions but otherwise chronic dermatitis involves a shift from Th2 to Th1 signaling where IL-4 is decreased and interferon gamma, IL-12, GM-CSF, Th1 T cells overall are increased (Hamid, Boguniewicz et al. 1994; Correale, Walker et al. 1999; Maintz and Novak 2007; Bieber 2008).

Thus different acute versus chronic inflammatory environments may activate different itch mechanisms but both depend on the presence of eosinophils. Neuropathic effects in my acute allergic inflammatory asthma model might be limited to anti-inflammatory sensory nerves that produce VIP whereas chronic neuropathic effects may be limited itch-producing C fibers. Both neuropathy of anti-inflammatory nerves and outgrowth of itch-sensing nerves could increase itch sensation in eosinophil-dependent acute and chronic dermatitis inflammatory environments.

Here I used three-dimensional computer mapping to investigate the role of eosinophils in causing increased epidermal nerves in models of atopic dermatitis. The physiologic consequences of increased nerves is potentially linked to increased itch in dermatitis by causing increased receptive field size and increases the likelihood of multiple receptive fields (Sandkuhler 2009) resulting in sensitivity to otherwise sub-threshold stimuli (Chu, Faltynek et al. 2004). I used three-dimensional mapping to quantify specific changes to nerve architecture and appreciate regional heterogeneity. I found nerve branching and length initially retract and subsequently undergo outgrowth in chronic dermatitis both of which were dependent on eosinophils. These opposite neurotrophic and neurotoxic effects of eosinophils may likely reflect unique activation states of eosinophils influencing their release of different neuromediators. Future studies using three-dimensional computer mapping should be useful to understand the timecourse of nerve retraction, regrowth, and hyperinnervation. Subtler changes like axonal swelling can also be calculated using my approach and have been shown to be present in milder forms of peripheral neuropathy (Lauria, Cornblath et al. 2005). In addition, markers of eosinophil activation, neurotrophins, and granule proteins will permit studying how eosinophils exhibit both neurotrophic and neurotoxic roles in disease.

CHAPTER 6: DISCUSSION

Peripheral neuroplasticity is implicated in the pathogenesis and symptoms of asthma but the complexity of airway sensory innervation makes it difficult to study using conventional approaches. After determining conventional tissue sectioning and two-dimensional approaches were insufficient, I developed an approach using computational mapping capable of sampling regional and layer-specific heterogeneity in the airway and capable of quantifying three-dimensional nerve architecture (Chapter 2). I found that heterogeneity of three-dimensional epithelial nerve architecture depends on airway tissue layer and location proximal-to-distal and dorsal-to-ventral. Computational mapping was sensitive enough to capture mouse epithelial nerves for the first time and furthermore to quantify a minority subpopulation of epithelial nerves that expressed substance P. This increased sensitivity should be useful in future studies since pan-neuronal architecture and heterogeneity was not predictive of the substance P subpopulation. I also showed computational mapping can be used with tissue specimens obtained in the clinic and in other organs with disease neuroplasticity. Using airway biopsies, I am currently testing if human asthma is associated with structural neuroplasticity (read below). Thus the dissertation has added both a more comprehensive method to image large-scale whole-organ innervation and introduces computer modeling to more accurately quantify the smaller-scale three-dimensional structure of peripheral nerves. In the future this technique should allow for improved identification of earlier changes to nerves when the causal signaling mechanism behind neuroplasticity is perhaps easier to detect. This technique can also greatly reduce inter-operator variability that has plagued previous studies of structural neuroplasticity.

Returning to the question of peripheral neuroplasticity in asthma, I quantified three-dimensional nerve structure in mouse models of asthma and found that branched outgrowth of epithelial nerves occurred in a model of chronic allergic inflammatory asthma (NJ.1726 mice)

associated with increased reflex bronchoconstriction (Chapter 4). Using mice lacking eosinophils (PHIL) and a double-transgenic control (NJ.1726/PHIL) I showed that eosinophils were necessary for both branched outgrowth of epithelial nerves and reflex bronchoconstriction. This suggests that in chronic allergic inflammatory asthma eosinophils contribute to airway narrowing in part by causing epithelial sensory nerves to grow and branch leading to increased sensitivity. This serves as additional evidence that eosinophils are not merely part of a cytotoxic infiltrate in asthma but exhibit specific signaling cross-talk with resident cells. This data also reiterates that asthma is not merely a sequence of exacerbations but is a disease of long-term airway remodeling and demonstrates that neuroplasticity is an important aspect of these chronic changes. Future treatment of asthma may need to treat the structural growth of peripheral nerves in order to prevent airway hyper-responsiveness.

In mouse models of dermatitis I showed eosinophils can produce both neurotrophic and neuropathic effects on epidermal nerves (Chapter 5). Neurotrophic effects were seen in a chronic dermatitis model whereas eosinophils were necessary for neuropathic loss of epidermal nerves in acute dermatitis. In co-culture experiments, eosinophils without any pre-treatment exhibited neurotrophic effects suggesting additional activation of eosinophils may be needed to produce neurotoxic effects. This suggests that unique eosinophil populations or activation states contribute to acute versus chronic symptoms of dermatitis such as itch by causing opposite neurotrophic or neuropathic peripheral neuroplasticity.

These data in this thesis show three-dimensional organ-wide imaging and computational mapping are a powerful tool to quantify peripheral nerves. This thesis also shows that eosinophils can cause profound structural neuroplasticity in allergic disease which in the airways manifests as increased reflex bronchoconstriction. Thus chronic treatment to

reduce airway eosinophils or newer drugs targeting sensory nerves themselves may provide therapeutic benefit in allergic disease of the airways and skin. In addition, this technique allows us for the first time to assess whether or not approved asthma therapies act by causing neuroplasticity. For example, bronchial thermoplasty is an approved asthma treatment where the epithelium and airway smooth muscle are burned to reduce airway narrowing (Thomson, Bicknell et al. 2012). The current technique could determine if bronchial thermoplasty is efficacious by damaging epithelial sensory nerves or causing their neuroplasticity.

CHAPTER 7: APPENDIX

7.1 Developing Nerve Imaging and Quantification: Additional Material Excluded from Chapter 2

Prior to developing computer nerve mapping, I tested multiple conventional techniques for imaging nerves and quantifying their structure with the overall hypothesis that nerve density increases and A/C fiber phenotype changes in mouse models of acute allergic inflammatory asthma.

7.1.1 Pilot Experiments of Conventional Tissue Preparation and Immunolabeling to Quantify Nerve Density and Phenotype in a Mouse Model of Acute Asthma

I initially used chromogenic staining (eg. 3,3'-diaminobenzidine) of nerve segments in paraffin embedded lung sections (Figure 3). However paraffin embedding masked antibody epitopes which either prevented specific staining or required unmasking (eg. citrate buffer and microwaving) at the cost of disrupting normal tissue architecture. Thin tissue sections captured only a small piece of nerve material which prevented quantifying nerve structural information other than nerve density. Chromogenic staining, although highly sensitive, also produced background staining that obviated most computer analysis approaches I was considering at the time. I gradually transitioned to using thick (60 μm) cryosectioned tissue and then whole mounts in order to image more complete nerve structure. However, even in whole mounts chromogenic staining intensity is not quantifiable, produces background signal, and is difficult to use for producing distinct multi-color labeling. Thus at the same time I was testing thin tissue sections, thick tissue sections, and whole mounts I also optimized protocols for fluorescently

labeling nerves rather than using chromogenic staining. Fluorescent labeling reduced background and non-specific staining and allowed for multi-color labeling which was necessary for studying nerve phenotype.

7.1.2 Experiments of Whole Mount Immunolabeling and Confocal Microscopy Followed by Image Flattening to Quantify Nerve Density and Phenotype in a Mouse Model of Acute Asthma.

Once I optimized fluorescent labeling of nerves in tissue whole mounts I also developed protocols to label nerve C and A fiber phenotype using substance P (SP) and neurofilament 160kDa (NF160) markers respectively (Figure 4). At the same time I also began testing three-dimensional imaging of nerves using laser-scanning confocal microscopy. Once these protocols and image approaches were developed I returned to the initial hypothesis that nerve quantity and nerve phenotype change in a mouse model of acute allergic inflammatory asthma. I imaged three-dimensional nerves in airway tissue, flattened data into two-dimensional images, and tested if nerve density, substance P, or NF160 changes in the ovalbumin model of acute allergic inflammatory asthma. In randomly acquired images of airway whole mounts I found that both substance P and NF160 signal intensity in nerves decreased in mouse models of acute allergic inflammatory asthma (Figure 11, Figure 12, Figure 13). This suggested nerve phenotype is changing in acute allergic inflammatory asthma, but flattening images meant discounting distinct nerve populations in different tissue layers. Thus if an image happened to capture a location with thicker submucosa, the overall amount of nerves, substance P, and NF160 would drastically change. This variability made it difficult to tell if nerve density or phenotype resulted from true disease-associated neuroplasticity or from undersampling and post-processing data

reduction. Thus I attempted to develop a method for quantifying three-dimensional nerve structure.

7.1.3 Quantification of Airway Three-Dimensional Nerve Structure Using Computational Filtering, Processing, and Modeling

Initially I wrote all software and macros used for identifying nerves in three-dimensional images and only later replaced some of my software with the commercial software, Imaris (Figure 5). In order to help identify nerves I initially tested image filtering algorithms in C++, Matlab, and ImageJ including seeded region growing, watershed segmentation, adaptive contours, and Sobel edge detection. Diffusion-based algorithms (CED and Hessian filtering, discussed below) enhanced nerve signal and were less susceptible to background signal than other approaches. Subsequently I wrote software in Matlab to automatically filter three-dimensional images and skeletonize nerve signal (Figure 14). Skeletonization is a process where the width of linear structures (eg. nerves) in an image is reduced to one pixel in order to facilitate structural analysis. Once nerves were skeletonized I wrote Matlab software to count branchpoints as three nerve segments sharing one contact point (colored circles in right panel of Figure 14) and software to calculate three-dimensional Cartesian lengths of nerve skeletons. I subsequently replaced my nerve skeletonization program with nerve modeling using the commercial software, Imaris, because it performed quantification faster, contained an interactive user interface for semi-automatic nerve modeling, and did not have random access memory (RAM) limitations of Matlab and Java-based software such as ImageJ.

7.2 Pilot Experiments to Measure Airway Nerve Function Excluded from Chapter 3

7.2.1 Pilot Experiments to Measure Non-cholinergic Neuronal Contractions in Mouse Trachea

I initially attempted to measure asthma functional neuroplasticity of non-parasympathetic nerves using mouse tracheas in an organ bath. The nerves that cause these contractions are thought to be substance P-expressing nerves which were shown to change phenotype in acute allergic inflammatory asthma models in my earlier imaging studies (Figure 4, Figure 12, Figure 13). Previous studies reported that tracheal contractions in guinea pig and human could be elicited using longer pulse width (2millisecond) electrical field stimulation (Linden 1996). One laboratory suggested that non-cholinergic contractions could also be elicited in mouse trachea (Tournoy, De Swert et al. 2003). I replicated the electrical field stimulation parameters from guinea pig studies and could successfully elicit trachea contractions in mice. Trachea contractions were augmented in mice with IL-5 overexpression regardless of whether or not eosinophils were present (Figure 29). However, follow-up control experiments showed these contractions were not blocked by antagonists of neuronal signaling (tetrodotoxin, low dose atropine). Pilot experiments were unsuccessful to cause neuronal (tetrodotoxin sensitive) non-cholinergic contractions in mouse trachea using different electrical field stimulation parameters or direct sensory agonists including: capsaicin, cinnemaldehyde, acrolein, adenosine, adenosine monophosphate, adenosine triphosphate, mustard oil, 4-oxo-2-nonenal, substance P, and neurokinin A. Trachea contractions mediated by cholinergic parasympathetic nerves were possible to elicit using shorter pulse width (0.2ms) electrical field stimulation that were sensitive to both atropine and tetrodotoxin demonstrating they were neuronal in origin.

7.2.2 Pilot Experiments to Measure Sensory Nerve Plasma Exudation in Mice

I also attempted to assay sensory nerve function in mice by measuring plasma exudation of Evan's blue dye bound to serum albumin. Since sensory nerves can cause inflammation (in part through substance P release) which increases leakage of Evan's blue dye into the affected area (Figini, Emanueli et al. 1997; Baluk, Thurston et al. 1999), I hypothesized that this neuronal response would be increased in mouse asthma models. However in my initial positive control experiments, large intravenous doses of capsaicin or substance P did not cause increased Evan's blue dye leakage into the airways over injection of saline or ethanol vehicle control (data not shown). There was also no difference in Evan's blue dye leakage when controlling for tissue weight or harvesting the entire airways versus individual lobes or trachea. These experiments in part provided the motivation to utilize an in vivo mouse ventilation protocol in collaboration with the MacDonald laboratory in order to robustly elicit neuronal reflex bronchoconstriction.

7.3 Future Studies

7.3.1 Ongoing Studies in a Mouse Model of Chronic Severe Asthma and in Human Biopsies

From collaborators I am currently receiving airways from a mouse model of chronic severe asthma. These mice (described in Chapter 2 "Transgenic Mouse Model of Severe Chronic Asthma") have lung eosinophila similar to the NJ.1726 (++IL5/++Eos) mice used above but have more pronounced airway remodeling and eosinophil activation (Ochkur, Jacobsen et al. 2007). I am performing airway whole mount three-dimensional nerve imaging followed by computational nerve mapping in these mice. Low resolution images of the carina were un-

blinded (Figure 39) and these images suggest epithelial nerve density is markedly increased in the mouse model of chronic severe asthma.

From a second collaborator I am receiving human airway tissue from patients with asthma and other lung diseases. Currently I have imaged twenty five biopsies but variability in patient population disease status has prevented us from un-blinding my data. I also currently have biopsies from only four control patients. I will ultimately quantify the presence or absence of peripheral neuroplasticity associated with disease or with eosinophils. I am imaging epithelial nerves in biopsy whole mounts and performing three-dimensional computer mapping (Figure 40). I also image eosinophils in these biopsies and will correlate eosinophil presence and proximity to nerves with branched outgrowth of nerves.

7.3.2 Ongoing Study: Mechanism of Eosinophil-Induced Branched Outgrowth

I am currently performing human eosinophil and human sensory nerve co-culture experiments similar to Figure 38. I am culturing sensory nerves with eosinophils or eosinophil-conditioned medium with the hypothesis that eosinophil-induced branched outgrowth is not contact dependent as was shown previously using mouse-derived cells (Foster, Simpson et al. 2011). I also plan to obtain human nodose and jugular ganglia from Dr. Woltjer at OHSU in order to co-culture eosinophils with airways-specific nerves. This will allow us to test eosinophil-induced plasticity of placodal-derived sensory nerves (nodose ganglion) for the first time in addition to neural crest (jugular ganglion or dorsal root ganglion) derived nerves. Future experiments will attempt to narrow down an eosinophil signaling mechanism(s) responsible for neurotrophic effects using antagonists of neurotrophin and GFL signaling. In addition it will be

important to study different populations of eosinophils which is one potential mechanism for causing the opposite neuroplasticity in Chapter 5. My lab already isolates unique populations of eosinophils using fluorescence-activated cell sorting (FACS) which could then be co-cultured with sensory nerves to look for different forms of neuroplasticity. For example, future studies could employ a uridine-derivative, BrdU (routinely used by my lab), to distinguish newly differentiated eosinophils versus old/resident eosinophils, and CD69, a cell surface marker associated with eosinophil activation (Hartnell, Robinson et al. 1993) in order to see if eosinophil age or activation causes opposite neurotrophic versus neuropathic effects as was seen in my chronic versus acute dermatitis models (Chapter 5).

7.3.3 Future Study: Quantify Regional Epithelial Neuroplasticity in our Mouse Model of Chronic Allergic Inflammatory Asthma

Chapter 3 demonstrated that epithelial nerves occur individually or in patches that vary in length and branching depending on their location in the airways. It will be important to quantify changes in the patchy distribution of epithelial nerves and differences in ventral versus dorsal and proximal versus distal airways. This more comprehensive quantification across different regions of the airway could identify “hotspots” of neuroplasticity in the airways. Thus a future study will repeat nerve quantification but more comprehensively across different airway regions similar to Chapter 3. A measure of local patchiness such as spatial variance will be measured within each region and across different regions.

7.3.4 Future Study: Quantify Eosinophil-Induced Plasticity of Sensory Receptors in Asthma and Atopic Dermatitis.

As discussed in Chapter 1, specific sensory receptors (eg TrpV1, TrpA1, TrpM8) are implicated in producing cough and itch in asthma and dermatitis respectively. An important future study will be to use three-dimensional mapping of nerves to test if the expression or distribution of these receptors changes in human asthma and dermatitis. Follow-up studies in my mouse models of chronic allergic inflammatory asthma and dermatitis in wildtype versus PHIL mice will determine if eosinophils are necessary for this form of neuroplasticity. Using in vivo airway mechanics with a mouse ventilator I can use specific agonists (eg. capsaicin, cinnemaldehyde, menthol) to test if nerve receptor plasticity is associated with functional plasticity. Similarly, measuring histamine receptor and TrpA1 receptor expression will help determining which form of itch underlies my chronic dermatitis model. TrpA1 has been recently shown to mediate antihistamine-insensitive itch caused by either chloroquine or BAM8-22 (discussed in Chapter 5).

Not only nerve structural heterogeneity (addressed in Chapter 3) but also nerve phenotype and ganglion origin will be important to quantify. Similar to three-dimensional structural heterogeneity, different nodose versus jugular ganglia-derived and different phenotype populations are rarely appreciated in previous studies despite their differential expression of sensory receptors such as TrpA1 and their overall importance in determining nerve structure/function. As discussed above, previous data showed each nerve population contains unique signaling (eg. Trk and GFL receptors, Trp receptors, purinergic receptors) and responds differently to asthma inflammation (Lieu, Kollarik et al. 2011). My preliminary data in flattened whole mounts suggest that nerve phenotype changes in a mouse model of acute allergic inflammatory asthma (Figure 4, Figure 11, Figure 12, Figure 13). My three-dimensional computational mapping can be used to determine where this change occurs (eg. airway region and tissue layer). This will help determine nerve phenotype and whether nerves are derived

from the nodose or jugular ganglion. Identifying nodose versus jugular origin (ie embryologic origin) will identify potential neurotrophic and GFL signaling mechanisms involved in asthma neuroplasticity. My preliminary data suggest both phenotype and ganglionic origin can be identified and studied in airway tissue (Figure 4), airway ganglia (Figure 42), and in culture (Figure 41).

7.3.5 Future Study: Quantifying Structural and Phenotypic Plasticity in Virus-Induced Hyperreactivity

My previous data and an earlier study suggest nerve structural and phenotypic plasticity are also caused by airway viral infection rather than just allergic sensitization and this could represent another future direction of research. My lab and a collaborator have previously shown airway virus infection causes airway hyperreactivity (Jacoby, Tamaoki et al. 1988) and phenotypic plasticity in sensory nerves (Carr, Hunter et al. 2002). After airway infection with a parainfluenza virus, A fibers in the nodose ganglion increased production of a C fiber phenotype marker, substance P. This effect occurred rapidly four days after infection and was transient by disappearing 28 days after virus inoculation. In early studies using flattened whole mounts, I also showed that parainfluenza virus infection was associated with an intermediate change in nerve phenotype, measured as a decrease in NF160, an A fiber marker (Figure 43). Future studies could measure the timecourse of NF160 and substance P expression after virus infection in both the airways and nodose/jugular ganglion. This would begin to resolve phenotypic changes manifested in the nerve cell body versus airway periphery and also could potentially capture different plasticity associated with virus infection versus an acute allergic inflammatory asthma model. Moreover, three-dimensional computer mapping could determine if and how nerve structure changes with virus infection.

TABLES

Table 1. Characteristics of A and C Fiber Phenotypes

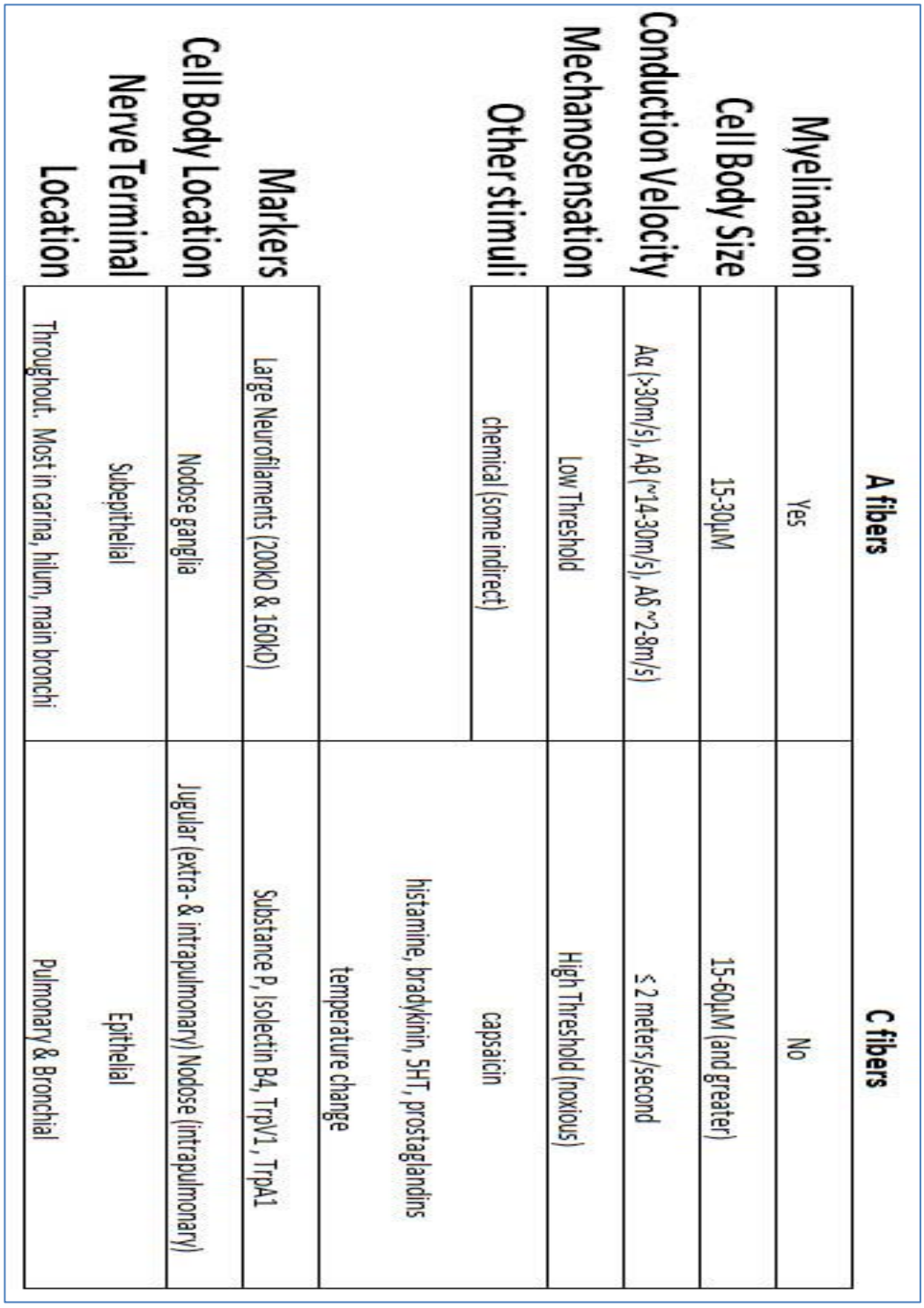

	A fibers	C fibers
Myelination	Yes	No
Cell Body Size	15-30μM	15-60μM (and greater)
Conduction Velocity	Aα (>30m/s), Aβ (~14-30m/s), Aδ ~2-8m/s)	≤ 2 meters/second
Mechanosensation	Low Threshold	High Threshold (noxious)
Other stimuli	chemical (some indirect)	capsaicin histamine, bradykinin, 5HT, prostaglandins temperature change
Markers	Large Neurofilaments (200kD & 160kD)	Substance P, Isolectin B4, TrpV1, TrpA1
Cell Body Location	Nodose ganglia	Jugular (extra- & intrapulmonary) Nodose (intrapulmonary)
Nerve Terminal Location	Subepithelial Throughout. Most in carina, hilum, main bronchi	Epithelial Pulmonary & Bronchial

FIGURES

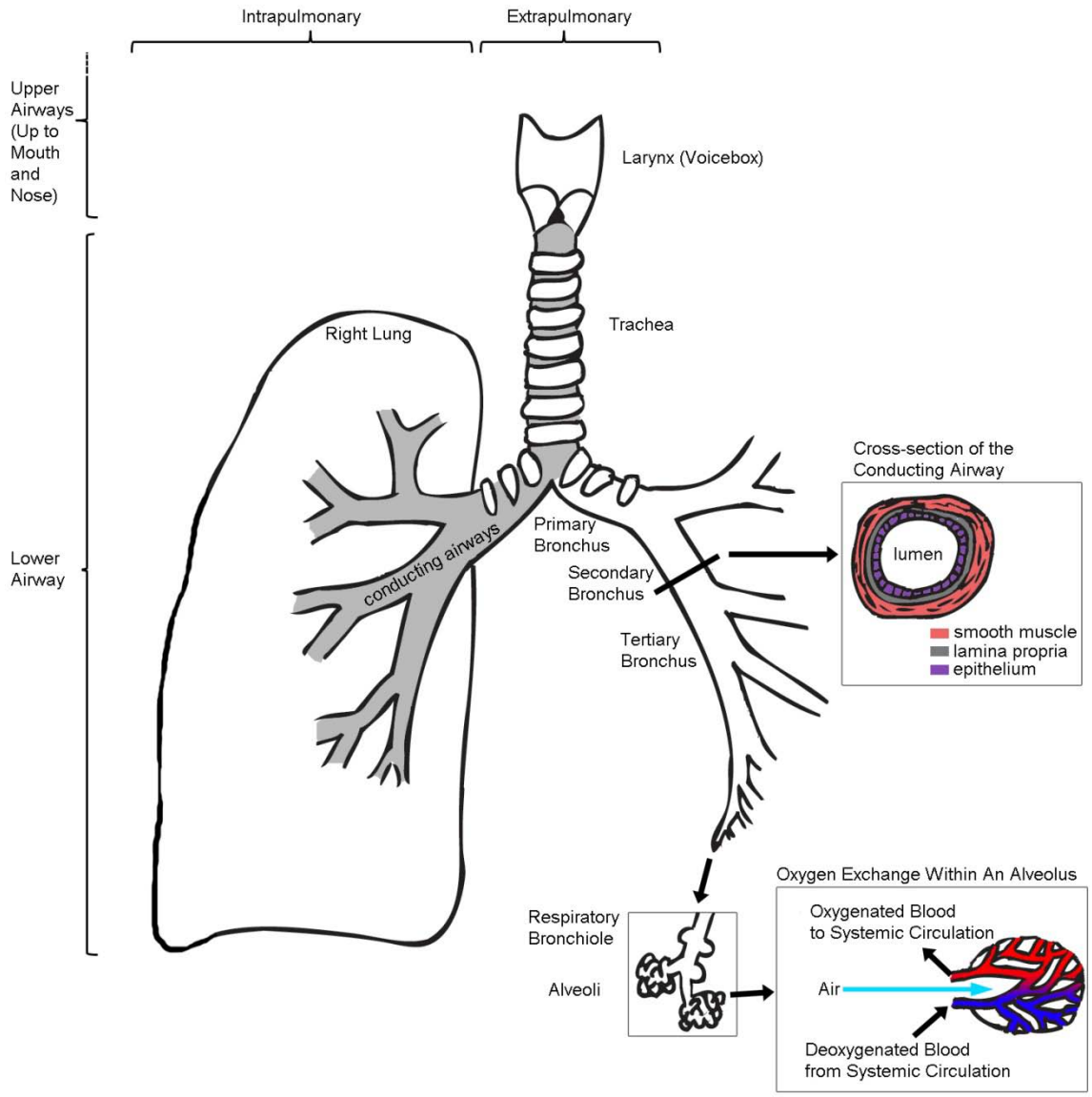

Figure 1. Diagram of the Conducting Airways and Lungs.

Inhaled air passes through the upper airway (nose, mouth, larynx) and then lower airways (trachea, bronchi, bronchioles, alveoli) where oxygen from the air diffuses across alveolar walls into blood. The conducting airways of the lower airway lack alveoli and include the trachea, bronchi to terminal bronchioles. A cross-section of the conducting airways shows the airway lumen in contact with epithelium and a deeper smooth muscle layer that can narrow the lumen and cause increased airway resistance (and cough, wheezing) in asthma. The carina is the first bifurcation where the trachea splits into two primary bronchi. Intra- and extra-pulmonary refer to parts of the lower airway inside or outside the lungs respectively.

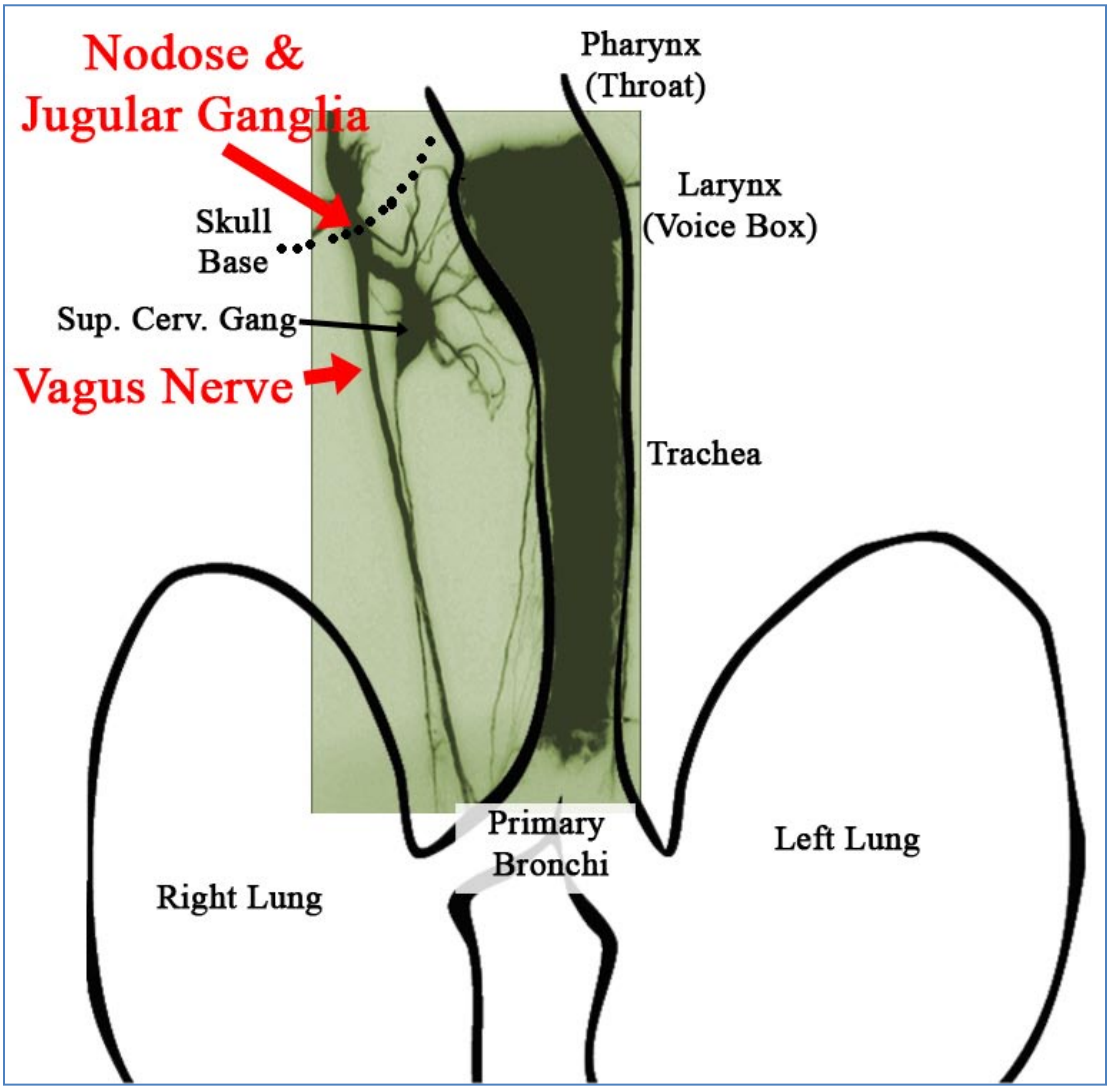

Figure 2. Sensory Innervation of the Airways.

Diagram of the airways overlaid on a brightfield microdissection image of the vagus nerve innervating the trachea (image from B. Undem, personal correspondence). The vagus nerve emerges from the base of the skull and is encircled by two ganglia called the nodose and jugular ganglia. These two ganglia are fused into one circular structure and harbor the cell bodies of sensory nerves innervating the airways. Sensory nerves send one half of their axon toward the central nervous system and the other half (shown here) in nerve bundles to the airways. Also shown is the superior cervical ganglion, a nearby ganglion that supplies sympathetic innervation to airway tissues. Sympathetic innervation does not relax airway smooth muscle or innervate the epithelium.

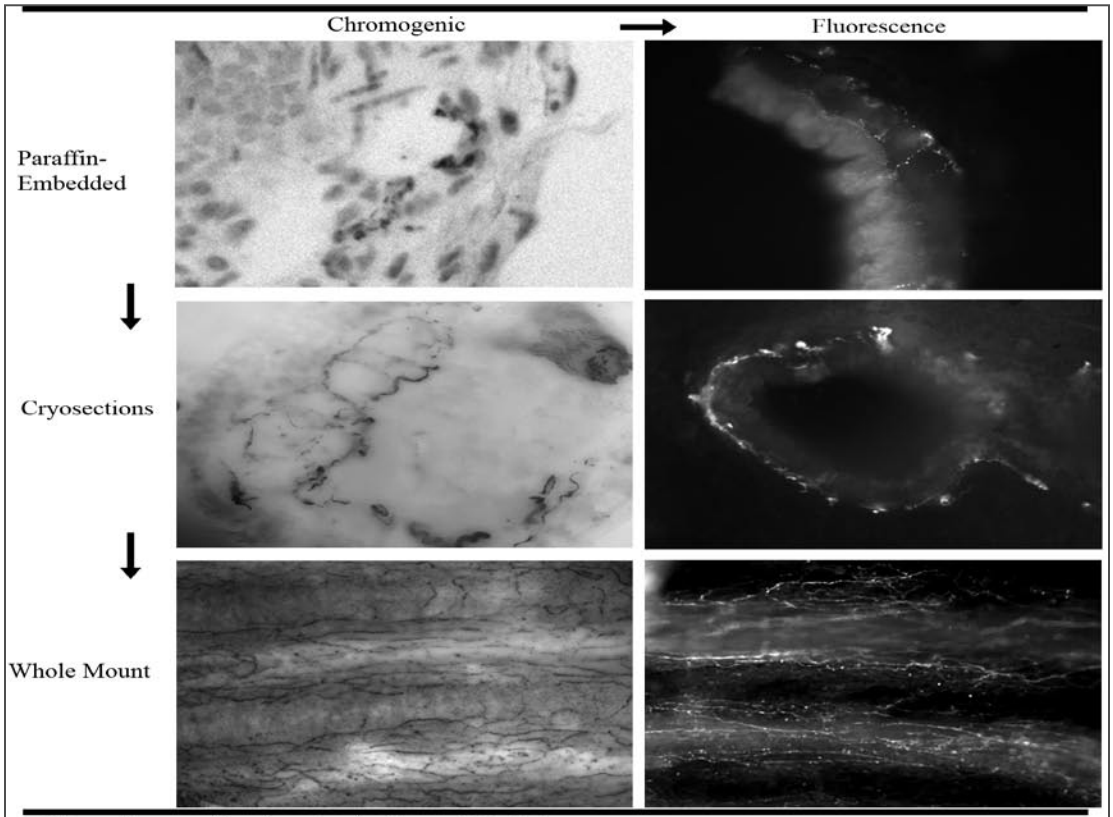

Hypotheses for Acute Asthma Model:
1) Nerve Density Increases
2) Nerve Phenotype Changes (ΔSubP, ΔNF160)

Results:

Paraffin:
Masked epitopes and non-specific binding.

Cryosections:
Improved antibody specificity but loss of morphology

Whole Mount:
Specific labeling, preserved morphology, but limited imaging depth and out-of-focus background signal

Chromogenic:
High signal density but non-specific labeling

Fluorescence:
Reduced non-specific labeling, facilitated multi-color labeling

All:
Limited imaging depth and out-of-focus background using epifluorescent and brightfield microscopy
Lack of full neuron structure (2D representations of 3D structure)

Figure 3. Pilot Experiments of Conventional Tissue Preparation and Immunolabeling to Quantify Nerve Density and Phenotype in a Mouse Model of Acute Allergic Inflammatory Asthma

Top half: A series of pilot experiments were performed in order to test tissue preparation techniques (egs. paraffin-embedding, cryosectioning, whole mount) and immunolabeling approaches (egs. chromogenic and fluorescence) in mouse airway tissue. Lower right image: whole mount fluorescence improved immunolabeling but still contained background fluorescence and just two-dimensional nerve structure. Bottom half: limitations of each approach ultimately leading to subsequent studies using confocal microscopy of whole mounts.

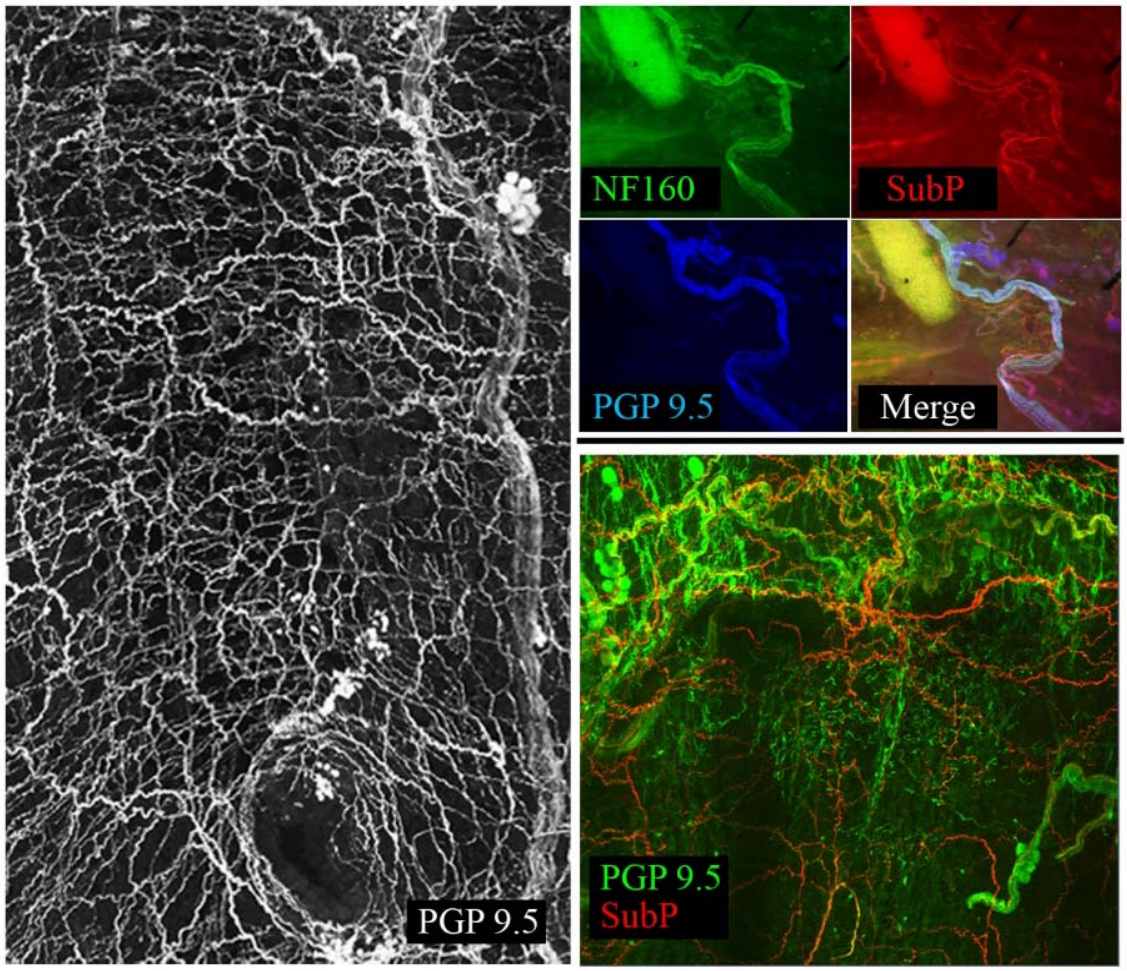

Acute Asthma Model Hypotheses:

1) Nerve Phenotype Changes (ΔSubP, ΔNF160)
2) Nerve Density Increases

Acute Asthma Model Results:

1) Changed Nerve Phenotype: ↓SubP , ↓NF160
2) Nerve Density ?

Nerves (and density) segregate by layer

Figure 4. Experiments of Whole Mount Immunolabeling and Confocal Microscopy Followed by Image Flattening to Quantify Nerve Density and Phenotype in a Mouse Model of Acute Allergic Inflammatory Asthma.

Left panel shows microdissection and immunolabeling of a murine airway whole mount labeled with the pan-neuronal marker, PGP 9.5. Right panels show co-staining of PGP 9.5 with markers of nerve phenotype, substance P (SubP) and the neurofilament 160 kDa isoform (NF160). Upper right: murine airway stained with the pan-neuronal marker, PGP 9.5 (blue), the neuropeptide C fiber marker, substance P (red), and the A fiber marker, neurofilament 160kDa (NF160kDa, green). Lower right: airway stained with the pan-neuronal marker, PGP 9.5 (green), the neuropeptide C fiber marker, substance P (red). Tissue layer and 3D nerve structure was discarded by image flattening similar to previous studies using maximum intensity projection. Nerve heterogeneity prevented quantifying nerve density using flattened whole mount images of nerves.

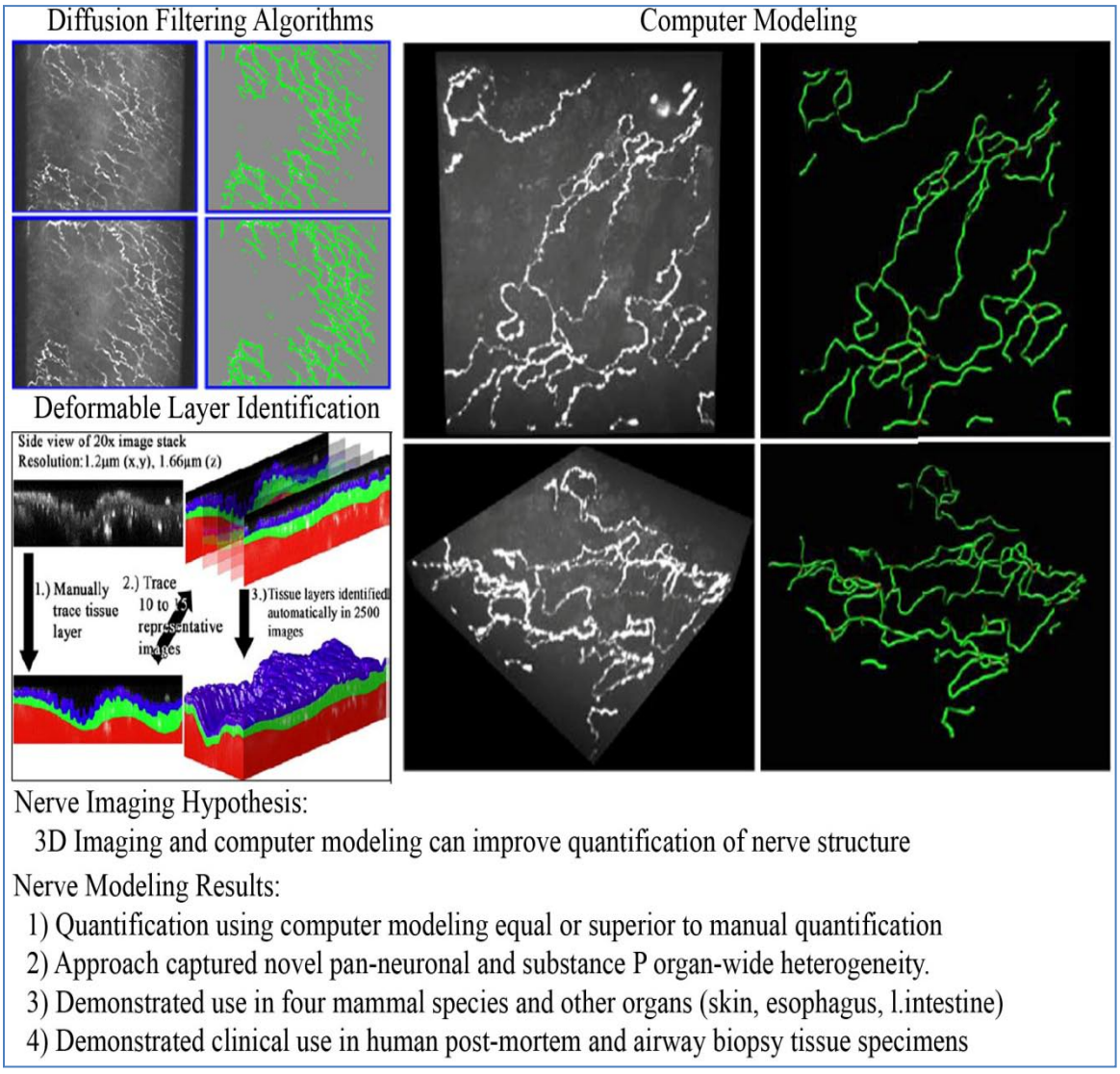

Figure 5. Quantification of Airway Three-Dimensional Nerve Structure Using Computational Filtering, Processing, and Modeling.

Development of techniques to quantify nerves in whole airway microdissected tissue imaged with confocal microscopy. Upper left panel: diffusion filtering using coherence-enhancing diffusion improved signal-to-noise of nerve images. Lower left panel: use of computer-generated deformable surfaces to distinguish tissue layer boundaries. Right panel: computer modeling (green) of airway nerves (white) labeled with the pan-neuronal marker, PGP 9.5 allowed for quantification of 3D nerve structure.

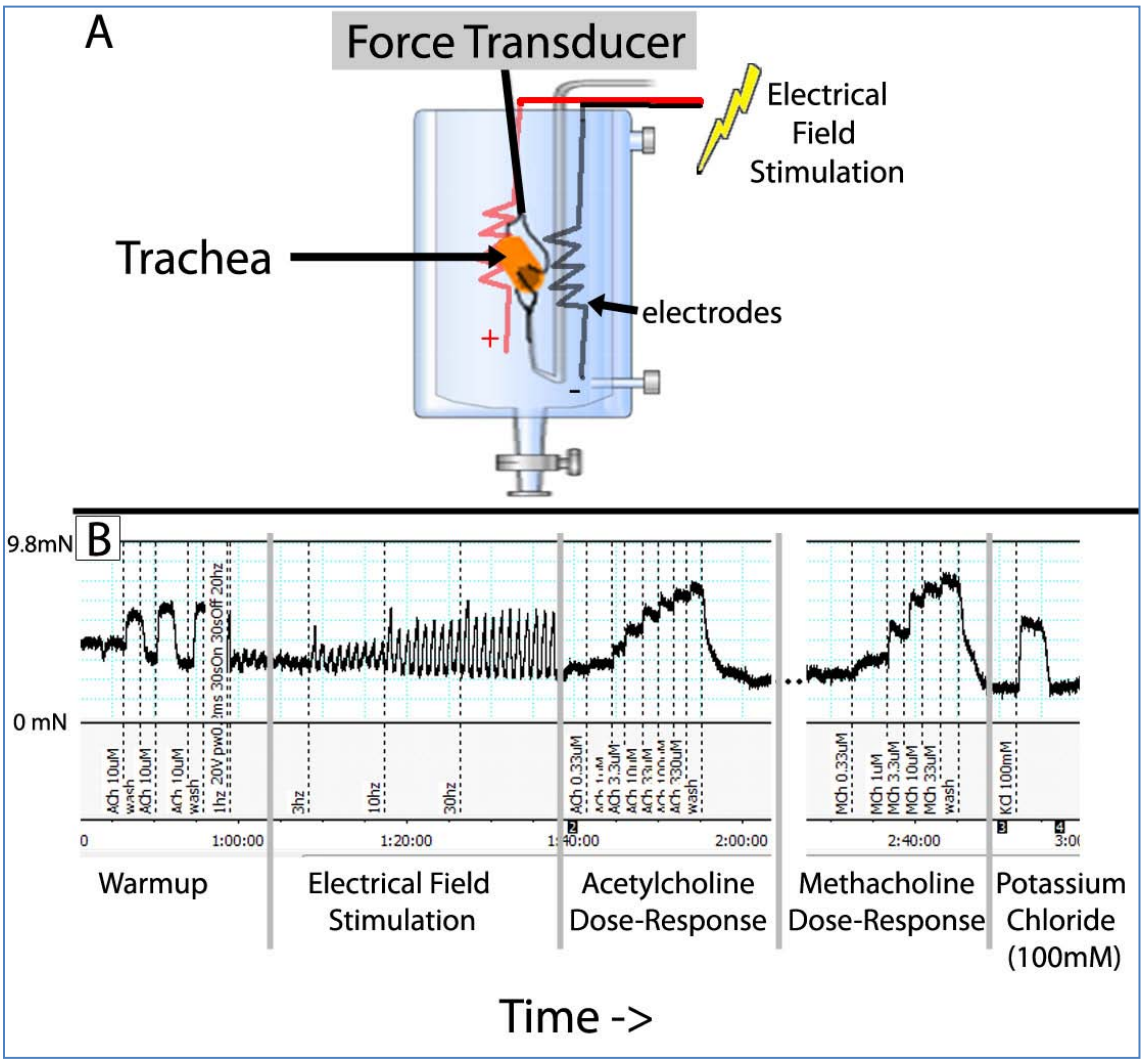

Figure 6. Measuring Airway Muscle Contraction Ex Vivo in an Organ Bath.

Panel A: A mouse trachea is suspended in a 5ml bath by two looped strings. Contractions are measured by a force transducer attached to the upper string. Panel B: Tracing of contraction force (y-axis) over the duration of the experiment (x-axis). Direct contraction of smooth muscle is caused by administration of agonists directly into the organ bath (Acetylcholine Dose-Response, Methacholine Dose-Response) and neuronal cholinergic contractions are caused by short (0.2ms) pulse width electrical field stimulation. A warmup period and final contraction with potassium chloride are performed to ensure tissue viability and measure maximal non-cholinergic contraction. Y-axis shows isometric force in millinewtons.

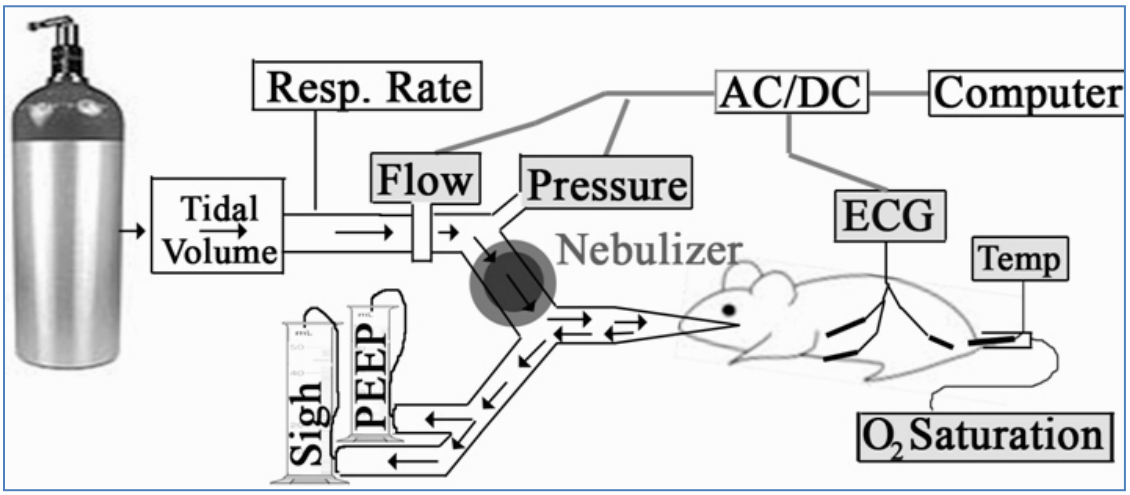

Figure 7. Mouse Ventilator Setup.

Diagram showing mouse ventilator circuit and data acquired. Mouse is anesthetized, intubated, and ventilated in the low dead-space ventilatory circuit shown above. Pressure: an in-line pressure transducer measures the pressure needed to inflate the lungs. This is the principle dependent variable. Flow: an in-line spirometer measures air flow through the circuit. Tidal volume: an in-line valve adjusts how much gas enters the circuit from the tank supply (far left). Tidal volume is calculated by integrating flow over one breath. Nebulizer: an in-line mesh nebulizer aerosolizes compounds (serotonin in the current dissertation) into the ventilator circuit. ECG: an electrocardiogram measures heart function during the experiment. Temp: a rectal thermometer measures body temperature. PEEP: Positive end expiratory pressure is maintained after every breath by having expiration pass through a short water column. Sigh: Airways are prevented from collapse by occasionally increasing inflation pressure to 25 cm H2O using a taller water column in the expiratory circuit. This is performed consistently before each administration of serotonin or control. O2 Saturation: an optional tail monitor can measure oxygen saturation in the blood.

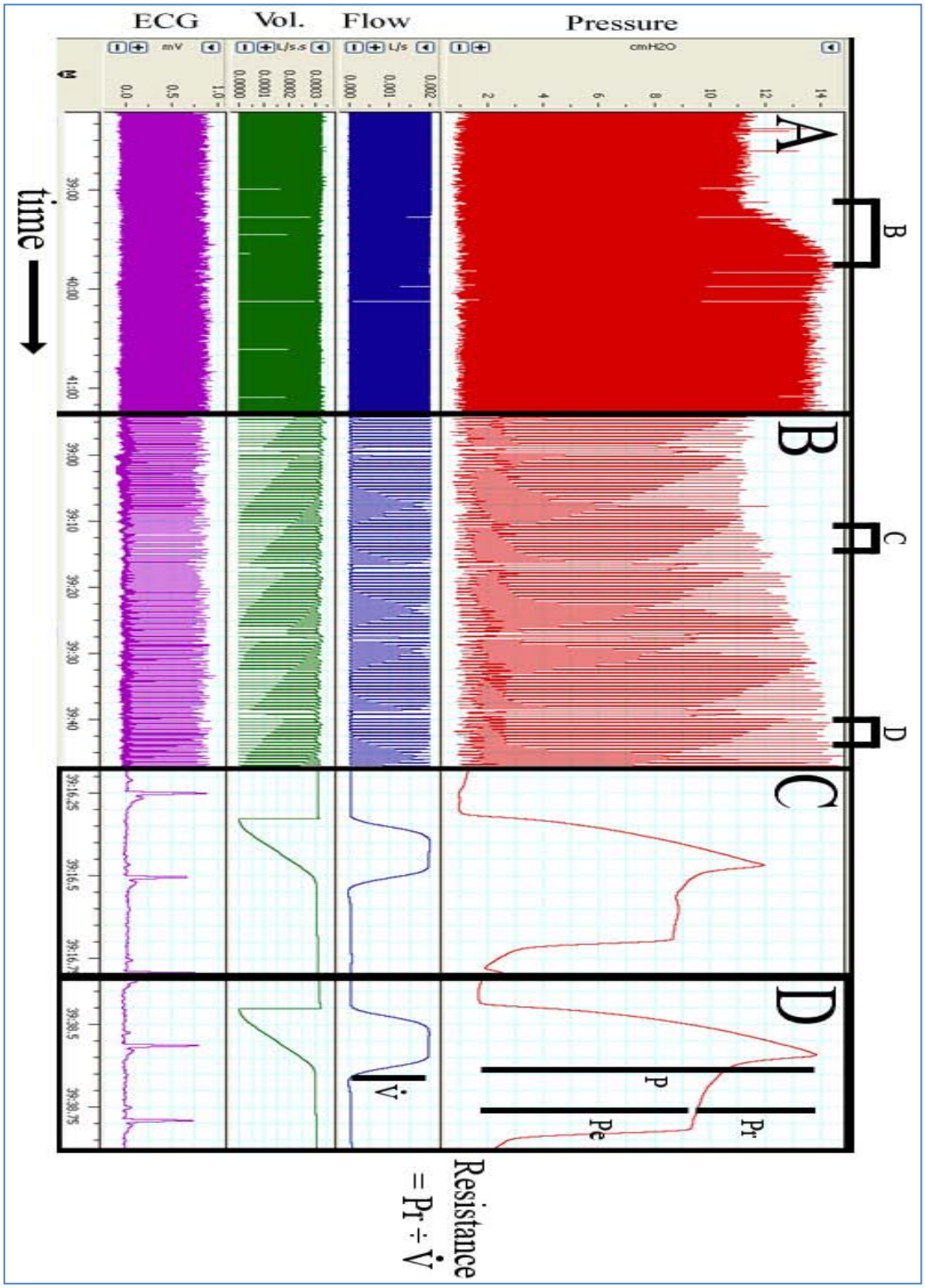
Pressure
Flow
Vol.
ECG
A
B
C
D
Pr
P
Pe
$\dot{V}$
Resistance
= Pr ÷ $\dot{V}$
time

Figure 8. Measuring Airway Mechanics in a Mouse.

Mice are mechanically ventilated in order to measure airway resistance which represents the degree of narrowing of the conducting airways. A constant respiratory rate is maintained and for each breath the same air flow speed (V-dot, blue) and tidal volume (green) are used. The amount of pressure in the ventilator circuit needed to inflate the lungs (red) is measured for each breath before and after administering serotonin which narrows the airways. Panel A shows the increase in inflation pressure after a single aerosol dose of serotonin (given at start of B). B is a magnified view of the data right before and after serotonin exposure. Changes in inflation pressure (red) are measured during maneuvers (C & D) where the lungs are inflated and held open. Note in C and D that the peak pressure required to inflate the lungs (P) is greater than the plateau amount of pressure needed to hold the lungs open (Pe). This difference between peak and plateau pressure (Pr) is directly proportional to airway resistance and is calculated by dividing by flow (V-dot).

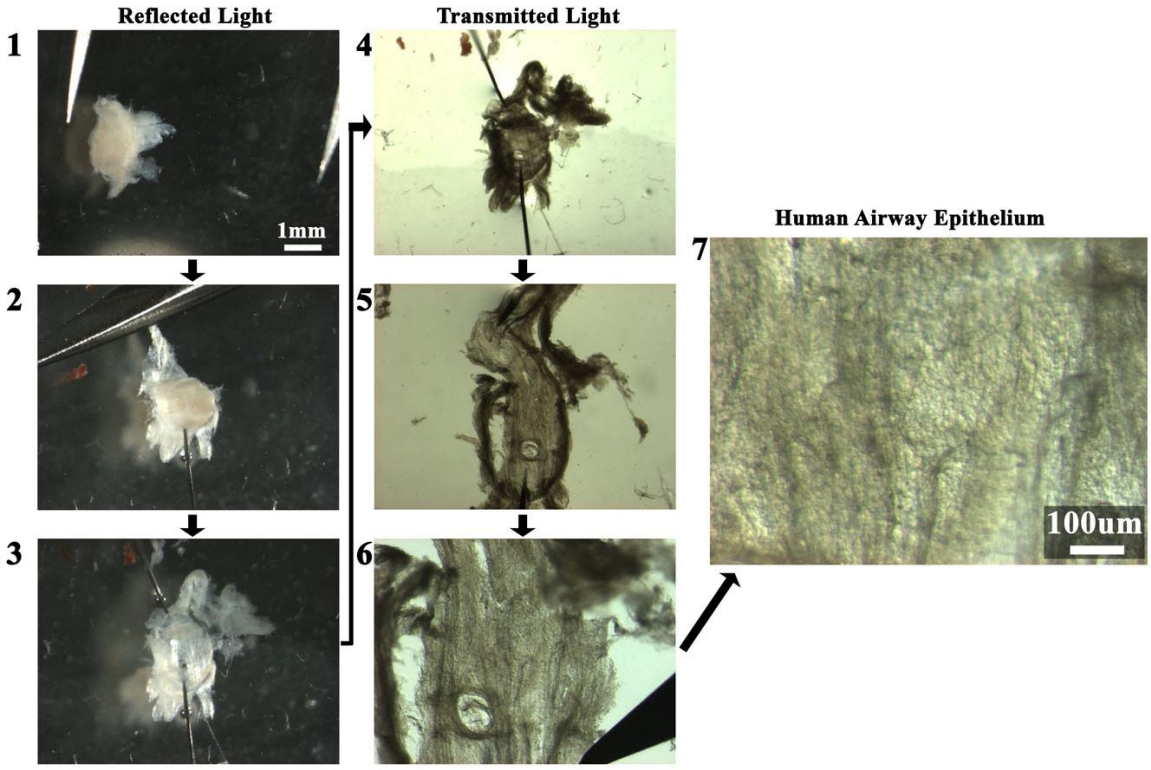

Figure 9. Microdissection of Human Airway Biopsy to Image Epithelium.

Steps for removing sub-epithelial tissue from airway forceps biopsy specimens are shown in brightfield images from the microdissecting microscope (1-7). Initially tissue is viewed by light reflectance (1), pinned to sylgard plate epithelium-side-down (2), and the majority of submucosal tissue is removed (3). Under transmitted light (4) the remaining sub-epithelial tissue is carefully removed using fine forceps and microdissection scissors (5-6). Panel 7 shows a higher magnification of airway epithelium now visible after removal of intervening tissue.

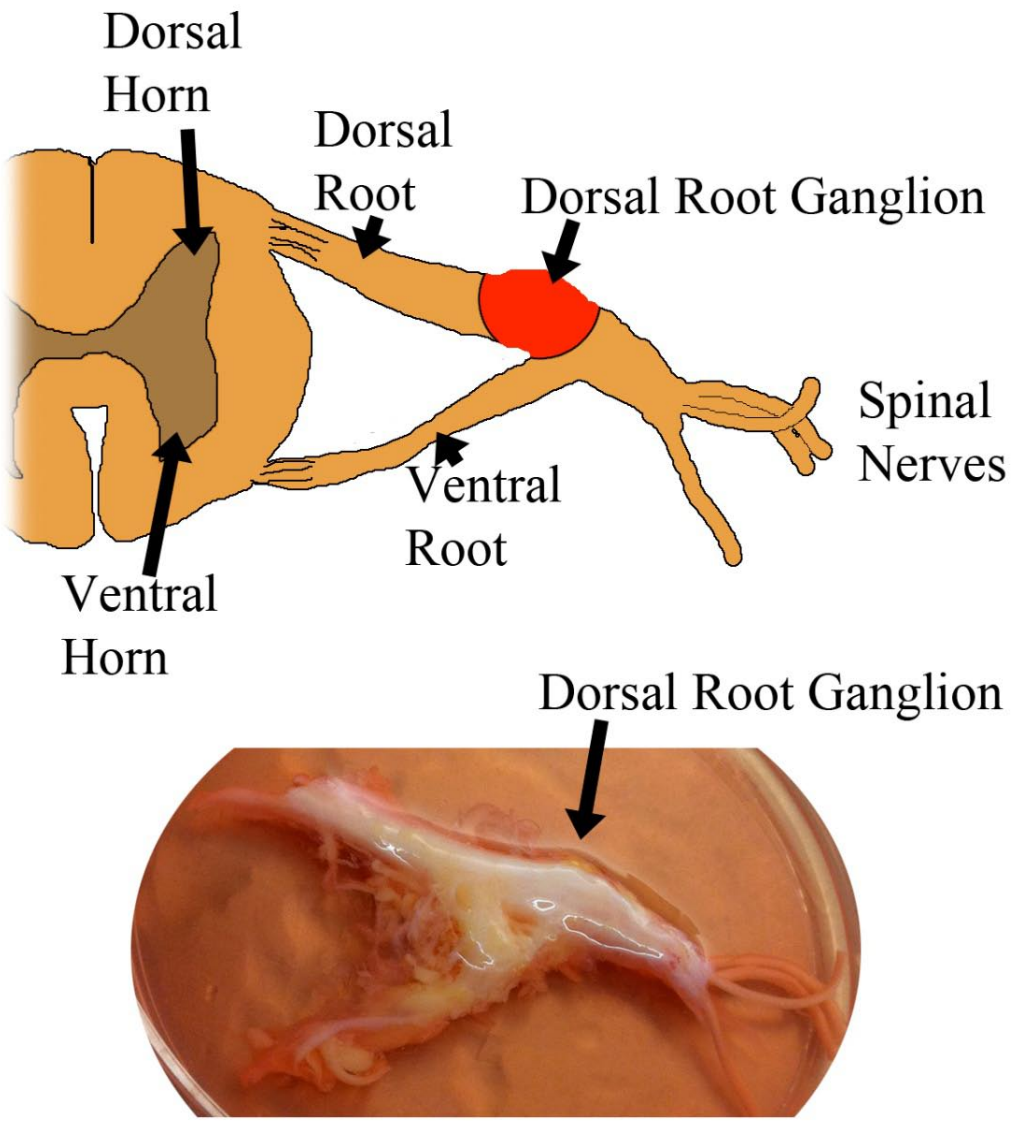

Figure 10. Harvesting Sensory Neurons from Human Dorsal Root Ganglia.

Human dorsal root ganglia are dissected from ventral/dorsal roots and spinal nerves shown above. Dorsal root ganglia are then manually fragmented, enzymatically digested, purified by pre-plating, and then plated for tissue culture experiments.

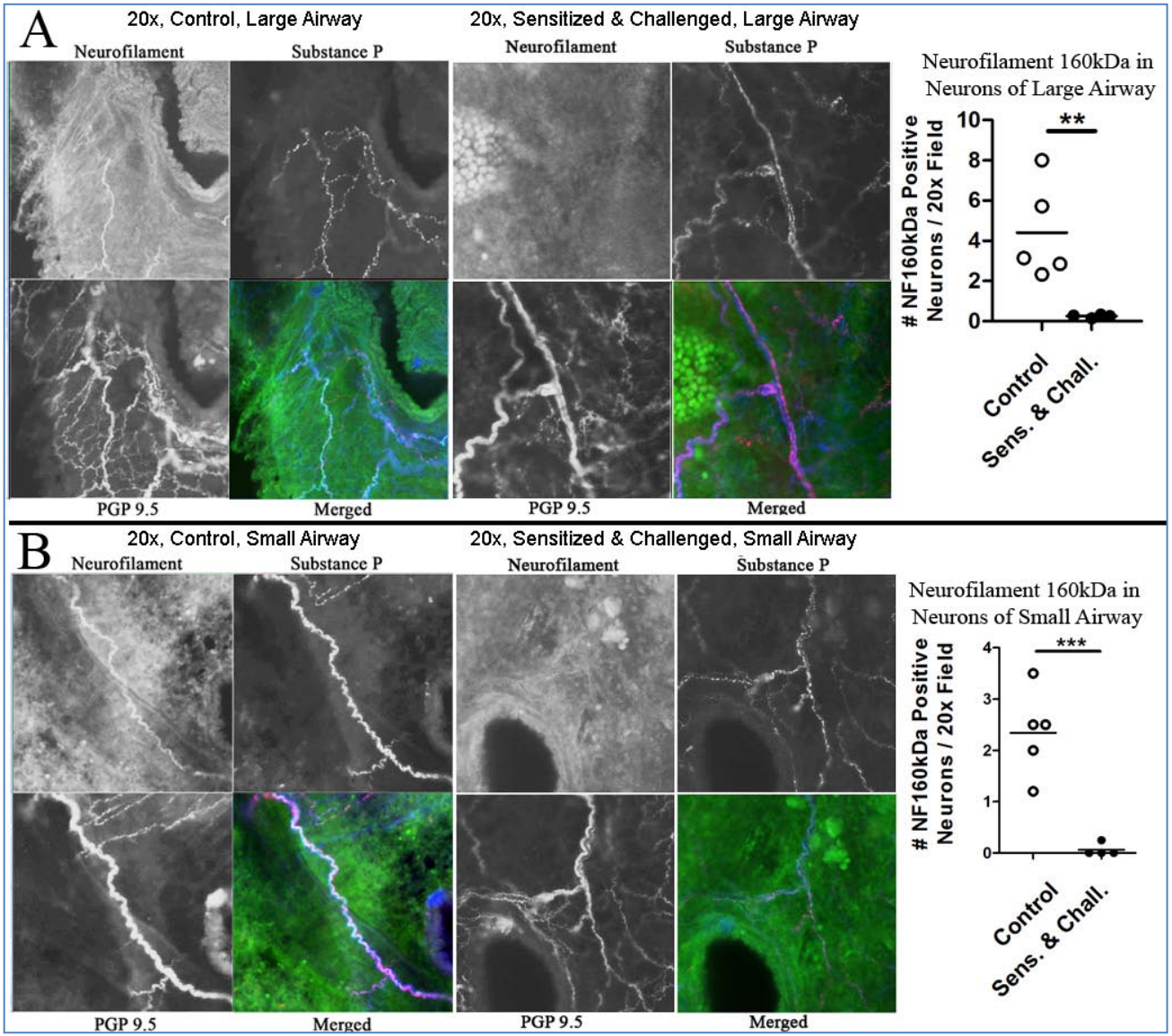
A
20x, Control, Large Airway
Neurofilament
Substance P
PGP 9.5
Merged
20x, Sensitized & Challenged, Large Airway
Neurofilament
Substance P
PGP 9.5
Merged
Neurofilament 160kDa in Neurons of Large Airway
NF160kDa Positive Neurons / 20x Field
10
8
6
4
2
0
**
Control
Sens. & Chall.
B
20x, Control, Small Airway
Neurofilament
Substance P
PGP 9.5
Merged
20x, Sensitized & Challenged, Small Airway
Neurofilament
Substance P
PGP 9.5
Merged
Neurofilament 160kDa in Neurons of Small Airway
NF160kDa Positive Neurons / 20x Field
4
3
2
1
0
***
Control
Sens. & Chall.

Figure 11. Decreased A-Fiber Phenotype Marker, Neurofilament 160kDa (NF160), in a Model of Acute Allergic Inflammatory Asthma.

Airway nerve phenotype was imaged in whole mounts of murine airways stained with the pan-neuronal marker, PGP 9.5 (blue), the neuropeptide C fiber marker, substance P (red), and the A fiber marker, neurofilament 160kDa (NF160kDa, green). A blinded observer counted the number of NF160kDa-positive fibers per image. Mice that are sensitized and challenged to foreign antigen (n=4), a model of acute allergic inflammatory asthma, contained significantly less NF160kDa fibers in their airways than untreated control mice (n=5). 20x fields are 425 µm x 425 µm.

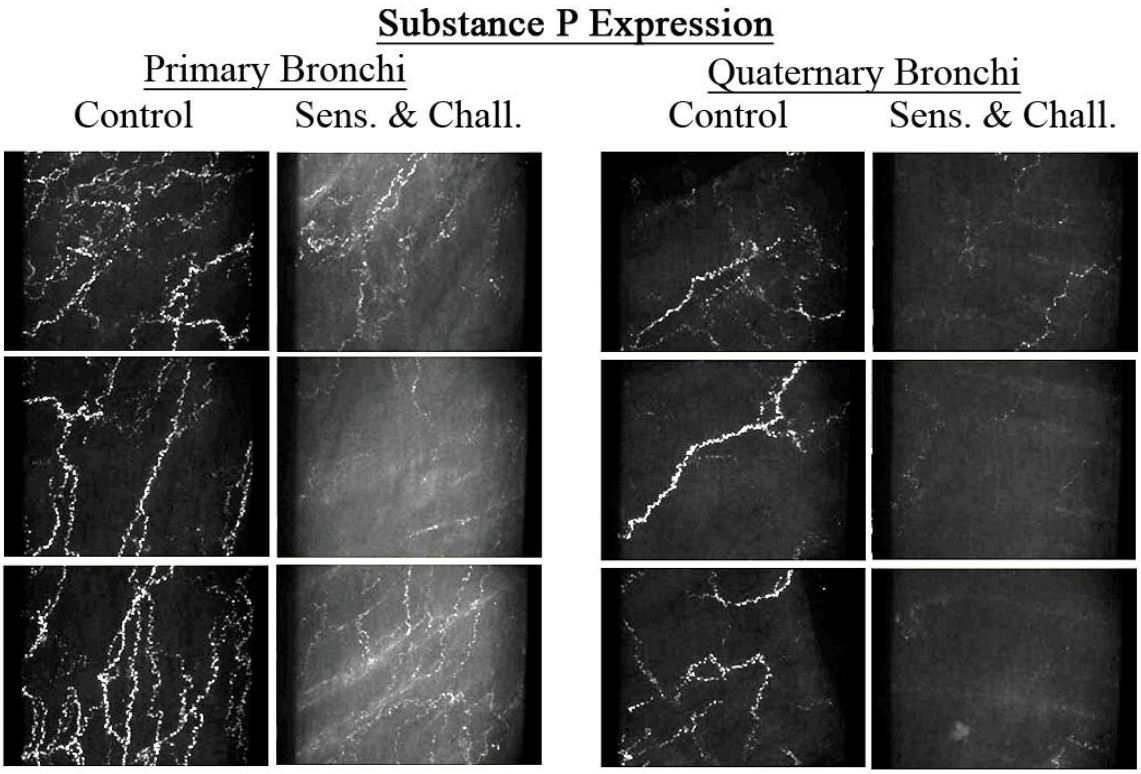

Figure 12. Imaging Neuronal Substance P in a Mouse Model of Acute Allergic Inflammatory Asthma.

Murine airway whole mounts were labeled with the pan-neuronal marker, PGP 9.5, and the C-fiber neuropeptide, substance P. 20x images (425 µm x 425 µm) of airway innervation were acquired at primary and quaternary bronchi locations. The amount of neuronal substance P appeared decreased in an antigen sensitization and challenge model of acute allergic inflammatory asthma suggesting increased release or decreased synthesis.

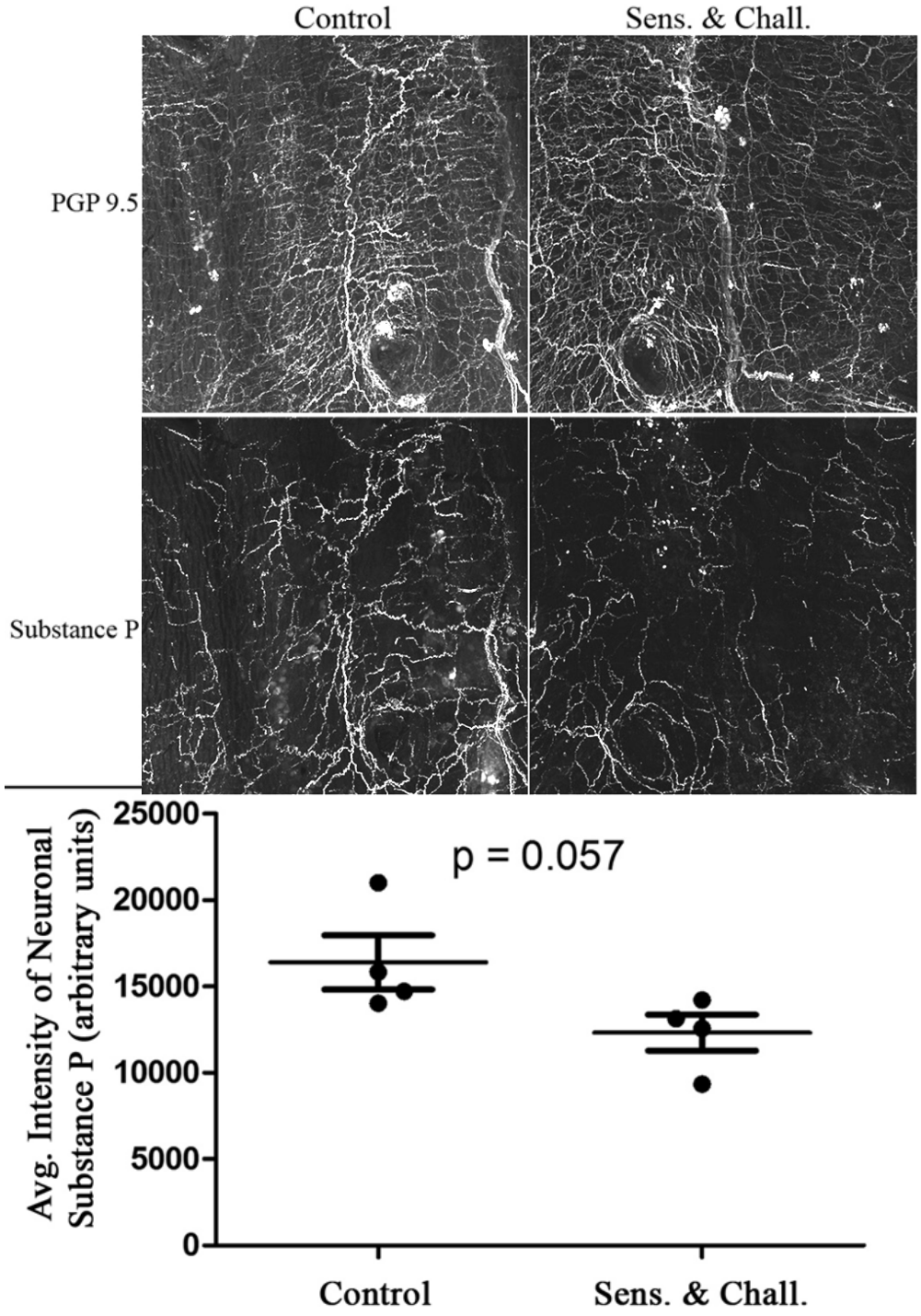

Figure 13. Decreased Neuronal Substance P in a Model of Acute Allergic Inflammatory Asthma.

Flattened large-scale 1700 µm x 1700 µm images of the primary bronchi innervation. Images were flattened using maximum intensity projection, gaussian filtered, and nerve signal identified using manual intensity thresholding of the PGP 9.5 channel. Substance P intensity was measured for nerve (PGP 9.5 positive) pixels. n=4.

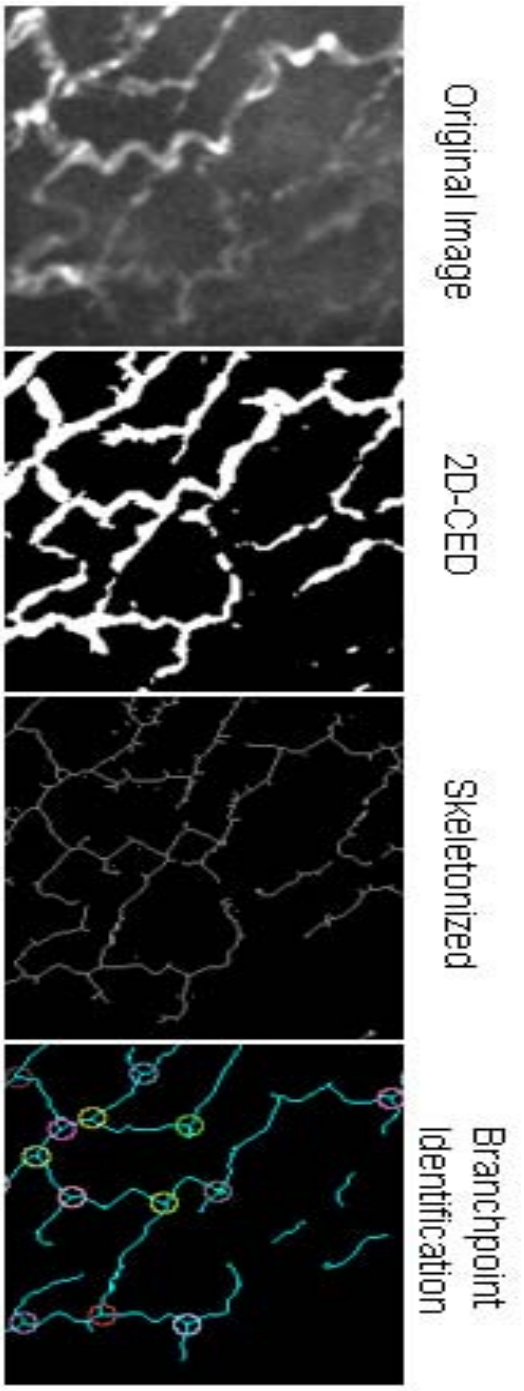

Figure 14. Initial Approach to Quantify Nerve Morphology.

Custom software was developed to analyze nerve morphology of 3D images ("Original Image"). This software was eventually replaced by the commercial software, Imaris. (2D-CED) Nerves were identified using 2D coherence enhancing diffusion (2D-CED), a filter that enhances linear objects. (Skeletonized) Nerves were reduced to one pixel width using skeletonization and branchpoints identified as colored circles in "Branchpoint Identification".

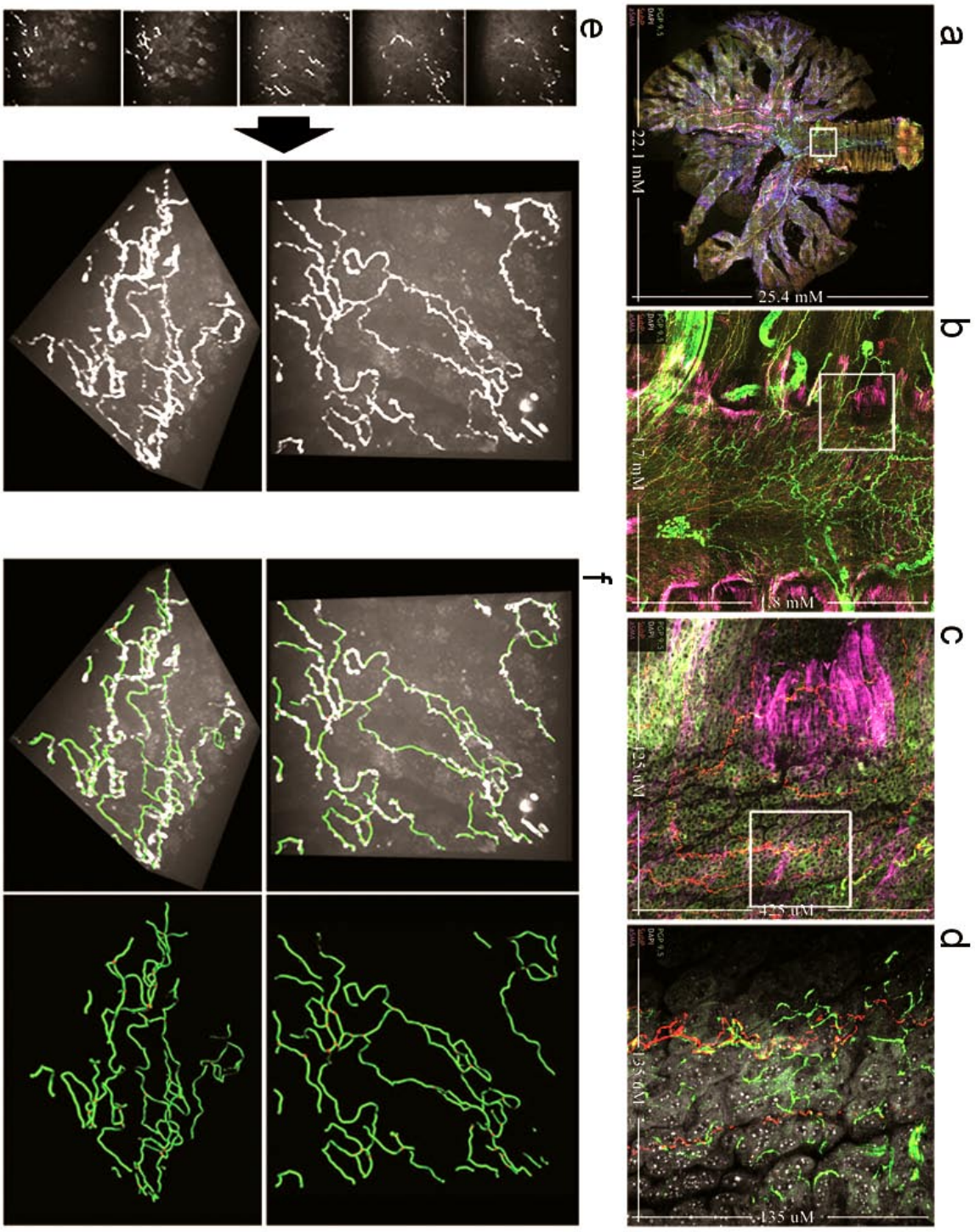
a
22.1 mM
25.4 mM
b
1.7 mM
8 mM
c
25 uM
12.5 uM
d
135 uM
135 uM
e
f

Figure 15. Whole Organ Innervation and Computer Modeling of Peripheral Nerves.

(a-d) Flattened projections of 3D airway images at four magnifications capturing (a) whole airway innervations up to (d) higher resolution epithelial nerve structure. Nerves are labeled with a pan-neuronal antibody, PGP 9.5 (green). Identification of tissue compartments and sub-typing nerves is demonstrated using α-smooth muscle actin (pink) for airway smooth muscle, DAPI (white) for epithelial nuclei, and substance P (red) for a subpopulation of sensory nerves. (e-f) Computer modeling of epithelial nerves. (e) optical sectioning (z-stack) image series of airway epithelial nerves and 3D visualization of images at orthogonal and oblique angles using maximum intensity projection. (f) computer nerve model (green) overlaid on raw image data (white). Once modeled, nerve structural characteristics are automatically identified and quantified. See videos 1 and 2 in supplemental material. Dimensions for panel A = 22.1x25.4mm, panel B = 1.7x1.8mm, panel C = 425x425 µm, panels D-F = 135x135 µm.

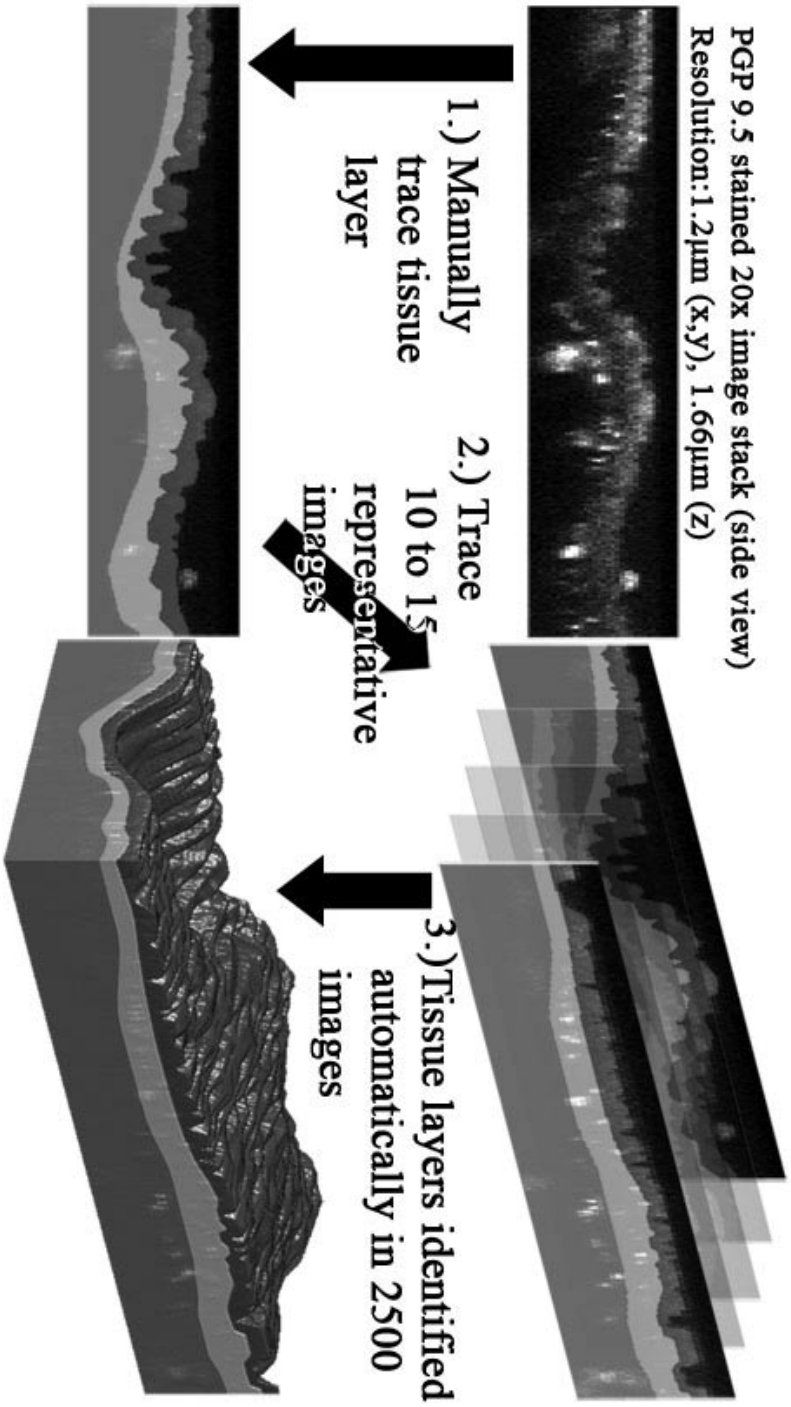

Figure 16. Computer assisted tissue layer identification.

Confocal image stacks of airway tissue (450 µm x 450 µm) are rotated to a lateral view and tissue layers are manually identified in 10-15 representative images. A custom program generates mallea

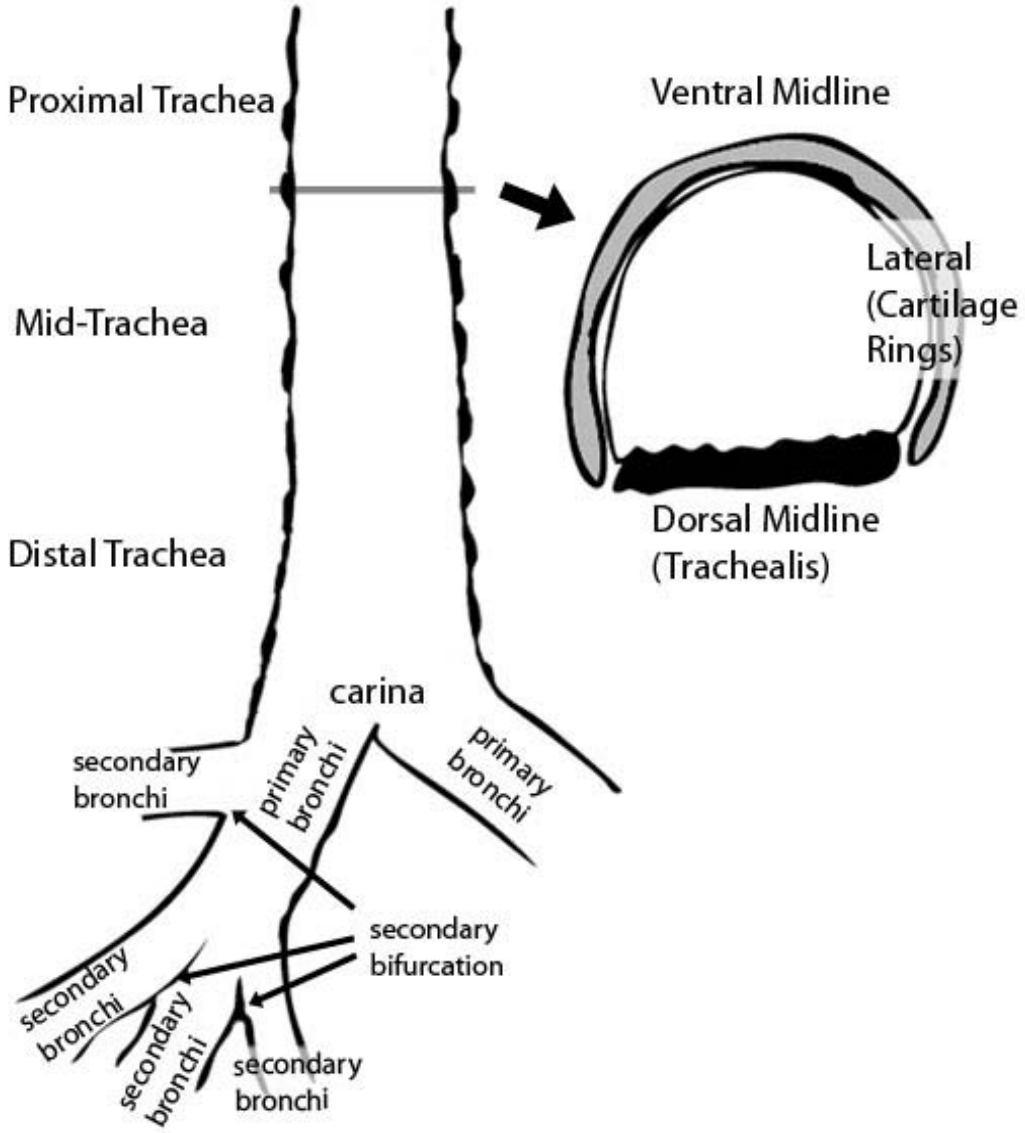

Figure 17. Airway Regions in the Mouse where Epithelial Nerves are Quantified

The trachea was divided into three even proximal-to-distal and three dorsal-lateral-ventral regions. The carina (first airway division) and secondary bifurcations were quantified separately from distal trachea/primary bronchi and primary bronchi/secondary bronchi respectively.

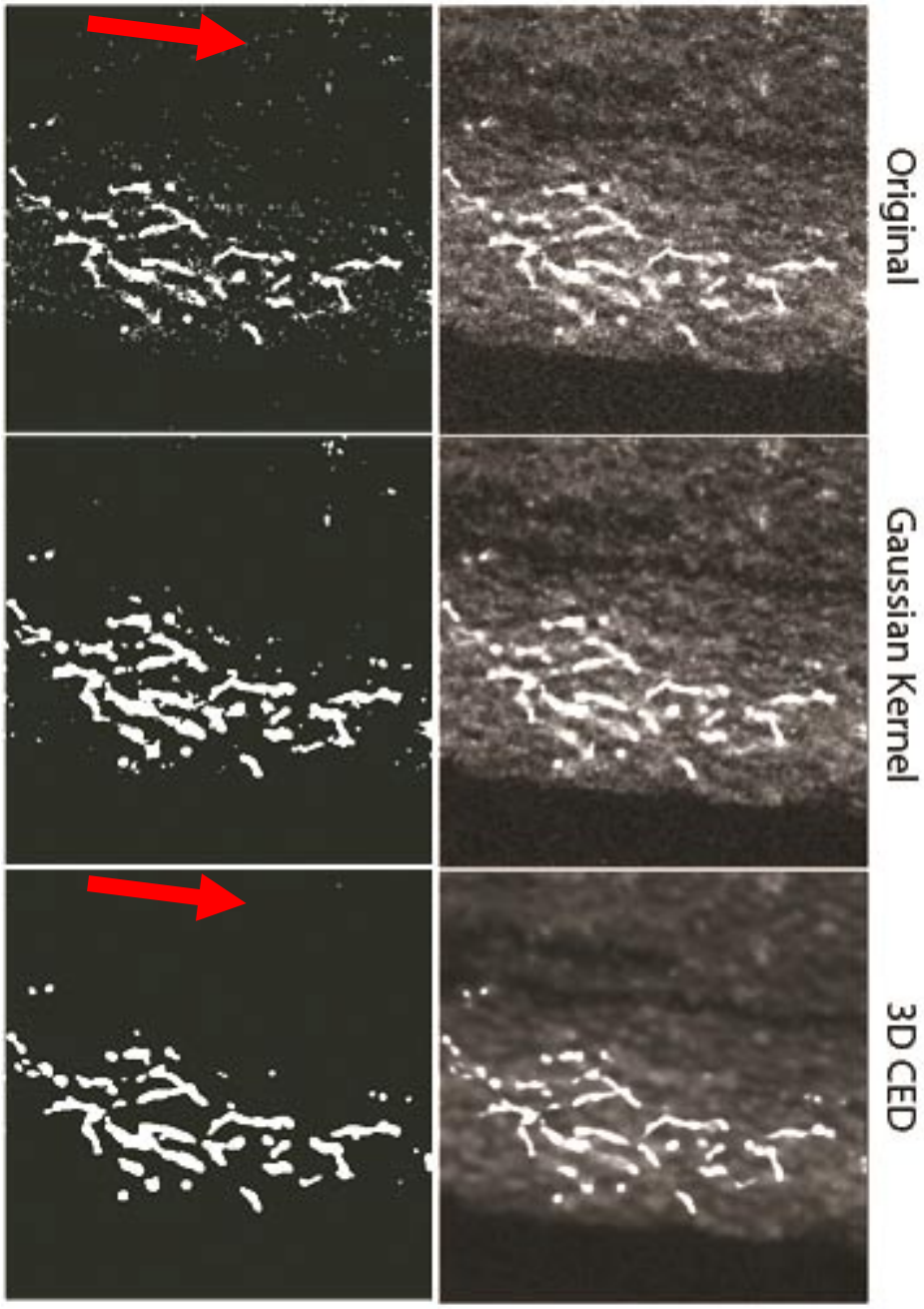

Figure 18. Diffusion Filtering to Enhance 3D Nerve Images.

(top row) Image data before and after pre-processing filters. (bottom row) binary mask after intensity threshold. (left) Slice of raw 3D nerve data with brightness increased to show image noise. (middle) Slice of gaussian filtered (1 pixel radius) 3D nerve data. (right) Slice of 3D nerve data filtered with 3D coherence-enhancing diffusion. Lower row shows improved identification of nerve signal using coherence-enhancing diffusion. Arrow shows region where background noise was reduced by 3D CED.

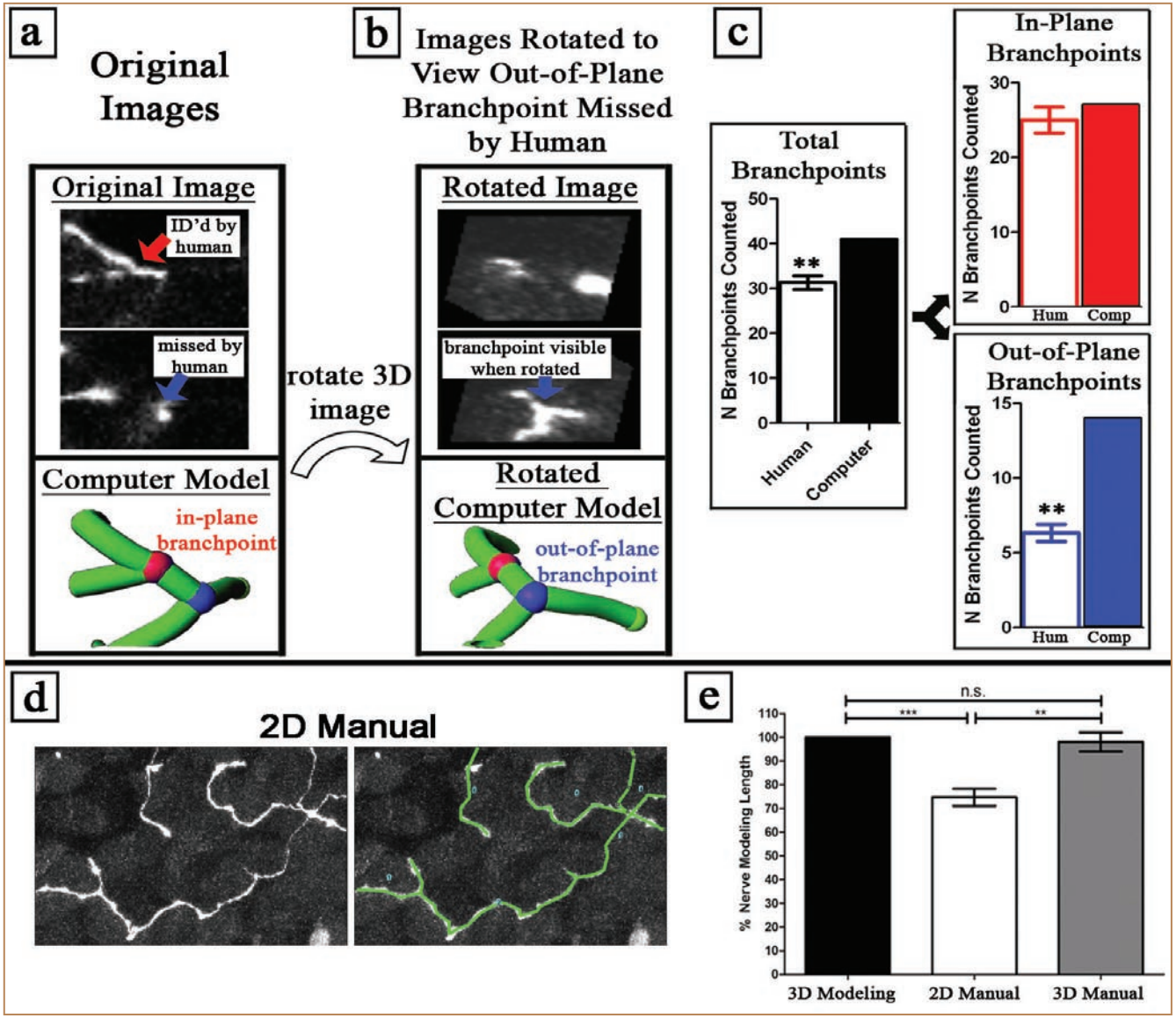
a
Original Images
Original Image
ID'd by human
missed by human
Computer Model
in-plane branchpoint
rotate 3D image
b
Images Rotated to View Out-of-Plane Branchpoint Missed by Human
Rotated Image
branchpoint visible when rotated
Rotated Computer Model
out-of-plane branchpoint
c
Total Branchpoints
N Branchpoints Counted
Human
Computer
In-Plane Branchpoints
Out-of-Plane Branchpoints
Hum
Comp
d
2D Manual
e
% Nerve Modeling Length
n.s.
3D Modeling
2D Manual
3D Manual

Figure 19. Computer Nerve Modeling Identifies Branchpoints and Nerve Length Missed By Manual Analysis.

(a-c) Out-of-plane branchpoints identified by nerve modeling and not by manual counting. (a) Image slice from non-rotated ("Original Image") data contains an in-plane branchpoint (red) with three branches viewable in the non-rotated plane. (b) Image slice from rotated data ("Rotated Image") contains an out-of-plane branchpoint (blue) with branches oriented in a different plane to original images and hence requires image rotation to visualize. Blinded humans counted branchpoints in the same 3D images. Humans were shown sample in-plane and out-of-plane branchpoints and taught to rotate images. (c) Comparison between human branchpoint counting (n=3) and computer nerve modeling. Humans consistently missed out-of-plane branchpoints that computer nerve modeling correctly identified. See video 3 in supplemental material. (d-g) Nerve length quantified using computer nerve modeling in six different sample images is equivalent to manual quantification of 3D image data ("3D Manual") and greater than manual quantification of 2D flattened image data ("2D Manual"). (d) Manual nerve tracing in 2D and 3D images. (e) Total nerve length was compared to computer modeling. ** $p < 0.01$, *** $p < 0.001$

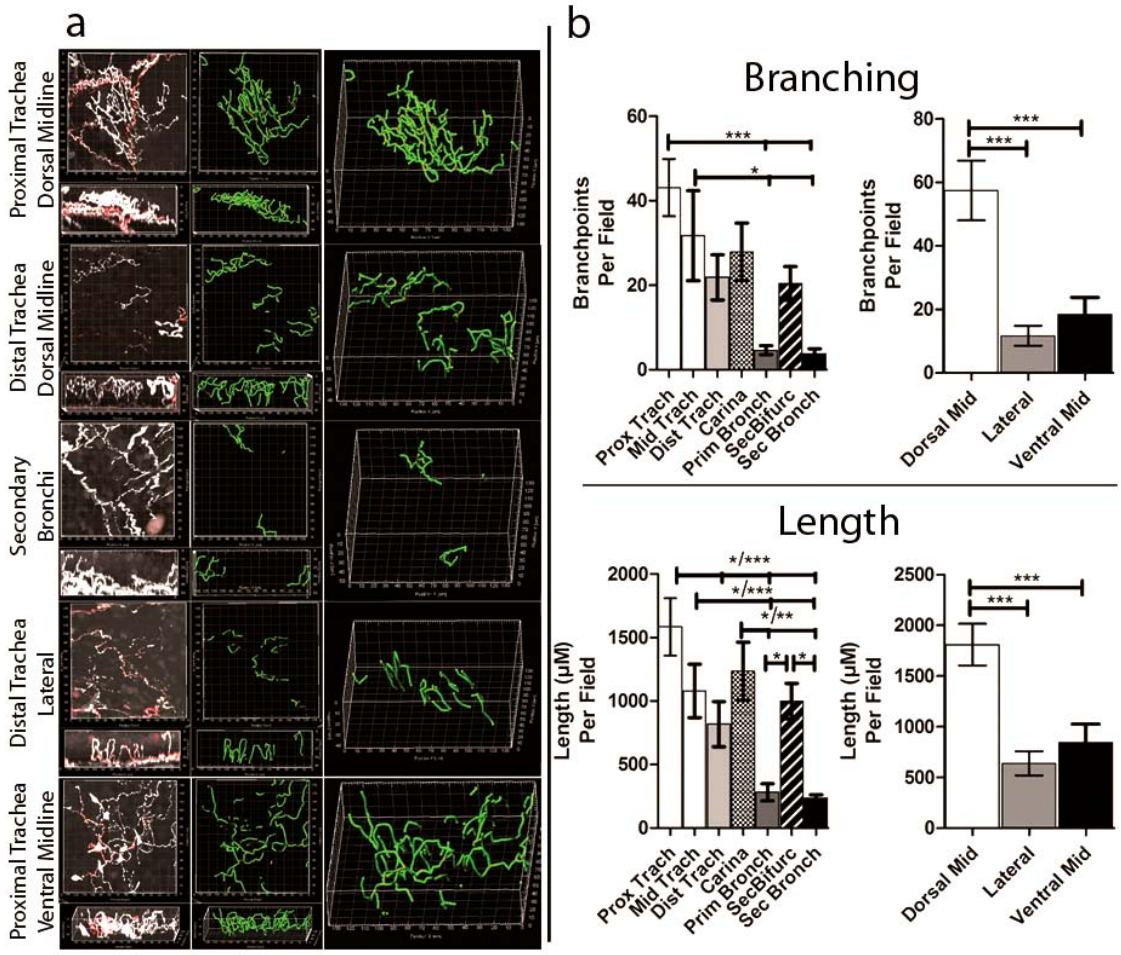

Figure 20. Organ-wide Structural Quantification of Murine Airway Epithelial Nerves, a Previously Unidentified Nerve Population.

(a) Lateral views of epithelial nerves (white) in different regions of the large airways with nerve model (green) overlaid on nerve image data. Substance P is labeled red and is discussed later. (b) Once modeled, nerve length and number of branchpoints was quantified by the computer per 135 μm x 135 μm field. Across multiple mice (N=6 mice), nerve length and branching decreased proximal-to-distal with regional increases at airway bifurcations. Nerve length and branching decreased from the dorsal midline to lateral and ventral positions in the trachea. N=6 MICE. * $p < 0.05$, ** $p < 0.01$, *** $p < 0.001$.

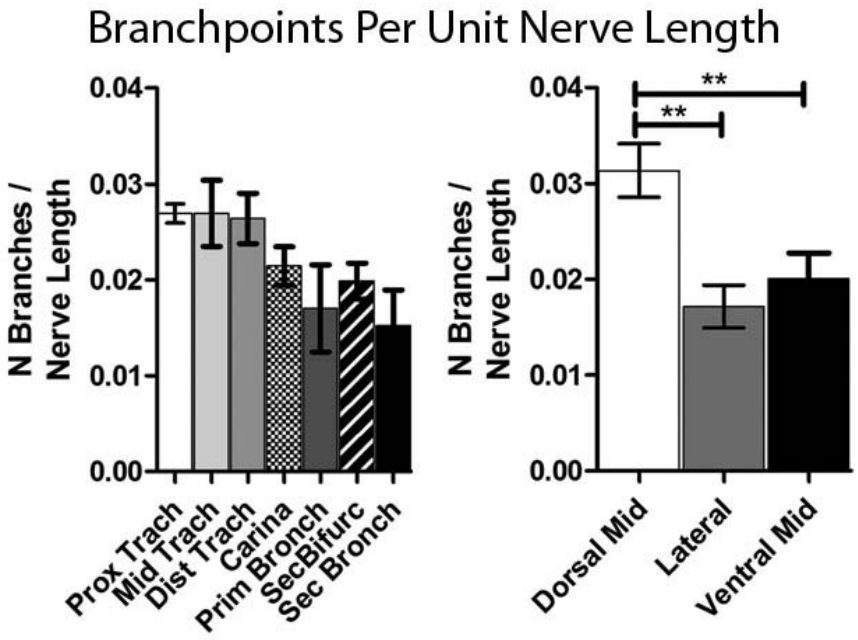

Figure 21. Changes in Nerve Branching Evaluated By Adjusting for Nerve Length.

Nerve branchpoints were divided by nerve length (µm) for all epithelial nerves per 135 µm x 135 µm field. Overall nerve branching per unit nerve length decreased proximal-to-distal and dorsal-to-lateral/ventral but proximal-to-distal was non-significant for post-test comparison of each location. N=6 mice.

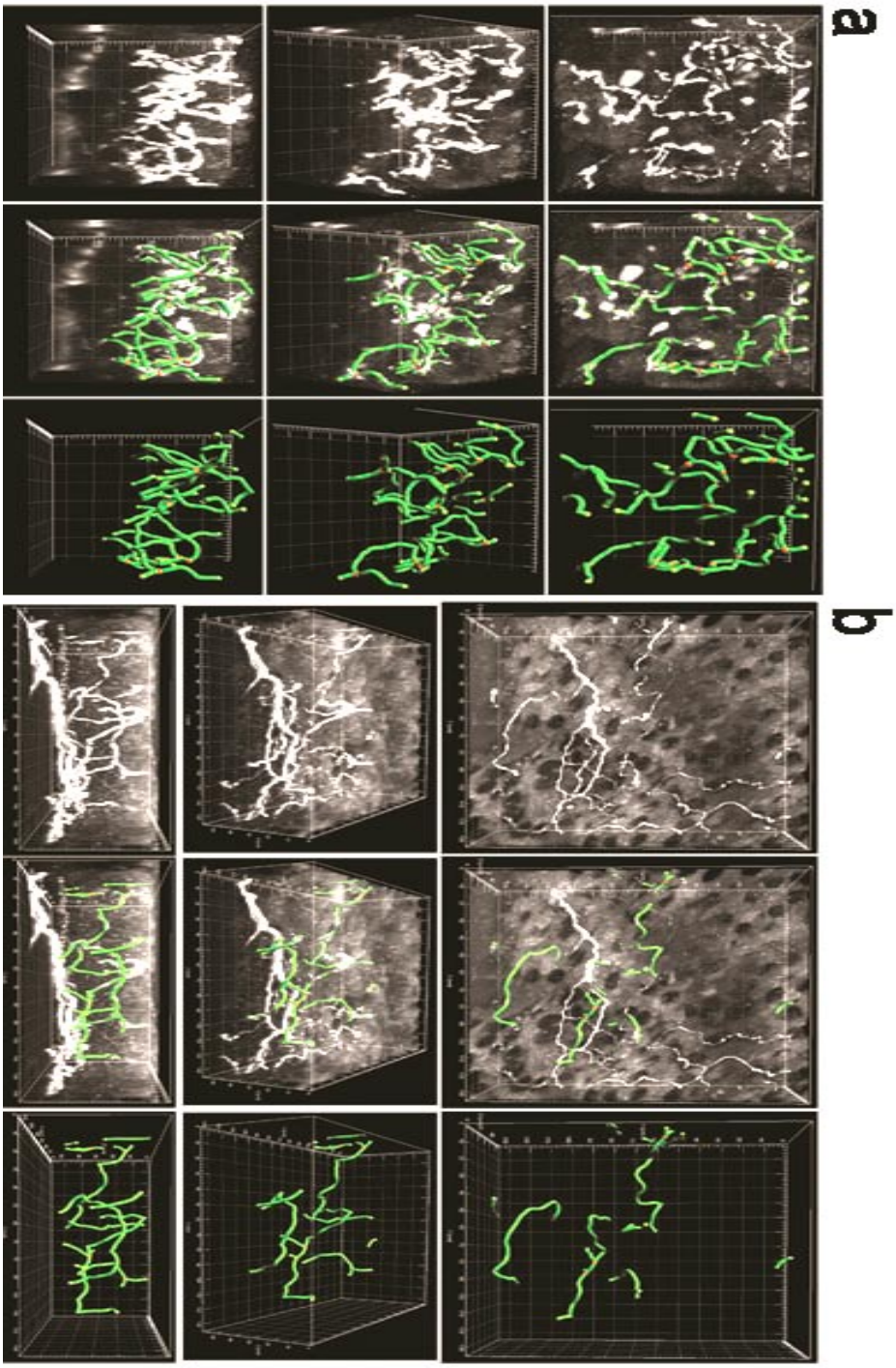

Figure 22. Epithelial Nerve Modeling Demonstrated in Large Animal Airway Tissue.

(a,b) Top (top row), oblique (middle row), and lateral (bottom row) projections of 3D nerve data alone and overlaid with computer modeling in a 135 µm x 135 µm field. (a) Guinea pig epithelial nerves (white) from trachea overlaid with the computer nerve model (green). (b) Epithelial nerves (white) and nerve modeling (green) demonstrated in canine airway tissue obtained using a forceps biopsy.

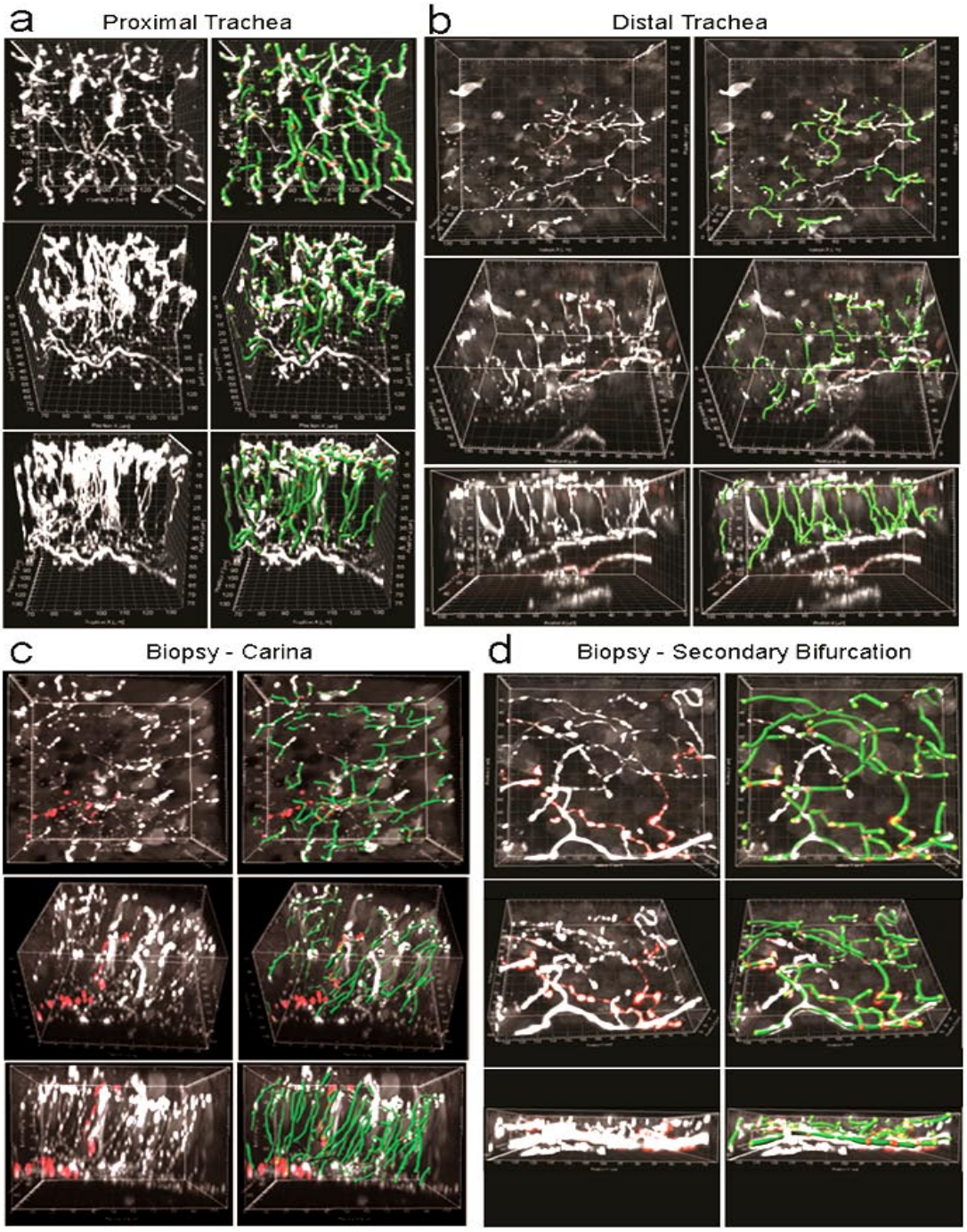

Figure 23. Epithelial Nerve Modeling in Human Airway Tissue.

(a,b) Top, oblique, and lateral projections of human epithelial nerves (white) in the proximal and distal trachea overlaid with computer nerve models (green) in a 135 µm x 135 µm field. (c,d) Epithelial nerves (white) and nerve modeling (green) in airway forceps biopsy tissue from airway bifurcations. Columnar epithelium present in the trachea autopsy specimens and carina biopsy specimen. Squamous epithelium present in the secondary bifurcation biopsy specimen.

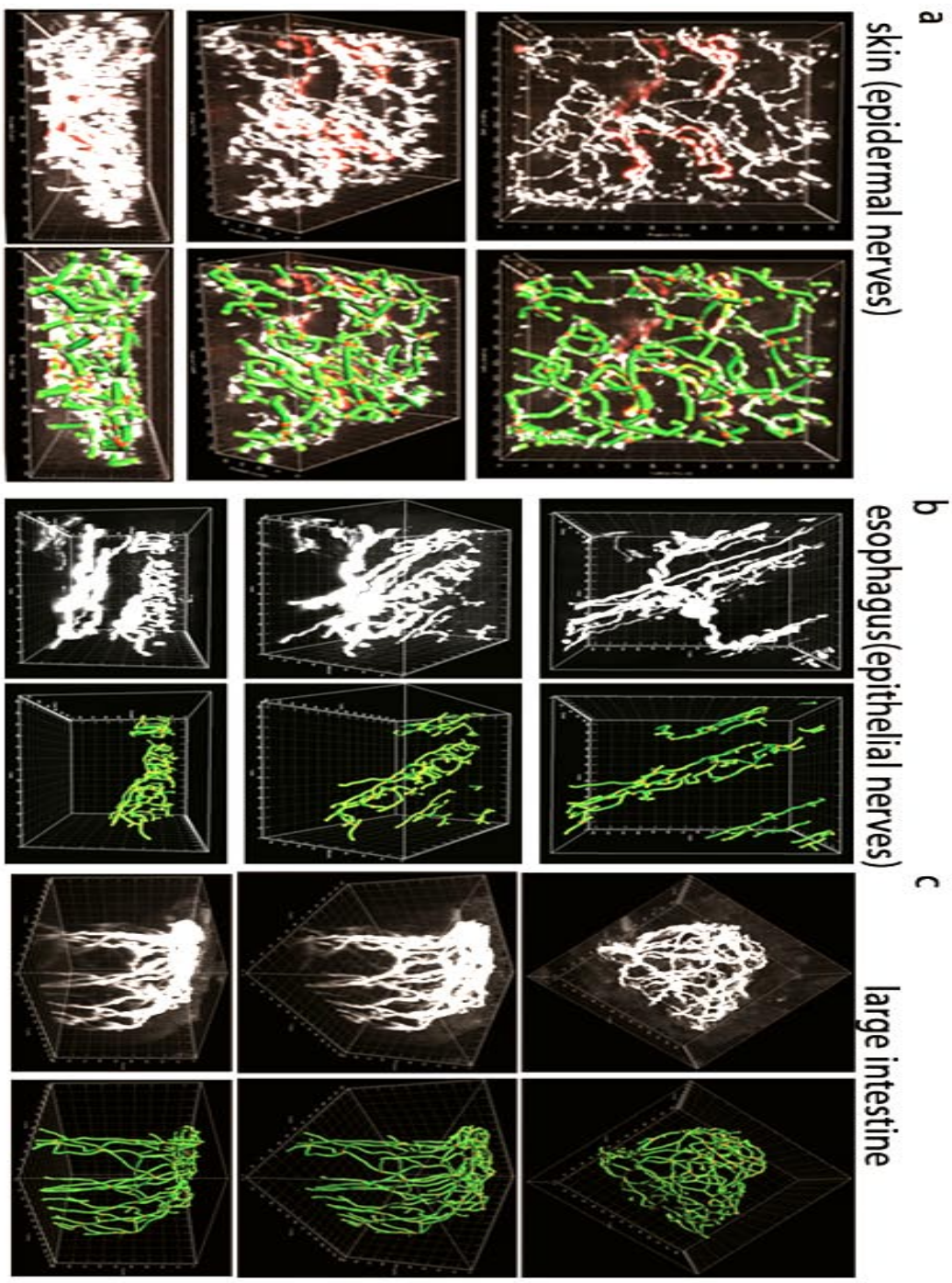

Figure 24. Nerve Modeling in Skin, Esophagus, and Large Intestine.

(a-c) Top, oblique, and lateral projections of nerve image data (white) alone, overlaid with the computer nerve model (green), or the nerve model alone in a 135 µm x 135 µm field. (a) Epidermal nerves (b) proximal esophageal epithelial nerves (c) intestinal nerves. Red pixels in epidermal image are discussed in Figure 28.

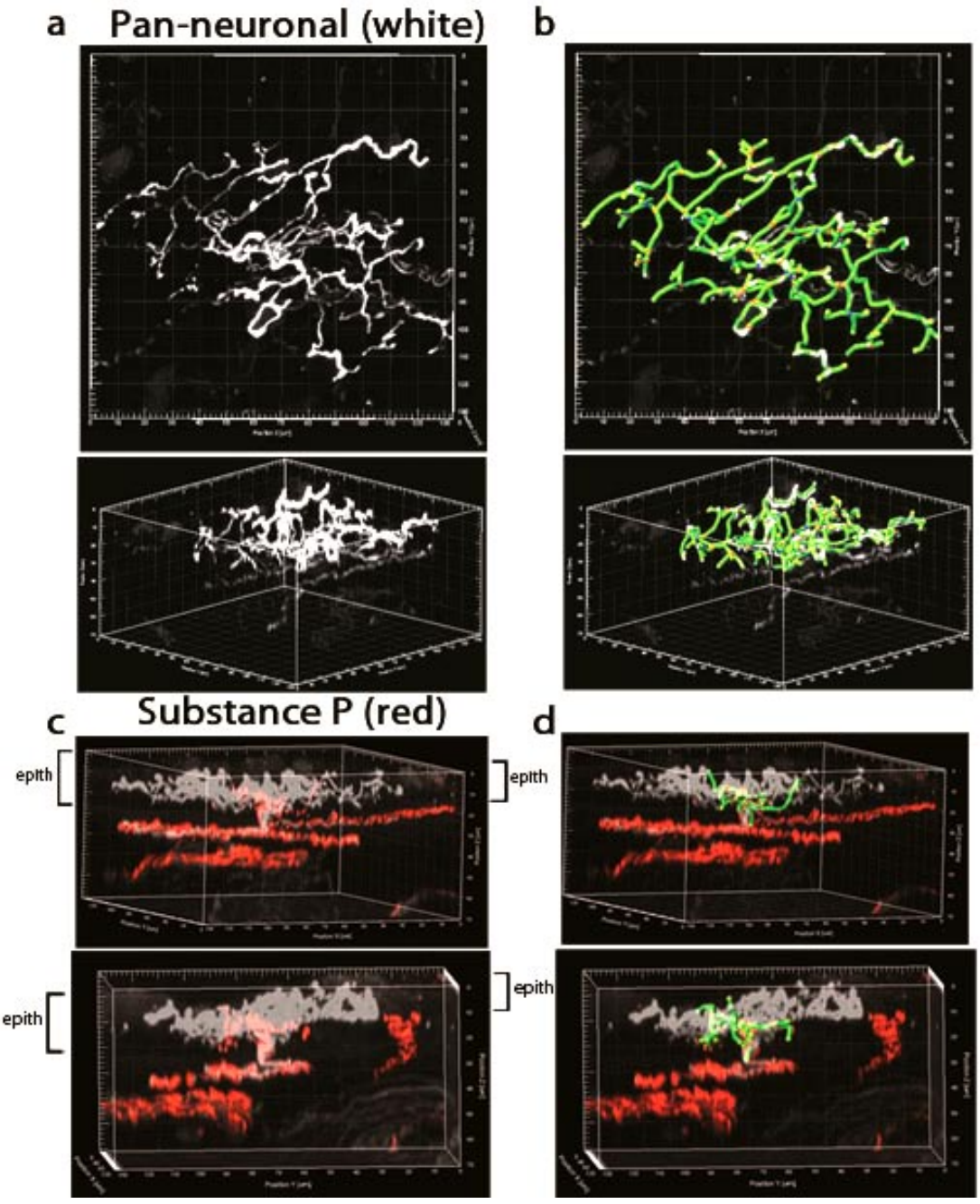

Figure 25. Computer Modeling Epithelial Nerves and the Substance P Subpopulation.

(a-d) Projections of an epithelial nerve patch containing a substance P subpopulation in a 135 µm x 135 µm field. (a) All nerves (white) were labeled using the pan-neuronal marker, PGP 9.5, and a sub-population (red) expressed substance P. (b) Overlay of raw image data and computer model of total epithelial nerves (green). (c) Substance P subpopulation (red) overlaid with total nerves (white-transparent) and (d) shown with the substance P nerve model (green).

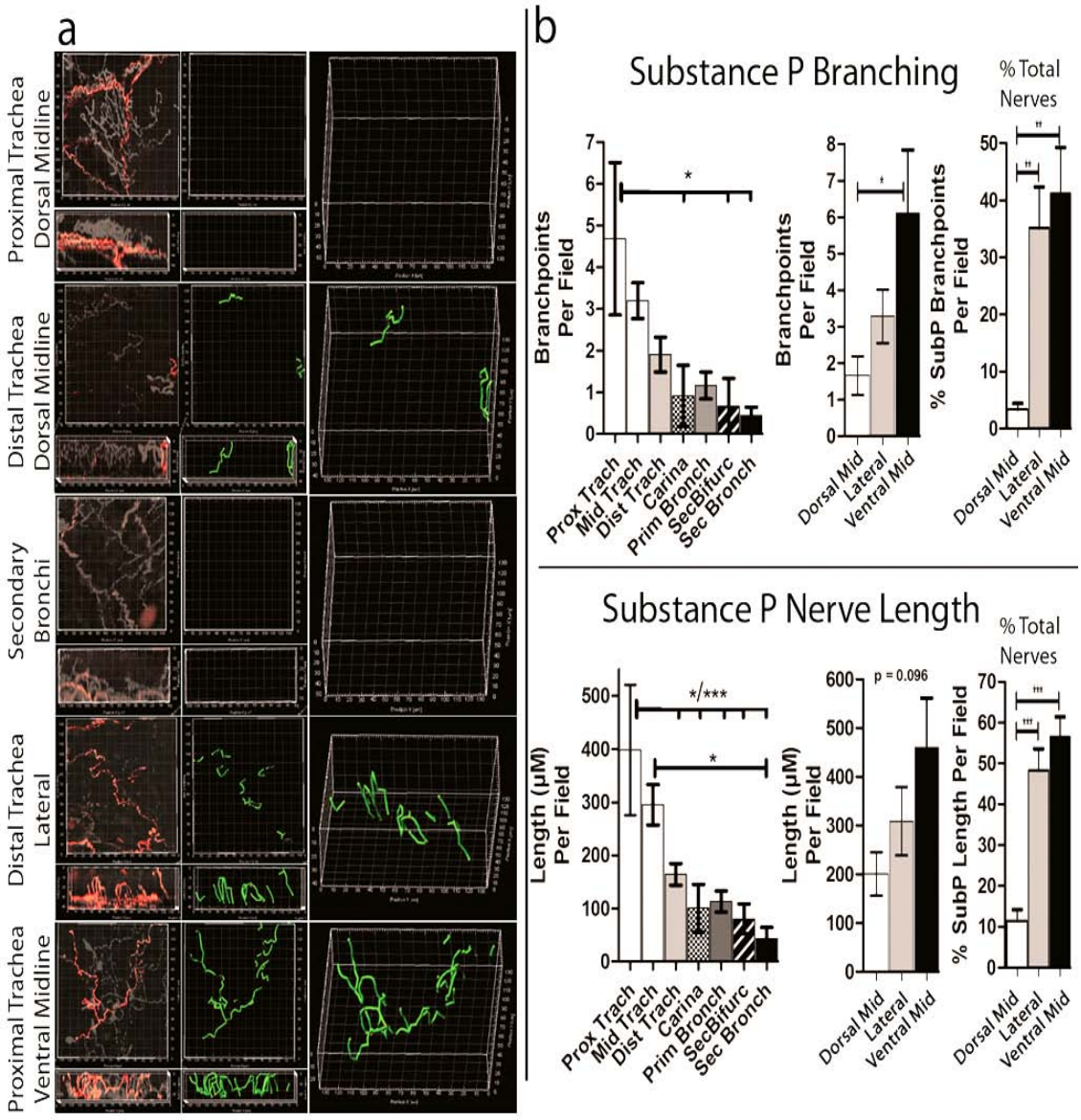

Figure 26. Distinct Organ-Wide Structure of an Airway Epithelial Nerve Subpopulation.

(a) Lateral views of substance P expressing nerves (red) overlaid on nerves labeled with a pan-neuronal marker (white – transparent). Computer substance P nerve model (green) overlaid on image data. (b) Once modeled, epithelial substance P nerve length and branching was quantified by the computer per 135 µm x 135 µm field. Similar to all epithelial nerves, substance P nerve length and branching decreased from proximal to distal airways. Unlike total epithelial nerves, substance P nerve length and branching increased from dorsal to lateral and ventral positions. This was also seen when substance P nerve length and branching was calculated as a percentage of total nerve length and branching (far right graphs). Unlike total nerves, substance P nerve length and branching also did not increase at airway bifurcations. N=6 MICE. * $p < 0.05$, ** $p < 0.01$, *** $p < 0.001$.

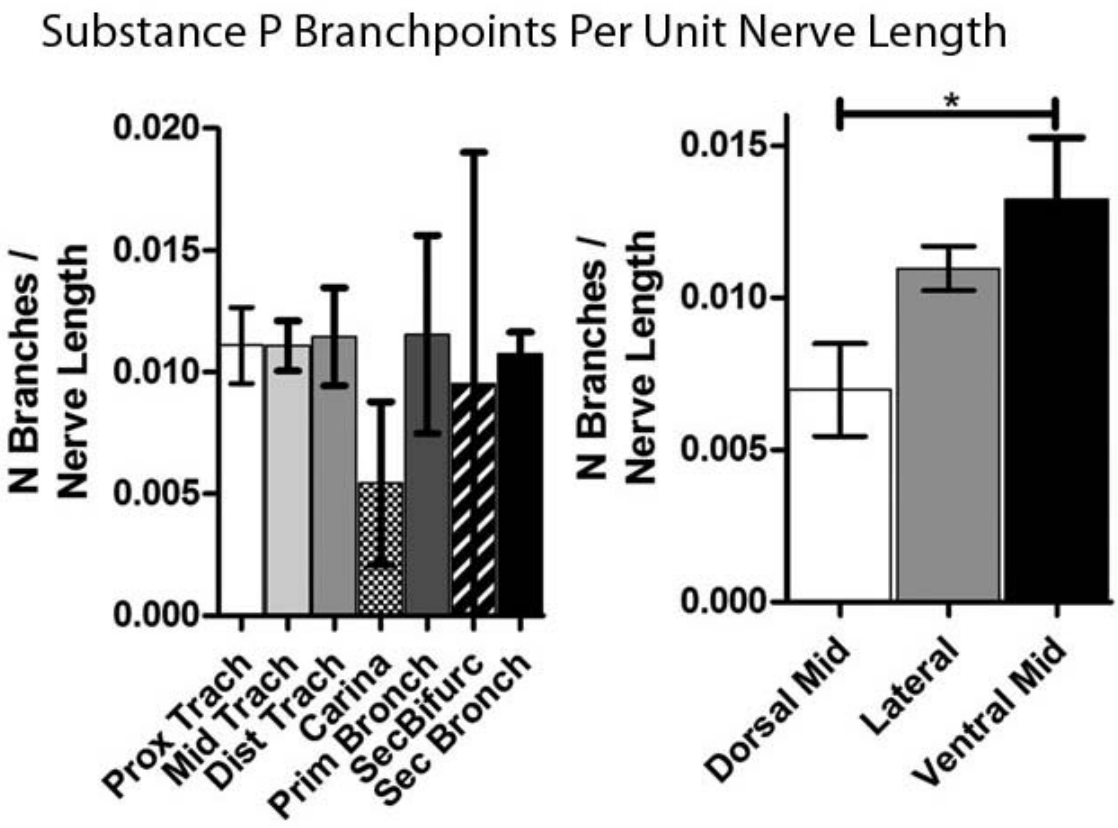

Figure 27. Changes in Substance P Nerve Branching Evaluated By Adjusting for Nerve Length.

Nerve branchpoints were divided by nerve length (µm) of the substance P subpopulation per 135 µm x 135 µm field. Overall nerve branching per unit nerve length decreased proximal-to-distal and dorsal-to-lateral/ventral but proximal-to-distal was non-significant for post-test comparison of each location. Unlike overall nerves, substance P branching per unit length increased dorsal-lateral-ventral but not proximal-to-distal. N=6 MICE. * $p < 0.05$, ** $p < 0.01$

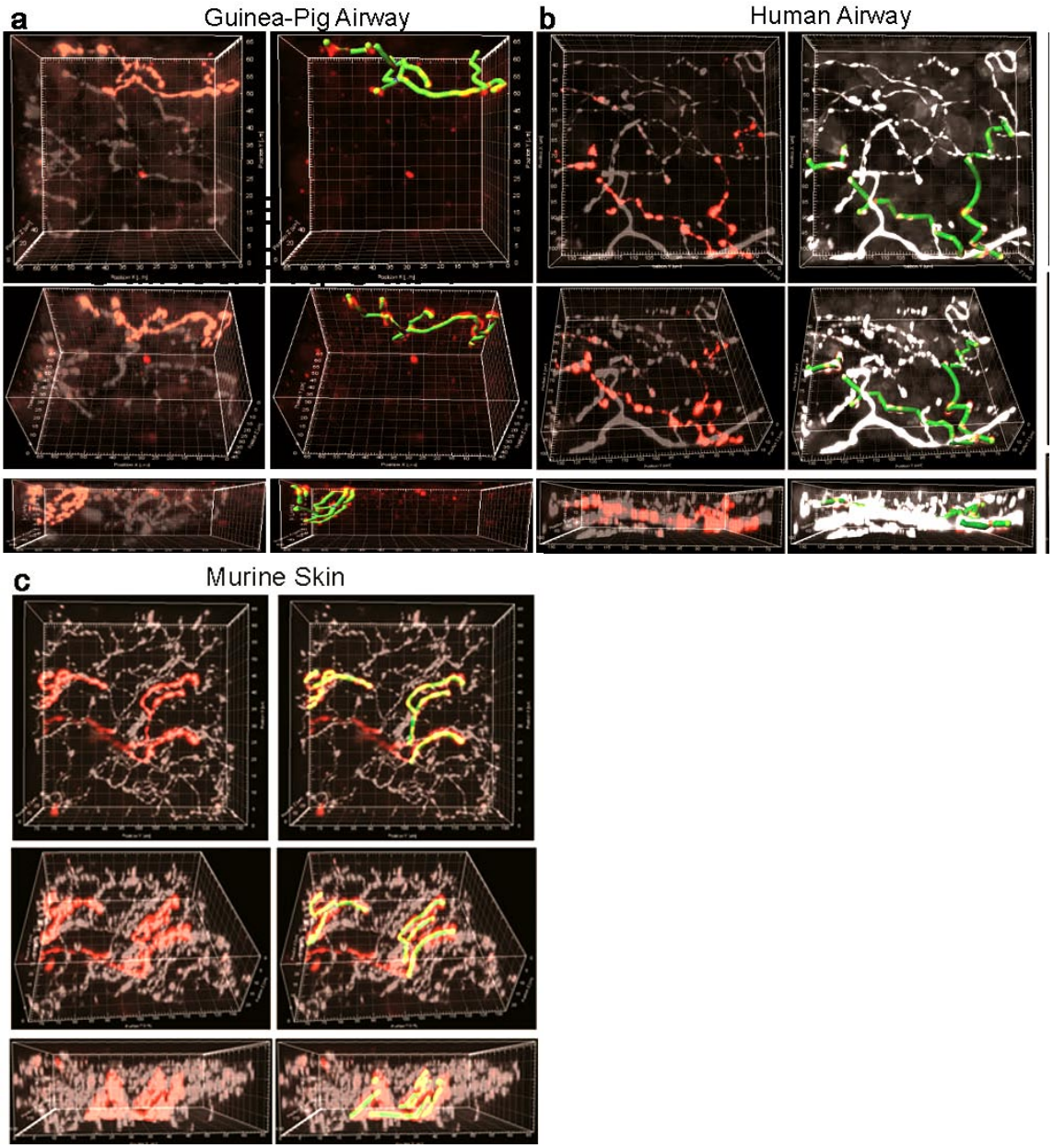

Figure 28. Modeling Substance P Epithelial Nerves in Guinea Pig and Human Airway, and Mouse SkinTissue.

(a-c) Top, oblique, and lateral projections of 3D nerve data alone and overlaid with computer modeling in a 135 µm x 135 µm field. Of the nerves (white - transparent) labeled using the pan-neuronal marker, PGP 9.5, a sub-population (red) labeled with an antibody against substance P. (a) Guinea pig tracheal epithelial nerves shown alone and overlaid with substance P nerve model. (b) Human epithelial nerves from forceps biopsy tissue (pan-neuronal staining shown in Figure 5) overlaid with the substance P nerve model. (c) Mouse epidermal nerves shown alone and overlaid with substance P nerve model.

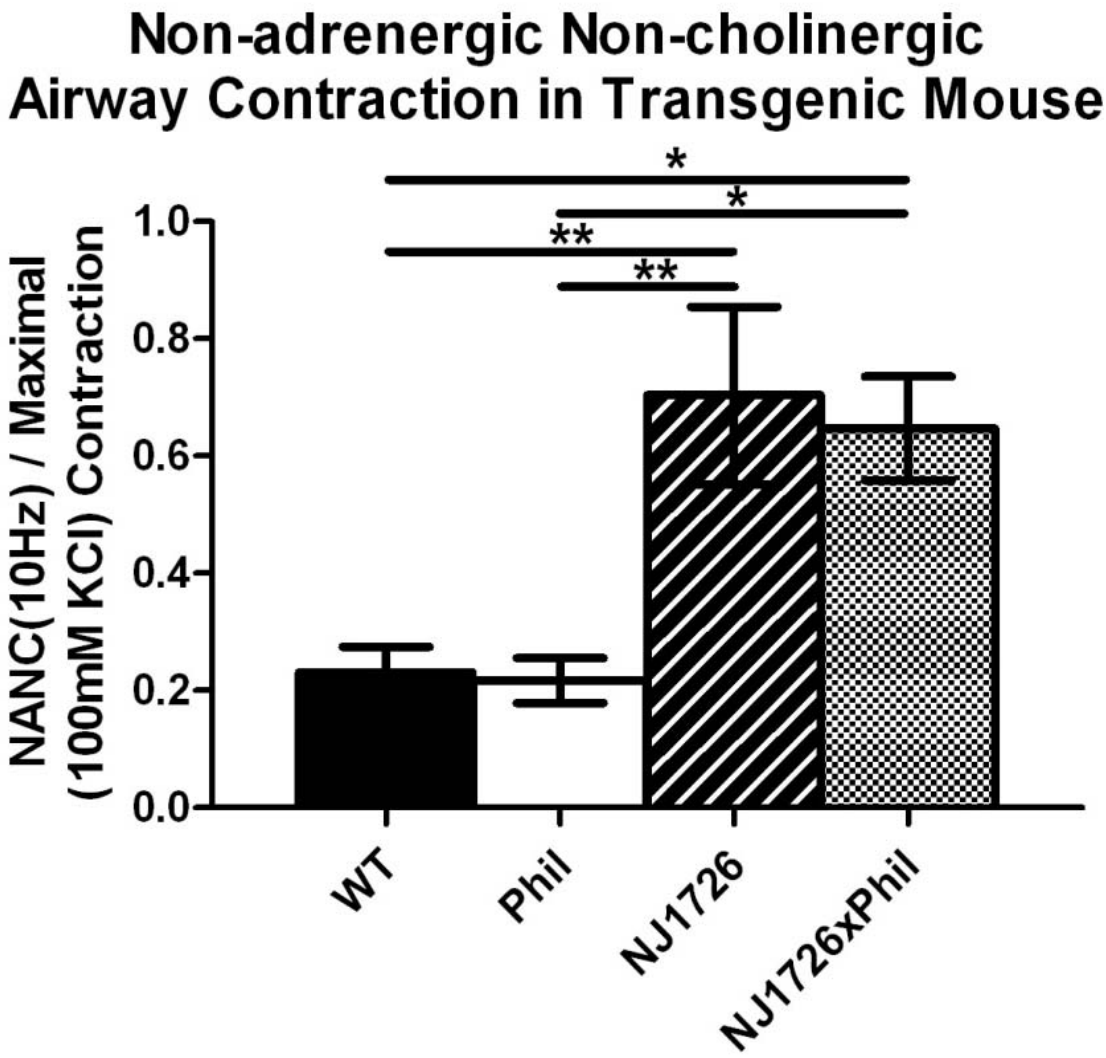

Figure 29. High Voltage (60V) and Long Pulse Width (2ms) Electrical Field Stimulated Reveals Increased Non-Neuronal Smooth Muscle Contractility Associated With Increased IL-5.

Trachea muscle contractions are induced in the presence of atropine (cholinergic antagonist) and propranolol (adrenergic antagonist). Standard trachea contractions are produced by administering 100mM KCl to ensure tissue viability. Data are shown for wildtype (N=6 mice), mice lacking eosinophils (PHIL, n=5), mice with lung eosinophilia due to IL-5 overexpression (NJ7126, n=5), and mice lacking eosinophils but overexpressing IL-5 in the lungs (NJ1726xPHIL, n=4). Contractions induced by this electrical stimulation were not inhibited by high doses of tetrodotoxin showing it was non-neuronal.

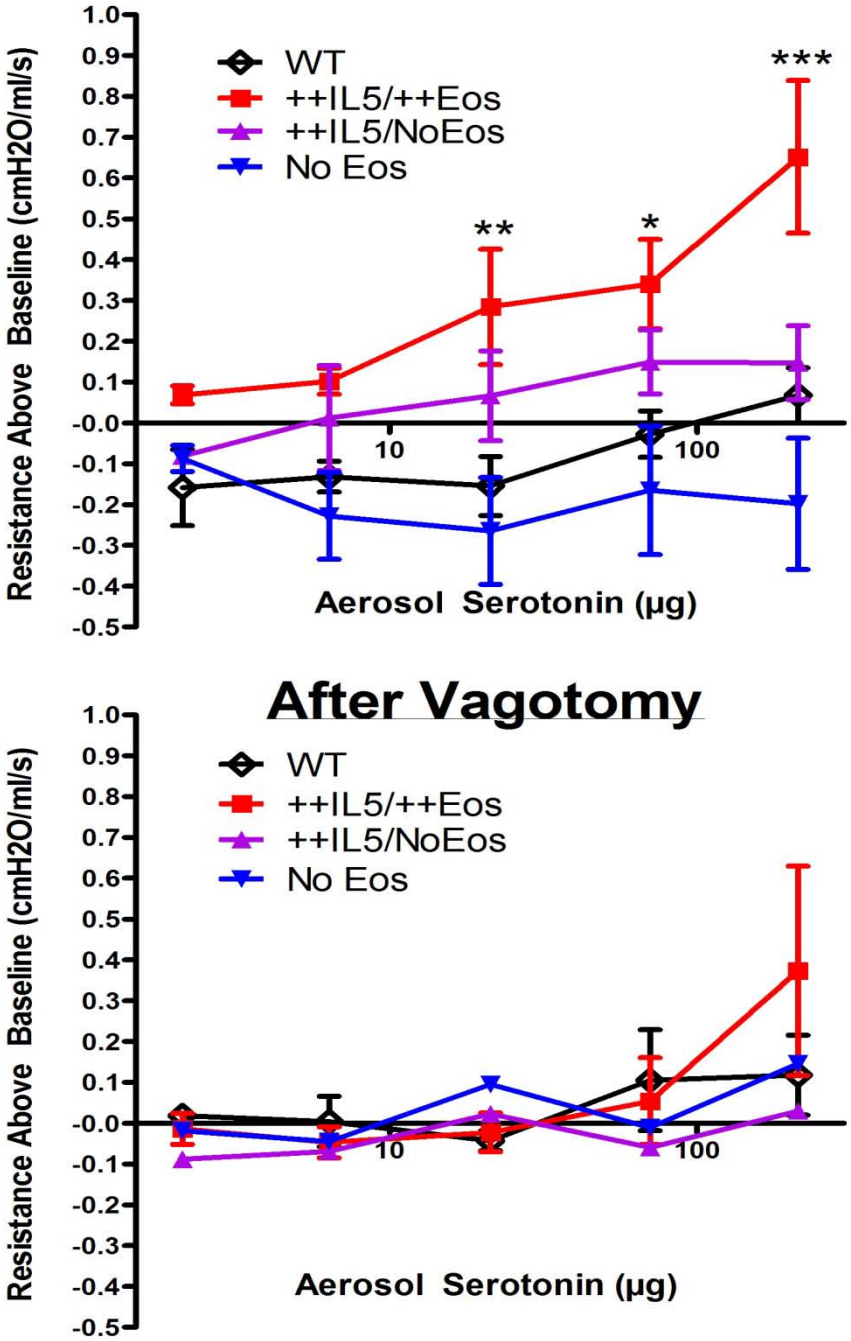

Figure 30. Increased Reflex Bronchoconstriction Associated with Lung Eosinophilia in a Chronic Allergic Inflammatory Asthma Model.

Airway contractions caused by increasing doses of aerosol serotonin were measured in mechanically ventilated wildtype mice (n=7), mice with chronic eosinophilia due to IL5 lung overexpression (++IL5/++Eos, n=9), mice lacking eosinophils (NoEos, n=3), and mice with IL-5 overexpression in the lung but lacking eosinophils (++IL5/NoEos, n=3). Mice with overabundant lung eosinophils had increased bronchoconstriction in response to aerosol serotonin that was eliminated by cutting airway innervation with vagotomy.

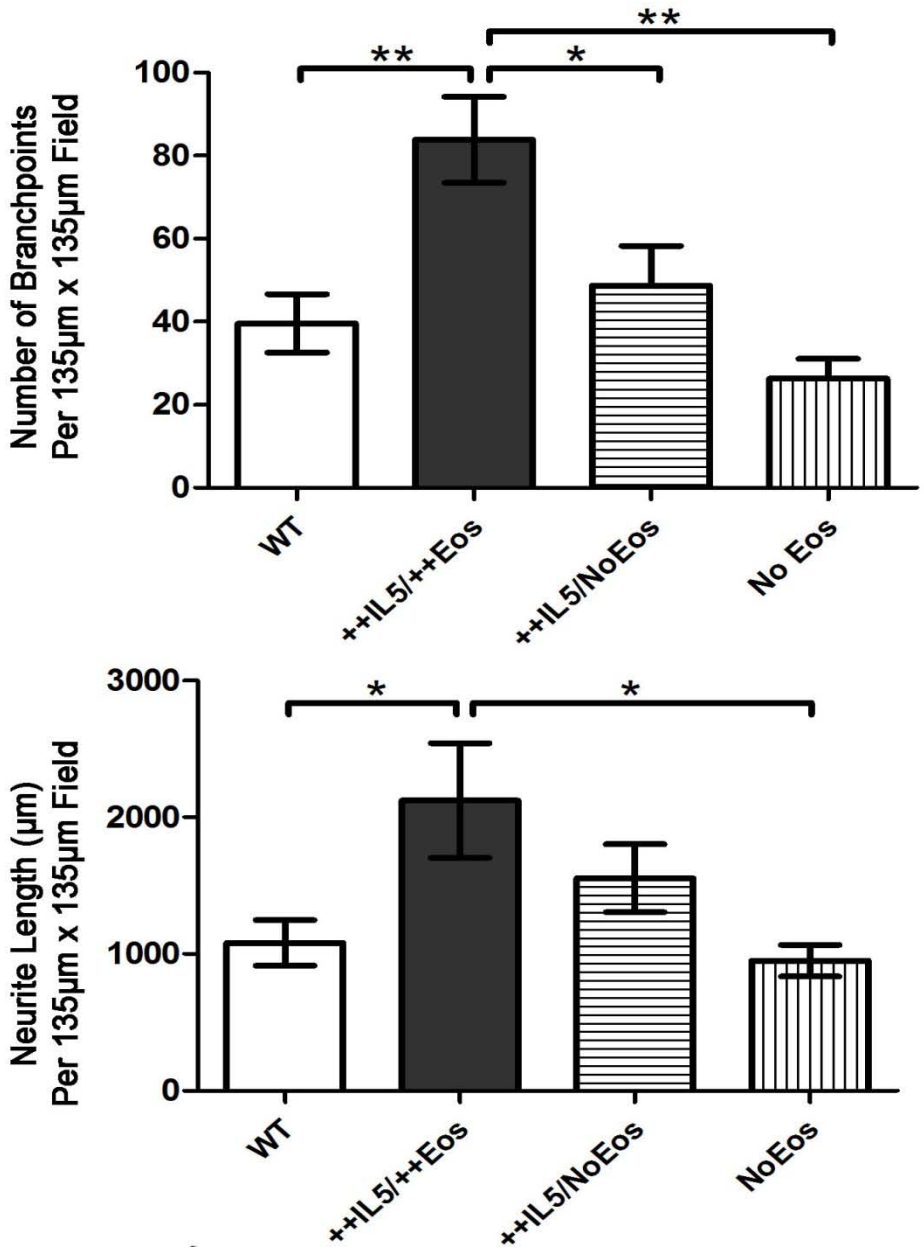

Figure 31. Increased Neuron Branching and Length in Airway Epithelium Associated with Lung Eosinophilia in a Chronic Allergic Inflammatory Asthma Model.

Three-dimensional epithelial nerve morphology was imaged in the large airways of wildtype mice (n=5), mice with chronic eosinophilia due to IL5 lung overexpression (++IL5/++Eos, n=4), mice lacking eosinophils (NoEos, n=4), and mice with IL-5 overexpression in the lung but lacking eosinophils (++IL5/NoEos, n=4). Computer models of nerve morphology were generated and nerve length and branching quantified per 135 µm x 135 µm field. Mice with overabundant lung eosinophils showed significantly increased nerve length and branching above wildtype and this required the presence of eosinophils. * $p < 0.05$

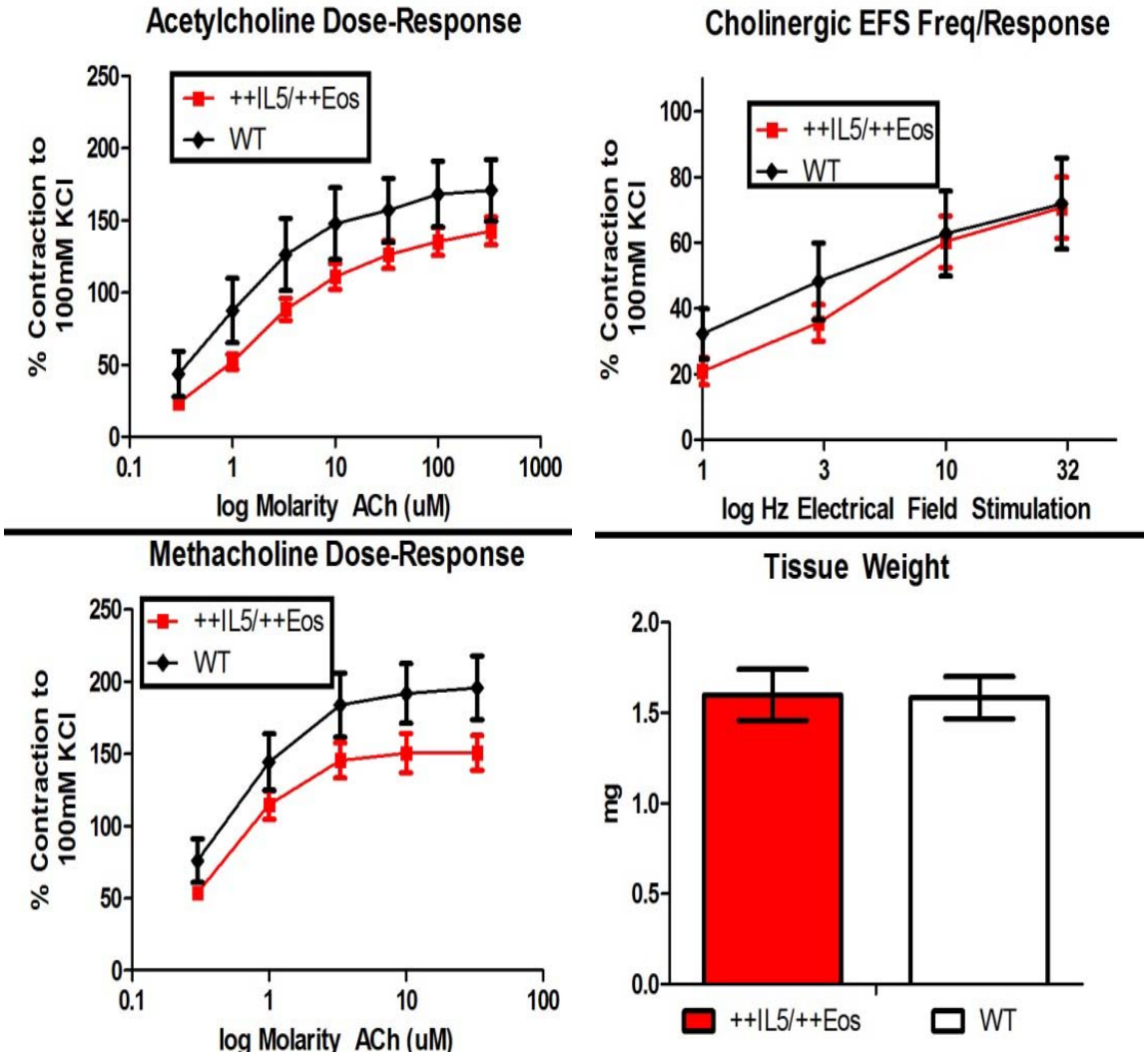

Figure 32. Increased Eosinophils Not Associated With Changes in Muscle Contractility Ex Vivo.

Tracheas from wildtype (WT) mice and NJ.1726 mice with overabundant eosinophils (++IL5/++Eos), were contracted with direct cholinergic agonists, acetylcholine (top left panel) and methacholine (lower left panel) (n=12 and n=17), and electrical field stimulation (EFS) (n=14 and n=19) of parasympathetic nerves (top right panel). Muscle contractions were not significantly different with any of these stimuli. An equivalent amount of smooth muscle was harvested as indicated by tissue weight (lower right panel).

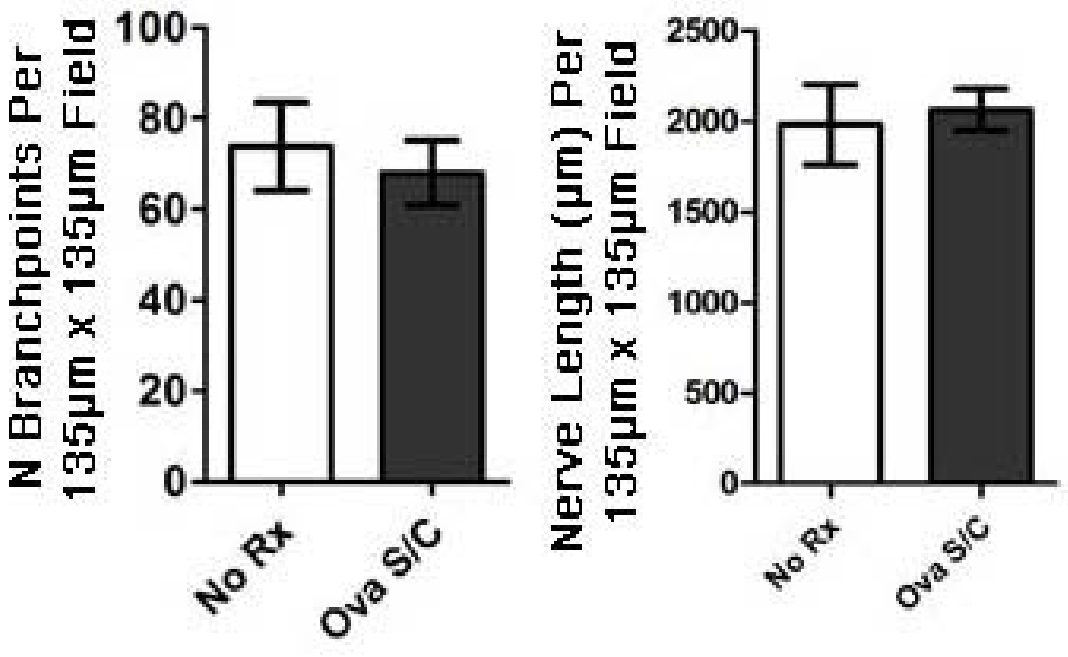

Figure 33. No Change in Neuron Branching and Length in Airway Epithelium in an Acute Allergic Inflammatory Asthma Model.

Three-dimensional epithelial nerve morphology was imaged in the large airways of untreated mice (NoRx, n=5) and mice sensitized to ovalbumin and administered ovalbumin in the airway (Ova S/C, n=4). Computer models of nerve morphology were generated and nerve length and branching automatically quantified. There was not a significant difference in nerve length or branching between treatment groups.

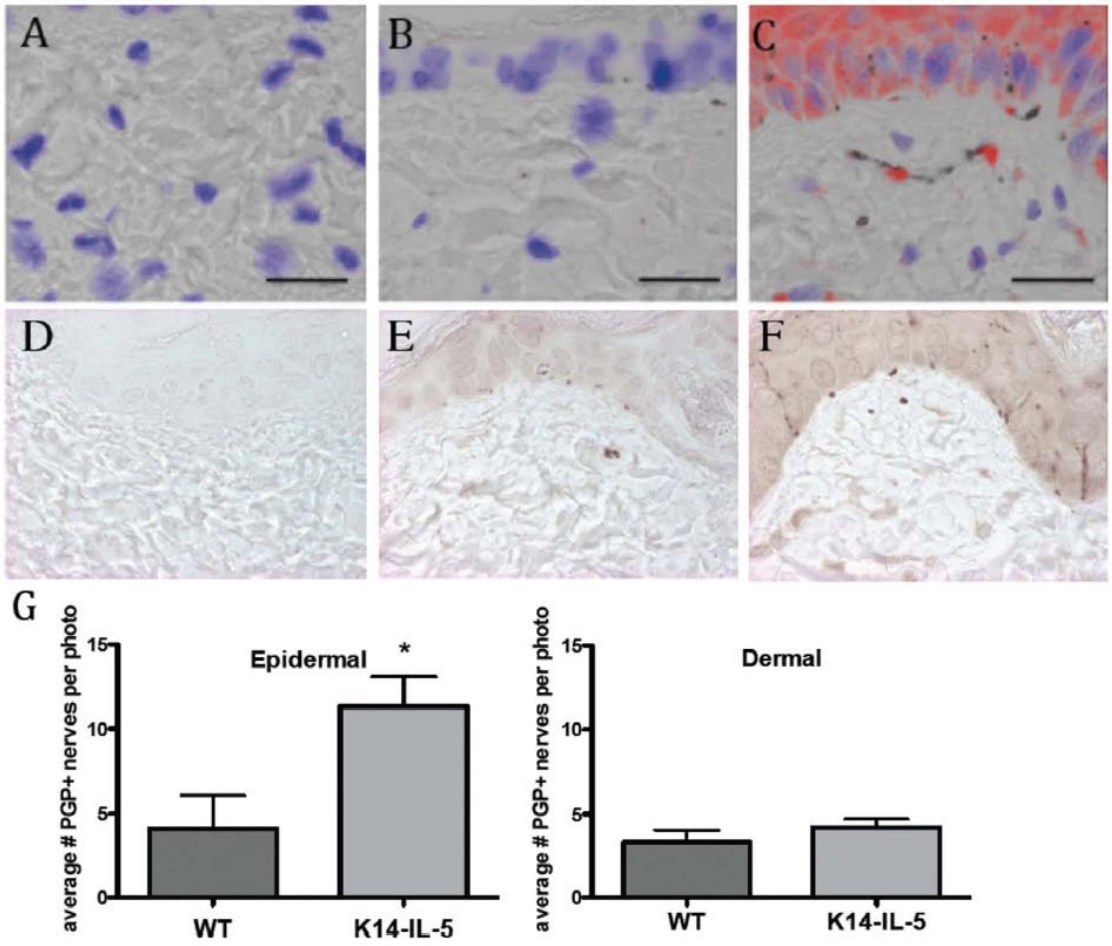

Figure 34. Keratin 14-interleukin 5 mice have eosionophil major basic protein (MBP) primarily in the epidermis, and have more nerves in epidermis and basement membrane zone than wild-type controls, but similar numbers in the dermis.

5 µm skin sections on slides were stained using anti-MBP (red, in top three sections) and anti-PGP9.5 to visualize nerves (brown, in bottom three sections). Photographs of each entire section were taken, and random numbers assigned to each for quantification of nerves by an observer blinded to the genotype. (A and D) IgG negative control, (B) anti-MBP staining of wild type mouse, (C) anti-MBP staining of K14-IL-5 skin section. MBP staining is largely seen in the epidermis, which is where the IL-5 is expressed. (E) PGP9.5 stained wild type mouse, (F) PGP9.5 stained K14-IL-5 skin section. Note the extensive linear nerves from the basement membrane zone through many layers of the epidermis. (G) Quantification of nerves shows an increase in the epidermis (where IL-5 is expressed and eosinophil major basic protein is seen) but not in the dermis. Scale bars = 50 µm.

From (Foster, Simpson et al. 2011)

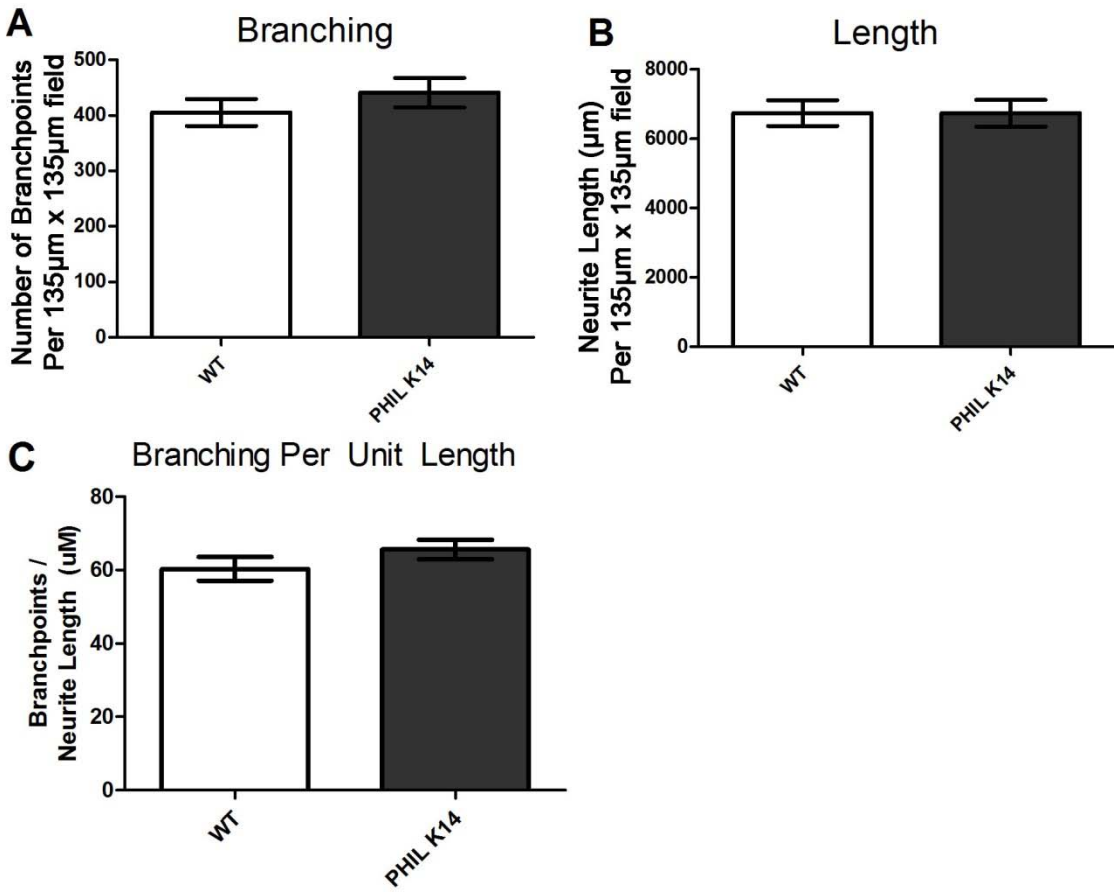

Figure 35. Epidermal Nerve Branching and Length are Not Changed in Mice with Skin Overexpression of IL-5 and Absence of Eosinophils.

Epidermis was dissected from the base of the right ear in wildtype mice (n=4) and mice (PHIL/K14, n=4) overexpressing IL-5 under a keratinocyte promoter but lacking eosinophils. Epidermis was then stained for nerves with the pan-neuronal marker, PGP 9.5. Epidermal nerves were imaged and computer modeled in five 135 µm x 135 µm images for each experimental replicate. N=4.

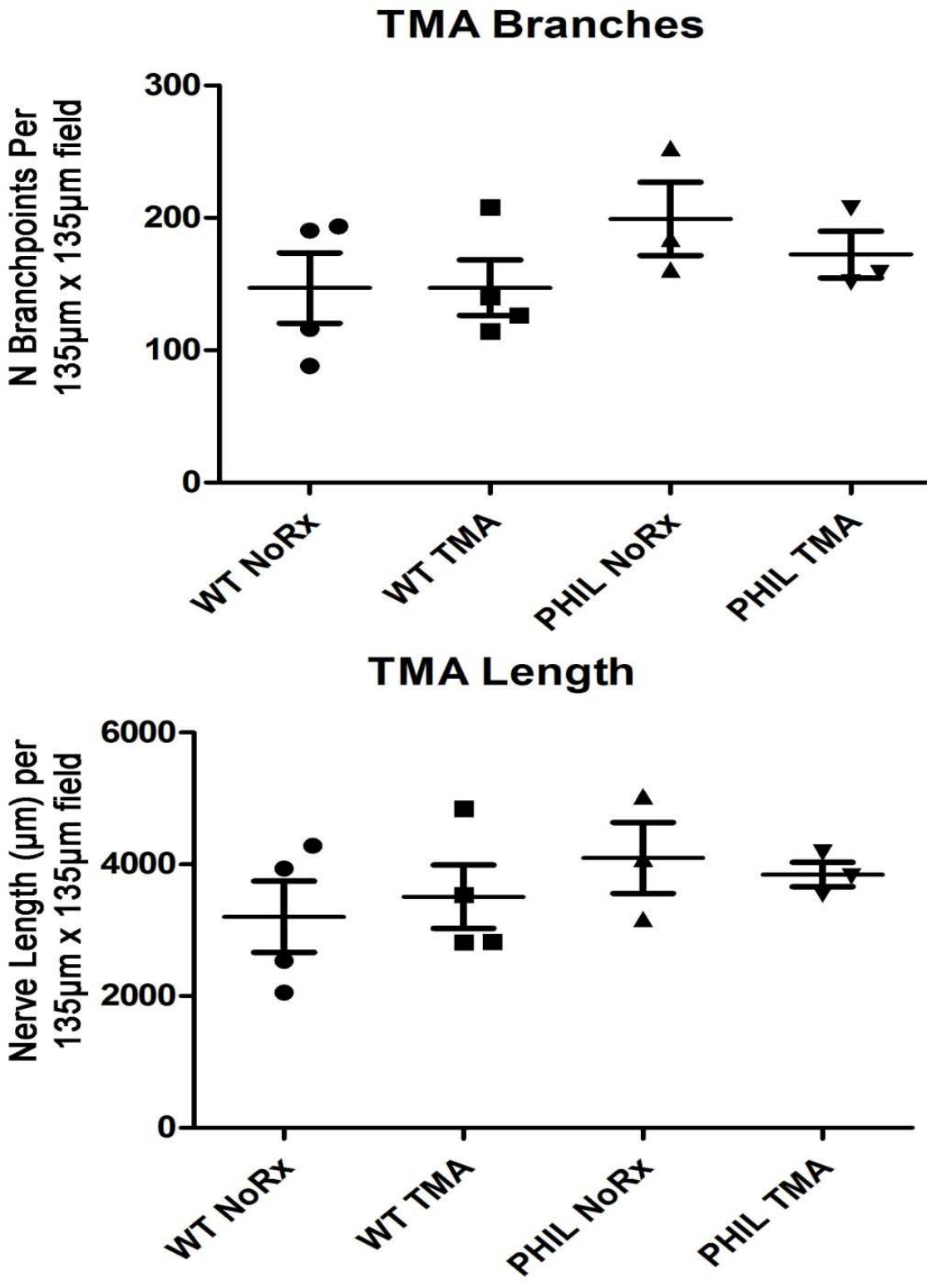
TMA Branches
N Branchpoints Per 135µm x 135µm field
300
200
100
0
WT NoRx
WT TMA
PHIL NoRx
PHIL TMA
TMA Length
Nerve Length (µm) per 135µm x 135µm field
6000
4000
2000
0
WT NoRx
WT TMA
PHIL NoRx
PHIL TMA

Figure 36. Chemical Treatment Model of Subacute Dermatitis is Not Associated With Structural Neuroplasticity.

Wildtype (n=4) and mice lacking eosinophils (PHIL, n=3) were administered trimetallic anhydride (TMA), a model of subacute dermatitis, in one ear and vector control into the opposite ear. The epidermis of TMA-treated and control ear tissue was stained with the pan-neuronal marker, PGP 9.5 and nerves were modeled with the computer to automatically calculate nerve length and branching per 135 µm x 135 µm field. In ears treated with TMA there was no change in nerve length and branching. In mice lacking eosinophils there was also no change in nerve length or branching after TMA treatment.

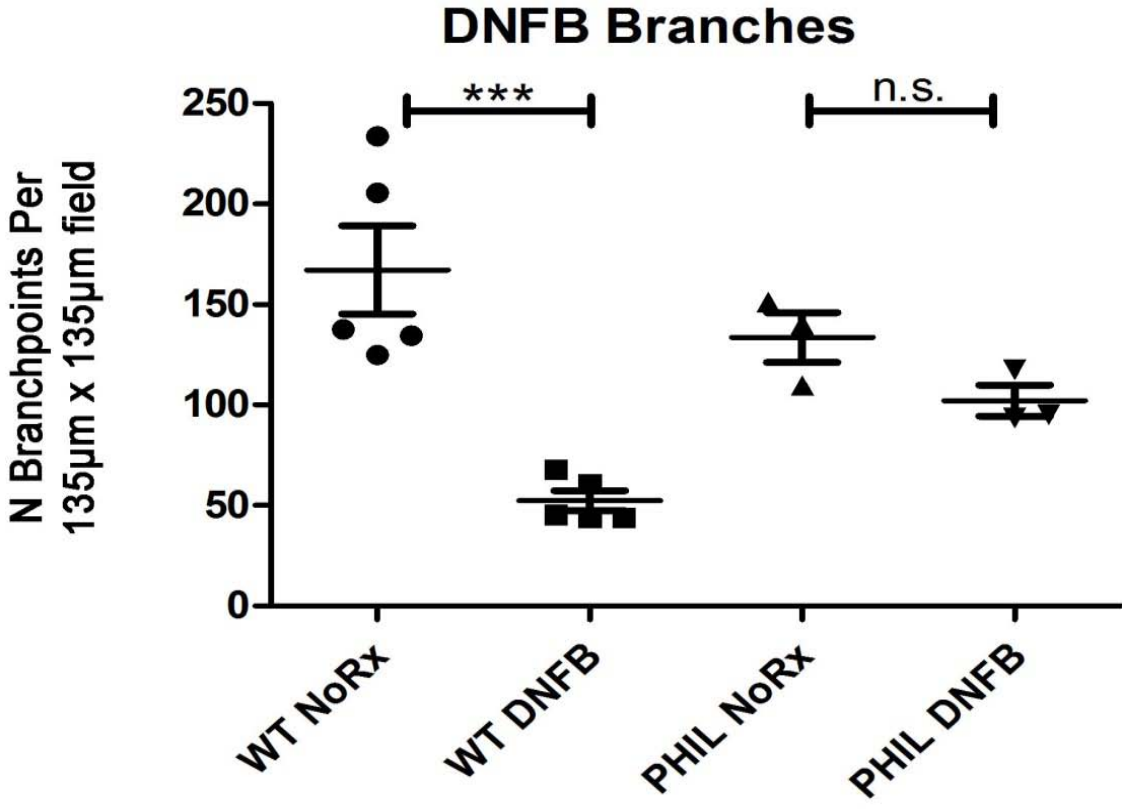
DNFB Branches
N Branchpoints Per 135µm x 135µm field
250
200
150
100
50
0
***
n.s.
WT NoRx
WT DNFB
PHIL NoRx
PHIL DNFB

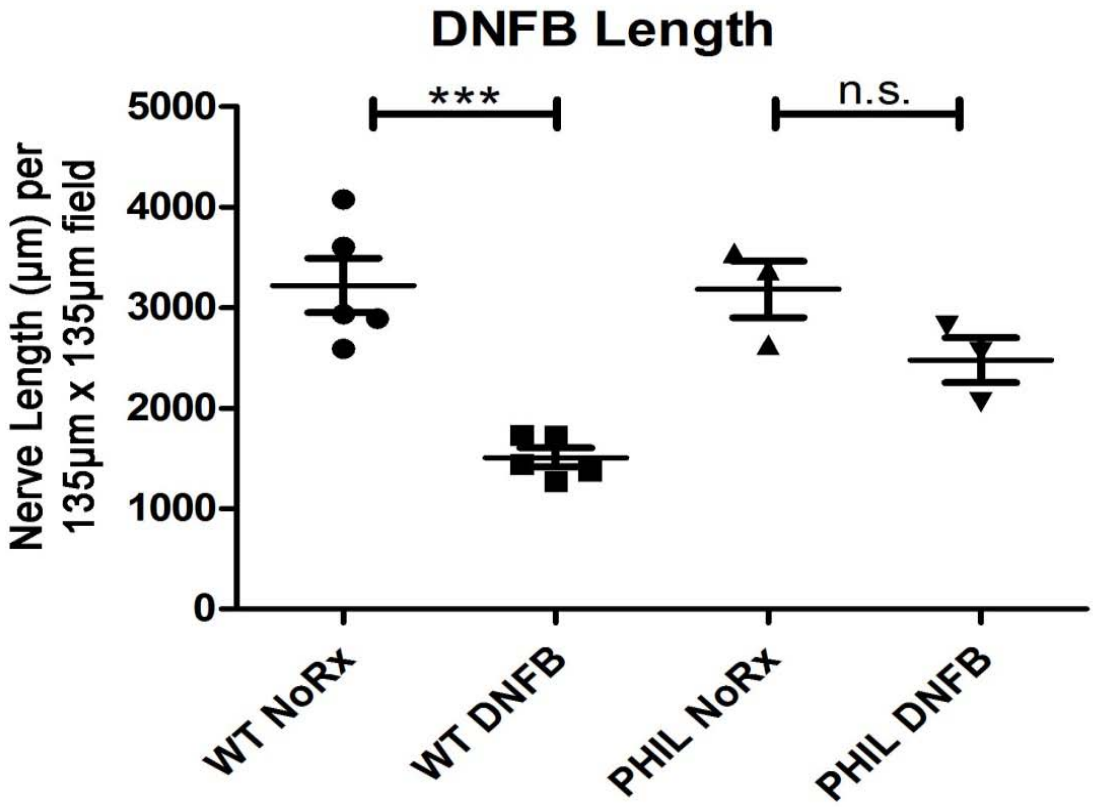
DNFB Length
Nerve Length (µm) per 135µm x 135µm field
5000
4000
3000
2000
1000
0
***
n.s.
WT NoRx
WT DNFB
PHIL NoRx
PHIL DNFB

Figure 37. Nerve Branching and Length Decrease in a Chemical Treatment Model of Acute Dermatitis and is Prevented by Loss of Eosinophils.

Wildtype (n=5) and mice lacking eosinophils (PHIL, n=3) were administered 2,4-dinitrofluorobenzene (DNFB), a model of acute dermatitis, in one ear and vector control (3:1 acetone/olive oil) into the opposite ear. The epidermis of DNFB-treated and control ear tissue was stained with the pan-neuronal marker, PGP 9.5 and three-dimensional nerves were modeled with the computer to automatically calculate nerve length and branching. In the ears of Wildtype mice treated with DNFB there was a significant decrease in epidermal nerve length and branching compared to the untreated ear. In mice lacking eosinophils there was not a significant decrease in either nerve length or branching in the DNFB treated ear. This suggests that acutely, eosinophils are associated with nerve destruction, recycling, or failed repair in chemically-treated skin. *** $p < 0.001$

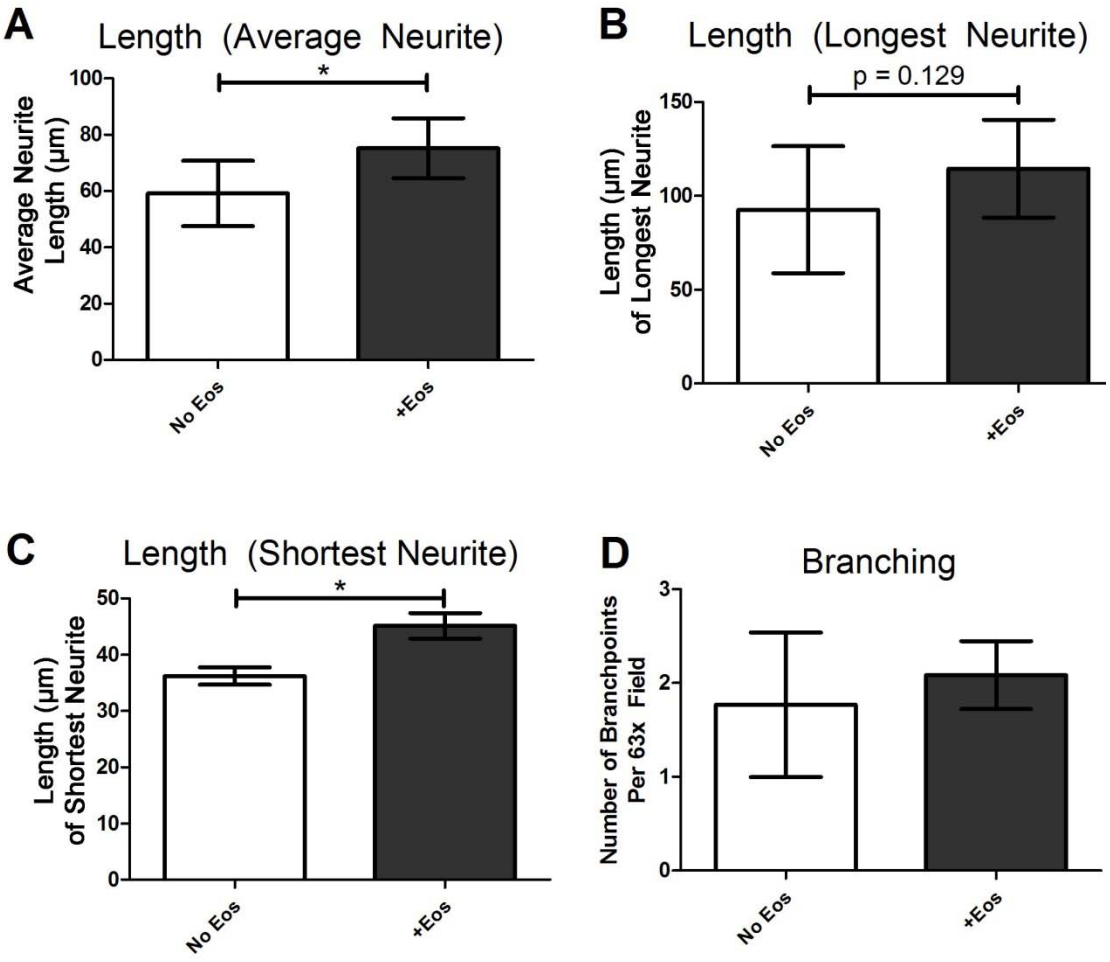

Figure 38. Co-culture of Human Sensory Neurons with Human Eosinophils Increases Nerve Length.

Human sensory neurons from lumbar dorsal root ganglia were cultured with and without eosinophils harvested from peripheral blood. Note that enrichment of sensory nerve cultures using cytosine arabinoside was not performed. When eosinophils were co-cultured with sensory nerves, the average length of a sensory neurite (A) and the minimum neurite length (C) were increased. B: There was also a trend for increased length of the longest neurite with eosinophil co-culture. D: The number of branchpoints was not significantly different between treatment groups and was highly variable between experimental replicates. N=3. * $P < 0.05$

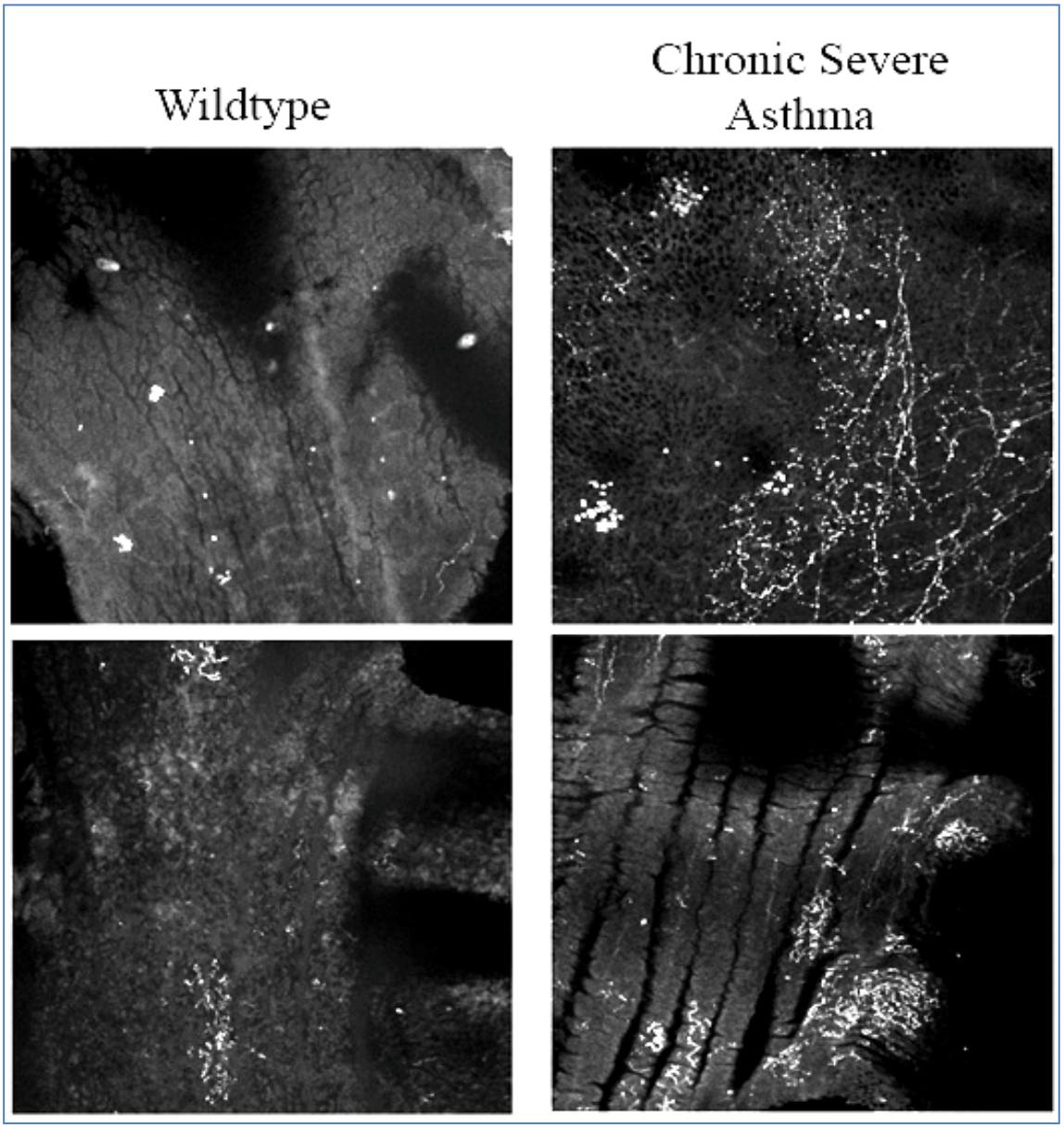

Figure 39. Pilot Data Showing Increased Epithelial Innervation in a Mouse Model of Chronic Severe Asthma.

Airway epithelium at the carina in wildtype mice and in a transgenic mouse model of chronic severe asthma where IL-5 is overexpressed systemically and eotaxin-2 is overexpressed in the lung leading to eosinophilia, asthma symptoms, and airway remodeling. Large field-of-view low resolution (10x, 850 µm x 850 µm) images of nerves labeled with PGP 9.5 (white) showing increased epithelial nerve signal in the mouse model of chronic severe asthma.

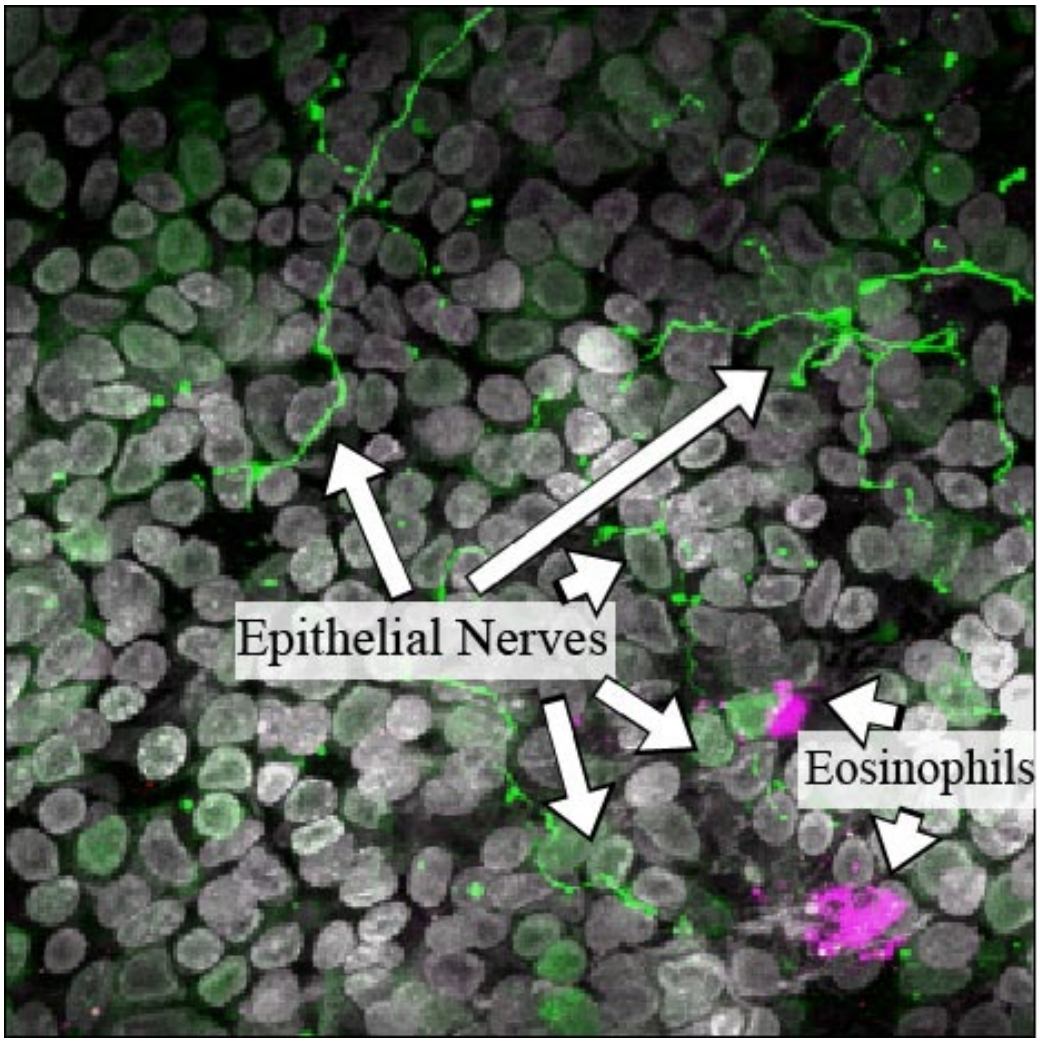

Figure 40. Imaging Human Epithelial Nerves and Eosinophils in Bronchoscopic Airway Biopsies.

Demonstration of human airway epithelial nerves (green), eosinophils (pink), and cell nuclei (white) imaged in airway biopsy specimens.

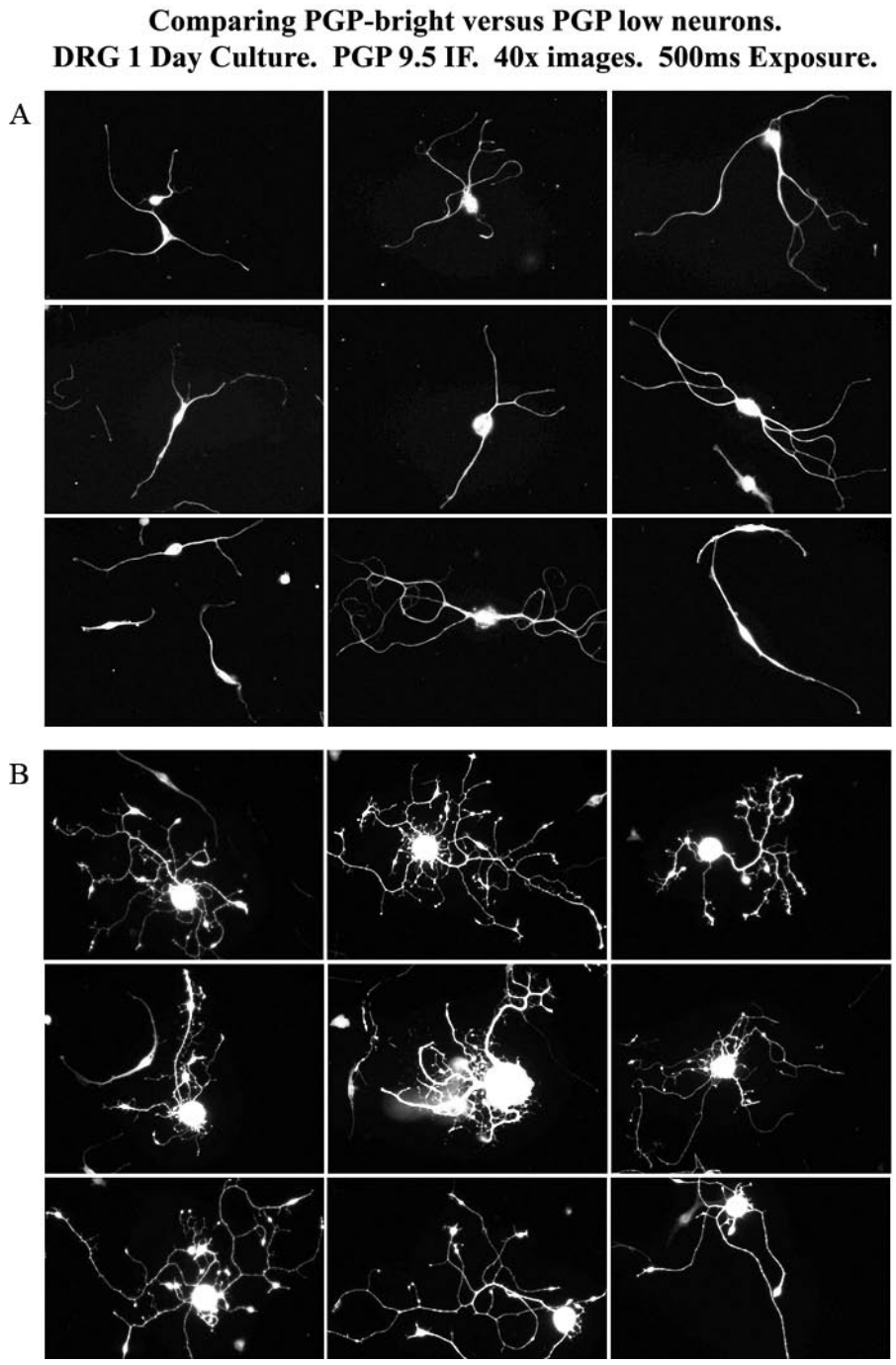

Figure 41. Imaging Neuronal Phenotype in Culture.

Panels A and B show cultured sensory nerves harvested from dorsal root ganglion. Neurons are labeled with the pan-neuronal marker, PGP 9.5. A: Smaller diameter neurons with rounded branching pattern likely representing C fibers. B: Larger diameter highly branched neurons likely representing A fibers. Future studies of airway neuroplasticity (phenotype or branched outgrowth) will likely need to distinguish these two unique neuronal populations.

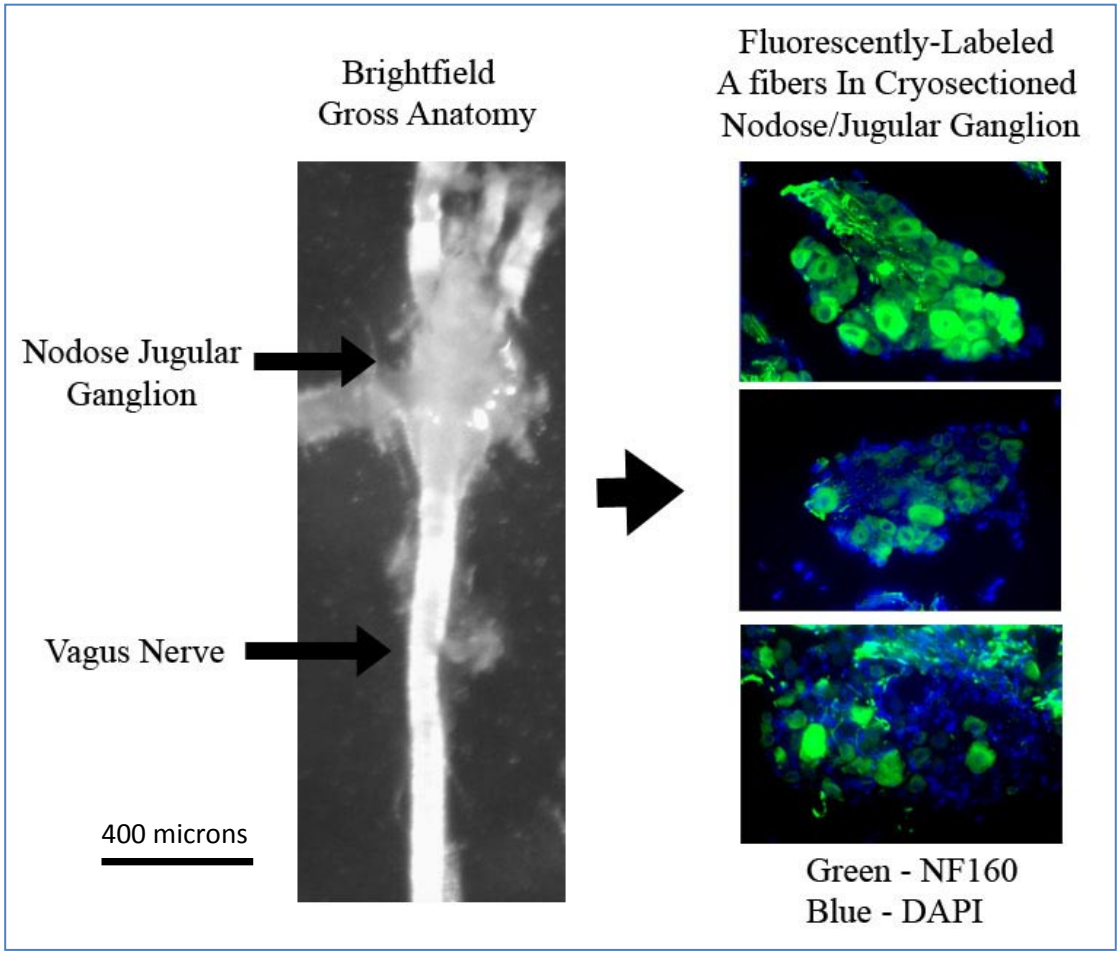

Figure 42. Imaging Nerve Phenotype in Nodose Versus Jugular Airway Sensory Ganglia of Mice.

Left panel: Low magnification brightfield image showing a single circular transparent structure, the fused mouse nodose/jugular ganglion. Right panel: Cryosectioned nodose/jugular ganglia stained for a nerve phenotype marker of large diameter A fibers, NF160. Note the variability in NF160 staining which is likely caused by imaging either the nodose or jugular ganglia. The nodose ganglion supplies the majority of A fibers to the airway (uppermost image) whereas the jugular ganglion supplies a minority of A fibers (middle and lowermost images). Future studies of airway neuroplasticity (phenotype or branched outgrowth) will likely need to distinguish these two unique nerve populations.

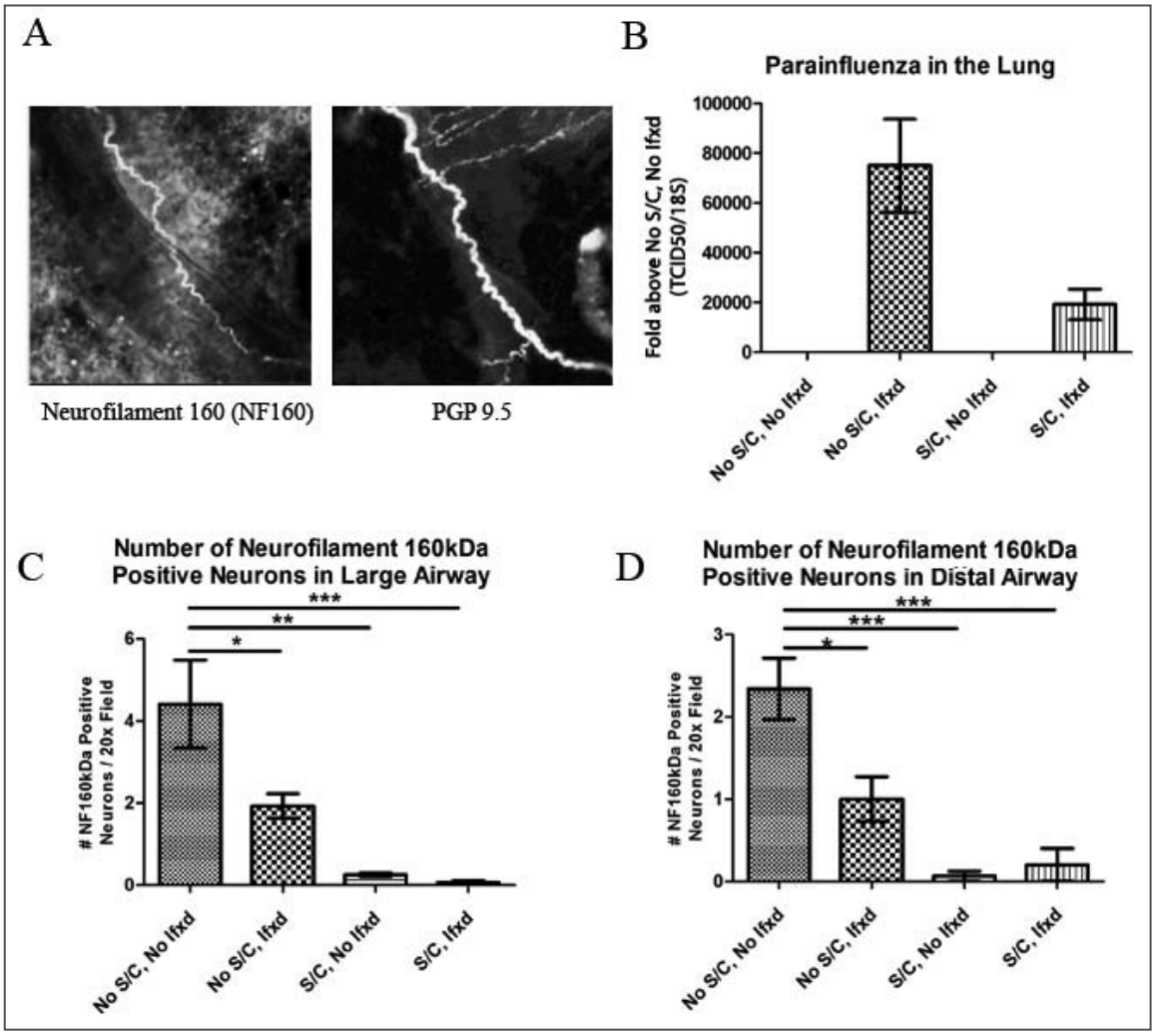

Figure 43. Virus Infection Associated With A Fiber Phenotypic Plasticity.

Mice were sensitized and challenged with ovalbumin ("S/C") in an acute allergic inflammatory asthma model and/or infected with parainfluenza virus ("Ifxd"). A: Airways were stained for nerve using the pan-neuronal marker, PGP 9.5 (blue), and the A fiber phenotype using NF160 (green). NF160 fibers were counted in flattened whole mount images. B: Infection with parainfluenza was confirmed by PCR of whole lung homogenates. C and D: Parainfluenza infection caused an intermediate loss of NF160 fiber phenotype ("No S/C, Ifxd") in both the large and small airways. 20x images are 450µm x 450µm.

WORKS CITED

Abramoff, M. D., P. J. Magalhaes, et al. (2004). "Image Processing with ImageJ." Biophotonics International **11**(7): 36-42.

Adamko, D. J., B. L. Yost, et al. (1999). "Ovalbumin sensitization changes the inflammatory response to subsequent parainfluenza infection. Eosinophils mediate airway hyperresponsiveness, m(2) muscarinic receptor dysfunction, and antiviral effects." J Exp Med **190**(10): 1465-1478.

Adriaensen, D., I. Brouns, et al. (2003). "Functional morphology of pulmonary neuroepithelial bodies: extremely complex airway receptors." Anat Rec A Discov Mol Cell Evol Biol **270**(1): 25-40.

Airaksinen, M. S. and M. Saarma (2002). "The GDNF family: signalling, biological functions and therapeutic value." Nat Rev Neurosci **3**(5): 383-394.

Akdis, C. A., M. Akdis, et al. (1999). "T cells and T cell-derived cytokines as pathogenic factors in the nonallergic form of atopic dermatitis." J Invest Dermatol **113**(4): 628-634.

Al-Chaer, E. D., M. Kawasaki, et al. (2000). "A new model of chronic visceral hypersensitivity in adult rats induced by colon irritation during postnatal development." Gastroenterology **119**(5): 1276-1285.

Albers, K. M., T. N. Perrone, et al. (1996). "Cutaneous overexpression of NT-3 increases sensory and sympathetic neuron number and enhances touch dome and hair follicle innervation." J Cell Biol **134**(2): 487-497.

Albers, K. M., C. J. Woodbury, et al. (2006). "Glial cell-line-derived neurotrophic factor expression in skin alters the mechanical sensitivity of cutaneous nociceptors." J Neurosci **26**(11): 2981-2990.

Albers, K. M., D. E. Wright, et al. (1994). "Overexpression of nerve growth factor in epidermis of transgenic mice causes hypertrophy of the peripheral nervous system." J Neurosci **14**(3 Pt 2): 1422-1432.

Almarestani, L., G. Longo, et al. (2008). "Autonomic fiber sprouting in the skin in chronic inflammation." Mol Pain **4**: 56.

Alsina, B., T. Vu, et al. (2001). "Visualizing synapse formation in arborizing optic axons in vivo: dynamics and modulation by BDNF." Nat Neurosci **4**(11): 1093-1101.

Andre, E., B. Campi, et al. (2008). "Cigarette smoke-induced neurogenic inflammation is mediated by alpha,beta-unsaturated aldehydes and the TRPA1 receptor in rodents." J Clin Invest **118**(7): 2574-2582.

Balogh, G., D. Dimitrov-Szokodi, et al. (1957). "Lung denervation in the therapy of intractable bronchial asthma." J Thorac Surg **33**(2): 166-184.

Baloh, R. H., M. G. Tansey, et al. (1998). "Artemin, a novel member of the GDNF ligand family, supports peripheral and central neurons and signals through the GFRalpha3-RET receptor complex." Neuron **21**(6): 1291-1302.

Baluk, P., J. A. Nadel, et al. (1992). "Substance P-immunoreactive sensory axons in the rat respiratory tract: a quantitative study of their distribution and role in neurogenic inflammation." J Comp Neurol **319**(4): 586-598.

Baluk, P., G. Thurston, et al. (1999). "Neurogenic plasma leakage in mouse airways." Br J Pharmacol **126**(2): 522-528.

Barnes, P. J. (2001). "Neurogenic inflammation in the airways." Respir Physiol **125**(1-2): 145-154.

Barnes, P. J., K. F. Chung, et al. (1998). "Inflammatory mediators of asthma: an update." Pharmacol Rev **50**(4): 515-596.

Barnes, P. J. and A. J. Woolcock (1998). "Difficult asthma." Eur Respir J **12**(5): 1209-1218.

Basoglu, O. K., A. Pelleg, et al. (2005). "Effects of aerosolized adenosine 5'-triphosphate vs adenosine 5'-monophosphate on dyspnea and airway caliber in healthy nonsmokers and patients with asthma." Chest **128**(4): 1905-1909.

Baudet, C., A. Mikaels, et al. (2000). "Positive and negative interactions of GDNF, NTN and ART in developing sensory neuron subpopulations, and their collaboration with neurotrophins." Development **127**(20): 4335-4344.

Bauer, C., T. Pock, et al. (2010). "Segmentation of interwoven 3d tubular tree structures utilizing shape priors and graph cuts." Med Image Anal **14**(2): 172-184.

Beirowski, B., A. Nogradi, et al. (2010). "Mechanisms of axonal spheroid formation in central nervous system Wallerian degeneration." J Neuropathol Exp Neurol **69**(5): 455-472.

Berry, M. A., B. Hargadon, et al. (2006). "Evidence of a role of tumor necrosis factor alpha in refractory asthma." N Engl J Med **354**(7): 697-708.

Bessac, B. F., M. Sivula, et al. (2008). "TRPA1 is a major oxidant sensor in murine airway sensory neurons." J Clin Invest **118**(5): 1899-1910.

Beuche, W. (1991). "Differential isolation of eosinophils and myelin phagocytes from mouse peripheral nerves during Wallerian degeneration by uncoated and immunoglobulin-coated sheep red blood cells." Brain Res **558**(1): 101-104.

Bieber, T. (2008). "Atopic dermatitis." N Engl J Med **358**(14): 1483-1494.

Bieber, T., D. Leung, et al. (2011). Atopic Eczema and Contact Dermatitis. World Allergy Organization (WAO) White Book On Allergy. R. Pawankar, G. W. Canonica, S. T. Holgate and R. F. Lockey. United Kingdom, World Allergy Organization.

Birdsall, H. H., C. Lane, et al. (1992). "Induction of VCAM-1 and ICAM-1 on human neural cells and mechanisms of mononuclear leukocyte adherence." J Immunol **148**(9): 2717-2723.

Birrell, M. A., M. G. Belvisi, et al. (2009). "TRPA1 agonists evoke coughing in guinea pig and human volunteers." Am J Respir Crit Care Med **180**(11): 1042-1047.

Blanchard, C. and M. E. Rothenberg (2009). "Biology of the eosinophil." Adv Immunol **101**: 81-121.

Bonini, S., A. Lambiase, et al. (1996). "Circulating nerve growth factor levels are increased in humans with allergic diseases and asthma." Proc Natl Acad Sci U S A **93**(20): 10955-10960.

Bos, I. S., R. Gosens, et al. (2007). "Inhibition of allergen-induced airway remodelling by tiotropium and budesonide: a comparison." Eur Respir J **30**(4): 653-661.

Botchkarev, V. A., N. V. Botchkareva, et al. (1998). "BDNF overexpression induces differential increases among subsets of sympathetic innervation in murine back skin." Eur J Neurosci **10**(10): 3276-3283.

Boucher, T. J., K. Okuse, et al. (2000). "Potent analgesic effects of GDNF in neuropathic pain states." Science **290**(5489): 124-127.

Bousbaa, H. and J. Fleury-Feith (1991). "Effects of a long-standing challenge on pulmonary neuroendocrine cells of actively sensitized guinea pigs." Am Rev Respir Dis **144**(3 Pt 1): 714-717.

Boyd, J. G. and T. Gordon (2003). "Glial cell line-derived neurotrophic factor and brain-derived neurotrophic factor sustain the axonal regeneration of chronically axotomized motoneurons in vivo." Exp Neurol **183**(2): 610-619.

Brandon, C. (1985). "Improved immunocytochemical staining through the use of Fab fragments of primary antibody, Fab-specific second antibody, and Fab-horseradish peroxidase." J Histochem Cytochem **33**(7): 715-719.

Braun, A., M. Lommatzsch, et al. (1999). "Neurotrophins: a link between airway inflammation and airway smooth muscle contractility in asthma?" Int Arch Allergy Immunol **118**(2-4): 163-165.

Braun, A., M. Lommatzsch, et al. (2004). "Brain-derived neurotrophic factor (BDNF) contributes to neuronal dysfunction in a model of allergic airway inflammation." Br J Pharmacol **141**(3): 431-440.

Braun, A., D. Quarcoo, et al. (2001). "Nerve growth factor induces airway hyperresponsiveness in mice." Int Arch Allergy Immunol **124**(1-3): 205-207.

Brown, R. H., D. M. Walters, et al. (1999). "A method of endotracheal intubation and pulmonary functional assessment for repeated studies in mice." J Appl Physiol **87**(6): 2362-2365.

Bumbacea, D., D. Campbell, et al. (2004). "Parameters associated with persistent airflow obstruction in chronic severe asthma." Eur Respir J **24**(1): 122-128.

Burki, N. K., M. Alam, et al. (2006). "The pulmonary effects of intravenous adenosine in asthmatic subjects." Respir Res **7**: 139.

Caceres, A. I., M. Brackmann, et al. (2009). "A sensory neuronal ion channel essential for airway inflammation and hyperreactivity in asthma." Proc Natl Acad Sci U S A **106**(22): 9099-9104.

Cai, Y. Q., S. R. Chen, et al. (2009). "Role of M2, M3, and M4 muscarinic receptor subtypes in the spinal cholinergic control of nociception revealed using siRNA in rats." J Neurochem **111**(4): 1000-1010.

Campenot, R. B. (1977). "Local control of neurite development by nerve growth factor." Proc Natl Acad Sci U S A **74**(10): 4516-4519.

Canning, B. J. (2006). "Anatomy and neurophysiology of the cough reflex: ACCP evidence-based clinical practice guidelines." Chest **129**(1 Suppl): 33S-47S.

Canning, B. J. (2009). "Central regulation of the cough reflex: therapeutic implications." Pulm Pharmacol Ther **22**(2): 75-81.

Canning, B. J. and Y. L. Chou (2009). "Cough sensors. I. Physiological and pharmacological properties of the afferent nerves regulating cough." Handb Exp Pharmacol(187): 23-47.

Canning, B. J., N. Mori, et al. (2006). "Vagal afferent nerves regulating the cough reflex." Respir Physiol Neurobiol **152**(3): 223-242.

Cantero-Recasens, G., J. R. Gonzalez, et al. (2010). "Loss of function of transient receptor potential vanilloid 1 (TRPV1) genetic variant is associated with lower risk of active childhood asthma." J Biol Chem **285**(36): 27532-27535.

Cao, J. M., M. C. Fishbein, et al. (2000). "Relationship between regional cardiac hyperinnervation and ventricular arrhythmia." Circulation **101**(16): 1960-1969.

Carr, M. J., D. D. Hunter, et al. (2002). "Expression of tachykinins in nonnociceptive vagal afferent neurons during respiratory viral infection in guinea pigs." Am J Respir Crit Care Med **165**(8): 1071-1075.

Carr, M. J. and B. J. Undem (2001). "Inflammation-induced plasticity of the afferent innervation of the airways." Environ Health Perspect **109 Suppl 4**: 567-571.

Cazzola, I. and M. G. Matera (2000). "5-HT modifiers as a potential treatment of asthma." Trends Pharmacol Sci **21**(1): 13-16.

CDC (May 2011). Vital Signs, Center for Disease Control and Prevention.

Chakrabarty, A., K. E. McCarson, et al. (2011). "Hypersensitivity and hyperinnervation of the rat hind paw following carrageenan-induced inflammation." Neurosci Lett **495**(1): 67-71.

Chanez, P., D. Springall, et al. (1998). "Bronchial mucosal immunoreactivity of sensory neuropeptides in severe airway diseases." Am J Respir Crit Care Med **158**(3): 985-990.

Chao, T., K. Pham, et al. (2008). "Chronic nerve compression injury induces a phenotypic switch of neurons within the dorsal root ganglia." J Comp Neurol **506**(2): 180-193.

Chen, C., X. F. Zhou, et al. (1996). "Neurotrophin-3 and trkC-immunoreactive neurons in rat dorsal root ganglia correlate by distribution and morphology." Neurochem Res **21**(7): 809-814.

Chen, Y., J. Zeng, et al. (2009). "Multiple roles of the p75 neurotrophin receptor in the nervous system." J Int Med Res **37**(2): 281-288.

Cheng, J. F., N. L. Ott, et al. (1997). "Dermal eosinophils in atopic dermatitis undergo cytolytic degeneration." J Allergy Clin Immunol **99**(5): 683-692.

Chou, D. L., B. L. Daugherty, et al. (2005). "Chronic aeroallergen during infancy enhances eotaxin-3 expression in airway epithelium and nerves." Am J Respir Cell Mol Biol **33**(1): 1-8.

Chu, K. L., C. R. Faltynek, et al. (2004). "Increased WDR spontaneous activity and receptive field size in rats following a neuropathic or inflammatory injury: implications for mechanical sensitivity." Neurosci Lett **372**(1-2): 123-126.

Chuaychoo, B., D. D. Hunter, et al. (2005). "Allergen-induced substance P synthesis in large-diameter sensory neurons innervating the lungs." J Allergy Clin Immunol **116**(2): 325-331.

Chuaychoo, B., M. G. Lee, et al. (2006). "Evidence for both adenosine A1 and A2A receptors activating single vagal sensory C-fibres in guinea pig lungs." J Physiol **575**(Pt 2): 481-490.

Chuaychoo, B., M. G. Lee, et al. (2005). "Effect of 5-hydroxytryptamine on vagal C-fiber subtypes in guinea pig lungs." Pulm Pharmacol Ther **18**(4): 269-276.

Colebatch, H. J. and D. F. Halmagyi (1963). "Effect of Vagotomy and Vagal Stimulation on Lung Mechanics and Circulation." J Appl Physiol **18**: 881-887.

Coleridge, J. C. and H. M. Coleridge (1984). "Afferent vagal C fibre innervation of the lungs and airways and its functional significance." Rev Physiol Biochem Pharmacol **99**: 1-110.

Collins, J. J., S. Usip, et al. (2002). "Sensory nerves and neuropeptides in uterine cervical ripening." Peptides **23**(1): 167-183.

Colsoul, B., B. Nilius, et al. (2009). "On the putative role of transient receptor potential cation channels in asthma." Clin Exp Allergy **39**(10): 1456-1466.

Correale, C. E., C. Walker, et al. (1999). "Atopic dermatitis: a review of diagnosis and treatment." Am Fam Physician **60**(4): 1191-1198, 1209-1110.

Correale, J. and M. Fiol (2004). "Activation of humoral immunity and eosinophils in neuromyelitis optica." Neurology **63**(12): 2363-2370.

Corry, D. B., H. G. Folkesson, et al. (1996). "Interleukin 4, but not interleukin 5 or eosinophils, is required in a murine model of acute airway hyperreactivity." J Exp Med **183**(1): 109-117.

Costantini, L. C. and O. Isacson (2000). "Immunophilin ligands and GDNF enhance neurite branching or elongation from developing dopamine neurons in culture." Exp Neurol **164**(1): 60-70.

Costello, R. W., D. B. Jacoby, et al. (2000). "Eosinophils and airway nerves in asthma." Histol Histopathol **15**(3): 861-868.

Costello, R. W., B. H. Schofield, et al. (1997). "Localization of eosinophils to airway nerves and effect on neuronal M2 muscarinic receptor function." Am J Physiol **273**(1 Pt 1): L93-103.

Cragg, B. G. and P. K. Thomas (1961). "Changes in conduction velocity and fibre size proximal to peripheral nerve lesions." J Physiol **157**: 315-327.

Crosby, J. R., H. H. Shen, et al. (2002). "Ectopic expression of IL-5 identifies an additional CD4(+) T cell mechanism of airway eosinophil recruitment." Am J Physiol Lung Cell Mol Physiol **282**(1): L99-108.

Crummy, F., M. Livingston, et al. (2005). "Endobronchial adenosine monophosphate challenge causes tachykinin release in the human airway." J Allergy Clin Immunol **116**(2): 312-317.

Curran, D. R., R. K. Morgan, et al. (2005). "Mechanism of eosinophil induced signaling in cholinergic IMR-32 cells." Am J Physiol Lung Cell Mol Physiol **288**(2): L326-332.

Cushley, M. J., A. E. Tattersfield, et al. (1983). "Inhaled adenosine and guanosine on airway resistance in normal and asthmatic subjects." Br J Clin Pharmacol **15**(2): 161-165.

Cushley, M. J., L. H. Wee, et al. (1986). "The effect of inhaled 5-hydroxytryptamine (5-HT, serotonin) on airway calibre in man." Br J Clin Pharmacol **22**(4): 487-490.

Cyphert, J. M., M. Kovarova, et al. (2009). "Cooperation between mast cells and neurons is essential for antigen-mediated bronchoconstriction." J Immunol **182**(12): 7430-7439.

Czech, W., S. Dichmann, et al. (2001). "Distinct amplification of the C5a-receptor pathways in normodense and hypodense eosinophils of patients with atopic dermatitis." Scand J Immunol **53**(3): 235-239.

Daugherty, B. L., S. J. Siciliano, et al. (1996). "Cloning, expression, and characterization of the human eosinophil eotaxin receptor." J Exp Med **183**(5): 2349-2354.

Day, I. N. and R. J. Thompson (2010). "UCHL1 (PGP 9.5): neuronal biomarker and ubiquitin system protein." Prog Neurobiol **90**(3): 327-362.

de Vries, A., F. Engels, et al. (2006). "Airway hyper-responsiveness in allergic asthma in guinea-pigs is mediated by nerve growth factor via the induction of substance P: a potential role for trkA." Clin Exp Allergy **36**(9): 1192-1200.

de Vries, A., C. van Rijnsoever, et al. (2001). "The role of sensory nerve endings in nerve growth factor-induced airway hyperresponsiveness to histamine in guinea-pigs." Br J Pharmacol **134**(4): 771-776.

Delescluse, I., H. Mace, et al. (2012). "Inhibition of Airway Hyperresponsiveness by Trpv1 Antagonists (SB-705498 And PF-04065463) in The Unanaesthetised, Ovalbumin-Sensitised Guinea-Pig." Br J Pharmacol.

DeVane, C. L. (2001). "Substance P: a new era, a new role." Pharmacotherapy **21**(9): 1061-1069.

Dey, R. D., B. Satterfield, et al. (1999). "Innervation of tracheal epithelium and smooth muscle by neurons in airway ganglia." Anat Rec **254**(2): 166-172.

Di Giulio, A. M., B. Tenconi, et al. (1989). "Denervation and hyperinnervation in the nervous system of diabetic animals. II. Monoaminergic and peptidergic alterations in the diabetic encephalopathy." J Neurosci Res **24**(3): 362-368.

di Mola, F. F., H. Friess, et al. (2000). "Nerve growth factor and Trk high affinity receptor (TrkA) gene expression in inflammatory bowel disease." Gut **46**(5): 670-679.

Diamond, J., M. Holmes, et al. (1992). "Endogenous NGF and nerve impulses regulate the collateral sprouting of sensory axons in the skin of the adult rat." J Neurosci **12**(4): 1454-1466.

Dijkhuizen, P. A. and A. Ghosh (2005). "BDNF regulates primary dendrite formation in cortical neurons via the PI3-kinase and MAP kinase signaling pathways." J Neurobiol **62**(2): 278-288.

Dinh, Q. T., D. A. Groneberg, et al. (2004). "Nerve growth factor-induced substance P in capsaicin-insensitive vagal neurons innervating the lower mouse airway." Clin Exp Allergy **34**(9): 1474-1479.

Dinh, Q. T., D. A. Groneberg, et al. (2004). "Expression of tyrosine hydroxylase and neuropeptide tyrosine in mouse sympathetic airway-specific neurons under normal situation and allergic airway inflammation." Clin Exp Allergy **34**(12): 1934-1941.

Dixon, M., D. M. Jackson, et al. (1979). "The effects of histamine, acetylcholine and 5-hydroxytryptamine on lung mechanics and irritant receptors in the dog." J Physiol **287**: 393-403.

Dixon, M., D. M. Jackson, et al. (1979). "The effects of sodium cromoglycate on lung irritant receptors and left ventricular cardiac receptors in the anaesthetized dog." Br J Pharmacol **67**(4): 569-574.

Doherty, M. J., R. Mister, et al. (2000). "Capsaicin induced cough in cryptogenic fibrosing alveolitis." Thorax **55**(12): 1028-1032.

Doherty, M. J., R. Mister, et al. (2000). "Capsaicin responsiveness and cough in asthma and chronic obstructive pulmonary disease." Thorax **55**(8): 643-649.

Driver, A. G., C. A. Kukoly, et al. (1993). "Adenosine in bronchoalveolar lavage fluid in asthma." Am Rev Respir Dis **148**(1): 91-97.

Duarte, A. G., L. Terminella, et al. (2008). "Restoration of cough reflex in lung transplant recipients." Chest **134**(2): 310-316.

Dunzendorfer, S., C. Meierhofer, et al. (1998). "Signaling in neuropeptide-induced migration of human eosinophils." J Leukoc Biol **64**(6): 828-834.

Dupont, L. J., J. L. Pype, et al. (1999). "The effects of 5-HT on cholinergic contraction in human airways in vitro." Eur Respir J **14**(3): 642-649.

Durack, D. T., S. J. Ackerman, et al. (1981). "Purification of human eosinophil-derived neurotoxin." Proc Natl Acad Sci U S A **78**(8): 5165-5169.

Durcan, N., R. W. Costello, et al. (2006). "Eosinophil-mediated cholinergic nerve remodeling." Am J Respir Cell Mol Biol **34**(6): 775-786.

Dusser, D. J., D. B. Jacoby, et al. (1989). "Virus induces airway hyperresponsiveness to tachykinins: role of neutral endopeptidase." J Appl Physiol **67**(4): 1504-1511.

Dvorak, A. M., A. B. Onderdonk, et al. (1993). "Ultrastructural identification of exocytosis of granules from human gut eosinophils in vivo." Int Arch Allergy Immunol **102**(1): 33-45.

Ehrlich, P. and A. Lazarus (1900). Histology of the Blood: Normal and Pathological. Cambridge, Cambridge: At the university press.

Eilers, H., F. Cattaruzza, et al. (2010). "Pungent general anesthetics activate transient receptor potential-A1 to produce hyperalgesia and neurogenic bronchoconstriction." Anesthesiology **112**(6): 1452-1463.

Elbon, C. L., D. B. Jacoby, et al. (1995). "Pretreatment with an antibody to interleukin-5 prevents loss of pulmonary M2 muscarinic receptor function in antigen-challenged guinea pigs." Am J Respir Cell Mol Biol **12**(3): 320-328.

Elitt, C. M., S. L. McIlwrath, et al. (2006). "Artemin overexpression in skin enhances expression of TRPV1 and TRPA1 in cutaneous sensory neurons and leads to behavioral sensitivity to heat and cold." J Neurosci **26**(33): 8578-8587.

Ellman, L. K., P. Chatchatee, et al. (2002). "Food hypersensitivity in two groups of children and young adults with atopic dermatitis evaluated a decade apart." Pediatr Allergy Immunol **13**(4): 295-298.

Elsner, J., R. Hochstetter, et al. (1996). "Human eotaxin represents a potent activator of the respiratory burst of human eosinophils." Eur J Immunol **26**(8): 1919-1925.

Erin, E. M., T. J. Williams, et al. (2002). "Eotaxin receptor (CCR3) antagonism in asthma and allergic disease." Curr Drug Targets Inflamm Allergy **1**(2): 201-214.

Erjefalt, J. S., L. Greiff, et al. (1999). "Allergen-induced eosinophil cytolysis is a primary mechanism for granule protein release in human upper airways." Am J Respir Crit Care Med **160**(1): 304-312.

Erjefalt, J. S., M. Korsgren, et al. (1997). "Association between inflammation and epithelial damage-restitution processes in allergic airways in vivo." Clin Exp Allergy **27**(11): 1344-1355.

Erjefalt, J. S., F. Sundler, et al. (1996). "Eosinophils, neutrophils, and venular gaps in the airway mucosa at epithelial removal-restitution." Am J Respir Crit Care Med **153**(5): 1666-1674.

Evans, C. M., K. E. Belmonte, et al. (2000). "Substance P-induced airway hyperreactivity is mediated by neuronal M(2) receptor dysfunction." Am J Physiol Lung Cell Mol Physiol **279**(3): L477-486.

Evans, C. M., A. D. Fryer, et al. (1997). "Pretreatment with antibody to eosinophil major basic protein prevents hyperresponsiveness by protecting neuronal M2 muscarinic receptors in antigen-challenged guinea pigs." J Clin Invest **100**(9): 2254-2262.

Evans, C. M., D. B. Jacoby, et al. (2001). "Effects of dexamethasone on antigen-induced airway eosinophilia and M(2) receptor dysfunction." Am J Respir Crit Care Med **163**(6): 1484-1492.

Ewart, S., R. Levitt, et al. (1995). "Respiratory system mechanics in mice measured by end-inflation occlusion." J Appl Physiol **79**(2): 560-566.

Fang, X., L. Djouhri, et al. (2006). "Intense isolectin-B4 binding in rat dorsal root ganglion neurons distinguishes C-fiber nociceptors with broad action potentials and high Nav1.9 expression." J Neurosci **26**(27): 7281-7292.

Fernandes, E., M. Fernandes, et al. (2012). "The functions of TRPA1 and TRPV1: moving away from sensory nerves." Br J Pharmacol **166**(2): 510-521.

Figini, M., C. Emanueli, et al. (1997). "Differential activation of the epithelial and smooth muscle NK1 receptors by synthetic tachykinin agonists in guinea-pig trachea." Br J Pharmacol **121**(4): 773-781.

Figini, M., C. Emanueli, et al. (1997). "Substance P and bradykinin stimulate plasma extravasation in the mouse gastrointestinal tract and pancreas." Am J Physiol **272**(4 Pt 1): G785-793.

Fiocchi, A., H. A. Sampson, et al. (2011). Food Allergy. World Allergy Organization (WAO) White Book On Allergy. R. Pawankar, G. W. Canonica, S. T. Holgate and R. F. Lockey. United Kingdom, World Allergy Organization.

Fischer, A., G. P. McGregor, et al. (1996). "Induction of tachykinin gene and peptide expression in guinea pig nodose primary afferent neurons by allergic airway inflammation." J Clin Invest **98**(10): 2284-2291.

Fischer, A., A. Wussow, et al. (2005). "Neuronal plasticity in persistent perennial allergic rhinitis." J Occup Environ Med **47**(1): 20-25.

Fitzgerald, M. and S. Beggs (2001). "The neurobiology of pain: developmental aspects." Neuroscientist **7**(3): 246-257.

Forsberg, K., J. A. Karlsson, et al. (1988). "Cough and bronchoconstriction mediated by capsaicin-sensitive sensory neurons in the guinea-pig." Pulm Pharmacol **1**(1): 33-39.

Foster, E. L., E. L. Simpson, et al. (2011). "Eosinophils increase neuron branching in human and murine skin and in vitro." PLoS One **6**(7): e22029.

Foster, P. S., S. P. Hogan, et al. (1996). "Interleukin 5 deficiency abolishes eosinophilia, airways hyperreactivity, and lung damage in a mouse asthma model." J Exp Med **183**(1): 195-201.

Fox, A. J., P. J. Barnes, et al. (1993). "An in vitro study of the properties of single vagal afferents innervating guinea-pig airways." J Physiol **469**: 21-35.

Frangi, A. F., W. J. Niessen, et al. (2001). "Quantitative analysis of vascular morphology from 3D MR angiograms: In vitro and in vivo results." Magn Reson Med **45**(2): 311-322.

Freund-Michel, V. and N. Frossard (2008). "Overexpression of functional TrkA receptors after internalisation in human airway smooth muscle cells." Biochim Biophys Acta **1783**(10): 1964-1971.

Freytag, C., J. Seeger, et al. (2008). "Immunohistochemical characterization and quantitative analysis of neurons in the myenteric plexus of the equine intestine." Brain Res **1244**: 53-64.

Frossard, N., K. J. Rhoden, et al. (1989). "Influence of epithelium on guinea pig airway responses to tachykinins: role of endopeptidase and cyclooxygenase." J Pharmacol Exp Ther **248**(1): 292-298.

Fryer, A. D., R. W. Costello, et al. (1997). "Antibody to VLA-4, but not to L-selectin, protects neuronal M2 muscarinic receptors in antigen-challenged guinea pig airways." J Clin Invest **99**(8): 2036-2044.

Fryer, A. D. and J. Maclagan (1984). "Muscarinic inhibitory receptors in pulmonary parasympathetic nerves in the guinea-pig." Br J Pharmacol **83**(4): 973-978.

Fryer, A. D., L. H. Stein, et al. (2006). "Neuronal eotaxin and the effects of CCR3 antagonist on airway hyperreactivity and M2 receptor dysfunction." J Clin Invest **116**(1): 228-236.

Fulkerson, P. C., C. A. Fischetti, et al. (2006). "A central regulatory role for eosinophils and the eotaxin/CCR3 axis in chronic experimental allergic airway inflammation." Proc Natl Acad Sci U S A **103**(44): 16418-16423.

Garland, A., J. Necheles, et al. (1997). "Activated eosinophils elicit substance P release from cultured dorsal root ganglion neurons." Am J Physiol **273**(5 Pt 1): L1096-1102.

Gatti, R., E. Andre, et al. (2006). "Protease-activated receptor-2 activation exaggerates TRPV1-mediated cough in guinea pigs." J Appl Physiol **101**(2): 506-511.

Gerber, B. O., M. P. Zanni, et al. (1997). "Functional expression of the eotaxin receptor CCR3 in T lymphocytes co-localizing with eosinophils." Curr Biol **7**(11): 836-843.

Gold, W. M., G. F. Kessler, et al. (1972). "Role of vagus nerves in experimental asthma in allergic dogs." J Appl Physiol **33**(6): 719-725.

Goldie, R. G., L. B. Fernandes, et al. (1998). "Airway structure: a role for confocal microscopy?" Pulm Pharmacol Ther **11**(5-6): 349-354.

Gosens, R., J. Zaagsma, et al. (2006). "Muscarinic receptor signaling in the pathophysiology of asthma and COPD." Respir Res **7**: 73.

Green, R. H., C. E. Brightling, et al. (2002). "Asthma exacerbations and sputum eosinophil counts: a randomised controlled trial." Lancet **360**(9347): 1715-1721.

Griffiths-Johnson, D. A., P. D. Collins, et al. (1993). "The chemokine, eotaxin, activates guinea-pig eosinophils in vitro and causes their accumulation into the lung in vivo." Biochem Biophys Res Commun **197**(3): 1167-1172.

Groneberg, D. A., G. Folkerts, et al. (2004). "Neuropeptide Y (NPY)." Pulm Pharmacol Ther **17**(4): 173-180.

Groneberg, D. A., W. Heppt, et al. (2003). "Aspirin-sensitive rhinitis-associated changes in upper airway innervation." Eur Respir J **22**(6): 986-991.

Groneberg, D. A., A. Niimi, et al. (2004). "Increased expression of transient receptor potential vanilloid-1 in airway nerves of chronic cough." Am J Respir Crit Care Med **170**(12): 1276-1280.

Groneberg, D. A., D. Quarcoo, et al. (2004). "Neurogenic mechanisms in bronchial inflammatory diseases." Allergy **59**(11): 1139-1152.

Grossmann, L., N. Gorodetskaya, et al. (2009). "Cutaneous afferent C-fibers regenerating along the distal nerve stump after crush lesion show two types of cold sensitivity." Eur J Pain **13**(7): 682-690.

Gu, Q., M. E. Lim, et al. (2009). "Mechanisms of eosinophil major basic protein-induced hyperexcitability of vagal pulmonary chemosensitive neurons." Am J Physiol Lung Cell Mol Physiol **296**(3): L453-461.

Gu, Q., M. E. Wiggers, et al. (2008). "Sensitization of isolated rat vagal pulmonary sensory neurons by eosinophil-derived cationic proteins." Am J Physiol Lung Cell Mol Physiol **294**(3): L544-552.

Hajos, M. K. (1962). "Clinical studies on the role of serotonin in bronchial asthma." Acta Allergol **17**: 358-370.

Haldar, P., C. E. Brightling, et al. (2009). "Mepolizumab and exacerbations of refractory eosinophilic asthma." N Engl J Med **360**(10): 973-984.

Hallgren, R., A. Terent, et al. (1983). "Eosinophil cationic protein (ECP) in the cerebrospinal fluid." J Neurol Sci **58**(1): 57-71.

Hamann, K. J., R. L. Barker, et al. (1991). "The molecular biology of eosinophil granule proteins." Int Arch Allergy Appl Immunol **94**(1-4): 202-209.

Hamid, Q., M. Boguniewicz, et al. (1994). "Differential in situ cytokine gene expression in acute versus chronic atopic dermatitis." J Clin Invest **94**(2): 870-876.

Hanani, M., L. G. Ermilov, et al. (1998). "The three-dimensional structure of myenteric neurons in the guinea-pig ileum." J Auton Nerv Syst **71**(1): 1-9.

Harper, A. A. and S. N. Lawson (1985). "Conduction velocity is related to morphological cell type in rat dorsal root ganglion neurones." J Physiol **359**: 31-46.

Hartnell, A., D. S. Robinson, et al. (1993). "CD69 is expressed by human eosinophils activated in vivo in asthma and in vitro by cytokines." Immunology **80**(2): 281-286.

Hasan, W., A. Jama, et al. (2006). "Sympathetic hyperinnervation and inflammatory cell NGF synthesis following myocardial infarction in rats." Brain Res **1124**(1): 142-154.

Hastie, A. T., W. C. Moore, et al. (2010). "Analyses of asthma severity phenotypes and inflammatory proteins in subjects stratified by sputum granulocytes." J Allergy Clin Immunol **125**(5): 1028-1036 e1013.

Hayashida, K. I., T. Bynum, et al. (2006). "Inhibitory M2 muscarinic receptors are upregulated in both axotomized and intact small diameter dorsal root ganglion cells after peripheral nerve injury." Neuroscience **140**(1): 259-268.

Hefti, F. F., A. Rosenthal, et al. (2006). "Novel class of pain drugs based on antagonism of NGF." Trends Pharmacol Sci **27**(2): 85-91.

Heppt, W., Q. T. Dinh, et al. (2004). "Phenotypic alteration of neuropeptide-containing nerve fibres in seasonal intermittent allergic rhinitis." Clin Exp Allergy **34**(7): 1105-1110.

Hogan, S. P., K. I. Matthaei, et al. (1998). "A novel T cell-regulated mechanism modulating allergen-induced airways hyperreactivity in BALB/c mice independently of IL-4 and IL-5." J Immunol **161**(3): 1501-1509.

Hogan, S. P., A. Mishra, et al. (2001). "A pathological function for eotaxin and eosinophils in eosinophilic gastrointestinal inflammation." Nat Immunol **2**(4): 353-360.

Holgate, S. T., G. W. Canonica, et al. (2011). Asthma. World Allergy Organization (WAO) White Book On Allergy. R. Pawankar, G. W. Canonica, S. T. Holgate and R. F. Lockey. United Kingdom, World Allergy Organization.

Holtzman, M. J., H. L. Hahn, et al. (1982). "Selective effect of general anesthetics on reflex bronchoconstrictor responses in dogs." J Appl Physiol **53**(1): 126-133.

Howarth, P. H., D. R. Springall, et al. (1995). "Neuropeptide-containing nerves in endobronchial biopsies from asthmatic and nonasthmatic subjects." Am J Respir Cell Mol Biol **13**(3): 288-296.

Hoyer, D., J. P. Hannon, et al. (2002). "Molecular, pharmacological and functional diversity of 5-HT receptors." Pharmacol Biochem Behav **71**(4): 533-554.

Hua, X., C. J. Erikson, et al. (2007). "Involvement of A1 adenosine receptors and neural pathways in adenosine-induced bronchoconstriction in mice." Am J Physiol Lung Cell Mol Physiol **293**(1): L25-32.

Huang, E. J. and L. F. Reichardt (2001). "Neurotrophins: roles in neuronal development and function." Annu Rev Neurosci **24**: 677-736.

Humbles, A. A., C. M. Lloyd, et al. (2004). "A critical role for eosinophils in allergic airways remodeling." Science **305**(5691): 1776-1779.

Hunter, D. D., A. C. Myers, et al. (2000). "Nerve growth factor-induced phenotypic switch in guinea pig airway sensory neurons." Am J Respir Crit Care Med **161**(6): 1985-1990.

Hunter, D. D. and B. J. Undem (1999). "Identification and substance P content of vagal afferent neurons innervating the epithelium of the guinea pig trachea." Am J Respir Crit Care Med **159**(6): 1943-1948.

Hyde, D. M., J. R. Harkema, et al. (2006). "Design-based sampling and quantitation of the respiratory airways." Toxicol Pathol **34**(3): 286-295.

Ikoma, A., M. Steinhoff, et al. (2006). "The neurobiology of itch." Nat Rev Neurosci **7**(7): 535-547.

Ito, K., K. F. Chung, et al. (2006). "Update on glucocorticoid action and resistance." J Allergy Clin Immunol **117**(3): 522-543.

Jackson, P. and R. J. Thompson (1981). "The demonstration of new human brain-specific proteins by high-resolution two-dimensional polyacrylamide gel electrophoresis." J Neurol Sci **49**(3): 429-438.

Jacoby, D. B., R. M. Costello, et al. (2001). "Eosinophil recruitment to the airway nerves." J Allergy Clin Immunol **107**(2): 211-218.

Jacoby, D. B., G. J. Gleich, et al. (1993). "Human eosinophil major basic protein is an endogenous allosteric antagonist at the inhibitory muscarinic M2 receptor." J Clin Invest **91**(4): 1314-1318.

Jacoby, D. B., J. Tamaoki, et al. (1988). "Influenza infection causes airway hyperresponsiveness by decreasing enkephalinase." J Appl Physiol **64**(6): 2653-2658.

Jan, Y. N. and L. Y. Jan (2010). "Branching out: mechanisms of dendritic arborization." Nat Rev Neurosci **11**(5): 316-328.

Jancso, G., E. Kiraly, et al. (1985). "Selective degeneration by capsaicin of a subpopulation of primary sensory neurons in the adult rat." Neurosci Lett **59**(2): 209-214.

Janig, W., L. Grossmann, et al. (2009). "Mechano- and thermosensitivity of regenerating cutaneous afferent nerve fibers." Exp Brain Res **196**(1): 101-114.

Janse, C., B. Peretz, et al. (1999). "Excitability and branching of neuroendocrine cells during reproductive senescence." Neurobiol Aging **20**(6): 675-683.

Jayaram, L., M. M. Pizzichini, et al. (2006). "Determining asthma treatment by monitoring sputum cell counts: effect on exacerbations." Eur Respir J **27**(3): 483-494.

Jia, Y., R. L. McLeod, et al. (2002). "Anandamide induces cough in conscious guinea-pigs through VR1 receptors." Br J Pharmacol **137**(6): 831-836.

Jiang, M., Q. Ji, et al. (2006). "Model-based automated extraction of microtubules from electron tomography volume." IEEE Trans Inf Technol Biomed **10**(3): 608-617.

Johansson, O., Y. Liang, et al. (2000). "Eosinophil cationic protein- and eosinophil-derived neurotoxin/eosinophil protein X-immunoreactive eosinophils in prurigo nodularis." Arch Dermatol Res **292**(8): 371-378.

Johansson, S. G., T. Bieber, et al. (2004). "Revised nomenclature for allergy for global use: Report of the Nomenclature Review Committee of the World Allergy Organization, October 2003." J Allergy Clin Immunol **113**(5): 832-836.

Jonsson, M., O. Norrgard, et al. (2005). "Substance P and the neurokinin-1 receptor in relation to eosinophilia in ulcerative colitis." Peptides **26**(5): 799-814.

Joos, G. F. (2001). "The role of neuroeffector mechanisms in the pathogenesis of asthma." Curr Allergy Asthma Rep **1**(2): 134-143.

Joos, G. F., P. R. Germonpre, et al. (2000). "Neural mechanisms in asthma." Clin Exp Allergy **30 Suppl 1**: 60-65.

Jordt, S. E., D. M. Bautista, et al. (2004). "Mustard oils and cannabinoids excite sensory nerve fibres through the TRP channel ANKTM1." Nature **427**(6971): 260-265.

Julius, D. and A. I. Basbaum (2001). "Molecular mechanisms of nociceptions " Nature **413**: 203-210.

Kaatz, M., L. Berod, et al. (2004). "Interleukin-5, interleukin-3 and granulocyte-macrophage colony-stimulating factor prime actin-polymerization in human eosinophils: a study with hypodense and normodense eosinophils from patients with atopic dermatitis." Int J Mol Med **14**(6): 1055-1060.

Kajekar, R., E. M. Pieczarka, et al. (2007). "Early postnatal exposure to allergen and ozone leads to hyperinnervation of the pulmonary epithelium." Respir Physiol Neurobiol **155**(1): 55-63.

Kallinikos, P., M. Berhanu, et al. (2004). "Corneal nerve tortuosity in diabetic patients with neuropathy." Invest Ophthalmol Vis Sci **45**(2): 418-422.

Kamei, J., T. Hosokawa, et al. (1986). "Effects of methysergide on the cough reflex." Jpn J Pharmacol **42**(3): 450-452.

Kamei, J., T. Hosokawa, et al. (1986). "Involvement of central serotonergic mechanisms in the cough reflex." Jpn J Pharmacol **42**(4): 531-538.

Kamei, J., Y. Takahashi, et al. (2005). "Involvement of P2X receptor subtypes in ATP-induced enhancement of the cough reflex sensitivity." Eur J Pharmacol **528**(1-3): 158-161.

Karaosmanoglu, T., B. Aygun, et al. (1996). "Regional differences in the number of neurons in the myenteric plexus of the guinea pig small intestine and colon: an evaluation of markers used to count neurons." Anat Rec **244**(4): 470-480.

Karczewski, W. and J. G. Widdicombe (1969). "The role of the vagus nerves in the respiratory and circulatory reactions to anaphylaxis in rabbits." J Physiol **201**(2): 293-304.

Karczewski, W. and J. G. Widdicombe (1969). "The role of the vagus nerves in the respiratory and circulatory responses to intravenous histamine and phenyl diguanide in rabbits." J Physiol **201**(2): 271-291.

Karlsson, J. A., G. Sant'Ambrogio, et al. (1988). "Afferent neural pathways in cough and reflex bronchoconstriction." J Appl Physiol **65**(3): 1007-1023.

Keast, J. R., S. L. Forrest, et al. (2010). "Sciatic nerve injury in adult rats causes distinct changes in the central projections of sensory neurons expressing different glial cell line-derived neurotrophic factor family receptors." J Comp Neurol **518**(15): 3024-3045.

Kelly, D. E., M. Denis, et al. (1992). "Release of tumour necrosis factor alpha into bronchial alveolar lavage fluid following antigen challenge in passively sensitized guinea-pigs." Mediators Inflamm **1**(6): 425-428.

Kerschensteiner, M., M. E. Schwab, et al. (2005). "In vivo imaging of axonal degeneration and regeneration in the injured spinal cord." Nat Med **11**(5): 572-577.

Kim, H. Y., R. H. DeKruyff, et al. (2010). "The many paths to asthma: phenotype shaped by innate and adaptive immunity." Nat Immunol **11**(7): 577-584.

Kingham, P. J., W. G. McLean, et al. (2003). "Effects of eosinophils on nerve cell morphology and development: the role of reactive oxygen species and p38 MAP kinase." Am J Physiol Lung Cell Mol Physiol **285**(4): L915-924.

Knudsen, U. B. (1996). "Cervical ripening. A rat model for investigation of contractile and passive biomechanical properties, with focus on antigestagens, eosinophil granulocytes and mast cells." Acta Obstet Gynecol Scand **75**(1): 88-89.

Kobayashi, H., G. J. Gleich, et al. (2002). "Human eosinophils produce neurotrophins and secrete nerve growth factor on immunologic stimuli." Blood **99**(6): 2214-2220.

Kollarik, M., M. J. Carr, et al. (2010). "Transgene expression and effective gene silencing in vagal afferent neurons in vivo using recombinant adeno-associated virus vectors." J Physiol **588**(Pt 21): 4303-4315.

Kollarik, M., Q. T. Dinh, et al. (2003). "Capsaicin-sensitive and -insensitive vagal bronchopulmonary C-fibres in the mouse." J Physiol **551**(Pt 3): 869-879.

Kollarik, M., F. Ru, et al. (2010). "Vagal afferent nerves with the properties of nociceptors." Auton Neurosci **153**(1-2): 12-20.

Kopf, M., F. Brombacher, et al. (1996). "IL-5-deficient mice have a developmental defect in CD5+ B-1 cells and lack eosinophilia but have normal antibody and cytotoxic T cell responses." Immunity **4**(1): 15-24.

Koyama, S., E. Sato, et al. (1998). "Acetylcholine and substance P stimulate bronchial epithelial cells to release eosinophil chemotactic activity." J Appl Physiol **84**(5): 1528-1534.

Krimm, R. F., B. M. Davis, et al. (2006). "Overexpression of neurotrophin 4 in skin enhances myelinated sensory endings but does not influence sensory neuron number." J Comp Neurol **498**(4): 455-465.

Krylova, O., J. Herreros, et al. (2002). "WNT-3, expressed by motoneurons, regulates terminal arborization of neurotrophin-3-responsive spinal sensory neurons." Neuron **35**(6): 1043-1056.

Kuo, Y. L. and C. J. Lai (2008). "Ovalbumin sensitizes vagal pulmonary C-fiber afferents in Brown Norway rats." J Appl Physiol **105**(2): 611-620.

Kwong, K., M. Kollarik, et al. (2008). "P2X2 receptors differentiate placodal vs. neural crest C-fiber phenotypes innervating guinea pig lungs and esophagus." Am J Physiol Lung Cell Mol Physiol **295**(5): L858-865.

Lach-Trifilieff, E., R. A. McKay, et al. (2001). "In vitro and in vivo inhibition of interleukin (IL)-5-mediated eosinopoiesis by murine IL-5Ralpha antisense oligonucleotide." Am J Respir Cell Mol Biol **24**(2): 116-122.

Lagente, V., M. P. Pruniaux, et al. (1995). "Modulation of cytokine-induced eosinophil infiltration by phosphodiesterase inhibitors." Am J Respir Crit Care Med **151**(6): 1720-1724.

Lambert, A. R., P. O'Shaughnessy, et al. (2011). "Regional deposition of particles in an image-based airway model: large-eddy simulation and left-right lung ventilation asymmetry." Aerosol Sci Technol **45**(1): 11-25.

Lange, P., J. Parner, et al. (1998). "A 15-year follow-up study of ventilatory function in adults with asthma." N Engl J Med **339**(17): 1194-1200.

Langley, J. N. (1898). "On the Union of Cranial Autonomic (Visceral) Fibres with the Nerve Cells of the Superior Cervical Ganglion." J Physiol **23**(3): 240-270.

Larson, S. D., E. S. Schelegle, et al. (2003). "The three-dimensional distribution of nerves along the entire intrapulmonary airway tree of the adult rat and the anatomical relationship between nerves and neuroepithelial bodies." Am J Respir Cell Mol Biol **28**(5): 592-599.

Larson, S. D., E. S. Schelegle, et al. (2004). "Postnatal remodeling of the neural components of the epithelial-mesenchymal trophic unit in the proximal airways of infant rhesus monkeys exposed to ozone and allergen." Toxicol Appl Pharmacol **194**(3): 211-220.

Lauria, G., D. R. Cornblath, et al. (2005). "EFNS guidelines on the use of skin biopsy in the diagnosis of peripheral neuropathy." Eur J Neurol **12**(10): 747-758.

Lawson, S. N. and A. A. Harper (1984). Neonatal capsaicin is not a specific neurotoxin for sensory C-fibers or small dark cells of rat dorsal root ganglia. Antidromic Vasodilation and Neurogenic Inflammation. L. A. Chahl, J. Szolcsanyi and F. Lembeck. Budapest, Akademiai Kiado.

Lechin, F., B. van der Dijs, et al. (2002). "Severe asthma and plasma serotonin." Allergy **57**(3): 258-259.

Lechin, F., B. van der Dijs, et al. (2004). "Treatment of bronchial asthma with tianeptine." Methods Find Exp Clin Pharmacol **26**(9): 697-701.

Lee, J. J., D. Dimina, et al. (2004). "Defining a link with asthma in mice congenitally deficient in eosinophils." Science **305**(5691): 1773-1776.

Lee, J. J., M. P. McGarry, et al. (1997). "Interleukin-5 expression in the lung epithelium of transgenic mice leads to pulmonary changes pathognomonic of asthma." J Exp Med **185**(12): 2143-2156.

Lee, L. Y., Q. Gu, et al. (2001). "Effects of human eosinophil granule-derived cationic proteins on C-fiber afferents in the rat lung." J Appl Physiol **91**(3): 1318-1326.

Lee, L. Y., Y. Shuei Lin, et al. (2003). "Functional morphology and physiological properties of bronchopulmonary C-fiber afferents." Anat Rec A Discov Mol Cell Evol Biol **270**(1): 17-24.

Lein, P., M. Johnson, et al. (1995). "Osteogenic protein-1 induces dendritic growth in rat sympathetic neurons." Neuron **15**(3): 597-605.

Lembeck, F. (1953). "[Central transmission of afferent impulses. III. Incidence and significance of the substance P in the dorsal roots of the spinal cord]." Naunyn Schmiedebergs Arch Exp Pathol Pharmakol **219**(3): 197-213.

Leung, D. Y., M. Boguniewicz, et al. (2004). "New insights into atopic dermatitis." J Clin Invest **113**(5): 651-657.

Levi-Montalcini, R. (1987). "The nerve growth factor 35 years later." Science **237**(4819): 1154-1162.

Lewin, G. R., A. M. Ritter, et al. (1993). "Nerve growth factor-induced hyperalgesia in the neonatal and adult rat." J Neurosci **13**(5): 2136-2148.

Li, C. Q., J. M. Xu, et al. (2008). "Brain derived neurotrophic factor (BDNF) contributes to the pain hypersensitivity following surgical incision in the rats." Mol Pain **4**: 27.

Li, L., C. J. Xian, et al. (2006). "Upregulation of brain-derived neurotrophic factor in the sensory pathway by selective motor nerve injury in adult rats." Neurotox Res **9**(4): 269-283.

Liang, Y., H. H. Jacobi, et al. (2000). "CGRP-immunoreactive nerves in prurigo nodularis--an exploration of neurogenic inflammation." J Cutan Pathol **27**(7): 359-366.

Lieu, T., M. Kollarik, et al. (2011). "Neurotrophin and GDNF family ligand receptor expression in vagal sensory nerve subtypes innervating the adult guinea pig respiratory tract." Am J Physiol Lung Cell Mol Physiol **300**(5): L790-798.

Lieu, T., A. C. Myers, et al. (2012). "TRPV1 Induction In Airway Vagal Low-Threshold Mechanosensory Neurons By Allergen Challenge and Neurotrophic Factors." Am J Physiol Lung Cell Mol Physiol.

Lilly, C. M., T. R. Bai, et al. (1995). "Neuropeptide content of lungs from asthmatic and nonasthmatic patients." Am J Respir Crit Care Med **151**(2 Pt 1): 548-553.

Lim, Y. S., T. McLaughlin, et al. (2008). "p75(NTR) mediates ephrin-A reverse signaling required for axon repulsion and mapping." Neuron **59**(5): 746-758.

Lin, R. L., D. Hayes, Jr., et al. (2009). "Bronchoconstriction induced by hyperventilation with humidified hot air: role of TRPV1-expressing airway afferents." J Appl Physiol **106**(6): 1917-1924.

Linden, A. (1996). "NANC neural control of airway smooth muscle tone." Gen Pharmacol **27**(7): 1109-1121.

Lindsay, R. M. (1996). "Role of neurotrophins and trk receptors in the development and maintenance of sensory neurons: an overview." Philos Trans R Soc Lond B Biol Sci **351**(1338): 365-373.

Liu, Q., Z. Tang, et al. (2009). "Sensory neuron-specific GPCR Mrgprs are itch receptors mediating chloroquine-induced pruritus." Cell **139**(7): 1353-1365.

Logan, C. Y. and R. Nusse (2004). "The Wnt signaling pathway in development and disease." Annu Rev Cell Dev Biol **20**: 781-810.

Lu, B., P. T. Pang, et al. (2005). "The yin and yang of neurotrophin action." Nat Rev Neurosci **6**(8): 603-614.

Lu, S. G. and M. S. Gold (2008). "Inflammation-induced increase in evoked calcium transients in subpopulations of rat dorsal root ganglion neurons." Neuroscience **153**(1): 279-288.

Lucchinetti, C. F., R. N. Mandler, et al. (2002). "A role for humoral mechanisms in the pathogenesis of Devic's neuromyelitis optica." Brain **125**(Pt 7): 1450-1461.

Lucchini, R. E., F. Facchini, et al. (1997). "Increased VIP-positive nerve fibers in the mucous glands of subjects with chronic bronchitis." Am J Respir Crit Care Med **156**(6): 1963-1968.

Lundberg, J. M. and A. Saria (1983). "Capsaicin-induced desensitization of airway mucosa to cigarette smoke, mechanical and chemical irritants." Nature **302**(5905): 251-253.

Lundgren, J. D., R. T. Davey, Jr., et al. (1991). "Eosinophil cationic protein stimulates and major basic protein inhibits airway mucus secretion." J Allergy Clin Immunol **87**(3): 689-698.

Ma, Q. P. and C. J. Woolf (1997). "The progressive tactile hyperalgesia induced by peripheral inflammation is nerve growth factor dependent." Neuroreport **8**(4): 807-810.

MacDonald, K. D., H. Y. Chang, et al. (2009). "An improved simple method of mouse lung intubation." J Appl Physiol **106**(3): 984-987.

Maintz, L. and N. Novak (2007). "Getting more and more complex: the pathophysiology of atopic eczema." Eur J Dermatol **17**(4): 267-283.

Malcangio, M., M. S. Ramer, et al. (2000). "Intrathecally injected neurotrophins and the release of substance P from the rat isolated spinal cord." Eur J Neurosci **12**(1): 139-144.

Malin, S., D. Molliver, et al. (2011). "TRPV1 and TRPA1 function and modulation are target tissue dependent." J Neurosci **31**(29): 10516-10528.

Malin, S. A., D. C. Molliver, et al. (2006). "Glial cell line-derived neurotrophic factor family members sensitize nociceptors in vitro and produce thermal hyperalgesia in vivo." J Neurosci **26**(33): 8588-8599.

Manniesing, R., M. A. Viergever, et al. (2006). "Vessel enhancing diffusion: a scale space representation of vessel structures." Med Image Anal **10**(6): 815-825.

Mannion, R. J., M. Costigan, et al. (1999). "Neurotrophins: peripherally and centrally acting modulators of tactile stimulus-induced inflammatory pain hypersensitivity." Proc Natl Acad Sci U S A **96**(16): 9385-9390.

Mantelli, F., A. Micera, et al. (2010). "Neurogenic inflammation of the ocular surface." Curr Opin Allergy Clin Immunol **10**(5): 498-504.

Manzini, S. and L. Ballati (1990). "2-Chloroadenosine induction of vagally-mediated and atropine-resistant bronchomotor responses in anaesthetized guinea-pigs." Br J Pharmacol **100**(2): 251-256.

Mapp, C. E., R. E. Lucchini, et al. (1998). "Immunization and challenge with toluene diisocyanate decrease tachykinin and calcitonin gene-related peptide immunoreactivity in guinea pig central airways." Am J Respir Crit Care Med **158**(1): 263-269.

Markus, A., T. D. Patel, et al. (2002). "Neurotrophic factors and axonal growth." Curr Opin Neurobiol **12**(5): 523-531.

Marler, K. J., E. Becker-Barroso, et al. (2008). "A TrkB/EphrinA interaction controls retinal axon branching and synaptogenesis." J Neurosci **28**(48): 12700-12712.

Marshak, S., A. M. Nikolakopoulou, et al. (2007). "Cell-autonomous TrkB signaling in presynaptic retinal ganglion cells mediates axon arbor growth and synapse maturation during the establishment of retinotectal synaptic connectivity." J Neurosci **27**(10): 2444-2456.

Marvizon, J. C., X. Wang, et al. (2003). "Relationship between capsaicin-evoked substance P release and neurokinin 1 receptor internalization in the rat spinal cord." Neuroscience **118**(2): 535-545.

Mazzone, S. B. (2005). "An overview of the sensory receptors regulating cough." Cough **1**: 2.

Mazzone, S. B., S. M. Reynolds, et al. (2009). "Selective expression of a sodium pump isozyme by cough receptors and evidence for its essential role in regulating cough." J Neurosci **29**(43): 13662-13671.

McAllister, A. K., D. C. Lo, et al. (1995). "Neurotrophins regulate dendritic growth in developing visual cortex." Neuron **15**(4): 791-803.

McArthur, J. C., E. A. Stocks, et al. (1998). "Epidermal nerve fiber density: normative reference range and diagnostic efficiency." Arch Neurol **55**(12): 1513-1520.

McLeod, R. L., Y. Jia, et al. (2007). "Sulfur-dioxide exposure increases TRPV1-mediated responses in nodose ganglia cells and augments cough in guinea pigs." Pulm Pharmacol Ther **20**(6): 750-757.

Meeusen, E. N. and A. Balic (2000). "Do eosinophils have a role in the killing of helminth parasites?" Parasitol Today **16**(3): 95-101.

Michel, T., M. Theresine, et al. (2011). "Increased Th2 cytokine secretion, eosinophilic airway inflammation, and airway hyperresponsiveness in neurturin-deficient mice." J Immunol **186**(11): 6497-6504.

Mikaels, A., J. Livet, et al. (2000). "A dynamic regulation of GDNF-family receptors correlates with a specific trophic dependency of cranial motor neuron subpopulations during development." Eur J Neurosci **12**(2): 446-456.

Milici, A. J., L. A. Carroll, et al. (1998). "Early eosinophil infiltration into the optic nerve of mice with experimental allergic encephalomyelitis." Lab Invest **78**(10): 1239-1244.

Mille-Hamard, L., L. Bauchet, et al. (1999). "Estimation of the number and size of female adult rat C4, C5 and C6 dorsal root ganglia (DRG) neurons." Somatosens Mot Res **16**(3): 223-228.

Moffatt, J. D., T. M. Cocks, et al. (2004). "Role of the epithelium and acetylcholine in mediating the contraction to 5-hydroxytryptamine in the mouse isolated trachea." Br J Pharmacol **141**(7): 1159-1166.

Moitra, J., S. Sammani, et al. (2007). "Re-evaluation of Evans Blue dye as a marker of albumin clearance in murine models of acute lung injury." Transl Res **150**(4): 253-265.
Molliver, D. C., J. Lindsay, et al. (2005). "Overexpression of NGF or GDNF alters transcriptional plasticity evoked by inflammation." Pain **113**(3): 277-284.
Moqbel, R. and J. J. Coughlin (2006). "Differential secretion of cytokines." Sci STKE **2006**(338): pe26.
Morgan, R. K., P. J. Kingham, et al. (2004). "Eosinophil adhesion to cholinergic IMR-32 cells protects against induced neuronal apoptosis." J Immunol **173**(10): 5963-5970.
Moriyama, T., T. Higashi, et al. (2005). "Sensitization of TRPV1 by EP1 and IP reveals peripheral nociceptive mechanism of prostaglandins." Mol Pain **1**: 3.
Mould, A. W., A. J. Ramsay, et al. (2000). "The effect of IL-5 and eotaxin expression in the lung on eosinophil trafficking and degranulation and the induction of bronchial hyperreactivity." J Immunol **164**(4): 2142-2150.
Muhlfeld, C., T. Papadakis, et al. (2010). "An unbiased stereological method for efficiently quantifying the innervation of the heart and other organs based on total length estimations." J Appl Physiol **108**(5): 1402-1409.
Murray, T. C. and D. B. Jacoby (1992). "Viral infection increases contractile but not secretory responses to substance P in ferret trachea." J Appl Physiol **72**(2): 608-611.
Nadel, J. A., H. Salem, et al. (1965). "Mechanism of Bronchoconstriction during Inhalation of Sulfur Dioxide." J Appl Physiol **20**: 164-167.
Nagase, T., M. J. Dallaire, et al. (1996). "Airway and tissue behavior during early response in sensitized rats: role of 5-HT and LTD4." J Appl Physiol **80**(2): 583-590.
Nair, P., M. M. Pizzichini, et al. (2009). "Mepolizumab for prednisone-dependent asthma with sputum eosinophilia." N Engl J Med **360**(10): 985-993.
Nassenstein, C., D. Dawbarn, et al. (2006). "Pulmonary distribution, regulation, and functional role of Trk receptors in a murine model of asthma." J Allergy Clin Immunol **118**(3): 597-605.
Nassenstein, C., T. Kammertoens, et al. (2007). "Neuroimmune crosstalk in asthma: dual role of the neurotrophin receptor p75NTR." J Allergy Clin Immunol **120**(5): 1089-1096.
Nassenstein, C., K. Kwong, et al. (2008). "Expression and function of the ion channel TRPA1 in vagal afferent nerves innervating mouse lungs." J Physiol **586**(6): 1595-1604.
Nassenstein, C., T. E. Taylor-Clark, et al. (2010). "Phenotypic distinctions between neural crest and placodal derived vagal C-fibres in mouse lungs." J Physiol **588**(Pt 23): 4769-4783.
Nault, M. A., S. G. Vincent, et al. (1999). "Mechanisms of capsaicin- and lactic acid-induced bronchoconstriction in the newborn dog." J Physiol **515 (Pt 2)**: 567-578.
Nemeth, L., U. Rolle, et al. (2003). "Nitrergic hyperinnervation in appendicitis and in appendices histologically classified as normal." Arch Pathol Lab Med **127**(5): 573-578.
Neumann, S., T. P. Doubell, et al. (1996). "Inflammatory pain hypersensitivity mediated by phenotypic switch in myelinated primary sensory neurons." Nature **384**(6607): 360-364.
Neves, J. S., S. A. Perez, et al. (2008). "Eosinophil granules function extracellularly as receptor-mediated secretory organelles." Proc Natl Acad Sci U S A **105**(47): 18478-18483.
Newton, D. L., S. Walbridge, et al. (1994). "Toxicity of an antitumor ribonuclease to Purkinje neurons." J Neurosci **14**(2): 538-544.
NHLBI (2007). Guidelines for the Diagnosis and Managements of Asthma., National Heart, Lung, and Blood Institute.
Nie, Z., D. B. Jacoby, et al. (2009). "Etanercept prevents airway hyperresponsiveness by protecting neuronal M2 muscarinic receptors in antigen-challenged guinea pigs." Br J Pharmacol **156**(1): 201-210.

Nie, Z., C. S. Nelson, et al. (2007). "Expression and regulation of intercellular adhesion molecule-1 on airway parasympathetic nerves." J Allergy Clin Immunol **119**(6): 1415-1422.

Noga, O., C. Englmann, et al. (2003). "The production, storage and release of the neurotrophins nerve growth factor, brain-derived neurotrophic factor and neurotrophin-3 by human peripheral eosinophils in allergics and non-allergics." Clin Exp Allergy **33**(5): 649-654.

Numao, T. and D. K. Agrawal (1992). "Neuropeptides modulate human eosinophil chemotaxis." J Immunol **149**(10): 3309-3315.

O'Brien, L. M., E. Fitzpatrick, et al. (2008). "Eosinophil-nerve interactions and neuronal plasticity in rat gut associated lymphoid tissue (GALT) in response to enteric parasitism." J Neuroimmunol **197**(1): 1-9.

O'Connell, F., D. R. Springall, et al. (1995). "Abnormal intraepithelial airway nerves in persistent unexplained cough?" Am J Respir Crit Care Med **152**(6 Pt 1): 2068-2075.

O'Connor, T. M., J. O'Connell, et al. (2004). "The role of substance P in inflammatory disease." J Cell Physiol **201**(2): 167-180.

Ochkur, S. I., E. A. Jacobsen, et al. (2007). "Coexpression of IL-5 and eotaxin-2 in mice creates an eosinophil-dependent model of respiratory inflammation with characteristics of severe asthma." J Immunol **178**(12): 7879-7889.

Oh, Y. S., A. Y. Jong, et al. (2006). "Spatial distribution of nerve sprouting after myocardial infarction in mice." Heart Rhythm **3**(6): 728-736.

Olerud, J. E., D. S. Chiu, et al. (1998). "Protein gene product 9.5 is expressed by fibroblasts in human cutaneous wounds." J Invest Dermatol **111**(4): 565-572.

Ollerenshaw, S., D. Jarvis, et al. (1989). "Absence of immunoreactive vasoactive intestinal polypeptide in tissue from the lungs of patients with asthma." N Engl J Med **320**(19): 1244-1248.

Ollerenshaw, S. L., D. Jarvis, et al. (1991). "Substance P immunoreactive nerves in airways from asthmatics and nonasthmatics." Eur Respir J **4**(6): 673-682.

Ollerenshaw, S. L. and A. J. Woolcock (1992). "Characteristics of the inflammation in biopsies from large airways of subjects with asthma and subjects with chronic airflow limitation." Am Rev Respir Dis **145**(4 Pt 1): 922-927.

Osoegawa, M., H. Ochi, et al. (2003). "Eosinophilic myelitis associated with atopic diathesis: a combined neuroimaging and histopathological study." Acta Neuropathol **105**(3): 289-295.

Ostlere, L. S., T. Cowen, et al. (1995). "Neuropeptides in the skin of patients with atopic dermatitis." Clin Exp Dermatol **20**(6): 462-467.

Ostro, B. D., M. J. Lipsett, et al. (1991). "Asthmatic responses to airborne acid aerosols." Am J Public Health **81**(6): 694-702.

Othumpangat, S., L. F. Gibson, et al. (2009). "NGF is an essential survival factor for bronchial epithelial cells during respiratory syncytial virus infection." PLoS One **4**(7): e6444.

Paterson, S., M. Schmelz, et al. (2009). "Facilitated neurotrophin release in sensitized human skin." Eur J Pain **13**(4): 399-405.

Pauwels, R. A., G. J. Brusselle, et al. (1997). "Cytokine manipulation in animal models of asthma." Am J Respir Crit Care Med **156**(4 Pt 2): S78-81.

Pawankar, R., M. Sanchez-Borges, et al. (2011). Rhinitis, Conjunctivitis, and Rhinosinusitis. World Allergy Organization (WAO) White Book On Allergy. R. Pawankar, G. W. Canonica, S. T. Holgate and R. F. Lockey. United Kingdom, World Allergy Organization.

Peleshok, J. C. and A. Ribeiro-da-Silva (2012). "Neurotrophic factor changes in the rat thick skin following chronic constriction injury of the sciatic nerve." Mol Pain **8**: 1.

Peters, S. P., S. J. Kunselman, et al. (2010). "Tiotropium bromide step-up therapy for adults with uncontrolled asthma." N Engl J Med **363**(18): 1715-1726.
Pisarri, T. E., J. Yu, et al. (1986). "Background activity in pulmonary vagal C-fibers and its effects on breathing." Respir Physiol **64**(1): 29-43.
Premkumar, L. S. and G. P. Ahern (2000). "Induction of vanilloid receptor channel activity by protein kinase C." Nature **408**(6815): 985-990.
Price, J. (1985). "An immunohistochemical and quantitative examination of dorsal root ganglion neuronal subpopulations." J Neurosci **5**(8): 2051-2059.
Proskocil, B. J. and A. D. Fryer (2005). "Beta2-agonist and anticholinergic drugs in the treatment of lung disease." Proc Am Thorac Soc **2**(4): 305-310; discussion 311-302.
Raap, U. and G. J. Braunstahl (2010). "The role of neurotrophins in the pathophysiology of allergic rhinitis." Curr Opin Allergy Clin Immunol **10**(1): 8-13.
Rajan, B., M. Polydefkis, et al. (2003). "Epidermal reinnervation after intracutaneous axotomy in man." J Comp Neurol **457**(1): 24-36.
Ralevic, V. and G. Burnstock (1998). "Receptors for purines and pyrimidines." Pharmacol Rev **50**(3): 413-492.
Ramalho, R., R. Soares, et al. (2011). "Tachykinin receptors antagonism for asthma: a systematic review." BMC Pulm Med **11**: 41.
Reinhard, C., G. Eder, et al. (2002). "Inbred strain variation in lung function." Mamm Genome **13**(8): 429-437.
Rho, N. K., W. S. Kim, et al. (2004). "Immunophenotyping of inflammatory cells in lesional skin of the extrinsic and intrinsic types of atopic dermatitis." Br J Dermatol **151**(1): 119-125.
Riccio, M. M., A. C. Myers, et al. (1996). "Immunomodulation of afferent neurons in guinea-pig isolated airway." J Physiol **491 (Pt 2)**: 499-509.
Ricco, M. M., W. Kummer, et al. (1996). "Interganglionic segregation of distinct vagal afferent fibre phenotypes in guinea-pig airways." J Physiol **496 (Pt 2)**: 521-530.
Rice, F. L., K. M. Albers, et al. (1998). "Differential dependency of unmyelinated and A delta epidermal and upper dermal innervation on neurotrophins, trk receptors, and p75LNGFR." Dev Biol **198**(1): 57-81.
Rizzo, C. A., R. Yang, et al. (2002). "The IL-5 receptor on human bronchus selectively primes for hyperresponsiveness." J Allergy Clin Immunol **109**(3): 404-409.
Roosterman, D., T. Goerge, et al. (2006). "Neuronal control of skin function: the skin as a neuroimmunoendocrine organ." Physiol Rev **86**(4): 1309-1379.
Rosenberg, H. F., S. Phipps, et al. (2007). "Eosinophil trafficking in allergy and asthma." J Allergy Clin Immunol **119**(6): 1303-1310; quiz 1311-1302.
Rothenberg, M. E. and S. P. Hogan (2006). "The eosinophil." Annu Rev Immunol **24**: 147-174.
Ruda, M. A., Q. D. Ling, et al. (2000). "Altered nociceptive neuronal circuits after neonatal peripheral inflammation." Science **289**(5479): 628-631.
Rukwied, R., G. Lischetzki, et al. (2000). "Mast cell mediators other than histamine induce pruritus in atopic dermatitis patients: a dermal microdialysis study." Br J Dermatol **142**(6): 1114-1120.
Ruscheweyh, R., L. Forsthuber, et al. (2007). "Modification of classical neurochemical markers in identified primary afferent neurons with Abeta-, Adelta-, and C-fibers after chronic constriction injury in mice." J Comp Neurol **502**(2): 325-336.
Sahin-Yilmaz, A., C. C. Nocon, et al. "Immunoglobulin E-mediated food allergies among adults with allergic rhinitis." Otolaryngol Head Neck Surg **143**(3): 379-385.
Sandkuhler, J. (2009). "Models and mechanisms of hyperalgesia and allodynia." Physiol Rev **89**(2): 707-758.

Sato, E., S. Koyama, et al. (1998). "Acetylcholine stimulates alveolar macrophages to release inflammatory cell chemotactic activity." Am J Physiol **274**(6 Pt 1): L970-979.

Sawatzky, D. A., P. J. Kingham, et al. (2002). "Eosinophil adhesion to cholinergic nerves via ICAM-1 and VCAM-1 and associated eosinophil degranulation." Am J Physiol Lung Cell Mol Physiol **282**(6): L1279-1288.

Schafer, K. H. and P. Mestres (1999). "The GDNF-induced neurite outgrowth and neuronal survival in dissociated myenteric plexus cultures of the rat small intestine decreases postnatally." Exp Brain Res **125**(4): 447-452.

Schleimer, R. P., S. A. Sterbinsky, et al. (1992). "IL-4 induces adherence of human eosinophils and basophils but not neutrophils to endothelium. Association with expression of VCAM-1." J Immunol **148**(4): 1086-1092.

Schofield, J. N., I. N. Day, et al. (1995). "PGP9.5, a ubiquitin C-terminal hydrolase; pattern of mRNA and protein expression during neural development in the mouse." Brain Res Dev Brain Res **85**(2): 229-238.

Schwerk, N., M. Ballmann, et al. (2008). "Development of allergic asthma in an asthmatic recipient of a nonatopic lung under systemic immunosuppression." Allergy **63**(5): 628-629.

Scott, S. A. (1992). Sensory neurons : diversity, development, and plasticity. New York, Oxford University Press.

Sears, M. R., J. M. Greene, et al. (2003). "A longitudinal, population-based, cohort study of childhood asthma followed to adulthood." N Engl J Med **349**(15): 1414-1422.

Sharma, A. K. and P. K. Thomas (1974). "Peripheral nerve structure and function in experimental diabetes." J Neurol Sci **23**(1): 1-15.

Shimosegawa, T. and S. I. Said (1991). "Pulmonary calcitonin gene-related peptide immunoreactivity: nerve-endocrine cell interrelationships." Am J Respir Cell Mol Biol **4**(2): 126-134.

Sibaev, A., H. Franck, et al. (2003). "Structural differences in the enteric neural network in murine colon: impact on electrophysiology." Am J Physiol Gastrointest Liver Physiol **285**(6): G1325-1334.

Singh, U. S., A. Malhotra, et al. (2008). "Eosinophils, mast cells, nerves and ganglion cells in appendicitis." Indian J Surg **70**: 231-234.

Smith, C. H., J. N. Barker, et al. (1993). "Neuropeptides induce rapid expression of endothelial cell adhesion molecules and elicit granulocytic infiltration in human skin." J Immunol **151**(6): 3274-3282.

Snashall, P. D. and C. Baldwin (1982). "Mechanisms of sulphur dioxide induced bronchoconstriction in normal and asthmatic man." Thorax **37**(2): 118-123.

Sofroniew, M. V., C. L. Howe, et al. (2001). "Nerve growth factor signaling, neuroprotection, and neural repair." Annu Rev Neurosci **24**: 1217-1281.

Sorensen, L., L. Molyneaux, et al. (2006). "The relationship among pain, sensory loss, and small nerve fibers in diabetes." Diabetes Care **29**(4): 883-887.

Spahn, J. D. and R. Covar (2008). "Clinical assessment of asthma progression in children and adults." J Allergy Clin Immunol **121**(3): 548-557; quiz 558-549.

Spergel, J. M. "From atopic dermatitis to asthma: the atopic march." Ann Allergy Asthma Immunol **105**(2): 99-106; quiz 107-109, 117.

Steinhoff, M., U. Neisius, et al. (2003). "Proteinase-activated receptor-2 mediates itch: a novel pathway for pruritus in human skin." J Neurosci **23**(15): 6176-6180.

Sternini, C., D. Su, et al. (1995). "Cellular sites of expression of the neurokinin-1 receptor in the rat gastrointestinal tract." J Comp Neurol **358**(4): 531-540.

Stone, R. A., Y. M. Worsdell, et al. (1993). "Effects of 5-hydroxytryptamine and 5-hydroxytryptophan infusion on the human cough reflex." J Appl Physiol **74**(1): 396-401.

Stretton, D., M. G. Belvisi, et al. (1992). "The effect of sensory nerve depletion on cholinergic neurotransmission in guinea pig airways." J Pharmacol Exp Ther **260**(3): 1073-1080.

Stucky, C. L., M. Koltzenburg, et al. (1999). "Overexpression of nerve growth factor in skin selectively affects the survival and functional properties of nociceptors." J Neurosci **19**(19): 8509-8516.

Stucky, C. L. and G. R. Lewin (1999). "Isolectin B(4)-positive and -negative nociceptors are functionally distinct." J Neurosci **19**(15): 6497-6505.

Sugiura, H., M. Omoto, et al. (1997). "Density and fine structure of peripheral nerves in various skin lesions of atopic dermatitis." Arch Dermatol Res **289**(3): 125-131.

Sunohara, N., S. Furukawa, et al. (1989). "Neurotoxicity of human eosinophils towards peripheral nerves." J Neurol Sci **92**(1): 1-7.

Tada, T. and M. Sheng (2006). "Molecular mechanisms of dendritic spine morphogenesis." Curr Opin Neurobiol **16**(1): 95-101.

Taha, R. A., E. M. Minshall, et al. (2000). "Evidence for increased expression of eotaxin and monocyte chemotactic protein-4 in atopic dermatitis." J Allergy Clin Immunol **105**(5): 1002-1007.

Tallini, Y. N., B. Shui, et al. (2006). "BAC transgenic mice express enhanced green fluorescent protein in central and peripheral cholinergic neurons." Physiol Genomics **27**(3): 391-397.

Tandrup, T. (2004). "Unbiased estimates of number and size of rat dorsal root ganglion cells in studies of structure and cell survival." J Neurocytol **33**(2): 173-192.

Tannemaat, M. R., R. Eggers, et al. (2008). "Differential effects of lentiviral vector-mediated overexpression of nerve growth factor and glial cell line-derived neurotrophic factor on regenerating sensory and motor axons in the transected peripheral nerve." Eur J Neurosci **28**(8): 1467-1479.

Taylor-Clark, T. and B. J. Undem (2006). "Transduction mechanisms in airway sensory nerves." J Appl Physiol **101**(3): 950-959.

Taylor-Clark, T. E., C. Nassenstein, et al. (2009). "TRPA1: a potential target for anti-tussive therapy." Pulm Pharmacol Ther **22**(2): 71-74.

Taylor-Clark, T. E. and B. J. Undem (2010). "Ozone activates airway nerves via the selective stimulation of TRPA1 ion channels." J Physiol **588**(Pt 3): 423-433.

Terada, M., H. Yasuda, et al. (1998). "Delayed Wallerian degeneration and increased neurofilament phosphorylation in sciatic nerves of rats with streptozocin-induced diabetes." J Neurol Sci **155**(1): 23-30.

Thiberville, L., S. Moreno-Swirc, et al. (2007). "In vivo imaging of the bronchial wall microstructure using fibered confocal fluorescence microscopy." Am J Respir Crit Care Med **175**(1): 22-31.

Thompson, R. J., J. F. Doran, et al. (1983). "PGP 9.5--a new marker for vertebrate neurons and neuroendocrine cells." Brain Res **278**(1-2): 224-228.

Thompson, S. W., A. Dray, et al. (1995). "Nerve growth factor induces mechanical allodynia associated with novel A fibre-evoked spinal reflex activity and enhanced neurokinin-1 receptor activation in the rat." Pain **62**(2): 219-231.

Thomson, N. C., S. Bicknell, et al. (2012). "Bronchial thermoplasty for severe asthma." Curr Opin Allergy Clin Immunol **12**(3): 241-248.

Throsby, M., A. Herbelin, et al. (2000). "CD11c+ eosinophils in the murine thymus: developmental regulation and recruitment upon MHC class I-restricted thymocyte deletion." J Immunol **165**(4): 1965-1975.

Tobin, D., G. Nabarro, et al. (1992). "Increased number of immunoreactive nerve fibers in atopic dermatitis." J Allergy Clin Immunol **90**(4 Pt 1): 613-622.

Tokuoka, S., Y. Takahashi, et al. (2001). "Disruption of antigen-induced airway inflammation and airway hyper-responsiveness in low affinity neurotrophin receptor p75 gene deficient mice." Br J Pharmacol **134**(7): 1580-1586.

Tollet, J., A. W. Everett, et al. (2002). "Development of neural tissue and airway smooth muscle in fetal mouse lung explants: a role for glial-derived neurotrophic factor in lung innervation." Am J Respir Cell Mol Biol **26**(4): 420-429.

Tolwani, R. J., J. M. Cosgaya, et al. (2004). "BDNF overexpression produces a long-term increase in myelin formation in the peripheral nervous system." J Neurosci Res **77**(5): 662-669.

Tomita, K., T. Kubo, et al. (2007). "Myelin-associated glycoprotein reduces axonal branching and enhances functional recovery after sciatic nerve transection in rats." Glia **55**(14): 1498-1507.

Torsney, C. and M. Fitzgerald (2003). "Spinal dorsal horn cell receptive field size is increased in adult rats following neonatal hindpaw skin injury." J Physiol **550**(Pt 1): 255-261.

Tournoy, K. G., K. O. De Swert, et al. (2003). "Modulatory role of tachykinin NK1 receptor in cholinergic contraction of mouse trachea." Eur Respir J **21**(1): 3-10.

Trevisani, M., D. Gazzieri, et al. (2004). "Ethanol causes inflammation in the airways by a neurogenic and TRPV1-dependent mechanism." J Pharmacol Exp Ther **309**(3): 1167-1173.

Uddman, R., R. Hakanson, et al. (1997). Distribution of neuropeptides in airways. Autonomic Innervation of the Respiratory Tract. P. J. Barnes. London, Harwood Academic**:** 22-37.

Undem, B. J. and M. J. Carr (2002). "The role of nerves in asthma." Curr Allergy Asthma Rep **2**(2): 159-165.

Undem, B. J., M. J. Carr, et al. (2002). "Physiology and plasticity of putative cough fibres in the Guinea pig." Pulm Pharmacol Ther **15**(3): 193-198.

Undem, B. J., B. Chuaychoo, et al. (2004). "Subtypes of vagal afferent C-fibres in guinea-pig lungs." J Physiol **556**(Pt 3): 905-917.

Undem, B. J., E. J. Oh, et al. (2003). "Effect of extracellular calcium on excitability of guinea pig airway vagal afferent nerves." J Neurophysiol **89**(3): 1196-1204.

Urashima, R. and M. Mihara (1998). "Cutaneous nerves in atopic dermatitis. A histological, immunohistochemical and electron microscopic study." Virchows Arch **432**(4): 363-370.

Vaughan, R. P., M. T. Szewczyk, Jr., et al. (2006). "Adenosine sensory transduction pathways contribute to activation of the sensory irritation response to inspired irritant vapors." Toxicol Sci **93**(2): 411-421.

Veres, T. Z., S. Rochlitzer, et al. (2009). "The role of neuro-immune cross-talk in the regulation of inflammation and remodelling in asthma." Pharmacol Ther **122**(2): 203-214.

Verleden, G. M. (1996). "Neural mechanisms and axon reflexes in asthma. Where are we?" Biochem Pharmacol **51**(10): 1247-1257.

Virchow, J. C., P. Julius, et al. (1998). "Neurotrophins are increased in bronchoalveolar lavage fluid after segmental allergen provocation." Am J Respir Crit Care Med **158**(6): 2002-2005.

Wagner, E. M. and D. B. Jacoby (1999). "Methacholine causes reflex bronchoconstriction." J Appl Physiol **86**(1): 294-297.

Walsh, M. T., D. R. Curran, et al. (2004). "Effect of eosinophil adhesion on intracellular signaling in cholinergic nerve cells." Am J Respir Cell Mol Biol **30**(3): 333-341.

Watt, A. H. and P. A. Routledge (1985). "Adenosine stimulates respiration in man." Br J Clin Pharmacol **20**(5): 503-506.

Weickert, J. (1999). "Coherence-Enhancing Diffusion Filtering." Int J Comp Vis **31**(2): 111-127.
Weinreich, D., K. A. Moore, et al. (1997). "Allergic inflammation in isolated vagal sensory ganglia unmasks silent NK-2 tachykinin receptors." J Neurosci **17**(20): 7683-7693.
Wenzel, S. E. (2006). "Asthma: defining of the persistent adult phenotypes." Lancet **368**(9537): 804-813.
Wenzel, S. E., L. B. Schwartz, et al. (1999). "Evidence that severe asthma can be divided pathologically into two inflammatory subtypes with distinct physiologic and clinical characteristics." Am J Respir Crit Care Med **160**(3): 1001-1008.
Wernli, G., W. Hasan, et al. (2009). "Macrophage depletion suppresses sympathetic hyperinnervation following myocardial infarction." Basic Res Cardiol **104**(6): 681-693.
Westby, M., M. Benson, et al. (2004). "Anticholinergic agents for chronic asthma in adults." Cochrane Database Syst Rev(3): CD003269.
WHO (2007). Global surveillance, prevention and control of chronic respiratory diseases: a comprehensive approach, World Health Organization.
Widdicombe, J. G. (1995). "Neurophysiology of the cough reflex." Eur Respir J **8**(7): 1193-1202.
Widdicombe, J. G. (2003). "Overview of neural pathways in allergy and asthma." Pulm Pharmacol Ther **16**(1): 23-30.
Wilkinson, K. D., K. M. Lee, et al. (1989). "The neuron-specific protein PGP 9.5 is a ubiquitin carboxyl-terminal hydrolase." Science **246**(4930): 670-673.
Wilson, S. R., K. A. Gerhold, et al. (2011). "TRPA1 is required for histamine-independent, Mas-related G protein-coupled receptor-mediated itch." Nat Neurosci **14**(5): 595-602.
Woods, R. K., F. Thien, et al. (2002). "Prevalence of food allergies in young adults and their relationship to asthma, nasal allergies, and eczema." Ann Allergy Asthma Immunol **88**(2): 183-189.
Woolf, C. J. (1996). "Phenotypic modification of primary sensory neurons: the role of nerve growth factor in the production of persistent pain." Philos Trans R Soc Lond B Biol Sci **351**(1338): 441-448.
Worth, A. and A. Sheikh "Food allergy and atopic eczema." Curr Opin Allergy Clin Immunol **10**(3): 226-230.
Wu, Z. X., K. B. Benders, et al. (2012). "Early postnatal exposure of mice to side-steam tobacco smoke increases neuropeptide Y in lung." Am J Physiol Lung Cell Mol Physiol **302**(1): L152-159.
Xia, C. M., M. A. Gulick, et al. (2012). "Up-regulation of brain-derived neurotrophic factor in primary afferent pathway regulates colon-to-bladder cross-sensitization in rat." J Neuroinflammation **9**: 30.
Xin, P., Y. Pan, et al. (2010). "Favorable effects of resveratrol on sympathetic neural remodeling in rats following myocardial infarction." Eur J Pharmacol **649**(1-3): 293-300.
Yang, D., H. F. Rosenberg, et al. (2003). "Eosinophil-derived neurotoxin (EDN), an antimicrobial protein with chemotactic activities for dendritic cells." Blood **102**(9): 3396-3403.
Yawalkar, N., M. Uguccioni, et al. (1999). "Enhanced expression of eotaxin and CCR3 in atopic dermatitis." J Invest Dermatol **113**(1): 43-48.
Yen, L. D., G. J. Bennett, et al. (2006). "Sympathetic sprouting and changes in nociceptive sensory innervation in the glabrous skin of the rat hind paw following partial peripheral nerve injury." J Comp Neurol **495**(6): 679-690.
Yost, B. L., G. J. Gleich, et al. (2005). "The changing role of eosinophils in long-term hyperreactivity following a single ozone exposure." Am J Physiol Lung Cell Mol Physiol **289**(4): L627-635.
Young, B., J. Lowe, et al. (2006). Weather's Functional Histology, Elsevier Limited.

Yu, M., X. Zheng, et al. (2008). "Perinatal environmental tobacco smoke exposure alters the immune response and airway innervation in infant primates." J Allergy Clin Immunol **122**(3): 640-647 e641.

Yu, S., F. Ru, et al. (2008). "5-Hydroxytryptamine selectively activates the vagal nodose C-fibre subtype in the guinea-pig oesophagus." Neurogastroenterol Motil **20**(9): 1042-1050.

Zacharasiewicz, A., N. Wilson, et al. (2005). "Clinical use of noninvasive measurements of airway inflammation in steroid reduction in children." Am J Respir Crit Care Med **171**(10): 1077-1082.

Zhang, G., R. L. Lin, et al. (2008). "Altered expression of TRPV1 and sensitivity to capsaicin in pulmonary myelinated afferents following chronic airway inflammation in the rat." J Physiol **586**(Pt 23): 5771-5786.

Zhang, G., R. L. Lin, et al. (2008). "Sensitizing effects of chronic exposure and acute inhalation of ovalbumin aerosol on pulmonary C fibers in rats." J Appl Physiol **105**(1): 128-138.

Zhou, X. F., E. T. Chie, et al. (1999). "Injured primary sensory neurons switch phenotype for brain-derived neurotrophic factor in the rat." Neuroscience **92**(3): 841-853.

Zihlmann, K. B., A. D. Ducray, et al. (2005). "The GDNF family members neurturin, artemin and persephin promote the morphological differentiation of cultured ventral mesencephalic dopaminergic neurons." Brain Res Bull **68**(1-2): 42-53.

Zimmermann, M. (1968). "Selective activation of C-fibers." Pflugers Arch Gesamte Physiol Menschen Tiere **301**(4): 329-333.

Supplemental Videos #1

Click on image to start movie
Click again to pause. Double-click to restart.
**Adjust view and zoom as desired before starting movie.*

1A 3D Nerve Imaging: Whole Mouse Airway

Demonstration of whole airway innervation with progressive magnification toward a patch of epithelial nerves. One epithelial nerve in this example expresses substance P.

Species: Murine

White - DAPI (nuclear stain)

Green - PGP 9.5 (pan-neuronal marker)

Red - Substance P

Magenta - Alpha Smooth Muscle Actin (smooth muscle marker)

1B Imaging Airway Epithelial Nerves

Demonstration of innervation through all layers at a location with a patch of epithelial nerves. Sparse substance P epithelial nerves highlighted.

Species: Murine

Blue - DAPI (nuclear stain)

Green - PGP 9.5 (pan-neuronal marker)

Red - Substance P

More on next page

1C

Computer Mapping of Epithelial Nerves

Demonstration of airway epithelial nerve computer map.
A projection of 3D data is presented and the computer map is overlaid as images are rotated. Afterward, magnification is reduced to contain the whole airway

Species: Murine

First Half

White - PGP 9.5 (pan-neuronal marker)

Green - Computer map of epithelial nerves

Red - Branchpoint

Second Half

White - DAPI (nuclear stain)

Green - PGP 9.5 (pan-neuronal marker)

Red - Substance P

Supplemental Video #2

Click on image to start movie
Click again to pause. Double-click to restart.
**Adjust view and zoom as desired before starting movie.*

In-plane and Out-of-plane Epithelial Nerve Branchpoints

Demonstration of an in-plane branchpoint visible in non-rotated image. Image slices move from the airway lumen to basement membrane, then rotate to an orthogonal views to show difficulty in visually identifying out-of-plane branchpoints. Images are then rotated to an oblique angle to demonstrate visibility of out-of-plane branchpoints once they are identified.

Species: Murine

White - PGP 9.5 (pan-neuronal marker)

Supplemental Videos #3
(For Figures 3 & 6)

Click on image to start movie
Click again to pause. Double-click to restart.
**Adjust view and zoom as desired before starting movie.*

Organ-wide Structural Quantification of Airway Epithelial Nerves and Substance P Epithelial Nerves

A All Epithelial Nerves

B Substance P Epithelial Nerves

Proximal trachea, dorsal midline

White - PGP 9.5 (pan-neuronal marker)

Red - Substance P

Green - Computer Map of Epithelial Nerves
- Red spheres are branchpoints

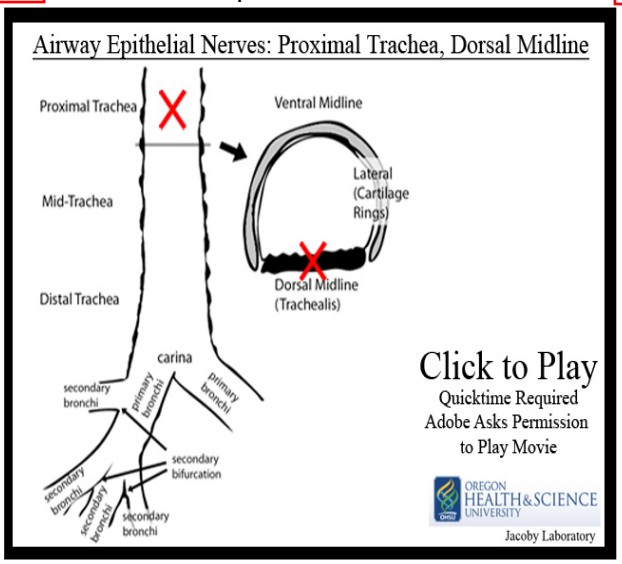

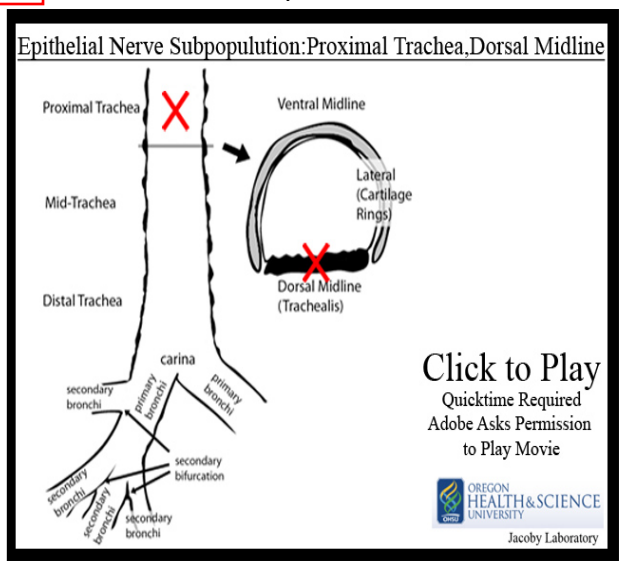

Distal trachea, dorsal midline

White - PGP 9.5 (pan-neuronal marker)

Red - Substance P

Green - Computer Map of Epithelial Nerves
- Red spheres are branchpoints

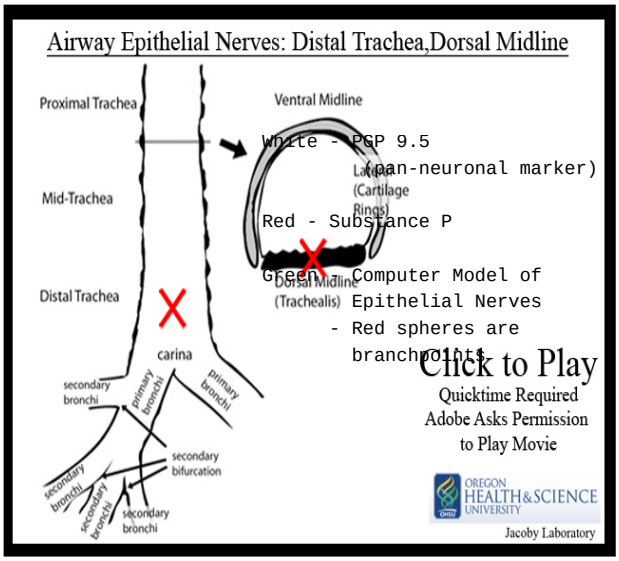

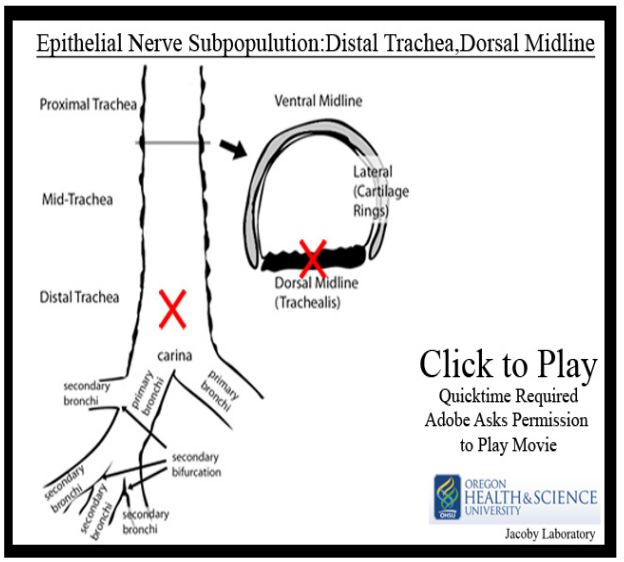

Proximal trachea, ventral midline

White - PGP 9.5 (pan-neuronal marker)

Red - Substance P

Green - Computer Map of Epithelial Nerves
- Red spheres are branchpoints

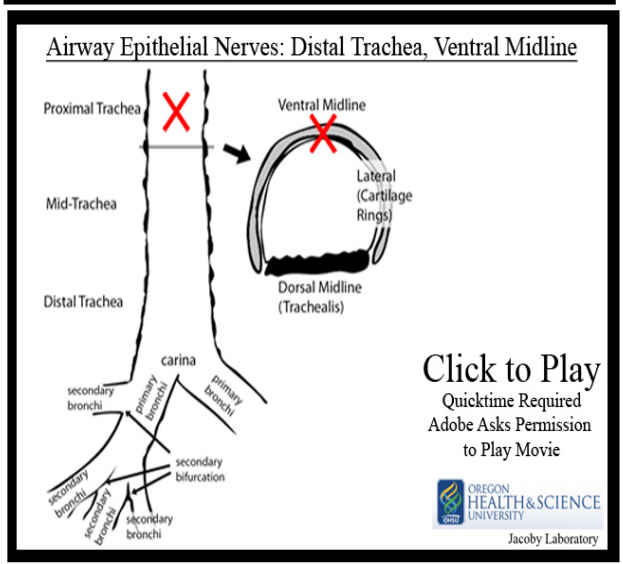

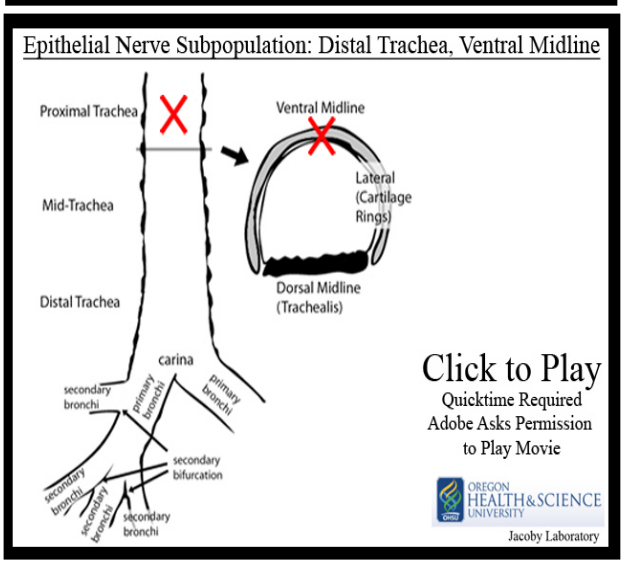

Supplemental Videos #4

Click on image to start movie
Click again to pause. Double-click to restart.
**Adjust view and zoom as desired before starting movie.*

4A 3D Nerve Mapping: Human Proximal Trachea

Innervation of proximal human trachea overlaid with computer map of epithelial nerves. Field contains columnar epithelium.

Species: Human

White - PGP 9.5 (pan-neuronal marker)

Green - Computer Map of Epithelial Nerves

4B 3D Nerve Mapping: Human Distal Trachea

Innervation of distal human trachea overlaid with computer map of epithelial nerves. Field contains columnar epithelium.

Species: Murine

Blue - DAPI (nuclear stain)

White - PGP 9.5 (pan-neuronal marker)

Red - Substance P

Green - Computer Map of Epithelial Nerves

More on next page

Epithelial Nerve Mapping

4C Human Airway Forceps Biopsy: Columnar Epithelium

Innervation of human airway bifurcation (tissue from airway biopsy) overlaid with computer map of epithelial nerves. Field contains columnar epithelium.

Species: Human

White - PGP 9.5 (pan-neuronal marker)

Red - Substance P

Green - Computer map of Epithelial Nerves

Epithelial Nerve Mapping:

4D Human Airway Forceps Biopsy: Squamous Epithelium

Innervation of human airway bifurcation (tissue from airway biopsy) overlaid with computer map of epithelial nerves. Field contains squamous epithelium

Species: Human

White - PGP 9.5 (pan-neuronal marker)

Red - Substance P

Blue - DAPI (nuclear stain)

Green - Computer map of Epithelial Nerves